New Approaches For Understanding Vehicle Emissions Using Remote Sensing

Jack Davison

Doctor of Philosophy

University of York

Chemistry

August, 2022

Abstract

Despite improvements in technology and increasingly strict legislation, road transport remains a key source of air quality pollutants. Accurate emission estimates are important for informing policy to combat the deleterious effects of exhaust species on human health. A key advantage of vehicle emission remote sensing is it can rapidly measure and characterise hundreds of thousands of vehicles. However, to fully realise the potential of remote sensing and gain a comprehensive assessment of emissions, new developments in calculating emission factors are needed. A recurring theme of this thesis is the calculation of emission-engine power models, which allow remote sensing to be used to address more facets of vehicle emissions than it is typically able. A method is developed to calculate distance-specific emission factors, which is validated using portable emission measurement system data. Distance-specific emissions can be compared with other measurement techniques and legislation, and can be used in emission inventory development. A remote sensing-based inventory is directly compared to the UK National Atmospheric Emissions Inventory, achieving excellent carbon balance (within 1%) but revealing that NO_x emissions may be being under-reported by up to 32% at a national level. Remote sensing data are also combined with a large driving activity database to address the effects of driver behaviour and challenge the COPERT approach for emission factor calculation. A robust statistical framework is used to assess emission deterioration, and it is shown that older gasoline cars show a skewed rate of deterioration whereas modern gasoline and diesel emissions are well controlled. A key conclusion is the importance of the differences between manufacturers, which are significant for individual vehicles, for emission deterioration, and in inventory development. This analysis shows that accounting for manufacturers in inventory calculations results in a 13.4% range in total NO_x emissions, an influence not currently reflected in European emission inventories.

Contents

List of Figures

List of Tables

Acknowledgements

To begin, I would like to thank my supervisor, Professor David Carslaw, for his invaluable direction, support, guidance and enthusiasm; I couldn't have picked a better PhD supervisor. Professor James Lee was my secondary supervisor and Professor Alastair Lewis was my independent panel member, and both were encouraging throughout my PhD.

I thank the National Environmental Research Council and UK Department for Transport for funding this PhD project (NE/S012044/1). I also thank my CASE partner, Ricardo Energy & Environment, for funding, support and provision of data. In particular I thank Drs Tim Murrels, Rebecca Rose and Jasmine Wareham for sharing their knowledge of road transport emission factor and inventory development.

This work could not be achieved without the collection of extensive vehicle emission remote sensing data. I thank Dr Gary Bishop from the University of Denver for access to the FEAT instrument, and Drs Naomi Farren, Adam Vaugahn, Stuart Young and Will Drysdale from the University of York for its use for data collection. I also thank the Ricardo Energy & Environment remote sensing team — especially Ben Fowler, Tom Green and Les Phelps — for the collection of data with the Opus RSD 5000, and the teams at OPUS Inspection in both the US and Madrid for their technical support.

Finally, my experience of completing a PhD would have been nothing without the support of my friends and colleagues in the Wolfson Atmospheric Chemistry Laboratories (WACL). I thank you all wholeheartedly.

Author's declaration

I declare that this thesis is a presentation of original work and I am the sole author. This work has not previously been presented for an award at this, or any other, University. All sources are acknowledged as References. Some of the contained work is based on peer reviewed publications with myself as the lead author[1–3], the details of which are provided below:

Ch 2 **Davison, J.**, Bernard, Y., Borken-Kleefeld, J., Farren, N. J., Hausberger, S., Sjödin, Å., Tate, J. E., Vaughan, A. R., Carslaw, D. C. (2020). **Distance-Based Emission Factors from Vehicle Emission Remote Sensing Measurements.** *Science of the Total Environment* 739, 139688
url: https://doi.org/10.1016/j.scitotenv.2020.139688

Ch 4 **Davison, J.**, Farren, N. J., Rose, R. R., Wagner, R. L., Carslaw, D. C. (2021). **Verification of a National Emission Inventory and Influence of On-road Vehicle Manufacturer-Level Emissions.** *Environmental Science & Technology* 55, 8, 4452–4461
url: https://doi.org/10.1021/acs.est.0c08363

Ch 5 **Davison, J.**, Rose, R. R., Farren, N. J., Wagner, R. L., Wilde, S. E., Wareham, J. V., Carslaw, D. C. (2021). **Gasoline and Diesel Passenger Car Emissions Deterioration using On-Road Emission Measurements and Measured Mileage.** *Atmospheric Environment: X* 14, 100162
url: https://doi.org/10.1016/j.aeaoa.2022.100162

Chapter 1

Introduction

1.1 Road Transport: Setting the Scene

In the UK, road vehicles and the roads upon which they drive could be described as ubiquitous. Urban centres are dominated by the presence of roads, with many of our homes, workplaces and recreational spaces connected and surrounded by them. At the end of September 2021 there were 39.2 million licensed vehicles in Great Britain, the majority (81.6%) being passenger cars[4]. For context, the estimated population of Great Britain in 2020 was around 65 million[5], meaning there are around 60 road vehicles per 100 people.

Transport is necessary to meet the needs of modern humans, and road transport is particularly useful for the transportation of both passengers and freight. Road transport uniquely offers travellers the ability to travel long distances, carrying cargo, and with near-total control over their scheduling, journey origin and destination. By comparison, active transport methods — most commonly walking and cycling — leave travellers exposed to the weather, have limited space for cargo, are restricted by fitness levels, and unavoidably can't transport people as far as powered vehicles. Air, sea and rail are restricted to stations or ports and specific scheduling times, and private ownership of their respective vehicles by the majority of the population is economically and practically unfeasible.

While undeniably useful, an over-reliance on road transport is not without detractors. Building cities without alternatives can disadvantage those unable to drive, such as the young, the elderly, and the disabled. Roads can be unsafe, particularly for vulnerable people; the UK Department for Transport reported 119,850 casualties on UK roads in 2021, 24,540 of which were killed or seriously injured[6]. Use of private road transport over active transport is suggested to have a damaging effect on mental health, physical health and social cohesion[7–9]. Road transport is a major contributor to greenhouse gas (GHG) emissions and, by extension, climate change; in 2019 transport was the largest emitting sector of UK GHG emissions (27% of the UK total), with 91% of its

emissions coming from road transport[10]. The focus of this thesis, however, is on other emission species with more local scale effects — what may be termed "air quality" pollutants.

Since road vehicles switched from manual power from humans or beasts of burden to the internal combustion engine (Subsection 1.2.1), road transport has emitted a myriad of tailpipe emissions that are deleterious to human health. Before "smokeless fuels" were legislated for, the sooty emissions of coal-burning road transport were much more visible to the naked eye. Cleaning up the visible pollution was far from the end of the story, however, as when one pollutant was dealt with through improvements in technology and legislation (Subsection 1.3.3), another would emerge as a new target. The soot and sulphur dioxide emissions of the 1940s gave way to a focus on carbon monoxide and lead emissions in the 1960s, which have since been superseded in the 2000s by oxides of nitrogen and a collection of particulate-phase emissions[11].

Road transport is far from the only source of combustion emissions, but it is arguably uniquely challenging to understand. Fossil-fuel power stations are also combustion sources, but they are much fewer in number, static, and highly regulated. Road transport is almost the complete opposite, and its associated challenges are effectively all knock-on effects of its aforementioned advantages; the road transport sector represents millions of independent privately owned mobile consumer products which move unpredictably in space and time. Each of the 39.2 million road vehicles in the UK represents a unique emission source, with even nominally identical vehicles (burning the same fuel in the same sized engine built by the same manufacturer) likely varying in emissions due to driving conditions, ambient conditions, driver behaviour, levels of maintenance, and so on.

Traditionally, road transport emissions have been estimated using data from a small number of vehicles to act as representatives of the whole fleet (Subsection 1.3.3). While not without merit, this approach is likely to miss the aforementioned distribution in a road transport fleet's emissions. This

thesis sets out to extract new information from vehicle emission remote sensing, which can measure thousands of vehicles relatively quickly, although is limited to capturing very brief "snapshots" of their journeys (Section 1.4). A key goal of this work is to gain a *comprehensive* understanding of emission behaviour despite this limitation.

This chapter serves as an introduction to three key background areas to this thesis and the subject of road transport emissions more widely. The chemistry of road transport emissions is first discussed in Section 1.2, followed by the legislation surrounding air quality and road transport type approval in Section 1.3, and finally a description of vehicle emission remote sensing is provided in Section 1.4. Section 1.5 and Section 1.6 will then outline the thesis objectives, structure and approach.

1.2 Chemistry of Road Transport Pollutants

1.2.1 Products of the Internal Combustion Engine

In the UK, the majority of road vehicles are powered by internal combustion engines fuelled by either diesel or gasoline (also called "petrol"). Both of these fuels are composed of mixtures of hydrocarbons, with gasoline being composed of more volatile, shorter-chain hydrocarbons (C_5–C_{10}) and diesel less volatile, longer-chain hydrocarbons (C_{10}–C_{15}). Regardless of the fuel type, road transport internal combustion engines operate in superficially similar ways — air is drawn into a cylinder, compressed with fuel, and the mixture is ignited which moves a piston. This drives the crankshaft and induces motion in the vehicle. The spent mixture of combustion products is the exhaust and is driven out of the engine, ready for the cycle to repeat.

The key difference between gasoline and diesel engines is related to how combustion is physically achieved. Gasoline is first mixed with air, compressed, and then ignited using a spark plug, with the amount of air "throttled" to

control the fuel-air ratio. Conversely, diesel is injected into already compressed, non-throttled air, the heat of which causes it to spontaneously ignite. Diesel engines have a higher "compression ratio" (the ratio of the volume of the cylinder at its maximum and minimum), which generates a greater twisting force ("torque") on the drive shaft. This, combined with the lack of throttling, means diesel engines are considered more efficient and are employed for heavier, load-bearing vehicles like light commercial vehicles (vans), heavy-goods vehicles, and agricultural equipment like tractors, although there are many diesel passenger cars in the UK and Europe. Gasoline is typically only used to fuel lighter vehicles that carry smaller loads, such as motorbikes and passenger cars.

The differences between gasoline and diesel combustion engines are behind the differences in the exhaust composition in the differently fuelled vehicles. In general, these differences are related to diesel engines running hotter, at higher pressures, and "lean" (i.e., having an excess of air), as well as injecting fuel rather than pre-mixing it with air. These different conditions can effect both the formation of emissions inside of the engine and the efficacy of exhaust after-treatment systems (Subsection 1.2.2). The chemical underpinnings of combustion emissions and their mitigation will now be discussed.

In chemistry, "combustion" refers to a category of exothermic redox chemical reactions between a *fuel* and an *oxidant*. "Fuels" are simply materials capable of releasing chemical energy by being burned, and an "oxidant" (or "oxidising agent") is a chemical that can accept the electrons of another substance. In combustion, the oxidising agent is commonly just atmospheric oxygen, O_2, in the air. An example equation for the complete combustion of the simplest saturated alkane, methane (CH_4), is given in Equation 1.1. In complete combustion — where there is sufficient oxygen to fully consume the fuels — the only products are carbon dioxide, CO_2, and water vapour, H_2O.

$$CH_4 + 2\,O_2 \longrightarrow CO_2 + 2\,H_2O \tag{1.1}$$

Carbon dioxide is a colourless, odourless, non-toxic and non-harmful gas

which exists naturally as a trace gas in the Earth's atmosphere. While not seen as an air quality gas, CO_2 is an important climate gas which contributes to climate change. In the context of remote sensing, measurement of CO_2 is still vital to understand air quality emissions; all other pollutants are expressed in a ratio to CO_2, and these ratios are then used to calculate emission factors. This is discussed later in Chapter 2.

With insufficient oxygen, *in*complete combustion occurs. This is undesirable as it produces less overall energy, as well as carbon monoxide (CO, Equation 1.2) and/or smoke (C, Equation 1.3).

$$CH_4 + \frac{3}{2}O_2 \longrightarrow CO + 2\,H_2O \tag{1.2}$$

$$CH_4 + \frac{1}{2}O_2 \longrightarrow C + H_2O \tag{1.3}$$

Carbon monoxide is another oxide of carbon, and takes the form of a colourless, odourless, and tasteless gas. Unlike many other road transport air quality pollutants, CO is not an irritant. Instead, it is both acutely and chronically poisonous through binding with haemoglobin in the blood, forming carboxyhaemoglobin. Carboxyhaemoglobin is incapable of bonding with oxygen, depriving cells within the body of oxygen and causing them to die. The UK National Health Service likens the symptoms of mild carbon monoxide poisoning to the flu or food poisoning. Symptoms of severe poisoning include intoxication and loss of consciousness followed by death[12]. Carbon monoxide also has an important role in the formation of tropospheric ozone, O_3, which comes with its own health effects (Subsection 1.2.3). Road transport was once the largest source of carbon monoxide in the United Kingdom, particularly from gasoline vehicles; the excess amounts of air in diesel engines promotes full combustion to CO_2. However, increasingly strict emissions regulations have caused carbon monoxide emissions to fall 95% between 1990 and 2017. Larger sources of CO are now seen to be residential and stationary combustion[13].

Smoke, given in Equation 1.3 as C, is a carbonaceous solid-phase emission sometimes also referred to as "soot", "smoke" or "black carbon". In emission

science, it is categorised as "particulate matter" (PM). Unlike the other pollutants mentioned so far, particulate matter — often abbreviated to "PM" — is not a discrete chemical species. Instead, it can be described as the sum of solid and liquid-phase particles in air, which include a combination of organic and inorganic chemical species of varying size, composition and origin. It has been demonstrated that particulate air pollution is associated with the development of cardiovascular diseases and lung cancer[14–16].

Particulate matter emissions are between six- to ten-times as high from diesel vehicles when compared to gasoline vehicles[17]. This is due to diesel fuel being injected rather than mixed, creating heterogeneous fuel-air mixtures. Fuel-dense pockets are not as exposed to air, leading to incomplete combustion and formation of black carbon which is emitted in the vehicle exhaust. While this carbon forms the bulk of diesel exhaust particulate, it also contains a soluble organic fraction (comprised of oil, unburnt fuel, and combustion by-products) and an inorganic fraction (metals)[17].

Another important emission is that of hydrocarbons (often abbreviated to "HC"). Hydrocarbons in exhausts are the emissions of unburnt or partially burnt fuel leaving the vehicle primarily through the tailpipe (although evaporative non-tailpipe "running-loss" emissions also occur). Much like particulate matter, "HC" isn't just one chemical species but instead refers to thousands of alkanes, alkenes, aromatics, and other hydrocarbons. Like NO_x, hydrocarbons play an important role in O_3 formation, and can cause respiratory irritation and cancer. Unlike NO_x, HC is higher in gasoline vehicles; the smaller-chain hydrocarbons in the lighter gasoline fuel are more volatile so more readily evaporate than the heavier diesel equivalents.

The preceding chemistry assumes a lack of elements other than hydrogen, oxygen and carbon in an engine, but this is practically untrue. Composing 78% of the Earth's atmosphere, nitrogen gas is unavoidably present in the fuel-air mixture in a combustion engine. The presence of nitrogen leads to the formation of nitrogen oxide (NO), which is described using the extended

Zeldovich mechanism (Equation 1.4), a series of reactions in which molecular nitrogen, oxygen and hydroxyl radicals react to give NO[18].

$$\begin{aligned} N_2 + O &\rightleftharpoons NO + N \\ N + O_2 &\rightleftharpoons NO + O \\ N + OH &\rightleftharpoons NO + H \end{aligned} \tag{1.4}$$

Nitrogen dioxide, NO_2, can also be formed in combustion engines (Equation 1.5), though much of it is a secondary product which will be discussed later (Subsection 1.2.3).

$$NO + HO_2 \rightleftharpoons NO_2 + OH \tag{1.5}$$

NO is odourless and colourless, whereas NO_2 is pungent and reddish-brown. Both are toxic gases, although the toxicity of NO_2 is around five times as great[17]. Collectively, NO and NO_2 are referred to as NO_x, and act as an irritant, lower the body's resistance to respiratory disease, and play an important role in the formation of tropospheric O_3 and secondary PM (Subsection 1.2.3). Oxides of nitrogen are key targets for legislation in the UK and Europe; NO_2 has limits set for ambient air (Subsection 1.3.1) and NO_x emission limits form part of the road vehicle type approval process (Subsection 1.3.3). In 2019, 33% of the UK's NO_x emissions came from road transport, especially from diesel vehicles. Diesel engines emit considerably more NO_x than gasoline engines; the higher operating temperatures of and excess oxygen in the cylinder promotes its formation. While road transport remains an important source of NO_x in the UK and Europe, it is important to mention that, since 1990, NO_x emissions from road transport have decreased in the UK by 78%, owing to stricter legislation on newer vehicles (Subsection 1.3.3)[19].

Another element which can be present in fuel is sulphur, the combustion product of which is sulphur dioxide (SO_2). SO_2 has health effects — irritating the nose and throat — and can react with water and oxygen in the atmosphere, producing H_2SO_4. The mechanism for the latter is provided in Equation 1.6.

Dilute H_2SO_4, alongside its nitrogen analogue HNO_3, is a component of acid rain which can damage both the natural and built environment. However, it is important to mention that, in the United Kingdom, legislation has meant fuel is now effectively sulphur-free. This severely cut SO_2 emissions from the transport sector by 91% from 1990 to 2017[20], and SO_2 is therefore not a focus of this thesis.

$$\begin{aligned} S + O_2 &\longrightarrow SO_2 \\ SO_2 + H_2O &\longrightarrow H_2SO_3 \\ 2\,H_2SO_3 + O_2 &\longrightarrow 2\,H_2SO_4 \end{aligned} \tag{1.6}$$

1.2.2 Emission Control Technology

To mitigate the emission of the harmful species discussed in Subsection 1.2.1, vehicle manufacturers employ a range of different technologies. At first these technologies focused on adapting the conditions *within* the engine. For example, one relatively early method developed for controlling NO_x in diesel vehicles was exhaust gas recirculation (EGR). An EGR system simply reintroudces some of the exhaust gas back into the cylinder, reducing its maximum temperature and therefore the amount of NO_x formed. This works due to exhaust gas having a higher specific heat capacity than air. While it is known that EGR is an effective method for reducing NO_x emissions, the lower amounts of oxygen in the cylinder can increase the amount of incomplete combustion, leading to more CO, PM and HC emissions[21–23].

As emission legislation became increasingly more strict (Subsection 1.3.3), engine-based interventions stopped being sufficient. As the unwanted by-products of combustion — NO_x, CO, particulates, etc. — and the evaporative emissions of volatile organic compounds are effectively inevitable side effects of fundamental chemical and physical processes, there are limited actions that can be taken within the engine itself to prevent their formation. Instead, vehicle manufacturers employ a series of "after-treatment" technologies which aim to destroy, convert or otherwise capture emissions *after* the engine but before they

exit the vehicle tailpipe. This is known as "after-treatment".

Perhaps the most well-known after-treatment systems are catalytic converters. In chemistry, "catalysis" is the process by which the rate of a chemical reaction is modified by the presence of a substance not consumed by the reaction — the "catalyst". Initially, road transport manufacturers relied on the two-way (or "oxidation") catalytic converter to meet emission regulations[24]. Both gasoline and diesel vehicles were equipped with these catalysts, which were designed to simultaneously oxidise harmful carbon monoxide and unburnt hydrocarbons to the less harmful carbon dioxide and, in the latter case, water (Equation 1.7, where hydrocarbons are represented by CH_2).

$$\begin{aligned} 2\,CO + O_2 &\longrightarrow 2\,CO_2 \\ CH_2 + O_2 &\longrightarrow CO_2 + H_2O \end{aligned} \tag{1.7}$$

Two-way catalysts were effective at their stated purpose, but were notably unable to deal with NO_x emissions. The two-way catalyst was therefore superseded by the *three*-way catalyst (TWC), which shared the objectives of oxidising the carbon-containing species but also reducing oxides of nitrogen (Equation 1.8)[24].

$$\begin{aligned} 2\,NO + 2\,CO &\longrightarrow N_2 + 2\,CO_2 \\ 2\,NO + 2\,H_2 &\longrightarrow 2\,H_2O + N_2 \\ 3\,NO + CH_2 &\longrightarrow CO_2 + H_2O + \frac{3}{2}\,N_2 \end{aligned} \tag{1.8}$$

While effective in their implementation in gasoline vehicles, three-way catalysts are known to give rise to an additional air quality pollutant. The TWC is designed to reduce NO to N_2, but it can be further reduced to result in the formation of ammonia, NH_3 (Equation 1.9). Ammonia plays an important role in a lot of environmental issues such as acidification, nitrification, and eutrophication, as well as acting as a precursor to secondary PM[25].

$$2\,NO + 2\,CO + 3\,H_2 \longrightarrow 3\,NH_3 + 2\,CO_2 \tag{1.9}$$

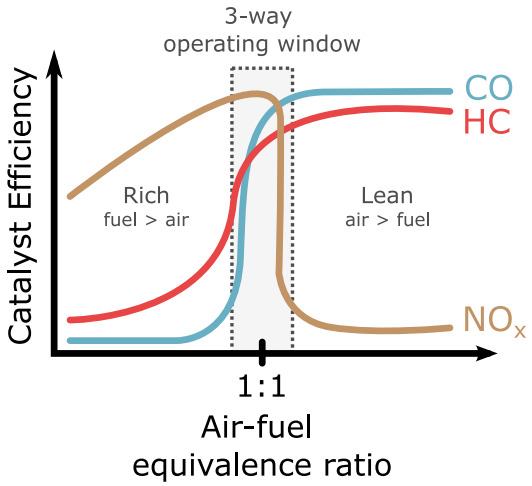

Figure 1.1: The efficiency of a three-way catalyst by air-fuel ratio. There is a "goldilocks" operating window found around the stochiometric ratio of air to fuel where three-way catalysts operate the most efficiently for all three species. Diagram adapted from Umicore Automotive Catalysts [26].

Three-way catalysts both reduce *and* oxidise species, processes that can be at odds with one another. Figure 1.1 visualises this; in rich conditions (low air) the reduction of NO_x is promoted but the oxidation of CO and hydrocarbons is poor, whereas in lean conditions (excess air) the oxidation of CO and hydrocarbons is rapid but the reduction of NO_x rapidly drops off. Three-way catalysts are therefore not used in diesel vehicles, which tend to run lean.

Instead, diesel vehicles use a combination of the diesel oxidation catalyst (DOC) and an additional NO_x control system. Much like other oxidation catalysts discussed, DOCs serve to oxidise carbon monoxide and hydrocarbons (as well as the soluble organic fraction of diesel particulate) to carbon dioxide and water. NO can also be oxidised to NO_2, which does not reduce overall NO_x emissions but can increase the efficiency of NO_x control after-treatment systems.

One common NO_x control system is the lean NO_x trap (LNT), which operates by adsorbing NO_x under lean conditions and periodically removing it under rich conditions. The chemistry of an LNT is outlined in Wang et al. [27], but

is reproduced here. In the lean periods, NO is oxidised to produce NO_2 and adsorbed to an oxide surface as nitrate ions, given in Equation 1.10.

$$\begin{aligned} NO + \frac{1}{2}O_2 &\rightleftharpoons NO_2 \\ BaCO_3 + 2\,NO_2 &\rightleftharpoons Ba(NO_3)_2 \end{aligned} \tag{1.10}$$

Under the periodic rich conditions, the barium nitrate is released from the trap and decomposes into barium oxide and nitrogen dioxide. The reduction of NO_2 by any of the reducing agents available in the exhaust (CO, HC, or H_2) is catalysed, and the barium carbonate used in Equation 1.10 is reformed through reaction with CO_2. These steps are laid out in Equation 1.11, where the reducing agent is given as CO.

$$\begin{aligned} Ba(NO_3)_2 &\rightleftharpoons BaO + 2\,NO_2 \\ 2\,NO_2 + 2\,CO &\xrightarrow{Pt/Rh} N_2 + 2\,CO_2 \\ BaO + CO_2 &\longrightarrow BaCO_3 \end{aligned} \tag{1.11}$$

An alternative (or, in some cases, complementary) NO_x control system in diesel engines is the selective catalytic reduction system (SCR). SCR systems use a reductant — commonly ammonia (NH_3) or urea ($CO(NH_2)_2$) — to reduce NO and NO_2 to N_2. The three reaction pathways for this — purely NO, purely NO_2, and a combination of both NO and NO_2— are provided in Equation 1.12. The combination reaction is the fastest of the three.

$$\begin{aligned} 2\,NO + 2\,NH_3 + \frac{1}{2}O_2 &\longrightarrow 2\,N_2 + 3\,H_2O \\ NO_2 + 2\,NH_3 + \frac{1}{2}O_2 &\longrightarrow \frac{3}{2}N_2 + 3\,H_2O \\ NO + NO_2 + 2\,NH_3 &\longrightarrow 2\,N_2 + 3\,H_2O \end{aligned} \tag{1.12}$$

SCR technology is neither new nor settled technology, being reviewed in the literature as early as 1996 and as recently as 2019[28,29]. Unlike the reduction systems in three-way catalysts, SCR systems are unaffected by the presence of oxygen, making them suitable for use in diesel engines. However, SCR-equipped diesel vehicles can undergo "ammonia slip" in which unreacted NH_3

is emitted from the tailpipe. Therefore, much like TWC-equipped gasoline vehicles, newer (Euro 6+) diesel vehicles can be a source of vehicular NH_3[30,31].

The final element of the diesel after-treatment system to be discussed is the diesel particulate filter (DPF). A DPF is a structure through which the exhaust gas travels and to which the particulate matter adsorbs. This is a different approach to the catalytic systems (e.g., TWC, DOC, SCR) which chemically convert their target pollutants to something less harmful; the particulates still exist, just trapped on the filter. DPFs therefore have an upper capacity after which they need regenerating, which is achieved by burning off the particulate. This can be "passive regeneration" during extended high engine load conditions — commonly motorway driving — or "active regeneration" where a control unit forces an increase in exhaust temperature when the DPF reaches a certain capacity. If neither of these regeneration methods are allowed to happen (for example, if a diesel passenger car almost exclusively operates in stop/start urban driving conditions), DPFs need to be manually cleaned or replaced.

This subsection has outlined several after-treatment strategies which vehicle manufacturers employ to reduce emissions and meet increasingly stringent emissions legislation (Subsection 1.3.3). While these methods are common and effective, they increase the cost, weight and complexity of combustion-powered road vehicles. The added expense of topping up SCR reductants or cleaning DPFs lead some fleet owners to pursue "DPF deletion" or use SCR "cheat devices" to bypass their vehicles' after-treatment systems. Furthermore, the chemistry promoted by the catalytic systems gives rise to additional air quality pollutants, such as ammonia.

1.2.3 Secondary and Non-Exhaust Pollutants

Not all air quality pollutants from road transport are products of combustion, or chemistry promoted by after-treatment systems. This subsection outlines air quality pollutants that are not emitted from a vehicle tailpipe, but instead

react in the atmosphere or are emitted from elsewhere. While this thesis is focused primarily on the direct tailpipe emissions of road transport vehicles, it is important to briefly mention these pollutants to fully contextualise how road transport contributes to poor air quality.

As previously mentioned, NO_x is the collective term for both NO and NO_2. The largest fraction of NO_x is nitrogen oxide, followed by *secondary* NO_2, with the smallest fraction being *primary* NO_2. *Secondary* means that it isn't produced in an engine, but rather by reactions between NO and O_3 in the atmosphere. NO and NO_2 exist in an equilibrium in the atmosphere, described by the *Leighton relationship* (Equation 1.13). NO_2 is photolysed into atomic oxygen, which quickly reacts to form ozone. Ozone molecules can react with nitrogen oxide to produce molecular oxygen and nitrogen dioxide again. Together these reactions form a null cycle, producing no net production or loss of the involved species. The ratio of NO to NO_2 depends on the intensity of sunlight (required in the first step) and the concentration of ozone (required in the third).

$$\begin{aligned} NO_2 &\xrightarrow{h\nu} NO + O \\ O + O_2 + M &\longrightarrow O_3 + M \\ O_3 + NO &\longrightarrow NO_2 + O_2 \end{aligned} \tag{1.13}$$

Another key secondary pollutant is tropospheric ozone, formed from reactions of primary pollutants and other species present in the atmopshere, such as those described in Equation 1.13. However, Equation 1.13 does not provide a complete picture — being a null cycle, no net production or destruction would occur if these reactions were all that occurred. In reality there are many competing reactions. The production of tropospheric ozone is complex and nonlinear, but a simplified summary of the photochemistry of ozone in "dirty air" is provided in Equation 1.14, where "VOC" refers to "volatile organic compounds" and "oVOC" their oxidation products (e.g., carbonyls).

$$VOC + 4\,O_2\,(+ NO_x + OH) \longrightarrow oVOC + 2\,O_3 + H_2O\,(+ NO_x + OH) \tag{1.14}$$

Ozone is a pale blue gas with a pungent smell. Stratospheric ozone is formed as a natural part of the atmospheric chemistry of Earth, and is essential for sustaining animal and plant life as it absorbs much of the ultra-violet (UV) radiation emitted by the sun. Tropospheric ozone, on the other hand, is primarily anthropogenic in origin and is far less desirable. Ground-level O_3 is harmful to breathe, causing respiratory damage, reduced lung function and increased mortality. It also has additional economic impacts through crop loss.

Earlier, particulate matter was discussed in the context of incomplete combustion of fuel, particularly diesel fuel, producing primary "soot" emissions. It was also mentioned that NO_x and NH_3 emissions can promote the formation of secondary PM in the atmosphere. Road transport also produces a third category of PM referred to as "non-exhaust" PM which arises from friction rather than chemistry. The main contributors to non-exhaust PM are brake wear (resulting from the action of a brake pad on a rotating mechanism), tyre and road surface wear (the action of a vehicle's tyre on the road surface), and resuspension (dust on the road being resuspended by the action of tyres on the road or by turbulence caused by the vehicle). It is estimated that, due to the success of DPFs, non-exhaust PM now exceeds exhaust PM in the UK[32]. Non-exhaust PM is also unique among all of the pollutants discussed in this chapter as it would remain an issue even if the entire road transport fleet completely electrified[33].

1.2.4 Summary of Road Transport Pollutants

Air pollutants resulting from road transport are summarised in Table 1.1. This includes pollutants arising from combustion and evaporative processes (Subsection 1.2.1), catalytic processes (Subsection 1.2.2), secondary reactions in the atmosphere and non-exhaust sources (Subsection 1.2.3).

	Pollutant	**Description**
CO_2	Carbon Dioxide	Formed from complete combustion. Not an air quality gas, but contributes to climate change.
CO	Carbon Monoxide	Formed from incomplete combustion. Acutely/chronically poisonous. Higher in gasoline engines — less oxygen to promote complete combustion.
NO_x	Nitrogen Oxides	Formed from the reaction of N_2 and O_2. Combination of NO and NO_2. Respiratory irritant and toxin. Contributes to O_3 and secondary PM formation. Higher in diesel engines — more oxygen and higher temperature.
HC	Hydro-carbons	Unburnt/partially burnt fuel. Thousands of chemically distinct hydrocarbons. Respiratory irritant and carcinogen. Contributes to O_3 formation. Higher in gasoline engines — more volatile fuel.
NH_3	Ammonia	Formed in three-way catalysts by over-reducing NO_x (gasoline) and slips from SCR systems (diesel). Contributes to acidification, nitrification, eutrophication and secondary PM formation. Higher in gasoline engines.
O_3	Ozone	Secondary pollutant, formed from reactions of HC and NO_x. Respiratory irritant, reduces lung function, destroys plant life.
PM	Particulate Matter	Mixtures of solid- and liquid-phase chemical compounds in the atmosphere. Cause/exacerbate respiratory and cardiovascular disease. Carcinogenic. *Primary*: Formed from incomplete combustion. Higher in diesel engines — heterogenous air-fuel mixture. *Secondary*: Formed in the atmosphere from primary NO_x and NH_3 emissions. *Non-Exhaust*: Formed from abrasive action on breaks/tyres/road, or resuspended from road surface.

Table 1.1: A summary of key pollutants resulting from road transport.

1.3 Road Transport and Air Quality Legislation

1.3.1 Air Quality Limits

As previously discussed, poor air quality has a negative effect on public health, acting as a risk factor for cardiovascular diseases, respiratory diseases and cancer. The World Health Organisation (WHO) takes the stance that air pollution is a global health risk on the same scale as unhealthy diets and smoking[34]. It is therefore in the interest of governments to legislate for better air to mitigate the health effects and their knock-on economic consequences.

To assist in developing legislation, the WHO sets out air quality guidelines. These are expressed as upper limits for specific pollutants — PM, O_3, NO_2, SO_2 and CO — over some averaging period (e.g., annual, daily, hourly, etc.). Varying averaging periods allows for long-term and short-term exposure to be legislated separately. Recently, the WHO released their 2021 guidelines[34] which significantly reduced guidelines for PM and NO_2, and introduced new guidelines for O_3, NO_2 and CO. These limits are tabulated in Table 1.2, alongside the relative changes between the 2005 and 2021 guidelines.

The WHO is an organisation of scientists and medical professionals; the limits it suggests are not necessarily feasible economically or technologically for any given country. Furthermore, while they are designed to aid in defining legislative limits for air quality pollutants, they themselves are not legally binding and governing bodies are free to set whichever limits they think are appropriate for their own circumstances. The UK's air quality objectives are set out by the Department for Environment, Food & Rural Affairs (Defra)[35] and are also tabulated in Table 1.2. The UK's limits are higher than even the 2005 iteration of the WHO guidelines for $PM_{2.5}$, PM_{10} and SO_2, and are higher than the newest guidelines for NO_2.

Naturally, air quality limits are set in response to more than just road transport. Countries can exceed their limits due to other anthropogenic activity

				WHO Guidelines		
Pollutant	**Unit**	**Averaging**	**UK**	**2021**	**2005**	**Change**
$PM_{2.5}$	$\mu g\,m^{-3}$	Annual	25	5	10	-50%
		24-hour	—	15	25	-40%
PM_{10}	$\mu g\,m^{-3}$	Annual	40	15	20	-25%
		24-hour	50	45	50	-10%
O_3	$\mu g\,m^{-3}$	Peak season	—	60	—	New
		8-hour	100	100	100	±0%
NO_2	$\mu g\,m^{-3}$	Annual	40	10	40	-75%
		24-hour	—	25	—	New
		1-hour	200	200	200	±0%
SO_2	$\mu g\,m^{-3}$	24-hour	125	40	20	+100%
		1-hour	350	—	—	—
		15-minute	266	—	—	—
		10-minute	—	500	500	±0%
CO	$mg\,m^{-3}$	24-hour	—	4	—	New
		8-hour	10	10	—	New
		1-hour	—	35	—	New
		15-minute	—	100	—	New

Table 1.2: UK National air quality objectives[35], alongside the World Health Organisation (WHO) air quality guidelines (2005 and 2021)[34,36]. "Peak season" is defined as the "average of daily maximum 8-hour mean O_3 concentration in the six consecutive months with the highest six-month running- average O_3 concentrations". WHO value table adapted from Breeze Technologies [37].

(e.g., other modes of transport, industry, agriculture, etc.) or unavoidable meteorological processes transporting pollution from elsewhere. Indeed, it has already been discussed that the road transport sector in the UK is of diminishing importance for CO and SO_2 emissions. However, it continues to dominate the issue of NO_x emissions, which in turn influences the ambient concentrations of the secondary pollutants O_3 and PM[19].

1.3.2 Emission Factors and Inventory Development

An "emission inventory" attempts to account for all pollutants emitted into the atmosphere, usually for a given location. The UK inventory is referred to as the National Atmospheric Emissions Inventory, often abbreviated to the "NAEI"[38]. It is funded by the UK Department for Business, Energy and Industrial Strategy (BEIS), the UK Department for Environment, Food and Rural Affairs (Defra), the Scottish and Welsh Governments and the Northern Ireland Department of Agriculture, Environment and Rural Affairs (DAERA). Emission inventories are required to meet international obligations; for example, data from the UK NAEI is presented to the United Nations Economic Commission for Europe (UNECE), United Nations Framework Convention on Climate Change (UNFCCC), and the European Union. Furthermore, inventories are essential for air quality modelling to understand trends in pollutant concentrations.

As it is impractical to measure every source of a pollutant at all times, generic emission factors are used when developing an emissions inventory. Emission factors are values which relate the quantity of a pollutant emission with an activity related to its release (Equation 1.15). For example, in road transport an emission factor may be expressed in units of g km^{-1}, which is to say the grams of a pollutant (the emission) emitted per kilometre the vehicle has driven (the activity).

$$Emission = Activity \times Factor \tag{1.15}$$

In Europe and the UK, the air quality community typically sources emission

factors from two modelling approaches; COPERT (the Computer Programme to calculate Emissions from Road Transport)[39,40] and HBEFA (the Handbook for Emission Factors)[41], both overseen by the ERMES (European Research for Mobile Emission Sources) Group[42]. Franco et al. [43] describes the different applications of the two approaches; COPERT is a "speed-dependent" approach (utilising speed-emission curves) which is relied upon by many European countries when reporting their national inventories of emissions, whereas HBEFA uses a "traffic-situation" approach which — due to requiring a deeper knowledge of local-scale traffic — is mainly used at smaller scales (i.e., individual road links rather than national inventories). Brown et al. [44] outlines the approach for the UK NAEI which — like many European countries — relies on the COPERT approach for emission factors alongside guidance from the EMEP/EEA (European Monitoring and Evaluation Programme/European Environment Agency) Emission Inventory Guidebook[45].

1.3.3 Type Approval Legislation & Emission Standards

Since 1992, all new road vehicles in the UK and Europe must meet certain emission standards. Meeting the relevant "Euro standard" is part of a vehicle's type approval process. The Euro standards for passenger cars are provided in Table 1.3, and the history and context behind these values will be discussed below.

In 1992, the Euro 1 legislation came into effect. At this stage, diesel and gasoline cars had near-identical emission standards, with the only difference being the additional limit on particulate matter for diesel cars. As well as the written limits, unleaded petrol and catalytic converters became compulsory. Four years later, the Euro 2 standards defined different limits for gasoline and diesel vehicles. To be tested against these type approval limits, manufacturers produce pre-production cars which are effectively identical to the final product to be put to market. For fairness, these pre-production cars undertake fixed

			Distance-Specific Emission (g km^{-1})				
Fuel	**Stage**	**Date**	**CO**	**HC+NO_x**	**HC**	**NO_x**	**PM**
Gasoline	Euro 1	07/1992	2.72	0.97	—	—	—
	Euro 2	01/1996	2.20	0.50	—	—	—
	Euro 3	01/2000	2.30	—	0.20	0.15	—
	Euro 4	01/2005	1.00	—	0.10	0.08	—
	Euro 5	09/2009	1.00	—	0.10	0.06	0.0045
	Euro 6	09/2014	1.00	—	0.10	0.06	0.0045
Diesel	Euro 1	07/1992	2.72	0.97	—	—	0.1400
	Euro 2	01/1996	1.00	0.70	—	—	0.0800
	Euro 3	01/2000	0.64	0.56	—	0.50	0.0500
	Euro 4	01/2005	0.50	0.30	—	0.25	0.0250
	Euro 5	09/2009	0.50	0.23	—	0.18	0.0045
	Euro 6	09/2014	0.50	0.17	—	0.08	0.0045

Table 1.3: European emission standards for passenger cars in g km^{-1}.

"drive cycles" on chassis dynamometers, also known as "rolling roads" — laboratory instruments designed to simulate driving in a controlled environment. At the time, the drive cycle used was the ECE+EUDC cycle[46]. This involved four repetitions of an urban cycle (meant to model typical driving in a European city) followed by one "extra-urban" cycle (accounting for more aggressive driving).

Under the Euro 1 and 2 standards, vehicles were allowed to idle for 40 seconds at the beginning of the test before emission sampling started. One of the key changes brought with the Euro 3 legislation was the removal of this idling period, capturing so-called "cold-start" emissions. The cold-start procedure was referred to as the "New European Drive Cycle" (NEDC), which is visualised in Figure 1.2. As well as introducing the NEDC, the Euro 3 legislation of 2000 further reduced CO and PM emissions, added separate NO_x limits for diesel cars, and added separate HC and NO_x limits for gasoline cars.

Over the next nine years, the Euro 4 and 5 standards continued to introduce increasingly strict limits on NO_x, CO, HC and PM for gasoline and diesel

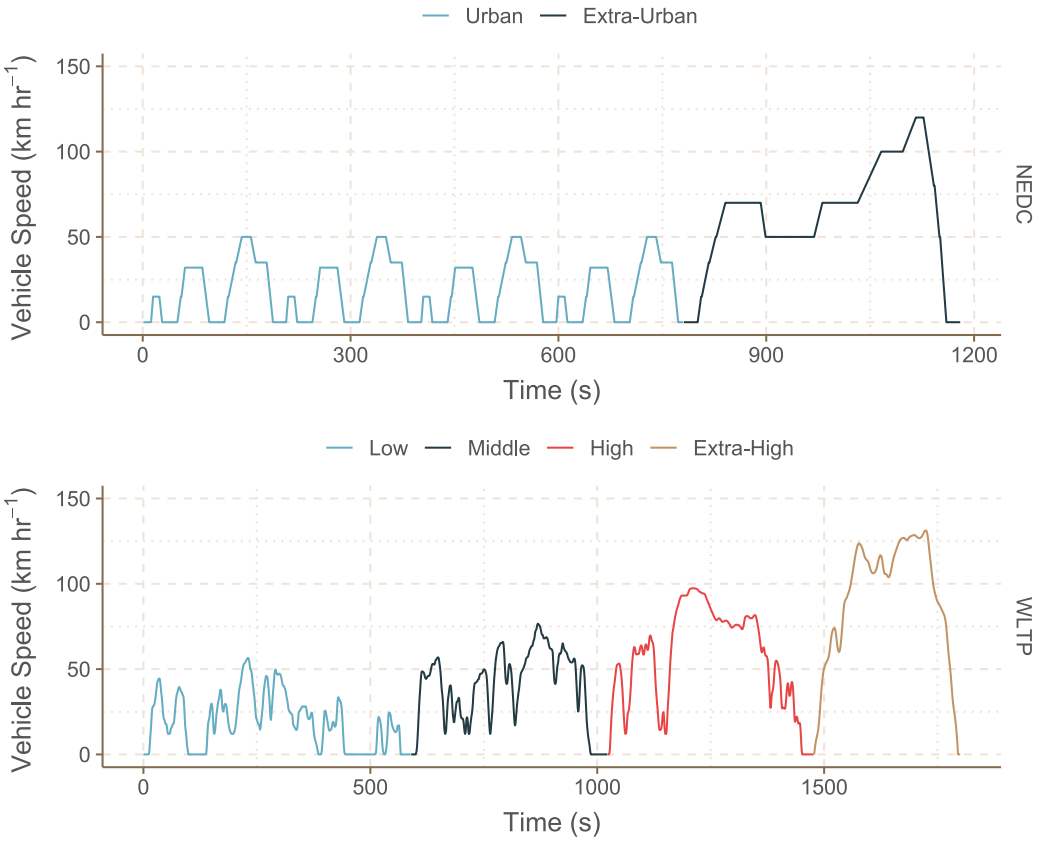

Figure 1.2: The New European Drive Cycle (NEDC, top) and World Harmonised Light Vehicle Test Procedure (WLTP, bottom).

cars. Euro 5, for the first time, also included a PM standard for gasoline cars. Furthermore, to mitigate the effects of very fine particulate emissions, Euro 5 introduced a particle *number* (PN) limit of 6×10^{11} km^{-1} for diesel cars. The increasingly stringent PM emission limits led to the mass adoption of the diesel particulate filter (DPF) in all diesel cars under the Euro 5 legislation, although there were some early Euro 4 adopters.

The most recent set of standards are the Euro 6 standards which broadly focus on reducing diesel emissions, with the NO_x limit dropping by roughly 60% to just 0.08 g km^{-1}. Importantly, the various stages of Euro 6 legislation brought significant changes to the way type approval was carried out[47]. Euro 6 legislation was set out in stages — Euro 6a through Euro 6d — with each step

introducing new legislation:

- Euro 6a was the first version, and effectively set out the standard limits and the start date of 1 September 2014.
- Euro 6b came into force in 2014, when new vehicles began needing to meet the Euro 6 standard. Furthermore, the particulate limits for both gasoline and diesel engines dropped to 0.0045 g km^{-1}.
- Euro 6c was introduced in 2017, which included two key changes. First, the particle number limit imposed on diesel vehicles under Euro 5 legislation was introduced to gasoline vehicles. This led to the adoption of the Gasoline Particle Filter — a similar technology to the Diesel equivalent that has been shown to effectively control gasoline PM emissions[48–50]. Secondly, and perhaps more significantly, Euro 6c replaced the NEDC with the World Harmonised Light Vehicle Test Procedure (WLTP), which is also visualised in Figure 1.2. This new drive cycle was meant to be more reflective of real-world driving, addressing criticism that the NEDC covers too limited a range of driving conditions to represent *actual* driving[51,52].
- Euro 6d-TEMP was valid between 2018 and 2020, and arguably introduced Euro 6's most significant change to the type approval process; for the first time, a "real-world" element was added in the form of the Real World Driving (RDE) emissions test. The pre-production cars are driven on public roads with Portable Emission Measurement Systems (PEMS) measuring NO_x and PM emissions, PEMS being an "on-board" measurement technique where instrumentation is carried inside a vehicle. Euro 6d-TEMP legislated a so-called "conformity factor" of 2.1 for the standards, effectively increasing the 0.08 g km^{-1} limit to 0.168 g km^{-1} for the RDE test. This was to allow manufacturers time to adjust to the change in the type approval procedure.

- Euro 6d is the current emission standard in the UK and Europe. The key change introduced was the compliance factor of the RDE test dropping from 110% to 50%.

Euro 6 will not be the final emission standard in Europe. As part of the European Green Deal, the European Commission has already set out intentions for Euro 7 legislation that will be even more stringent than Euro 6d[53–55]. Three options are being considered, all expressed as revisions to existing Euro 6 legislation: *1)* a "narrow revision" to simplify and standardise standards and testing, *2)* a "wide revision" to introduce even more stringent limits and begin legislating new pollutants (e.g., NH_3, non-CO_2 greenhouse gas emissions, etc.), and *3)* a "comprehensive revision" to begin real-world emission monitoring over a vehicle's lifetime. At the time of writing, the Euro 7 initiative has received 68 published articles of feedback, with the three biggest sources being business associations (23), individual companies or businesses (16) and public authorities (9)[56]. The non-governmental federation "Transport & Environment" has raised concerns about manufacturer groups opposition to Euro 7 proposals, referring to Euro 7 as "last opportunity to introduce stricter emissions standards to reduce toxic emissions from internal combustion engines"[57,58]. Indeed, it is commonly assumed that Euro 7 will be the final Euro emission standard before internal combustion engines begin to be phased out entirely.

While pollutants like CO, HC and PM have been broadly below the emission standards set out for them, NO_x emissions are understood to exceed the type approval limits in the real world[59]. Vehicles exceeding type limits has significant public health impacts, including premature deaths in Europe[60–62].

1.4 Vehicle Emission Remote Sensing

1.4.1 A Brief History of Remote Sensing

Vehicle Emission Remote Sensing (commonly abbreviated to either "RS" or "VERS") was invented by researchers at the University of Denver in 1987 with a grant from the Colorado Office of Energy Conservation[63]. The earliest publicly available reference to remote sensing technology was in Stedman et al. [64], a report to the Colorado Office of Energy Conservation, in which the authors describe the device in the context of its original funded purpose — to save fuel by identifying gasoline vehicles with high CO tailpipe emissions. Indeed, the name of the original "remote sensing device" (RSD) made no reference to air quality, being named the "Fuel Efficiency Automobile Test" (or FEAT) instrument.

> *"This device is the first of its kind in the world and has opened the way to monitoring a large number of "in-use" vehicles for excessive carbon monoxide emissions, which provides a direct relationship to the vehicle's energy efficiency, conveniently and economically."*[64]

In 1989 the first two FEAT articles in academic journals were published. Writing in *Environmental Science & Technology*, Donald H. Stedman — the project lead on the development of the FEAT instrument — reflected on remote sensing's role in clean air policy, and invited readers to consider how it may play into enforcement strategies. He also noted the observation that emissions from the studied fleet are dominated by small proportion of gross polluters — a recurring theme in remote sensing literature to this day[65]. The second article, Bishop et al. [66], is the first comprehensive description of the operation of the FEAT, and concludes by stating that *"[the authors] believe that the basic concept is sound and that it is feasible to expand the sensor to monitor additional species such as hydrocarbons, formaldehyde, and nitrogen oxides."*[66] — a prediction that would later come true.

In the late 1980s and early 1990s, the FEAT instrument was only capable of measuring CO_2 and CO using IR spectroscopy. Despite this limitation, over 100,000 measurements were taken using the FEAT device and used to comment on the success of then-recent legislation[67] and on the capability of RS to be an effective surveillance tool to identify high-emitting vehicles[68] — to list two examples. By 1992, the IR technology in the RSD had been upgraded to be able to measure unburnt hydrocarbon emissions[69]. One of the earlier applications of the HC capabilities was the FEAT's use in Mexico City, where vastly higher CO and HC emissions than had been seen in North America and Europe were observed[70].

In 1993, a patent was awarded to Donald Stedman and Gary Bishop for an "Apparatus for remote analysis of vehicle emissions", with the abstract beginning *"A gas analysis device for the remote detecting, measuring and recording of NO_x, CO, CO_2, HC and H_2O levels from the exhaust of moving motor vehicles"*[71]. NO was the next pollutant to be added to the FEAT system, being the first pollutant to be measured using ultraviolet rather than infrared spectroscopy[72,73]. At that time it was assumed that NO represented the majority of oxides present in NO_x, so it wasn't until later that a separate NO_2 channel was also included when primary NO_2 emissions were raised as a concern[74]. UV channels were also added to the FEAT to measure SO_2 and NH_3, further increasing its capabilities[75].

In the present day, the FEAT instrument is no longer the only cross-road, laser-based RSD. The company *Envirotest* were the first to commercialise the technology, and were then acquired by *OPUS Group* in 2014[76]. The OPUS *AccuScan* RSD is, in practice, very similar to the FEAT — although it possesses some key differences discussed in Subsection 1.4.2. Other commercially available RSDs are available; the EDAR system has been developed since 2009 which uses a 'top-down' approach to measure emissions rather than cross-road[77,78]. The top-down EDAR system is not a focus of this thesis, although its potential applications related to the contained work are briefly discussed in Chapter 2.

1.4.2 RSD Instrumentation: Principles and Practicalities

A vehicle emission remote sensing device (RSD) is not a singular instrument, but instead a collection of at least three key modules working in tandem - ultraviolet and infrared spectrometers used to measure concentrations of exhaust pollutants, speed-acceleration bars used to capture the instantaneous driving condition of the vehicle's being measured, and number plate cameras for photographing vehicle number plates. These modules all feed information to and are controlled by a field computer. A schematic of the set-up of a cross-road RSD is provided in Figure 1.3.

The underlying physical and chemical principles of cross-road RSDs have been described extensively in the literature, most often by the inventors of the FEAT instrument. A thorough review of the physical principles and individual instrumentation underpinning the FEAT instrument, many of which also apply to the OPUS instrument, is provided in Burgard et al. [79], but a brief overview is provided here.

CO_2, CO, and HC are measured using non-dispersive infra-red (NDIR) spectroscopy. While scanning IR spectrometers (such as those found as bench-top instruments in chemistry laboratories) are expensive, complex, and non-portable, NDIR sensors are cheap, simple and lightweight. NDIR sensors involve IR light shining from a lamp into a detector, passing through filters to isolate wavelengths corresponding to specific target gases. In the FEAT instrument IR light is focused across a road and, on entry to the detector, is refocused onto a spinning mirror, which sweeps the light across four IR detectors. The passband filters on these detectors filter for the following wavelengths: 2150 cm^{-1} for CO, 2350 cm^{-1} for CO_2, 2970 cm^{-1} for HC (specifically targeting the C−H stretch), and 2600 cm^{-1} for the IR reference.

The reference wavelength was chosen as it was in the same range as the pollutant wavelengths while being a wavelength where no pollutant should absorb. As HC emissions are mixtures of hundreds of different hydrocarbons

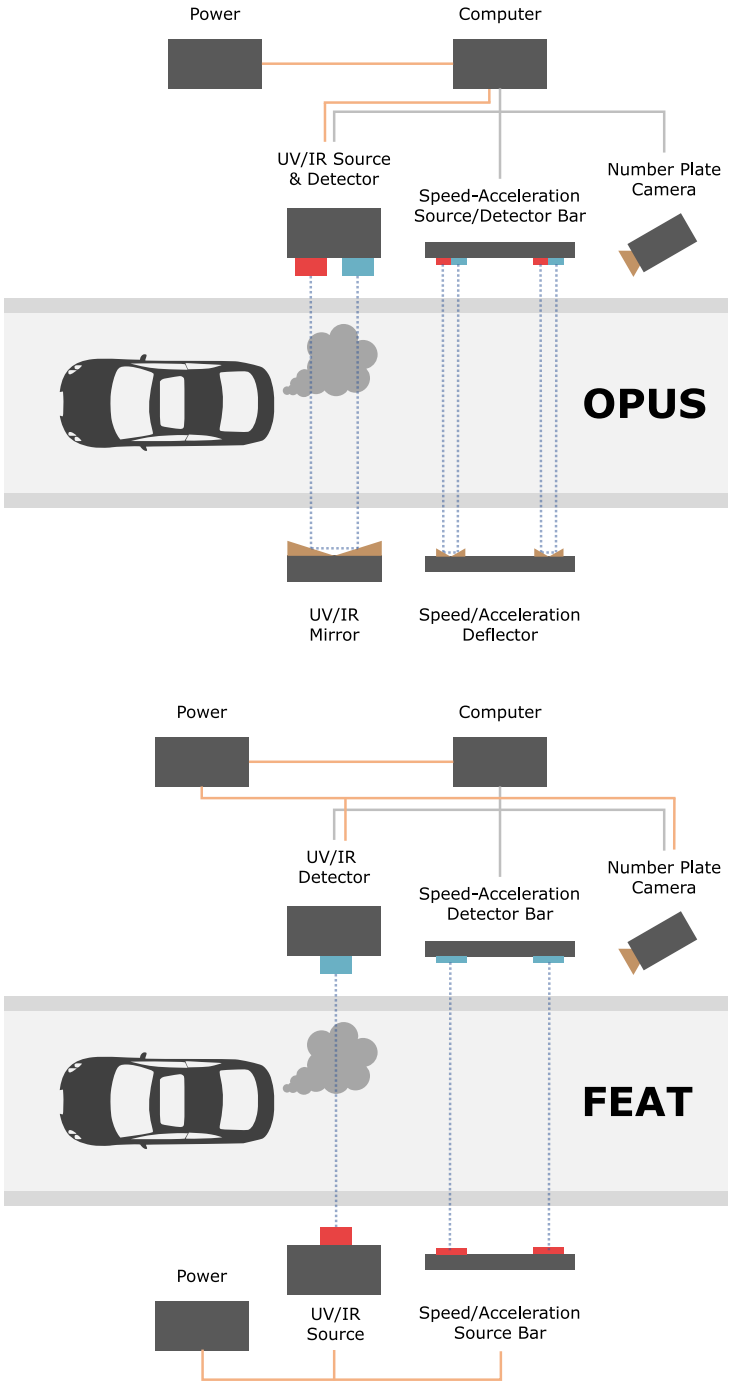

Figure 1.3: A schematic setup of the key modules of a roadside vehicle emission remote sensing device (RSD), for both the commercially available OPUS RSD (top) and the original Denver FEAT instrument (bottom).

the measurement is approximate and misses around half of hydrocarbons in the exhaust, so a scaling factor of 2 is applied[80]. The Beer-Lambert law (Equation 1.16) can be used to calculate the concentration of the target gas, c, using the intensity of light detected by the filtered light, I, the reference intensity, I_0, the molecular absorption coefficient of the gas, ε, and the path length, l.

$$\varepsilon cl = \log\left(\frac{I_0}{I}\right) \tag{1.16}$$

NO concentrations are not measured using NDIR as the fundamental absorption band of NO, 1800 cm^{-1}, overlaps with the absorption of water vapour, which is also present in the exhaust and air. Instead, NO — along with NO_2, SO_2 and NH_3— are measured using disperse ultraviolet (UV) spectroscopy. The UV and IR lights are collinear, so need to be split upon reaching the detector module of the RSD. While the IR is directed into the aforementioned spinning mirror, the UV light is focused onto the end of a quartz UV fibre bundle which — in the FEAT instrument — are coupled to two spectrometers: one to measure NO, SO_2 and NH_3 at the spectral range of 200–226 nm, and one to measure NO_2 between 430 and 447 nm. Until very recently, the OPUS RSDs only had one UV channel for measuring NO_x and NH_3, but the recent *AccuScan* RSD 5500 does include a second just for measuring NO_2 similar to the FEAT instrument[81]. Despite the slight differences in the spectroscopic approaches used by the FEAT and OPUS instruments, evidence from the literature suggests that the resulting data are comparable[82].

As well as measuring gaseous species, the OPUS RSD also measures particulate matter. Light is scattered or absorbed by particles in a vehicle's exhaust, so light opacity is used as a proxy for PM emissions. The UV absorbance at 248 nm is considered as there are limited responses from NO_x and other gaseous species at this wavelength. Opacity can be calculated by comparing the amount of light returning at this wavelength to the amount detected at the CO_2, CO and HC detection wavelengths. This opacity-based method is best suited for meas-

urements of high-emitting vehicles (such as pre-DPF diesel vehicles), as for "cleaner" vehicles the opacity readings are likely to fall within the instrument noise[83].

The speed-acceleration bars for both the FEAT and OPUS instruments are simple optical triggers. Passing vehicles blocking and unblocking the lasers as they pass allows the RSD computers to calculate vehicle speed and acceleration. These are important measurements for estimating the power demand on an engine, which usefully correlates with emissions better than speed or acceleration alone. Commonly, a metric known as vehicle specific power (VSP) is used, which is defined as the sum of the power demands on a vehicle (acceleration, drag, rolling resitance, gradient climbing, etc.) divided by the vehicle's mass[84]. The calculation and application of VSP is discussed more in Chapter 2.

The camera photographs number plates, which can be cross referenced with vehicle databases to obtain technical information about the passing vehicles. In the UK, technical information can be sourced from the UK Driver and Vehicle Licensing Agency (DVLA) and the Society of Motor Manufacturers and Traders Motor Vehicle Registration Information System (MVRIS), but sources and quantity of technical information will vary internationally. For the data used in this thesis, the commercial supplier CDL Vehicle Information Services Ltd. was used[85]. Vehicle technical information is vital to distinguish between different vehicle classifications (e.g., vehicle type, fuel type, and engine size). It also enables one of the greatest strengths of remote sensing as a method, which is considering a vehicle fleet on a very granular level (individual manufacturers, body types, years of manufacture, after-treatment technologies, etc.).

Figure 1.3 illustrates the similarities and differences between the practical deployment of the FEAT and OPUS RSDs. While the layout of the RSD modules is broadly similar, a key difference lies in the arrangement of the light sources and detectors. The Denver FEAT instrument places the UV/IR source and optical speed/acceleration bar source on the opposite side of the road to the detectors/spectrometers, whereas the OPUS RSD houses both source

and detector in one unit with the light being deflected back by mirrors. This means that the OPUS path length is effectively double that of the FEAT, which increases the signal-to-noise ratio and is suggested to potentially improve the accuracy of exhaust measurements[82]. The differing arrangements also mean that the FEAT instrument needs powering on both sides of the road, whereas the OPUS only requires a single power source on the curbside. The schematic in Figure 1.3 also simplifies the reality of the four FEAT modules; there are more individual units in the FEAT which need to be individually connected with communication and power cables. Conversely, the schematic accurately represents the OPUS system, where each of the modules are housed in one unit each which only need to be connected via communication cable to the control computer. Practically speaking, the differences between the systems mean that the OPUS RSD is easier to transport and faster, simpler and safer to deploy.

Site selection is an important consideration and limitation for the deployment of a remote sensing device. Cross-road RSDs can only work on single lanes of traffic. Setting up on a common single carriageway — with two lanes, one for each direction of travel — may lead to unlawful blocking of public roads, particularly in the UK where roads are broadly narrower compared to the US where RS was first invented. RSD operators therefore rely on road features such as pedestrian refuges or hatched road markings in the middle of the carriageway to non-obstructively deploy the "roadside" units of the RSD (FEAT sources/OPUS mirrors). Remote sensing also requires engines to be under load to produce a measurable exhaust plume. Site choices which optimise for these conditions include set-ups on motorway slip roads, on roundabout exits, after security gates or after speed limit increases, all of which are situations in which drivers are encouraged or required to accelerate. Remote sensing can also be described as "fair weather" technology as rain, snow, and fog cause light scattering which drastically decrease the number of valid emission measurements[86].

While RSD operators must be thoughtful when choosing measurement sites and days for the above reasons, the portability of remote sensing is one of its

key advantages. If a particular fleet is of interest — for example, the taxi fleet of a specific city — an RSD can be deployed in the city's urban centre and measure the actual taxi fleet under the conditions in which they are actually driven. If operators are interested in heavy-duty vehicle emissions, their RSD can be deployed in industrial estates or shipping ports. The FEAT instrument has even been adapted to measure high-exhaust heavy-duty road vehicles, snowmobiles, locomotives and aeroplanes, all of which are illustrated in Burgard et al. [79].

1.4.3 Common Applications of Remote Sensing

Before the commercialisation and wider adoption of remote sensing technology, the entirety of RS literature came from the Stedman group at the University of Denver. Some of this has been referenced in Subsection 1.4.1, and the earliest applications of the FEAT thoroughly reviewed in Burgard et al. [79]. This section intends to explore more recent applications of remote sensing, both from Denver and internationally.

Emission Factor Development

Remote sensing typically reports emissions as either ratios to CO_2 or, more commonly, fuel-specific (g kg^{-1}) emission factors. Due to having no access to the tailpipe, distance-specific (g km^{-1}) emission factors are more difficult to estimate. This is a disadvantage of remote sensing as a technique as it sets it apart from other methods (chassis dynamometers, PEMS) and the COPERT/HBEFA approaches for emission factor calculation. This is more thoroughly discussed in Chapter 2. Regardless, numerous studies present emission factors for others to use[31,87], including studies presented in this thesis (Appendix C).

As remote sensing measurements are instantaneous snapshot measurements of vehicle emissions, a natural question is how many are required to be representative of a given vehicle category. Chen et al. [88] uses Monte Carlo simulations to attempt to set a threshold, arriving at 200 measurements being

able to represent the mean emission rate for Euro 4+ diesel cars, and 300-800 being needed to also approximate the variance. In reality, there is considerable variation in the literature, with Smit et al. [89] presenting emissions data for vehicle categories with as few as 3 remote sensing observations.

Fleet Surveillance

Remote sensing has been conducted since the late 1980s, meaning that there is a wealth of RS measurements in existence up until the present day. Several studies undertake what may be termed "fleet surveillance" — examining long-term trends in vehicle fleets, both in composition and emissions. The University of Denver is particularly capable of this kind of analysis[90,91], with Bishop [91] examining three *decades* worth of emissions measurements. The Denver group has also published extensive fleet surveillance studies on Heavy-Duty vehicles[92–97].

In Europe, the CONOX project set out to pool European RS data into a centralised database which, similar to the FEAT databse, allows for long-term fleet surveillance[98,99]. Chen et al. [59] used the CONOX database to analyse light commercial vehicle (LCV) emissions trends alongside changing emission legislation. In the UK, Carslaw et al. [100] noted a substantial downward trend in primary NO_2 emissions from road transport. Smit et al. [89] summarises a decade worth of remote sensing in Australia, noting stabilising NO_x and PM emissions from vehicles in the Australian fleet. A common theme across the American, European and Australian studies is the unprecedentedly large amounts of data spanning many years of measurement campaigns, the likes of which would be nearly impossible to replicate with in-lab or on-board techniques.

Historic measurements also allow remote sensing to directly address how emissions respond to "hot topic" issues in the road transport sector. A contemporary example is the after-effects of dieselgate. While it would be challenging to do enough lab-based or on-board measurements to identify the fleet-wide

implications of post-dieselgate hardware and software fixes, two RS studies — Grange et al. [101] and Bishop [102] — were able to directly compare large samples of pre- and post-repair diesel vehicle emissions. Being able to examine different in-use fleets permitted the studies to come to different conclusions (36% vs 83% reductions in fuel-specific NO_x in Europe vs the US, respectively) which may have been hidden if only a small number of "representative" vehicles were studied using PEMS, for example. An earlier example is Bishop and Stedman [103], where the Denver group examine the impact of the 2008 global recession on US light-duty vehicle emissions.

Long-term monitoring of the same fleet also allows for emission deterioration to be examined[104–106], which is more thoroughly discussed in Chapter 5.

Influences on Emissions

As already mentioned, a common variable with an influence on emissions is vehicle specific power (VSP)[84,107]. This is common in much of the road transport emission science literature, but very frequently used in remote sensing literature in particular to capture the instantaneous driving condition of a vehicle. Additionally, the variation in RS measurement sites/conditions coupled with its large sample sizes of vehicles allows the technique to comment on a myriad of other influences on vehicle emissions. Of particular interest may be those that are difficult to replicate in a laboratory — for example, some Denver studies on the effects of altitude[92,108].

Remote sensing measurements are taken under true ambient conditions, similar to PEMS measurements but dissimilar to in-lab, climate controlled chassis dynamometer studies. RS has therefore been a useful tool to examine extremes of temperature and their effects on emissions. Bishop et al. [109] examined heavy-duty vehicle emissions in the US using remote sensing and noted a roughly 25% increase in NO_x between spring and winter. Grange et al. [110] examined light-duty vehicles in Europe and suggested 38% more NO_x may have been emitted in Europe than was predicted by in-lab test cycles owing

to temperature dependence.

Remote sensing is also uniquely suited to identifying the real-world emission differences between vehicle manufacturers. The literature commonly references differences between manufacturers[31,83,101,110–112], and the quantification of these differences is a common theme in this thesis (Chapter 2, Chapter 4 and Chapter 5).

Fleet Screening

RS as a technique has the potential to screen passing vehicles to identify "high-emitters" — the small proportion of individual vehicles that contribute disproportionately high amounts to total fleet emissions. This may not be as straightforward as it first seems; instantaneous emission measurements from passing vehicles are not the same as their average emissions (which remote sensing doesn't have access to), and the easiest solution of setting a high threshold may fail to detect high-emitters. As part of their review of remote sensing in Hong Kong, Huang et al. [113] suggests a three-point strategy for high-emitter detection; measurements only under moderate speed/acceleration, a threshold "safely" above the emissions of normal vehicles, and at least two high emission flags (from using two RSDs sequentially, for example). Even then they note that, in Hong Kong, this strategy only consistently worked for gasoline vehicles, with a high number of false flags for diesel vehicles. There are a number of alternative methods presented in the literature that use more robust — and complex — statistical methods for high-emitter detection[114–116]

Despite the concerns expressed in the literature, in practice there has been success at using a high threshold to identify real-world high emitters by the OPUS group. A recent example was a 2019 campaign in Spain, where OPUS Remote Sensing Europe successfully identified NO_x emission "cheats" in the HGV fleet, with the police on hand to immediately investigate. The investigation noted 15% of the measured fleet were using SCR-overriding cheat devices, leading to arrests and other legal action[117].

Fleet screening includes more than just identifying high NO_x emitters. Gautam et al. [118] determines thresholds for identifying compromised/removed diesel particulate filters using remote sensing, and Bishop et al. [119] outlines a screening method for running-loss hydrocarbon emissions. Regardless of the specific feature being screened *for*, all screening studies exploit the rapid, "live" measurements of vehicles to quickly identify vehicles of interest.

1.5 Thesis Aims, Objectives and Structure

The overall aim of this thesis is to develop novel methods for the analysis of vehicle emissions remote sensing data, allowing for new insight into road transport emissions. Much of these methods focus on the exploitation of an exhaust emission-engine power relationship to "map" remote sensing emissions data onto real-world driving activity data. To demonstrate and validate the methods outlined in this thesis, large data sets of hundreds of thousands of remote sensing observations were used, collected with both the University of Denver FEAT instrument[120] and the commercially available OPUS RSD5000[76]. In some cases, outputs were directly validated or challenged with the use of non-remote sensing data, such as the UK National Atmospheric Emissions Inventory or independent PEMS data. Specific objectives for each chapter are outlined below.

Chapter 2 presents the development of a method to calculate distance-specific (g km^{-1}) emission factors from remote sensing data through modelling instantaneous fuel consumption using a physics-based estimate of engine power. The method is validated through an initial application to portable emission measurement system (PEMS) data, with good correlation between measured and modelled distance-specific CO_2 emissions. The chapter also presents a brief investigation into manufacturer-specific emissions, which is expanded upon in Chapter 4.

Chapter 3 demonstrates the approach outlined in Chapter 2 used to model NO_x emissions over a very large data set of real-world driving data from multiple drivers and driving conditions. The synthesis of a large data set of real-world emissions data from remote sensing and an extensive data set of driving data allows for comprehensive assessment of emissions. This chapter uses the resulting data set to explore the significance of two local-scale influences on emissions: the variability of the speed-emission relationship with road speed limit, and the potential effect of individual driver behaviour.

In **Chapter 4**, a large UK-based remote sensing data set, UK government activity data and the approach outlined in Chapter 2 are used to calculate a bottom-up estimate of CO_2 and NO_x emissions for the UK. The calculated values are then used to directly challenge the UK National Atmospheric Emissions Inventory. Good carbon balance is achieved, validating this approach further, but NO_x is found to be underestimated in the UK NAEI — particularly in urban areas. Furthermore, a potentially significant manufacturer effect not currently directly accounted for in emissions inventories is identified.

Chapter 5 presents a combination of remote sensing data and measured mileage information from MOT tests, which are used to statistically analyse the deterioration of emissions. Quantile regression is employed to understand the skewed nature of emissions deterioration, and reveals distinct patterns of deterioration between gasoline and diesel passenger cars. The difference between manufacturers are also once again highlighted, illustrating variable levels of control over NO_x emissions between them.

Chapter 6 summarises and contextualises the presented work, and discusses potential future directions in this area of research.

As Chapter 2, Chapter 4 and Chapter 5 are all heavily based on peer-reviewed journal publications, they are written in a way that can be read independently without reference to other chapters in this thesis. Chapter 3 is unpublished work and, while it can be read as an individual study, it is best considered an extension or application of Chapter 2.

1.6 Data & Software

Each of the results chapters of this thesis use vehicle emission remote sensing data obtained by researchers at the University of York and at Ricardo Energy & Environment. As more data were made available over time, numbers of observations are inconsistent between chapters. Results chapters were written in the following order, with the number of remote sensing observations available increasing with each: Chapter 2, Chapter 4, Chapter 5, Chapter 3.

All analysis contained within this thesis was conducted using the R programming language[121] in the RStudio integrated development environment[122]. Most commonly the `tidyverse` suite of packages was employed[123], but for large data sets (most notably in Chapter 3) the `data.table` package was used[124]. All data visualisations in this thesis were produced using the `ggplot2` package[125] and a handful of extension packages[126–131], with some visual refinement performed in the vector graphics editor *Inkscape*[132]. Inkscape was also used to illustrate all graphical abstracts at the beginning of chapters.

Statistical modelling was undertaken using the "base" R `stats` package[121], the `tidymodels` suite of packages[133], as well as the following specialist packages: generalised additive models were fit using `mgcv`[134]. Decision trees were fit using `rpart`[135]. Quantile regression models were fit using `quantreg`[136]. Statistical summary tables found in the "methods and materials" sections of Chapter 2, Chapter 4 and Chapter 5 were generated using the `gt`[137] and `gtsummary`[138] packages.

The typesetting for this thesis was done with LaTeX using the *Overleaf* cloud-based LaTeX editor (`www.overleaf.com`).

Chapter 2

Absolute Emission Estimates from Remote Sensing Data

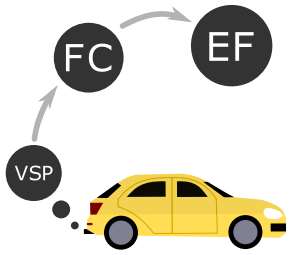

1 Estimate VSP, model fuel consumption and calculate emission factors.

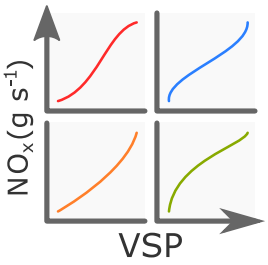

2 Fit emission-VSP GAMs using remote sensing data.

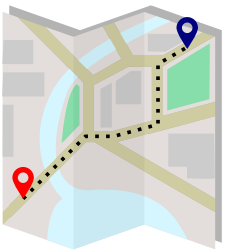

3 Use GAMs to map remote sensing data onto any drive cycle.

2.1 Abstract

Vehicle emission remote sensing has the potential to provide detailed emissions information at a highly disaggregated level owing to the ability to measure thousands of vehicles in a single day. Fundamentally, remote sensing provides a direct measure of the molar volume ratio of a pollutant to carbon dioxide, from which fuel-specific emissions factors can readily be calculated. However, vehicle emissions are more commonly expressed in emission per unit distance travelled, e.g., grams per km or mile. To express vehicle emission remote sensing data in this way requires an estimate of the fuel consumption at the time of the emission measurement. In this chapter, an approach is developed based on vehicle specific power that uses commonly measured or easily obtainable vehicle information such as vehicle speed, acceleration and mass. The method is tested against 55 independent comprehensive PEMS measurements for Euro 5 and 6 gasoline and diesel vehicles over a wide range of driving conditions, and is applied to individual vehicle model types to quantify distance-specific emission factors. The method will be appropriate for application to larger vehicle emission remote sensing databases, thus extending real-world distance-specific vehicle emissions information.

2.2 Introduction

Road vehicle emissions contribute significantly to a wide range of air pollution problems, particularly in urban areas. The European Environment Agency estimates that in 2017 86% of its monitoring stations which reported NO_2 concentrations above the World Health Organisation Air Quality Guidelines were traffic stations[139]. Important primary combustion products from vehicles include NO_x (NO + NO_2) and particulate matter (PM). Additionally, emissions of NO_x act as an ozone (O_3) precursor and are an important contributor to secondary particulate formation. Emissions of these species have been shown to have considerable deleterious effects on human health[16,140,141], with premature deaths in Europe having been attributed to poor air quality owing to exceedance of road transport type approval tests[60–62]. Recently, Schraufnagel et al. [142] suggested that air pollution could deal chronic damage to potentially every organ in the human body.

Robust emissions data are required to ensure that policies aiming to mitigate air pollution are effective. In the case of road vehicle emissions, robust quantification poses considerable challenges. Vehicle emissions vary by manufacturer, vehicle model, emission standard, engine size, fuel type and many other factors. Even nominally identical vehicles which share all these characteristics can vary in their mileage, their levels of maintenance, driver behaviour, the added weight of their passengers and cargo, the auxiliary systems being employed, and the ambient conditions in which they are driven. With tens of millions of road vehicles in the United Kingdom alone, it is challenging to robustly quantify the contribution of road transport to air quality.

In recent years there has been an increased focus on emissions under "real-world" conditions in addition to laboratory-based quantification. Historically, testing vehicles for type approval regulations has been solely conducted under controlled laboratory conditions on chassis dynamometers over drive cycles such as the New European Driving Cycle (NEDC). Originally introduced in

1996, the NEDC is criticised for poorly reflecting real driving conditions. To replace the NEDC, the Worldwide Harmonised Light Vehicles Test Procedure (WLTP) was introduced in Europe starting in 2017, which is more representative of real-world driving, alongside the Real Drive Emissions (RDE) test. The RDE test is conducted on roads in real traffic, with vehicles being measured with Portable Emission Measuring Systems (PEMS) undergoing a specified variety of driving conditions (urban, rural, and motorway)[143].

Remote sensing is in many ways complementary to PEMS. PEMS has some clear benefits: the full journey of a single vehicle can be measured under almost any driving condition — idling in traffic through to motorway driving. However, it can be expensive and time consuming to measure a large number of vehicles in this way and capture important variations due to ambient conditions, vehicle age profiles and the potential effects of vehicle deterioration. Moreover, it is also challenging to measure a broad range of vehicle types, including urban buses and the wide range of heavy duty diesel vehicles (HDV) that exist. The growing databases of PEMS measurements are strongly dominated by measurements of passenger cars.

On the other hand, vehicle emission remote sensing cannot measure an entire drive cycle; only measuring a snapshot of a given vehicle's journey (the average of 10 to 25 instantaneous measurements of an exhaust plume within 0.5 s of a vehicle's passing[111]). Nevertheless, an important advantage of remote sensing comes from the much larger sample size measured in a short space of time, full fleet coverage with little selection bias, and the unobtrusive nature of remote sensing. Applications of the technique have included the instantaneous identification of potential high-emitters[113,117] and investigations into longer term trends in fleet emissions[90,144]. Remote sensing data has also been used to analyse real-world conditions which can influence vehicle emissions, two examples being altitude[108] and ambient temperature[110].

A key limitation of remote sensing in terms of emission factor development, however, is that only a molar ratio of a pollutant to CO_2 is measured. This is a

consequence of measuring in a dispersing plume in the atmosphere rather than measuring emissions directly at the tailpipe. The concentrations of pollutants in a plume may change as it dilutes, but their ratios to CO_2 should remain the same for unreactive pollutants[145]. With a few basic assumptions about the combustion of hydrocarbon fuels, it is straightforward to calculate fuel-specific emission factors, most commonly expressed as grams of emission per kilogram of fuel burnt[79].

Fuel-specific emission factors have been argued to vary less with engine load than distance-specific equivalents[145,146]. Lee and Frey [147] went as far to suggest that remote sensing site-specific fuel-specific emission factors could be representative of area-wide emission rates if the distribution of vehicle specific power (VSP) values were similar between the measurement site and routes in the area of interest. However, the vehicle emissions type approval process and emission factors used in the development of emissions inventories instead express emissions as distance-specific factors, i.e., grams per mile or kilometre.

Previous studies have already attempted to calculate distance-specific emission factors from remote sensing data. Carslaw et al. [148] used UK emission factor estimates of CO_2 in g km^{-1} and measured NO_x to CO_2 ratios to calculate NO_x g km^{-1} emission factors; a major assumption being how accurate and representative the CO_2 estimates are. Similarly, Bernard et al. [149] combined average fuel-specific emission factors, the carbon content of fuel, and distance-specific CO_2 emission factors estimated based on type-approval information contained in number plate information, augmented by the reported consumer fuel economy average experience in real-world conditions. The authors note that this method is to be used with caution due to the real-world variance of CO_2 g km^{-1} values not reflected in the type-approval values.

More commonly, fuel consumption is used directly to transform fuel-specific emission factors into distance-specific emission factors. In some cases, the approach relies on preexisting measurements of fuel consumption. Andrés Aguilar-Gómez et al. [150] estimated fuel consumption based on fuel economy

data-bases available from maintenance programs in Mexico where their study took place, and Zhou et al. [151] relied on fuel consumption information derived from an earlier PEMS study by Wang et al. [152]. A natural drawback of methods such as these is the restriction of remote sensing to locations where these external data sets exist and are publicly available.

Other studies have chosen to model fuel consumption based on roadside measurements. For example, Chan and Ning [153] used work presented by Tong et al. [154] to model fuel consumption based on instantaneous vehicle speed. Later, Zhou et al. [155] modelled fuel consumption based on both binned vehicle specific power (VSP) and vehicle speed to better reflect real-world driving conditions, with each binned fuel consumption value adjusted by vehicle mass. Only four vehicles were used in the fuel economy testing to feed into this model, however, limiting its applicability.

The primary aim of this work is the development and validation of a method to estimate the instantaneous fuel consumption of a vehicle measured using remote sensing, which can then be used to estimate distance-specific emission factors. To estimate fuel consumption, vehicle specific power (VSP) is first estimated using curbside measurements and vehicle technical data, and is then used to model fuel consumption through relationships established using the Passenger Car and Heavy Duty Emission Model (PHEM). The calculated distance-specific emission factors are compared to PEMS data of 55 Euro 5 and 6 passenger cars and light duty vans. The comparison is made between the emissions of NO_x measured over a real-world driving test (similar to an RDE test) and emissions derived using the emissions model based on remote sensing data.

In order to demonstrate the methods in this work, certain assumptions have been made — for example relating to the power demands on vehicle engines, or the molecular formula of fuel. The methods are sufficiently modular such that if more specific values are known or if alternative assumptions are preferred, they can be used in the place of those assumptions presented here.

2.3 Materials and Methods

2.3.1 Calculation of Vehicle Power

The aim of the emissions model is to estimate the instantaneous fuel consumption of a vehicle at the time the remote sensing measurement is made. The approach is based on the estimate of the vehicle power demand at a particular point in time coinciding with when a remote sensing measurement is made. To calculate VSP[84], it is necessary to sum the power demands for a vehicle, given in Equation 2.1. In practice, this is the sum of the power to accelerate the vehicle (P_{accel}), to overcome rolling resistance from the road (P_{roll}), to overcome air resistance (P_{air}), to climb the road gradient (P_{grad}) and to operate auxiliary devices (P_{aux}), accounting for power losses in the transmission through multiplication by an adjustment factor (F_{trans}).

$$P_{total} = \left(P_{accel} + P_{roll} + P_{air} + P_{grad}\right) \times F_{trans} + P_{aux} \tag{2.1}$$

The total vehicle power demand (in Watts) is given by Equation 2.2. The terms used in Equation 2.2 and subsequent equations are defined in Table 2.1.

$$P_{total} = \left[\underbrace{m_{kg} \times a \times 1.04}_{P_{accel}} + \overbrace{R_0 + R_1 \times v}^{P_{roll}} + \underbrace{0.5 \times C_d \times A \times \rho \times v^2}_{P_{air}} + \overbrace{m_{kg} \times g \times Grad}^{P_{grad}} \right] \times \underbrace{1.08}_{F_{trans}} \times v + \overbrace{2500}^{P_{aux}} \tag{2.2}$$

To arrive at Equation 2.2, the following assumptions were made: the power to accelerate rotational accelerated mass is equivalent to 4% of the power for translational accelerated mass; the power losses in the transmission are equal to 8% of the power at the driven wheels; and the power demand of auxiliaries is taken to be a fixed value of 2.5 kW[98,156]. g is taken to be 9.81 m s^{-2} and ρ to be 1.2 kg m^{-3}, the density of air at 20 °C and 1 atm of pressure. To calculate

Term	Definition	Unit
VSP	Vehicle Specific Power	kW t^{-1}
FC_{gx}	Fuel Consumption	g x^{-1} ($x \in \{h, km\}$)
EF_{gx}	Emission Factor	g x^{-1} ($x \in \{kg, s, km\}$)
m_x	Vehicle Mass, including loading	x ($x \in \{kg, t\}$)
a	Vehicle Acceleration	m s^{-2}
v	Vehicle Speed	m s^{-1}
C_d	Aerodynamic Drag Coefficient	–
A	Frontal Surface Area	m^2
ρ	Density of Air	kg m^{-3}
R_0, R_1	Road Load Coefficients	N, N $(m\ s^{-1})^{-1}$
g	Acceleration due to Gravity	m s^{-2}
Grad	Altitude / Distance Travelled	–
r_P	Ratio of Species "P" to CO_2	–
MW_P	Molecular Weight of Species "P"	g mol^{-1}
Q	Exhaust Flow Rate	L s^{-1}
V_m	Molar Volume of Gas	L
n_P	Amount of Gas "P"	mol

Table 2.1: Definitions of terms in Chapter 2, including units.

VSP in kW t^{-1}, Equation 2.2 is divided by mass to arrive at Equation 2.3.

$$VSP = \frac{2500 + \left(R_0 \times v + R_1 \times v^2 + C_d \times A \times 0.5 \times \rho \times v^3\right) \times 1.08}{m_t \times 1000} + v \times 1.08 \times (1.04 \times a + g \times Grad) \tag{2.3}$$

Coefficients R_0, R_1 and C_dA are provided in Table 2.2 on a per-vehicle segment basis, as well as for *average* cars, vans and both cars and vans. These coefficients are average values taken from the test data base used for the Handbook Emission Factors for Road Transport (HBEFA) v3.3. The segmentation

used is that of the European Commission [157], with vehicle segments defined to group vehicles with similar characteristics together and make the analysis tractable. Vehicle segments are each given letters and names, with *A* corresponding to minis, *B* small cars, *C* medium-sized cars, *D* large cars, *E* executive cars, *F* luxury cars and *J* sports utility vehicles. *VanI-III* refer to increasing sizes of van. Segmentation is inexact, being based on factors such as price and accessories as well as vehicle size and shape; in principle, no segmentation is required, but it is especially useful for grouping vehicles with similar drag coefficients, where there is an absence of individual vehicle measured values of C_d.

2.3.2 Modelling Instantaneous Fuel Consumption

The Passenger Car and Heavy Duty Emission Model (PHEM) simulates fuel consumption and emissions from vehicles in any driving situation based on engine maps and vehicle longitudinal dynamics simulation[156]. PHEM is able to model fuel consumption values over a range of driving conditions. For the purposes of estimating the fuel consumption of vehicles measured by remote sensing, it provides relationships between fuel consumption and engine power. This relationship can be normalised by dividing through both variables by vehicle mass, effectively creating a relationship between normalised fuel consumption in (g h^{-1}) t^{-1} and VSP. VSP can therefore be converted to fuel consumption using Equation 2.4, where $\beta_{0,1}$ are the dimensionless parameters of the linear relationship. These parameters are provided in Table 2.2 on a per-vehicle segment basis, as well as for *average* cars, vans and both cars and vans. Specifically, these parameters were determined from characteristic fuel flow curves for different engines calculated using the HBEFA 3.3 test data base and the *Common Artemis Driving Cycle* (CADC)[98,156,158].

$$FC_{gh} = (\beta_1 \times VSP + \beta_0) \times m_t \tag{2.4}$$

	Diesel					Gasoline				
Segment	$\mathbf{R_0}$	$\mathbf{R_1}$	$\mathbf{C_dA}$	β_1	β_0	$\mathbf{R_0}$	$\mathbf{R_1}$	$\mathbf{C_dA}$	β_1	β_0
A+B	120	0.77	0.537	208	159	106	0.67	0.538	236	545
C	151	0.93	0.617	206	217	139	0.85	0.618	225	554
D	166	1.02	0.665	200	208	154	0.94	0.689	219	558
E+F+J	204	1.18	0.915	199	272	175	1.01	0.810	217	601
VanI	122	0.73	0.529	216	92	106	0.67	0.538	236	545
VanII	152	0.89	0.765	217	81	145	0.84	0.853	236	327
VanIII	213	1.24	1.307	220	85	198	1.14	1.158	234	209
Avg Car	157	0.95	0.660	204	221	127	0.78	0.598	229	552
Avg Van	174	1.02	0.965	218	87	114	0.71	0.601	236	501
Avg All	158	0.96	0.690	206	199	127	0.78	0.598	229	550

Table 2.2: Generic coefficients (R_0, R_1, C_dA) and dimensionless parameters ($\beta_{0,1}$) to be used in Equation 2.3 and Equation 2.4. The coefficients are average values taken from the test data base used for the Handbook Emission Factors for Road Transport (HBEFA) v3.3. The parameters were determined from characteristic fuel flow curves for different engines calculated using PHEM, again using the HBEFA 3.3 test data base and the *Common Artemis Driving Cycle* (CADC)[98,156,158].

A consequence of using a linear equation such as Equation 2.4 to model fuel consumption are negative modelled fuel consumption values, which are set to zero. These negative estimates of fuel consumption arise from negative power conditions resulting from the engagement of the mechanical braking system of a vehicle, so have no physical basis[98]. Using Equation 2.5 fuel consumption can be converted from grams per hour driven to grams per kilometre travelled through division by vehicle speed in kilometres per hour.

$$FC_{gkm} = \frac{FC_{gh}}{v \times 3.6} \tag{2.5}$$

Using modelled instantaneous fuel consumption from Equation 2.4 and Equation 2.5–Equation 2.8 allow for the calculation of emission factors by combination with remote sensing data. First, fuel-specific emission factors are calculated using pollutant ratios through Equation 2.6, where P corresponds to the pollutant being measured (NO_x, CO_2, HC, etc.). The denominator of this equation is the sum of all carbon containing exhaust pollutants multiplied by the molecular weight of a generic fuel with the formula CH_2 (MW_{fuel} is therefore 14 g mol^{-1}). r_{HC} is multiplied by six as HC is taken to be C_3H_6 (containing three carbons), and approximately half of HC in exhausts isn't visible to the RSD[80]. A more complete derivation of Equation 2.6 is outlined in Bernard et al. [149].

$$EF_{gkg} = \frac{r_P \times MW_P}{(1 + r_{CO} + 6r_{HC}) \times \left(MW_{fuel}/1000\right)} \tag{2.6}$$

Fuel-specific emission factors from Equation 2.6 can then be combined with the modelled fuel consumption from Equation 2.4 and Equation 2.5 to calculate instantaneous emissions (g s^{-1}) and instantaneous distance-specific emissions (g km^{-1}) using Equation 2.7 and Equation 2.8.

$$EF_{gs} = EF_{gkg} \times \frac{FC_{gh}}{3,600,000} \tag{2.7}$$

$$EF_{gkm} = EF_{gkg} \times \frac{FC_{gkm}}{1000} \tag{2.8}$$

Modelling fuel consumption is not necessary for PEMS data. As PEMS instruments report the flow rate of the exhaust, it is straightforward to calculate emission factors. Equation 2.9 demonstrates a method to calculate instantaneous emissions, and Equation 2.10 a transformation from instantaneous emissions to instantaneous distance-specific emission factors. V_m is taken to be 24.1 L (molar volume at a temperature of 20 °C and pressure of 1 atm).

$$EF_{gs} = \frac{Q}{V_m} \times n_P \times MW_P \tag{2.9}$$

$$EF_{gkm} = \frac{EF_{gs} \times 1000}{v} \tag{2.10}$$

2.3.3 Journey Average Emission Factors

For a vehicle completing a drive cycle of a known distance, the average distance-specific emission factor can be determined from a 1Hz PEMS data set via the sum of all instantaneous emissions divided by the distance covered in the journey in kilometres, shown in Equation 2.11.

$$EF_{gkm} = \frac{\sum EF_{gs}}{total\ distance} \tag{2.11}$$

While Equation 2.8 is a simple way to calculate instantaneous distance-specific (g km^{-1}) emission factors, there are potential issues with these factors being biased due to remote sensing typically measuring vehicles under load. Large parts of journeys taken by vehicles, particularly in urban centres, may involve idling and braking — conditions in which remote sensing is not suited to measure.

To overcome this issue, relationships between instantaneous emissions (g s^{-1}) and VSP may be determined from remote sensing and then, in principle, used to predict emissions over any drive cycle where VSP can be estimated. Generalised Additive Models (GAMs) can be used for this purpose. GAMs offer several advantages in this respect in that they are 'data-driven' and handle non-linear relationships between variables. GAMs relating NO_x g s^{-1} to VSP were fitted using the `gam()` function in the `mgcv` R package[134] using remote sensing data constrained to positive, i.e., non-zero NO_x g s^{-1} values. The default parameters of the `gam()` function were used throughout. In this study the drive cycle used to predict emissions over is taken from a PEMS study, described further in Subsection 2.3.4.

Predicting instantaneous emissions (g s^{-1}) corresponding to VSP values outside of the range of measured VSPs requires extrapolation of the GAM,

which can lead to unreliable predictions. For this reason, GAMs are only fitted using a VSP range between 0 and the 99th percentile of remote sensing VSPs, and then only used to predict over elements of the on-road drive cycle within the same VSP ranges. For elements of the drive cycle above the 99th percentile of the remote sensing data, the emissions and distance covered were disregarded in calculations, effectively truncating the drive cycle as a whole, to ensure a like-for-like comparison. With larger remote sensing data sets that cover a greater range of VSPs, truncating drive cycles should not be necessary.

2.3.4 Portable Emissions Measurement System Data

The UK Department for Transport, prompted by the Volkswagen emissions scandal, started an investigation into commonly used diesel vehicles in 2015[159]. The *Vehicle Emissions Testing Programme* focused on three different types of measurements. First, in-lab testing using variations of the New European Driving Cycle (NEDC). Second, track testing using PEMS instrumentation, attempting to replicate the NEDC as close as possible, and third, on-road testing on a test route approximating the then-not fully defined Real Driving Emissions (RDE) test, including urban, rural and motorway driving. The third data set is used in this study.

After being augmented with the similar *Vehicle Market Surveillance Unit Programme* in 2017, the full PEMS data set contained 19 Euro 5 diesel cars, 17 Euro 6 diesel cars, 14 Euro 6 gasoline cars, 4 Euro 5 diesel vans and a single Euro 6 diesel van, for a total of 55 vehicles in total[160]. Vehicles were tested only once for an average of 95 minutes, with the shortest test being 90 minutes and the longest 106 minutes. The PEMS equipment was validated against a laboratory emissions measurement system. More detailed information about the ways the PEMS tests were conducted is available from the UK Department for Transport and UK Driver Vehicle Standards Agency web pages[159,160].

The effect of applying a time offset to the PEMS data was considered to

check whether any time synchronisation between between variables such as CO_2, NO_x, vehicle speed and acceleration was necessary. A range of time offsets were applied to seek the best agreement between the PEMS CO_2 and that predicted by the developed method. The agreement between PEMS and modelled data was judged using the correlation coefficient, r, and the root mean squared error ($RMSE$); seeking maxima and minima, respectively. Additionally, the application of a rolling mean of 3 to 5 seconds to the data was considered to reduce the effect of any time offsets. However, the best overall agreement was found by not applying time offsets for the data sets considered.

The DfT route can be split into urban, rural and motorway driving by changes in the speed profile of the vehicle as it continues through its journey, mainly changes in maximum speeds and frequency of braking. Each vehicle is driven over a similar trip, so an example for just one is provided in Figure 2.1.

The PEMS data sets already include the majority of required variables for the calculation of instantaneous fuel consumption, but some required additional processing. Vehicle speed was estimated based on the measured distance throughout the test. An on-board GPS provided second-by-second altitude in metres. A cubic smoothing spline was fitted using the default parameters of the `smooth.spline()` function of the R `stats` package[121] to remove noise from the GPS altitude signal, and was divided by the second-to-second difference in distance to derive the road gradient. Acceleration was taken to be the second-by-second difference in the speed of the vehicle. Ratios of pollutants to CO_2 required for Equation 2.6 were calculated using the instantaneous measured concentrations of each in %/ppm.

The PEMS data set provided measurements of carbon monoxide, CO_2, water vapour, NO_x (NO and NO_2), but did not provide measurements for total hydrocarbons. This means that the HC:CO_2 ratio in Equation 2.6 is omitted from the final calculations. This omission is likely to have a negligible effect on calculated emissions for diesel vehicles due to their low emissions of hydrocarbons[17], and studies have shown that even the newest gasoline vehicles emit little HC

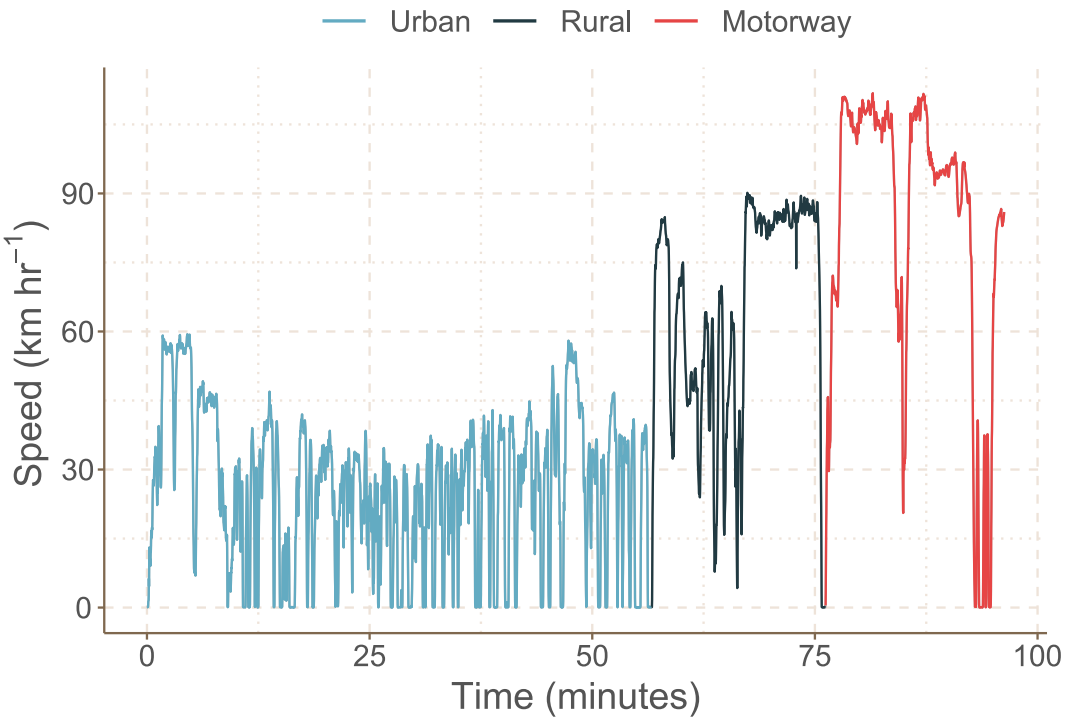

Figure 2.1: The speed profile of one of the passenger cars undergoing the Department for Transport's on-road test. The journey has been partitioned into motorway, urban and rural based on clear changes in the speed profile, including maximum speeds and frequency of braking.

relative to other carbon-containing pollutants[152].

The only variables that could not be estimated from the PEMS data sets were the masses of the vehicles, their vehicle segments and the road load and aerodynamic drag coefficients. Masses and vehicle segments were found using online research tools intended for car buyers, such as the *Parker's Car Guides*, with each mass having 150 kg added to approximate the added weight of the driver and PEMS instrumentation. The coefficients, alongside the $B_{0,1}$ parameters, were taken from the data outlined in Table 2.2 on a per-segment basis.

Two sets of emission factors were then calculated. First, Equation 2.3–Equation 2.8 were applied to the PEMS data set to calculate emission factors through modelling fuel consumption. Second, Equation 2.9 and Equation 2.10

were applied to calculate emission factors including the fuel consumption data contained within the PEMS data set. These two sets of emission factors facilitate comparisons and therefore validations of the fuel consumption model. To do so, GAMs were fitted to create smooth trends in CO_2 emission factors according to both the PEMS and modelled fuel consumption values through both speed and VSP values. Owing to the additional asymptotic effect of low speed values on distance-specific emission factors (i.e., as speed tends towards 0, fuel consumption per unit distance and therefore emissions per unit distance tend towards infinity) very low speeds are filtered out for the distance-specific emissions analysis. In practice this meant that these models used data which corresponded to VSP values of 0 to 30 kW t^{-1} for both GAMs, speeds of 0 to 111 km h^{-1} for the g s^{-1} GAM and speeds of 5 to 111 km h^{-1} for the g km^{-1} GAM.

Equation 2.11 was also applied to each vehicle in the PEMS data set for comparisons with distance-specific emission factors calculated from the remote sensing data set. These g km^{-1} factors were calculated for the journey as a whole as well as the individual urban, rural and motorway components.

2.3.5 Remote Sensing Data

To demonstrate an application of the distance-specific emission factor calculation methods outlined in Equation 2.3–Equation 2.8, remote sensing data were used. The data was acquired using the Fuel Efficiency Automobile Test (FEAT) instrument, the remote sensing (RS) device developed by the University of Denver. Its principles of operation have been described in detail elsewhere[79,145], but a brief overview is provided here.

The FEAT instrument consists of a UV/IR light source and detector for the measurement of exhaust gases, a set of laser-based speed bars for the measurement of speed and acceleration, a camera for photographing number plates, and a control computer. On the curbside is positioned the UV/IR

detector and the detecting speed bar, with the light source and emitting speed bar positioned directly opposite across a single lane carriageway. Pollutants in the exhaust plumes of passing vehicles interact with the collinear beam of IR and UV light produced by the source, permitting the measurement of CO, CO_2, hydrocarbons (HC), SO_2, NH_3, NO, and NO_2. Based on the blocking and unblocking of the two parallel lasers, the speed bars allow for the speed and acceleration of the vehicle to be calculated. Number plate photographs are cross referenced with vehicle databases to obtain further vehicle technical information, in this case obtained from a commercial supplier (CDL Vehicle Information Services Limited)[85].

The remote sensing data set combines data from measurement campaigns in two UK cities, York and London, conducted in 2017 and early 2018, with earlier measurements made in 2012/2013[87,100]. The data set consists of 37,421 measurements of Euro 5 and 6 light duty vehicles. The number of relevant measurements contained within the remote sensing data set are summarised in Table 2.3 alongside some statistical information pertaining to VSP, speed and road gradients.

Equation 2.3–Equation 2.8 were applied to the remote sensing data set to calculate emission factors. As the model is designed to be used with remote sensing data, its application is straightforward as most of the variables are already present in the data set. The mass of vehicles measured using remote sensing is also unknown but is estimated by adding 150 kg to the unladen weight of the vehicle, which is provided in the vehicle technical data.

One omission in the remote sensing data used is a lack of market segment information. The light commercial vehicles can be segmented into VI-III by their weight, but for passenger cars this is not possible. For passenger cars, segmentation was achieved with simple regression tree modelling based on the manually assigned market segments of the vehicles in the PEMS data set. Figure 2.2 shows the distributions of the vehicle frontal surface area (approximated simply through multiplying vehicle height times width) and mass for

Characteristic	Diesel LCV	Diesel PC	Gasoline PC
# Measurements	9,958	16,613	10,732
# Manufacturers	22	41	47
(w/ ≥100 measurements)	11	21	22
VSP (kW/t)	4.46 (5.45)	4.99 (5.93)	5.30 (5.83)
Speed (km/h)	22.25 (15.83)	22.95 (15.70)	21.12 (15.52)
Acceleration (km/h/s)	0.59 (2.09)	0.95 (2.26)	1.15 (2.36)
Gradient (alt/dist)	0.02 (0.01)	0.02 (0.01)	0.02 (0.01)
Euro standard			
Euro 5	8,652 (87%)	12,808 (77%)	7,488 (70%)
Euro 6	1,306 (13%)	3,805 (23%)	3,244 (30%)

Table 2.3: A statistical summary of the vehicle emission remote sensing data, split into diesel light commercial vehicles (LCV) and diesel and gasoline passenger cars (PC). The FEAT data set contains measurements of vehicles with different Euro standard and different vehicle types (e.g., HDVs and hybrid vehicles), which are not used in this study.

each passenger car vehicle segment in the UK Department for Transport PEMS data set. While vehicle dimensions are commonly available in remote sensing data sets, in this case the same online research tools used to find the vehicle segments and masses were used to determine width and height. Also shown is a simple decision tree for the segmentation of vehicles fit using the `rpart` R package, which utilises the *Classification and Regression Trees* (CART) algorithm to fit decision trees[135].

The decision tree presented in Figure 2.2 is based on a relatively small set of vehicles, albeit vehicles chosen for their high market share, so may be further refined by the addition of more vehicle data. However, it does demonstrate that partitioning vehicles into market segments is viable with a relatively simplistic method and, as discussed previously, the availability of aerodynamic drag

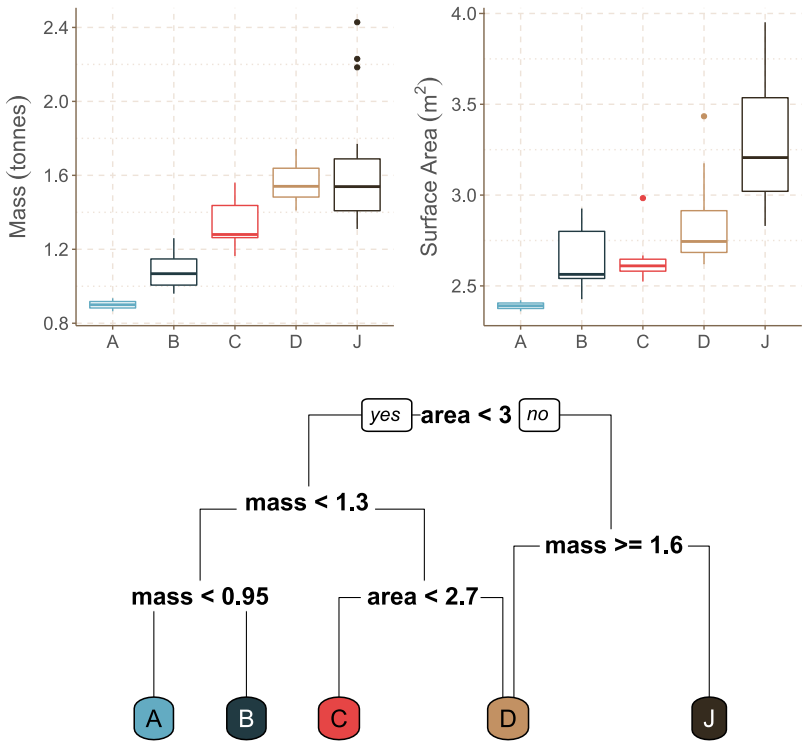

Figure 2.2: Box plots showing the range of surface areas and masses for each passenger car segment present in the UK Department for Transport PEMS data set, with a simple decision tree which could be used for the segmentation of passenger cars based on curb weights (*mass*, in tonnes) and frontal surface areas (*area*, in m^2). Note that there are no E- or F-Segment vehicles in the PEMS data set, reflective of their niche status in the UK fleet.

coefficients for individual vehicles would largely avoid the need to consider vehicle segments anyway.

One of the benefits of using vehicle emissions remote sensing data for estimating aggregate (e.g., Euro standard, fuel type, vehicle model) emissions is that an uncertainty can be calculated. When aggregating the g kg^{-1} emissions derived directly from individual vehicle emission measurements, the 95% confidence interval in the mean can be calculated. To account for the non-normal nature of vehicle emissions distributions, the 95% confidence interval is robustly estimated using bootstrap re-sampling approaches using the `openair` R

package[161]. The calculated uncertainties encompass many sources of variation including the uncertainty of the measurement itself but also issues related to the sampling conditions, such as sample size, ambient conditions and variation in vehicle dynamics remain.

The estimated uncertainties also provide a guide to whether two populations are statistically different from one another. For example, when considering the differences between individual vehicle manufacturer or vehicle models, the uncertainty helps to determine whether there is evidence or not for clear differences in the emission performance of vehicles. Such information is difficult to determine using PEMS as uncertainty information is rarely provided.

Uncertainty estimates can also be derived through GAM models relating the VSP to the emissions of NO_x. In this case, the estimated uncertainty in the GAM itself can be used to express an emissions uncertainty when applied to drive cycles over which predictions are made. The benefit of this approach is that where the original data have poor coverage, e.g., owing to a lack of measurements over high VSP conditions, the corresponding uncertainty estimated as part of the GAM development will also be higher. Consequently, the uncertainty in the prediction of emissions over different drive cycles will reflect the coverage of the original measurement data.

While this analysis does not explicitly include hybrid vehicles, the remote sensing measurements do provide insight into their operation. A vehicle plume is only considered valid if there is a measurement of CO_2. The absence of valid CO_2 plumes provides some indication of whether a hybrid vehicle was using an internal combustion engine or not. The data suggest that for all hybrid passenger cars, 27% of the measurements do not have a valid CO_2 plume, compared with only 2% of conventional vehicle measurements of CO_2. The data suggests that hybrid vehicles operate in battery mode approximately 25% of the time based on the remote sensing measurements. In principle it would be possible therefore to apply the methods developed in this study to a proportion of hybrid vehicle measurements only where there is a valid plume measurement

and assume zero emission otherwise.

2.4 Results and Discussion

2.4.1 Validation with a PEMS Data Set

Vehicle emission factors are typically not expressed at an individual vehicle model level but are aggregated in some way. For example, COPERT's emission factors separate passenger cars by Euro standard, fuel type and broad engine size. For simplicity, the vehicles studied were aggregated into three categories: Euro 5 diesel, Euro 6 diesel and Euro 6 gasoline (there being no Euro 5 gasoline vehicles in the PEMS data set). GAMs of the two sets of emission factors calculated using the PEMS data set are overlaid in Figure 2.3, with the lines labelled "PEMS" showing the factors calculated using Equation 2.9 & Equation 2.10 and "Modelled" showing the factors calculated using modelled fuel consumption detailed in Equation 2.3-Equation 2.8.

CO_2 emissions in g km^{-1} are shown as a speed-emission curve. In general, the emission factors calculated from the modelled fuel consumption data correspond well with those calculated from the PEMS fuel consumption, particularly in the case of the Euro 6 diesel vehicles. When using both curves to predict over a sequence of speeds from 5 to 110 km h^{-1}, the RMSE values between the two sets of predicted values was 28.2 (Euro 5 Diesel), 11.6 (Euro 6 Diesel) and 50.4 (Euro 6 Gasoline). The modelled values in the Euro 5 diesel and Euro 6 gasoline vehicles show some underestimation at lower speeds, though the gap rapidly shrinks and is closed by around 15 km h^{-1} in both cases; indeed the RMSE values drop to 18.5 and 14.3 respectively when only 15 to 110 km h^{-1} values are predicted over. There is slight underestimation at higher speeds seen in the Euro 5 diesel also.

CO_2 emissions in g s^{-1} are shown as a linear power-emission relationship, which demonstrates the overall concurrence between modelled and PEMS

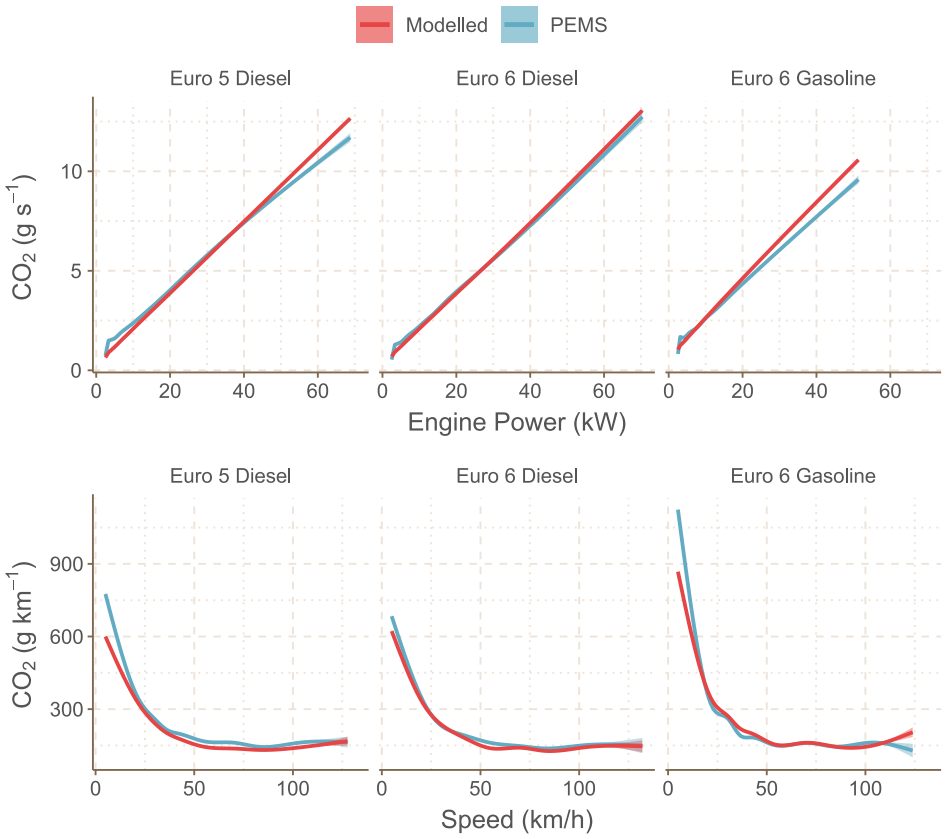

Figure 2.3: Generalised additive models (GAM) of CO_2 emissions (g s^{-1} and g km^{-1}) as functions of both power demand and speed. "PEMS" refers to emission factors calculated using Equation 2.9 & Equation 2.10 and "Modelled" the factors calculated using modelled fuel consumption detailed in Equation 2.3-Equation 2.8. All emission factors were calculated using the UK Department for Transport PEMS data set.

fuel consumption. A shared characteristic in all three of these curves is some deviation between the methods at higher engine powers, around 40 kW. There are fewer data at higher engine powers in the PEMS data set which may explain this observation. The curves were used to predict a sequence of engine powers from 1 to 70 kW (diesel vehicles) and from 1 to 50 kW (gasoline), giving RMSE values of 0.293 (Euro 5 Diesel), 0.579 (Euro 6 Diesel) and 0.514 (Euro 6 Gasoline).

2.4.2 Model Sensitivity

In practice, the application of the methods outlined in Subsection 2.3.1 and Subsection 2.3.2 depend on several assumptions concerning the vehicles measured using remote sensing. There are variables needed by the model for which direct measurements are not available. The mass of an unladen vehicle is obtainable from vehicle databases, but the true laden mass of a vehicle is unknown and will depend on factors such as number of passengers and cargo. The auxiliary power component is entirely estimated. While vehicle and acceleration can be measured accurately with speed bars, there will be some uncertainty over the location that is best suited to make the measurements[82,84].

To examine the sensitivity in emission factors related to the uncertainty in individual model parameters, a single vehicle was taken from the UK Department for Transport PEMS data set. A single vehicle was judged to be sufficient for this analysis as it is expected that the sensitivity of the model will be roughly consistent regardless of the vehicle to which it is being applied. The chosen vehicle was a D-Segment Euro 6 diesel passenger car, chosen for having a very good agreement between measured and modelled journey average CO_2 g km^{-1} values (calculated using Equation 2.11). The model outlined in Equation 2.3–Equation 2.7 was applied to this vehicle repeatedly to produce 1 Hz CO_2 instantaneous (g s^{-1}) emissions, with variations in the following parameters: C_dA, R_0/R_1, auxiliary power, acceleration, speed, road gradient and mass. C_dA, R_0 and R_1 were changed by ± 10%, acceleration by ± 5%, gradient by ± 20% and speed by ± 2 km h^{-1}. The range in mass is the curb weight (lower) to the curb weight plus 400 kg (higher). The range in P_{aux} is 250 W (lower) to 3 kW (higher). The impact on journey average CO_2 g km^{-1} values for the vehicle is visualised in Figure 2.4.

Auxiliary power has been shown to vary considerably in on-road driving[162]. The range of auxiliary powers investigated here (0.25 to 3 kW) induces a large change in estimated emissions of CO_2, particularly in urban driving. This

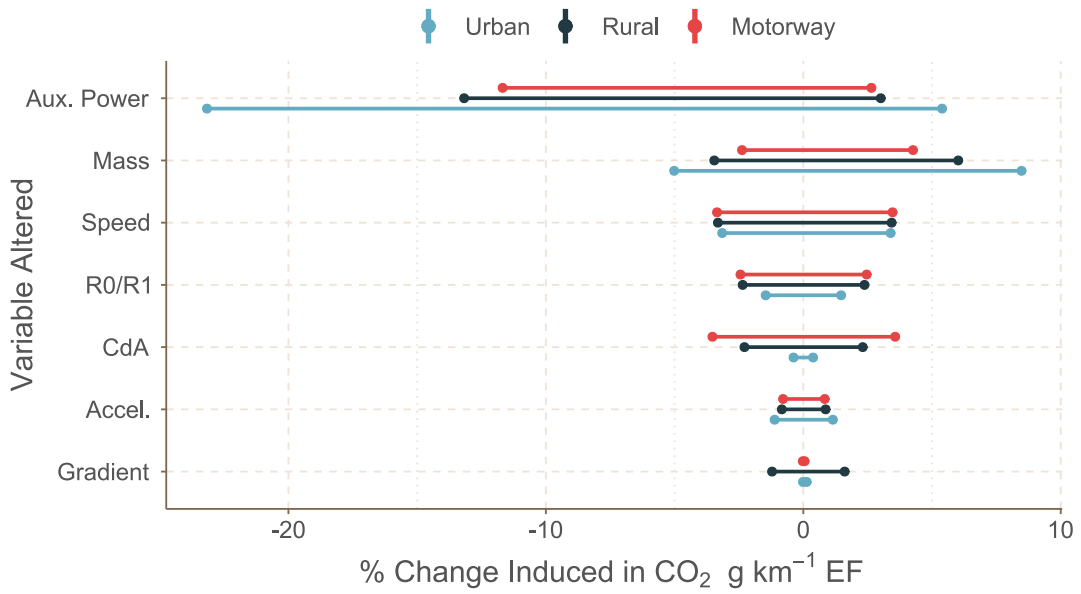

Figure 2.4: The percentage uncertainty in the D-Segment Euro 6 diesel passenger car CO_2 g km^{-1} induced by changes in model parameters. Percentage changes are relative to the base case, defined as the g km^{-1} factor determined using correct generic parameters for a D-segment diesel vehicle, unaltered speed, acceleration and gradient, curb weight plus 150 kg, and a P_{aux} of 2.5 kW.

behaviour is expected for urban driving conditions where there is a greater proportion of driving in lower power conditions, meaning that the auxiliary power accounts for a greater proportion of the total power consumption of the engine.

Uncertainty in vehicle mass also has a greater effect under urban driving conditions, which can be understood by the greater amount of acceleration and deceleration in urban driving. The opposite trend is seen in the air resistance parameter (C_d), with very little change observed in urban driving conditions. This behaviour is expected owing to the lower vehicle speeds under urban driving conditions, with P_{air} being proportional to the cube of vehicle speed. A similar but less extreme trend is seen for R_0/R_1.

A different trend is seen when varying the road gradient — little change is seen in both urban and motorway conditions, but a large effect is seen in hillier

rural driving. The overall influence of gradient uncertainty in this analysis is relatively small compared to other parameters, but it would likely be greater and therefore more important for vehicle emission measurements taken in hillier regions.

Focusing on urban-type driving conditions — where vehicle emissions remote sensing measurements are most commonly made — the variables to which estimated CO_2 emissions are most sensitive are seen to be vehicle mass, speed, acceleration, and auxiliary power demand.

An alternative way to consider uncertainty rather than the uncertainty of individual parameters is the misattribution of vehicle segments. Assuming inaccessibility of market segment information and the use of a decision tree similar to that which is described in Subsection 2.3.5, there will be unavoidable misattribution for vehicles that are uncharacteristically heavy or light for their market segment, or have an atypical frontal area. On an aggregate level this is not be a cause for concern; conversely this may be of benefit — an atypically shaped vehicle's 'true' C_dA, R_0 and R_1 values may be closer to those given for the segment to which it has been incorrectly assigned.

Table 2.4 summarises the effect of both misattributing the segments and applying the 'average car' parameters to the D-Segment vehicle. The greatest absolute difference, an increase of 22 g km^{-1}, is seen when attributing the vehicle an E-, F- or J-Segment, effectively assigning it the characteristics of a larger executive, luxury or sports utility vehicle. The second greatest absolute difference is a decrease of 12 g km^{-1} owing to an A-Segment assignment, assigning the D-Segment vehicle the characteristics of a mini car.

2.4.3 Method Application to Remote Sensing Data

The model was used used to estimate instantaneous emissions using remote sensing data, which were then directly compared with those of the PEMS data set. Figure 2.5 illustrates that similar relationships between instantaneous NO_x

	Journey Average CO_2 (g km^{-1})		
Attributed Segment	**Emission Factor**	**Absolute Difference**	**Percentage Change**
A/B	123	-12	-8.9%
C	136	+1	+0.7%
D	**135**	–	–
E/F/J	157	+22	+16.3%
Average Car	136	+1	+0.7%

Table 2.4: Journey average CO_2 g km^{-1} values for a chosen Euro 6 diesel D-Segment passenger car depending on Euro Segment attribution, including deviation from the correct D-Segment attribution.

emissions and VSP are seen in both remote sensing and PEMS, for example both showing similarly increasing NO_x emissions with engine load.

Figure 2.6 shows journey average distance-specific emission factors from remote sensing calculated using the GAM fitting methods outlined in Subsection 2.3.3, and journey average distance-specific emission factors calculated using PEMS data. To ensure a fair comparison, only vehicles present in both the PEMS and remote sensing data sets were used in GAM fitting (43 vehicles — 14 Euro 5 diesel cars, 11 Euro 6 diesel cars, 12 Euro 6 gasoline cars, and 4 Euro 5 diesel vans). This corresponds to 7939 remote sensing measurements. For this purpose, a 'vehicle' is defined by its make, engine size, fuel type, Euro standard and type approval category. Note that, for fairer comparison, the PEMS data set was constrained to the same VSP range over which the GAMs were fitted.

Overall, there is good agreement between the emission factors from PEMS and remote sensing for the passenger cars. The error bars showing 95% confidence intervals overlap for all passenger car columns in Figure 2.6. There is a much larger disparity seen in the emissions of the vans, particularly in urban driving. This disparity may be a consequence of having relatively few vans

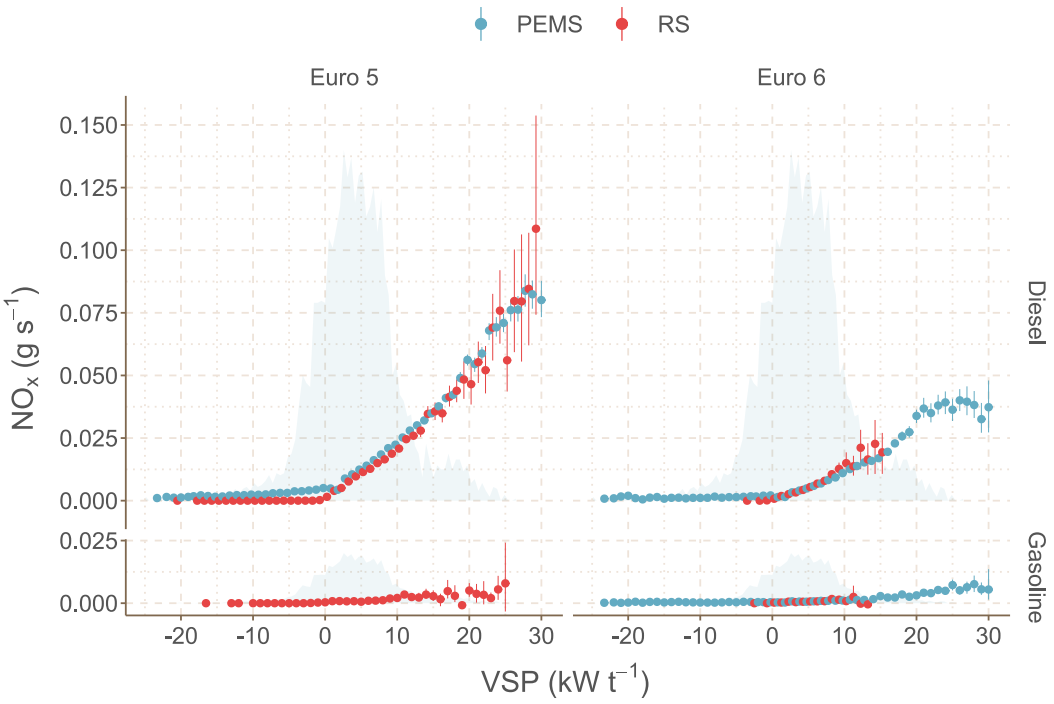

Figure 2.5: Trends in NO_x emissions as a function of vehicle specific power taken from the whole PEMS and RS data sets. The emissions from PEMS are calculated from 1 Hz measurements, and those from RS are taken from individual snapshot measurements. A normalised VSP density of a VSP-based Urban-Rural RDE drive cycle is shown in light blue, used later in Figure 2.8.

in the PEMS data set, as well as vans likely being heavier (owing to carrying cargo) in real-world use as opposed to the PEMS RDE test. There are instances in which the relative order of the driving conditions differs also — in Euro 6 diesel cars, for example, remote sensing suggests that motorway driving has the lowest emission factor whereas PEMS suggests that it is rural driving.

Journey average NO_x g km^{-1} values can also be calculated for *individual* vehicle models, shown in Figure 2.7. In this instance only urban and rural driving conditions were considered — i.e., similar conditions to those experienced for the remote sensing measurements. A lack of motorway measurements is a weakness of cross-road remote sensing as a method, although the top-down Emission Detection And Reporting system (EDAR) shows promise for use in

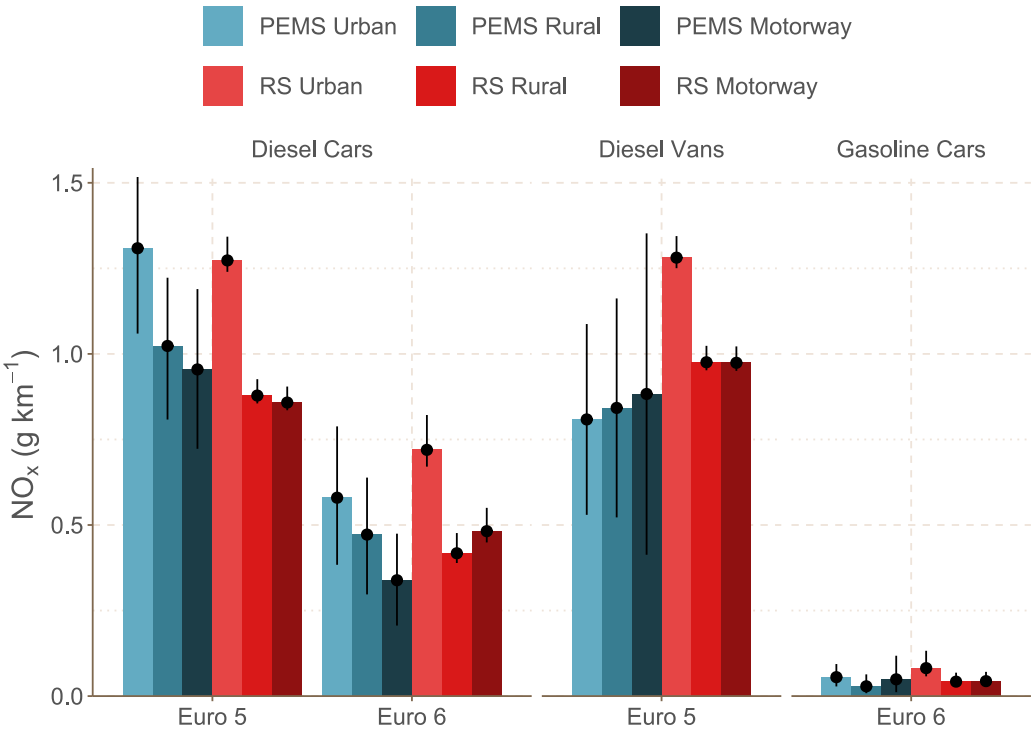

Figure 2.6: Journey average NO_x distance-specific emissions for different categories of vehicle. The RS factors are taken from the predictions of GAMs relating instantaneous NO_x emissions to VSP over a real driving emissions (RDE) drive cycle. The PEMS factors are the mean journey average distance-specific emission factors from all vehicles in each of the given categories. Error bars show the 95% confidence interval.

motorway conditions[77,78]. Of the diesel vehicles, the root mean square error (RMSE) between the PEMS and remote sensing (RS) emission factors varies from 0.230 (Euro 6 cars) to 0.616 (Euro 5 vans). A low RMSE is not necessarily expected; each RS emission factor reflects over a hundred individual vehicles whereas the PEMS data represents *single* vehicle measurements over a single drive cycle. Other work has shown significant variance in PEMS emission measurements for single vehicles tested multiple times, partly due to variance in testing conditions and procedures[163].

A strength of remote sensing is its ability to measure large numbers of vehicles non-obtrusively in a short space of time. In practice this means that

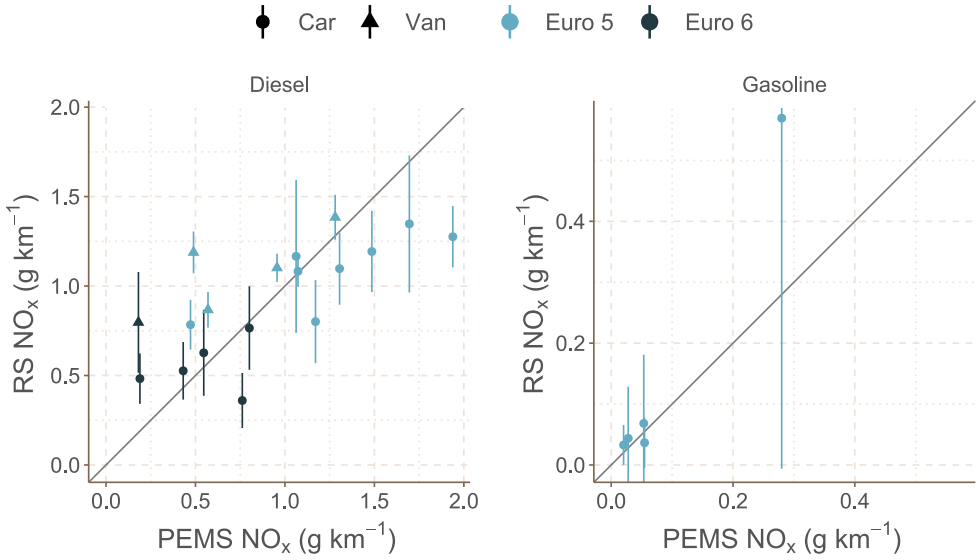

Figure 2.7: A comparison between journey average NO_x emissions calculated from RS and PEMS data. Each point represents a unique manufacturer–engine size combination with at least 100 measurements in the RS data set. The solid grey line shows the 1:1 relationship. The RS factors are taken from the predictions of GAMs relating instantaneous NO_x emissions to VSP over an urban-rural real driving emissions (RDE) drive cycle. The PEMS factors are the emission factors for the corresponding vehicle. The error bars show the 95% confidence interval of the mean for the RS emission predictions.

even in a relatively modest remote sensing data set there is likely a sufficient range of measurements over a large enough range of VSPs for GAMs to be fitted on an individual manufacturer or vehicle basis. Figure 2.8 shows urban-rural journey average distance-specific emissions from the remote sensing data set for individual vehicles, with a vehicle defined in the same way as in Figure 2.6 and Figure 2.7. Only vehicles with at least 100 measurements were used to ensure sufficient data to fit a GAM predicting NO_x emissions using VSP.

Figure 2.8 demonstrates the wide variation in individual vehicle emissions even within a single Euro standard. In the Euro 5 diesel cars category, for example, the cleanest vehicle is associated with a 0.55 g km^{-1} emission, 0.79 g km^{-1} lower than the highest at 1.34 g km^{-1}. Similarly for the Diesel Euro

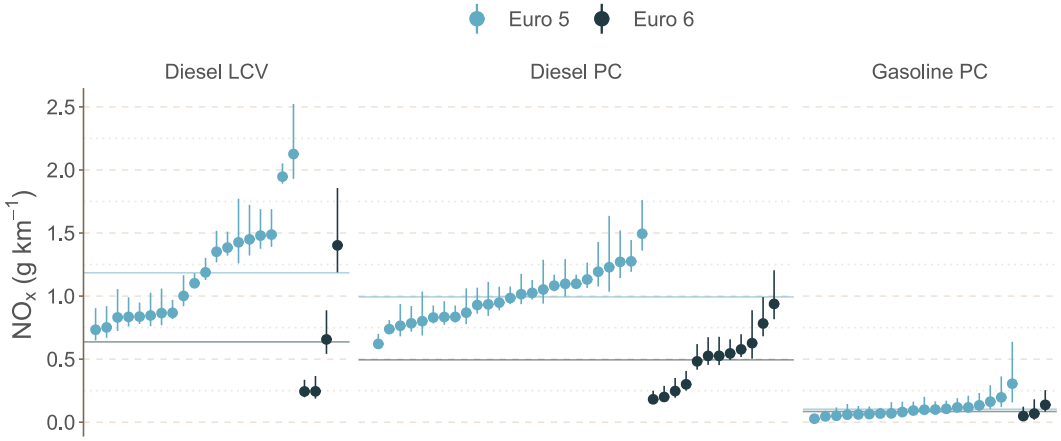

Figure 2.8: Distance-specific emissions for different vehicles calculated from RS data and an urban-rural on-road RDE drive cycle. Vehicles have been anonymised, but each is taken to be a unique manufacturer-engine size combination with at least 100 measurements. Error bars show the 95% confidence interval. Blue dashed lines show the mean emission in each vehicle category.

6 Cars category, the cleanest vehicle is at 0.17 g km^{-1} and the highest at 0.80 g km^{-1}, a range of 0.63 g km^{-1}. The vans show similar variation, both for Euro 5 (0.69–1.93 g km^{-1}) and Euro 6 (0.23–1.32 g km^{-1}). The variation shown in NO_x emissions provides an indication of the extent to which emissions could be reduced if "best-in-class" emissions performance was achieved. Furthermore, the differences observed between vehicle manufacturers provides information that is useful for understanding the expected variation in NO_x emissions resulting from different vehicle fleet compositions.

2.5 Conclusion

Remote sensing data offers large data sets of road vehicle emission measurements with good fleet coverage and little selection bias. However, without a measurement of instantaneous fuel consumption it is difficult to transform fuel-specific to distance-specific emission factors. As the vehicle type approval

process and emission inventory development both rely on distance-specific emission factors, this difficulty presents a limitation for the use of remote sensing data. Furthermore, comparisons with other commonly used road transport emission measurement techniques (chassis dynamometers, PEMS, etc.) are more limited without expressing emissions in this way.

A method to model fuel consumption from curbside measurements and vehicle technical data was developed, and is sufficiently general to be applied to any emission species measured using remote sensing and indeed any point-sampling measurement method that provides a pollutant to CO_2 ratio. In the current work, a relatively modest data set of remote sensing data was used to develop and demonstrate the method. However, there has been a considerable increase in the number of vehicle emission remote sensing data campaigns in recent years[78,164,165]. Large databases such as these would enable the methods outlined in this study to be used to calculate distance-specific emissions for a large range of vehicle models and driving conditions.

Arguably the main benefit of the approach is that it can in principle be applied to any vehicle drive cycle. This development is of importance for the analysis of vehicle emission remote sensing data where measurements tend to be made of vehicles mostly (but not always) under load. The potential to re-calculate emissions for more representative full drive cycles therefore addresses the potential issue of remote sensing site selection bias, where measured emissions would on average be higher than a typical full drive cycle. Indeed, with the increasing amounts of drive cycle data available, there is the potential to apply the method to large databases of actual vehicle activity over a large range of conditions. This is demonstrated in Chapter 3.

A common shortcoming of current remote sensing data sets is a lack of measurements under high speed and VSP conditions — particularly motorways. In this study, comparisons between remote sensing and PEMS distance-specific emissions were primarily carried out using urban and rural driving conditions to reflect this. This is not to say that motorway conditions cannot be modelled

using remote sensing (they are in Chapter 4), but the modelling must be done with an appreciation that the potentially unique behaviour of emissions under these conditions may not be captured (owing to, for example, the behaviour of after-treatment technologies under sustained high-speed driving). Regardless, as remote technology advances and motorway measurements become simpler and safer to make, this issue will be minimised.

Package Development

The methods outlined in this chapter were developed into an R package for expedient use. A brief overview of the package is provided in Appendix A.

Chapter 3

Influences on Local-scale Emissions from a Comprehensive Driving Database

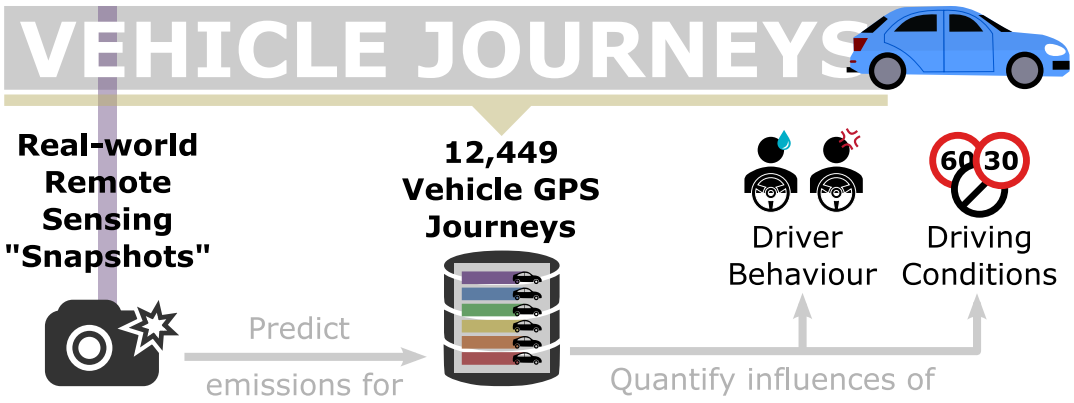

3.1 Abstract

While vehicle emission remote sensing can rapidly measure many different vehicles, it is limited in its journey coverage due to only measuring instantaneous, "snapshot" measurements of each vehicle. Journey-wide influences on emissions — for example, congestion or driver behaviour — are typically more easily studied using on-board measurement techniques which can capture a vehicle's whole journey. Through modelling the fuel consumption of passing vehicles, instantaneous emissions can be calculated and used to predict over any driving data for which GPS coordinates are available. In this study, this approach is demonstrated by modelling Euro 5 diesel passenger car NO_x emissions over a large database of over 100 days of continuous driving under different speed limits and undertaken by 79 different drivers. This substantial amount of modelled emission data is then used to reproduce COPERT-style NO_x speed-emission curves which are found to be consistently higher than the COPERT v5.5 equivalents regardless of driving condition, with an average underestimation of 0.21 g km^{-1}. Furthermore, the distributions of distance-specific emissions from different drivers is used to suggest a roughly ±22% relative percentage range owing to driver behaviour. While potentially important, comparisons with previous analysis suggest this is secondary to the distribution of emissions owing to different vehicle manufacturers. Overall, this study demonstrates the potential for remote sensing to comment on local-scale emissions, and to both quantify and rank the importance of real-world emission influences.

3.2 Introduction

Accurately estimating the emissions from road transport is challenging, yet it is a key step in introducing constructive air quality policy, developing effective vehicle technologies, and calculating accurate emissions inventories. To estimate emissions accurately, representative data of real-world driving is needed to both reflect the true emissions of vehicles in the environments in which they actually drive, and to understand real-world influences on emissions that cannot be easily recreated in laboratories such as ambient conditions[110,166–168], mileage- or age-based deterioration[104,105,169–171], and driver behaviour.

Driver behaviour is particularly difficult to measure. In-lab measurements will typically use consistent drive cycles (e.g., the New European Driving Cycle, or the Worldwide Harmonised Light Vehicles Test Procedure) which intrinsically do not address variations in driver behaviour. "On-road" measurements such as those taken using Portable Emissions Measurement Systems (PEMS) are more appropriate, however given their cost and time requirements it would be prohibitively expensive and time consuming to establish a true distribution of the behaviour of different drivers under different conditions. Furthermore, driver behaviour is difficult to isolate from uncontrollable factors like congestion, causing issues with repeatability outside of simulated drives. Regardless of the complexity of quantifying driver behaviour, it is still a useful thing to understand. If variations in driver behaviour are significant, "eco-driving" training or on-board behaviour monitoring tools could make for a cheaper, easier solution to air quality problems than relying on future advancements in engine and after-treatment technologies[172–174].

The literature includes several attempts to quantify driver behaviour and its influence on emissions, commonly focused on modelled emissions over measured journeys. For example, Zheng et al. [175] combines modelled emissions with survey data which was used to categorise drivers into one of four categories (aggressive, conservative, confident, and experienced; conservative

and confident drivers were the lowest emitters). Xu et al. [176] used machine learning on modelled emission data to show that extended idling, driver age, and route familiarity were key predictors for CO_2 and PM emissions. Huang et al. [177] used measured data from PEMS with two groups of drivers — "novice" and "experienced" drivers — and finds no significant difference in NO_x or PM emissions between them, though a large distribution *within* each group.

Vehicle emission remote sensing measurements are often referred to as "snapshots" of many vehicles' individual journeys. This is in contrast to techniques such as PEMS, which are effectively measurements of relatively very few vehicles' entire journeys. This makes remote sensing particularly useful for measuring in-use vehicles in a given fleet, monitoring trends in fleet composition and emissions, and studying influences on emissions that can be captured from single roadside measurements (e.g., differences between manufacturers, engine sizes, ambient conditions, etc.). The instantaneous measurements from remote sensing are not as useful to understand how emissions are influenced by different features of a vehicle's whole journey, such as the the aforementioned influence of driver behaviour.

In this study, NO_x emissions are modelled over a large data base of real driving data obtained through the use of GPS using the methodology described in Chapter 2/Davison et al. [1]. The driving data contains approximately 119 continuous days of driving and is conducted by 79 different drivers, and is therefore considerably larger than the driving data obtained from PEMS data sets used previously. Indeed, the greater purpose of this chapter is to demonstrate that the methods in Chapter 2 aren't limited to standard "real-driving emissions" drive cycles but can instead estimate emissions over drives of effectively any length — from small urban "links" of a few hundred metres to long motorway journeys of hundreds of kilometres. The synthesis of tens of thousands of remote sensing observations (effectively capturing the distribution of emissions across the vehicle fleet) and months of driving data (capturing all common driving conditions) allows for an unprecedentedly comprehensive

assessment of vehicle emissions, more comprehensive that could be achieved though any individual measurement technique — including remote sensing alone.

The specific research aims of this study is to use remote sensing to examine local-scale emissions on a sub-national scale, bridging the gap between the individual vehicle measurements remote sensing is known for and the national-scale emission inventory estimates which will be addressed in Chapter 4. An interesting feature of the driving data is the inclusion of speed limit data, which permits a more granular examination of the typical speed-emission curves employed by systems like COPERT (COmputer Programme to calculate Emissions from Road Transport)[40,44]. Furthermore, the vast numbers of drivers included in the driving data allows for remote sensing to be in a unique position to comment on driver behaviour and attempt to quantify the distribution in real-world NO_x emissions it can induce. Neither of these factors are typically considered in emission factor calculation or inventory development, but using comprehensive modelled emissions data could provide evidence as to whether they have significant effects.

3.3 Materials and Methods

3.3.1 Data Sets

Two key data sets form the bulk of the analysis; an instrumented vehicle data set of driving conditions, and a remote sensing data set of real-world emission measurements. This section describes both data sets, with their use described in Subsection 3.3.2.

The instrumented vehicle data set contains 10,255,088 seconds (approximately 119 continuous days) of driving across 12,449 individual journeys carried out by 79 different drivers over 5 investigation periods between 2003 and 2007. Drivers were based in Leeds and Sheffield in the United Kingdom

and journeyed predominately within, around and between these two cities. The data were originally collected as part of the UK External Vehicle Speed Control (EVSC) project, which reviewed the possible introduction of intelligent speed adaptation technology in the UK. A more thorough description of EVSC and the data set is provided in Carsten and Tate [178].

An important feature of this data set is the inclusion of the speed limit in which the vehicle is driving. This is a more granular and objective way to discuss driving conditions than a typical urban/rural/motorway split. 20 and 30 mph roads can safely be considered "urban" driving through cities and towns, with 20 mph zones usually reserved for areas with vulnerable pedestrians or road users (commonly outside of schools and nurseries). 70 mph is the UK national speed limit for cars on dual carriageways and motorways, so can be considereFd "motorway"-style driving. 60 mph is the UK national speed limit for cars on single carriageways so it, along with 50 mph limits, is often found on open "rural" roads. 40 mph limits are more ambiguous but commonly represent "out of town" roads that lead into towns or cities, or slower-moving rural roads.

A vehicle specific power-emission model was fit using 61,887 valid remote sensing NO_x observations of Euro 5 diesel passenger cars obtained using the OPUS RSD 5000 (n = 46,559, 75%) and Denver FEAT instrument (n = 15,328, 25%). Vehicle technical information such as type approval categories, fuel types and vehicle types were obtained from the commercial supplier CDL Vehicle Information Services Ltd.[85]. Diesel vehicles were selected for this study due to their great impact on air quality, and Euro 5 vehicles were selected due to being the most common Euro standard observed in the remote sensing database (Chapter 4, Davison et al. [2]). Euro 5 diesel passenger cars in the remote sensing data set represent 21 different manufacturer groups (16 of which feature 100 observations or greater), and collectively had a mean VSP of 7.26 kW t^{-1}, speed of 22.9 mph, and acceleration of 0.68 mph s^{-1}. The mean cumulative mileage for these vehicles was 111,716 km, based on data from annual MOT tests made available by CDL. Measurements were taken at 37 sites

across 14 regions in the UK, with a mean ambient temperature of 15.6 °C.

At time of writing, the instrumented vehicle data set is over a decade old and it is likely that the capabilities of vehicles and design of roads have since changed. Furthermore, the dates of the instrumented vehicle data (2003–2007) do not overlap with those of the remote sensing data or even Euro 5 legislation, which came into effect in 2009. While a more recent driving data set would be preferable, no recent data similar in scope and size is available. In addition, it is not expected that the key aims of this study — the comparisons with COPERT and the examination of driver behaviour — will necessarily be impacted by the use of older data. Emissions are considered on a bulk level and always in reference to their relationship with engine power, and not on a fine spatial scale with reference to individual roads or specific journeys which may have considerably changed over the last 15 years.

For comparisons with in-use emission factors, COPERT v5.5 speed-emission curves were obtained from Ntziachristos and Samaras [45]. The COPERT curves are calculated using Equation 3.1, where EF is some emission factor, v is a vehicle's speed, α through η are dimensionless constants, and RF is a reduction factor. For many diesel passenger cars, RF is equal to 0. COPERT v5.4 introduced a separate category with an RF value of 0.3 for Volkswagen vehicles that received a software update post-"dieselgate". This 30% reduction factor is consistent with evidence from remote sensing, which suggests a 30–36% reduction factor depending on whether just software or hardware *and* software had been updated[101].

$$EF = \frac{\alpha v^2 + \beta v + \gamma + \frac{\delta}{v}}{\varepsilon v^2 + \zeta v + \eta} \times (1 - RF) \tag{3.1}$$

3.3.2 Data Processing

To model the emissions of the journeys in the instrumented vehicle data set, the whole data set needed to be converted into a vehicle specific power-based

drive cycle. To do so, the methods outlined in Chapter 2 were used, which have been reproduced as Equation 3.2–Equation 3.7.

$$VSP = \frac{2500 + \left(R_0 \times v + R_1 \times v^2 + C_d \times A \times 0.5 \times \rho \times v^3\right) \times 1.08}{m \times 1000} + v \times 1.08 \times (1.04 \times a + g \times Grad) \tag{3.2}$$

$$FC_{gh} = (\beta_1 \times VSP + \beta_0) \times m \tag{3.3}$$

$$EF_{gs} = EF_{gkg} \times \frac{FC_{gh}}{3,600,000} \tag{3.4}$$

$$EF_{gs} = f(VSP) \tag{3.5}$$

$$EF_{gkm-inst} = \frac{EF_{gs}}{v_{ms} \,/\, 1000} \tag{3.6}$$

$$EF_{gkm-avg} = \frac{\sum EF_{gs}}{total\ distance} \tag{3.7}$$

To calculate VSP from the data set required several intermediate steps. First, the second-by-second change in each vehicle's speed was taken to be its acceleration. Then, a smooth spline was fit to the elevation of each journey to remove GPS noise, and the second-by-second change in that elevation was taken to be the road slope. VSP was modelled to represent a 'generic' car, using the following values taken from Chapter 2/Davison et al. [1]: $R_0 = 157$, $R_1 = 0.95$, $C_dA = 0.660$, $\beta_0 = 221$, $\beta_1 = 204$. The vehicle mass, m, was taken to the average weight of a passenger car in the remote sensing data set, 1.4 tonnes, plus an additional 0.15 kg to estimate the weight of passengers and cargo. Equation 3.2 could then be used to calculate VSP.

VSP, fuel consumption (FC_{gh}) and instantaneous emissions (EF_{gs}) were calculated using the Euro 5 diesel remote sensing data set using Equation 3.2–Equation 3.4. A generalised additive model (GAM) was fit to determine the relationship between instantaneous NO_x emissions and VSP (Equation 3.5), with analysis of variance (ANOVA) testing showed that VSP was a significant predictor ($P < .05$). The fitted GAM was then used to predict NO_x emissions over the vehicle journeys.

Instantaneous distance-specific (g km^{-1}) emissions were calculated through division by instantaneous vehicle speed (Equation 3.6). These are useful when plotting speed-emission curves in Subsection 3.4.2, which are compared to COPERT speed-emission curves from Ntziachristos and Samaras [45]. Murrells and Rose [179] employed 6^{th} order polynomial equations to fit speed-emission curves, shown in Equation 3.8 where EF is some emission factor, v is a vehicle's speed, and a through g are dimensionless constants. This approach is recreated in this analysis.

$$EF = \frac{a + bv + cv^2 + dv^3 + ev^4 + fv^5 + gv^6}{v} \tag{3.8}$$

Journey-average distance-specific emissions were calculated by summing the instantaneous emissions for a given journey and dividing by the total distance travelled in that journey (Equation 3.7). To fairly compare the emissions from individual drivers, journeys were divided into sub-journeys based on speed limit zones. A sub-journey is classed as a period of time wherein a vehicle was under a single speed limit for any amount of time. For example, an overall journey may have started in an urban centre (30 mph limit), progressed onto a motorway (70 mph) and then returned to urban driving (back to 30 mph). This journey would have been split into 3 sub-journeys. Having access to speed limit-based sub journeys allows for journey-average distance-specific emissions to be calculated for individual speed limits.

3.4 Results and Discussion

3.4.1 Exploratory Speed Limit Analysis

Figure 3.1 visualises the proportions of different speed limits in the data set.

A slight majority (51%) of the driving was under a 30 mph speed limit, which can be assumed to reflect urban driving. The remaining speed limits in the data set, in descending order of frequency, are 40, 70, 60, 50 and finally 20

mph. 20 mph limits can be considered a niche in the overall data set, although still represent a total of approximately 16 continuous hours of driving. For comparison, the data for 30 mph limits represent 61 continuous *days*.

Taking only the driving in which the signposted speed limit was broken shows an increase in the proportion of 20, 30 and 70 mph, indicating that the majority of speeding appears to occur under urban and motorway conditions. Indeed, when considering the proportion of driving under each of these limits, 25.1% of driving done in 20 mph zones was over the signposted limit, 21.2% in 30 mph zones, and 31.0% in 70 mph zones. This percentage in 40, 50, and 60 mph zones was 17.6%, 15.8% and 5.2%, respectively.

Despite representing 51% of driving and 54% of speeding in the data set, 30 mph limits only account for 36% of instantaneous modelled NO_x emissions. This is still a plurality, with 70 mph limits accounting for 30% of NO_x emissions, 40 and 60 mph accounting for 14% each, 50 mph 5% and 20 mph the remainder ($< 1\%$). This owes to the power-NO_x relationship used to determine emissions; the median (and interquartile range) of VSP is 2.12 (0.53–6.17) kW t^{-1} in the 30 mph zones and 11.62 (5.09–17.02) kW t^{-1} in the 70 mph zones.

All of vehicle speed, VSP and instantaneous NO_x follow a similar pattern, their median values increasing with the speed limit. Instantaneous distance-specific NO_x shows a different trend, however, decreasing from a median value of 0.91 g km^{-1} of NO_x at 20 mph to 0.53 g km^{-1} at 60 mph, before increasing to 0.70 g km^{-1} at 70 mph.

3.4.2 Speed-Emission Curves

Speed-emission curves are often used for emission factor development, visualising the trend of distance-specific emissions as a function of vehicle speed. These commonly possess a "U"-shaped appearance, with emissions being lowest at middling speeds, higher at high speeds, and highest at low speeds — in part owing to the asymptotic effect of distance-specific emissions approaching

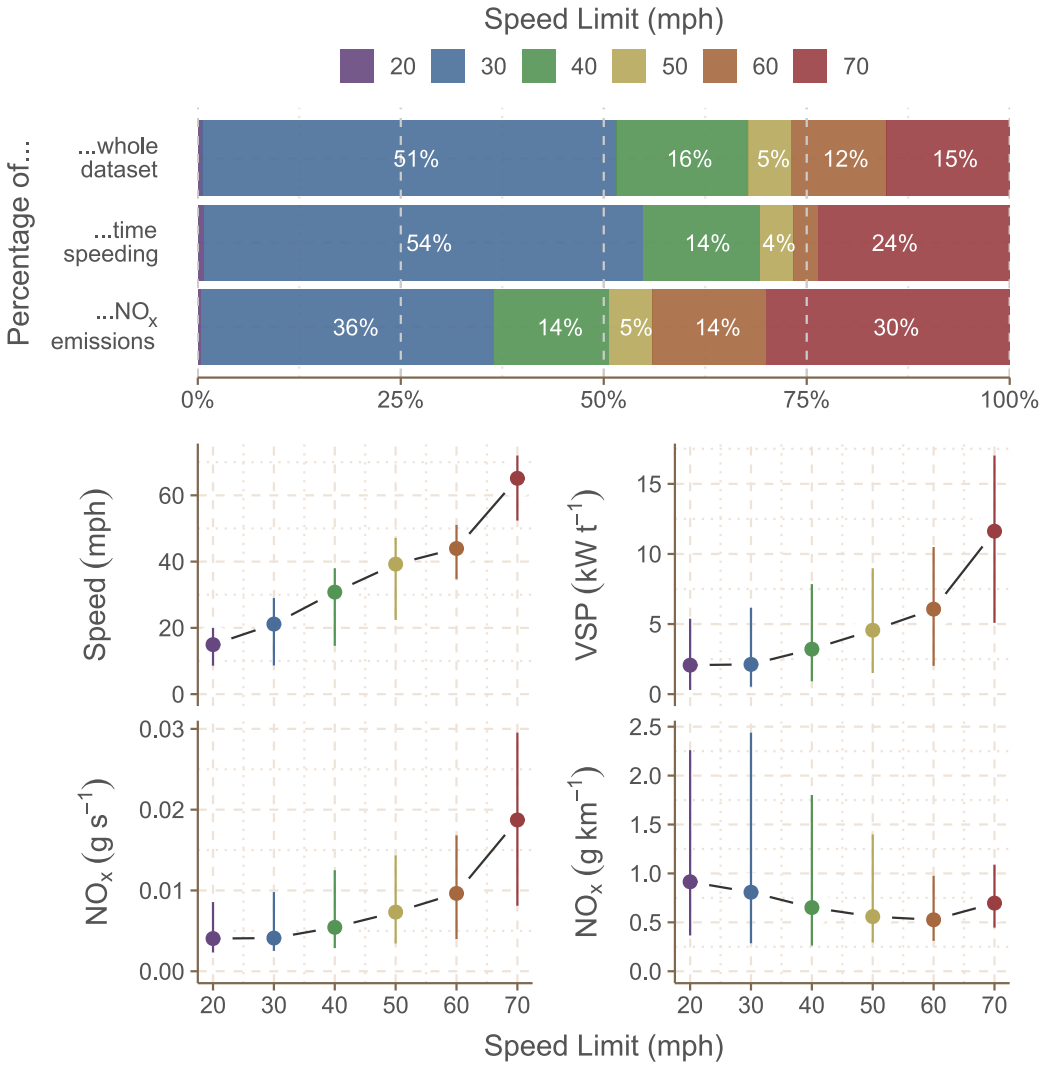

Figure 3.1: Exploratory speed limit analysis. **Top:** *a)*, the frequency of each speed limit in the data set, *b)*, the frequency of each speed limit when the vehicles were speeding, and *c)*, the proportion of NO_x each speed limit contributed to the overall sum of instantaneous NO_x emissions. 20 mph driving contributed < 1% to each total. **Bottom:** The median and interquartile range of vehicle speed, VSP, instantaneous NO_x and instantaneous distance-specific NO_x.

infinity as vehicle speed approaches zero.

There are several potential weaknesses of speed-emission curves that are worthy of examination, one being that the aforementioned asymptotic effect means that very low speed driving is often omitted from the curves. The key weakness, however, is that a vehicle's speed does not completely capture the demand on its engine. For example, a vehicle going 30 mph in an urban setting is driving unimpeded, likely neither accelerating nor decelerating and with little congestion. However, a vehicle going 30 mph on a motorway is likely either accelerating up to motorway speeds, decelerating in preparation to leave the motorway, or experiencing congestion. Furthermore, a vehicle going 30 mph uphill will have a greater power demand on its engine than a vehicle going 30 mph downhill.

Figure 3.2 shows a speed-emission curve at different speed limits, as well as a curve of all speed limits aggregated together. The slopes follow a similar overall trend, and display the previously mentioned "U"-shape. There are some differences revealed when considering vertical slices through the curves. For example, a Euro 5 diesel vehicle travelling at 30 mph emits 0.70 g km^{-1} of NO_x in a 30 mph zone, 0.77 g km^{-1} in a 40 mph zone, 0.82 in 50/60 mph zones and 0.88 in a 70 mph zone. This is a range of 0.17 g km^{-1} of NO_x. The aggregated curve predicts a value of 0.74 g km^{-1} of NO_x, halfway between the 30 mph and 40 mph values.

Speed-emission curves from COPERT are provided, plotted in the range of 10–130 km h^{-1} (roughly 6–81 mph) as directed by Ntziachristos and Samaras [45]. It is visibly apparent that the COPERT curves are lower than than the remote sensing curves for all speed limits, with an average difference of 0.21 g km^{-1} between the "no software update" (solid) COPERT and aggregated remote sensing curves. The difference between the curves tend to decrease at higher vehicle speeds; at 6mph (the lowest suggested speed for COPERT) the COPERT curve predicts emissions of 1.00 g km^{-1} (-0.60 g km^{-1}/-60% compared to the remote sensing curve) but by 30 mph the difference has

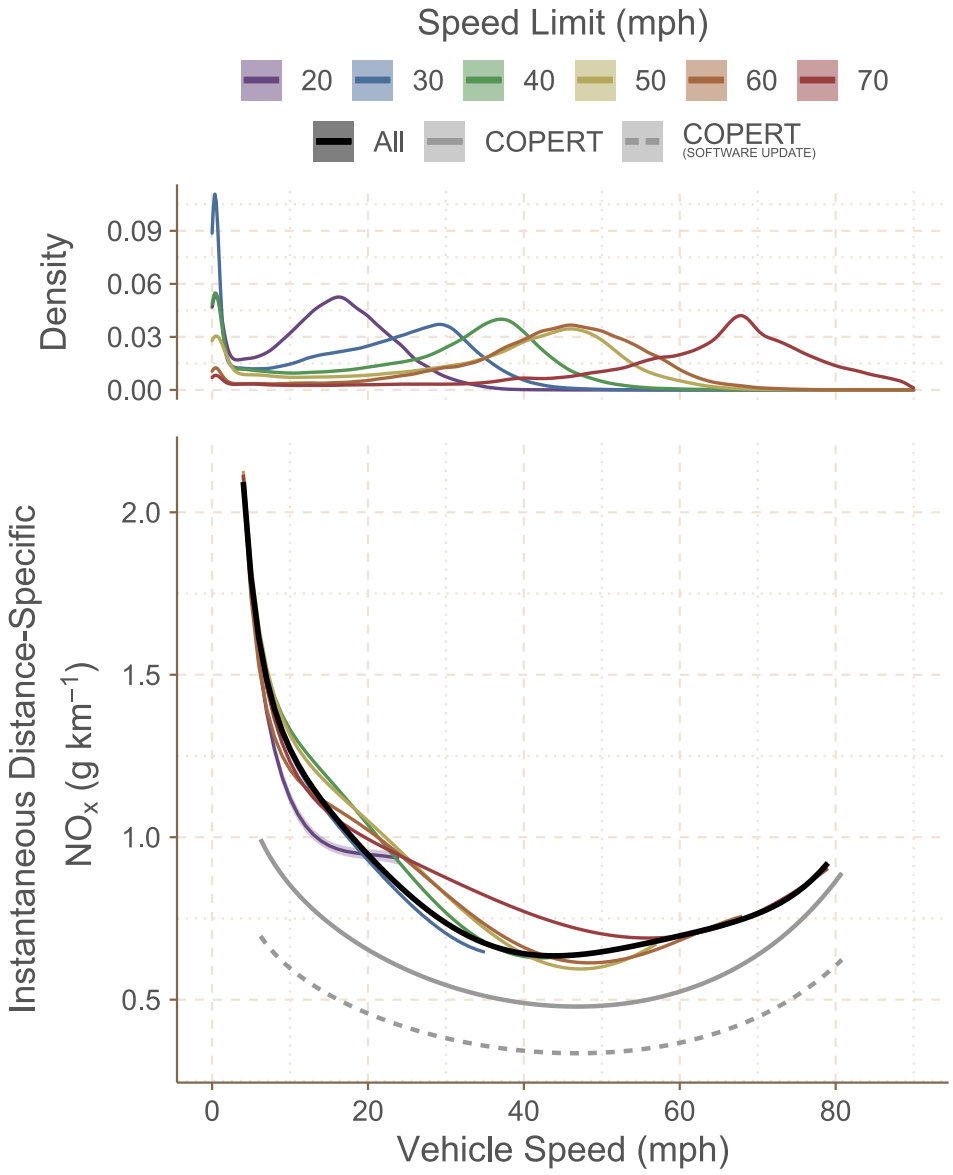

Figure 3.2: Top: Density functions of vehicle speed on roads under different speed limits. **Bottom:** Speed-emission curves for instantaneous distance-specific NO_x of Euro 5 diesel passenger cars as a function of vehicle speed. Curves are given on a per-speed limit basis, as well as all speed limits aggregated ("All"). A sixth-order polynomial fit was employed (Equation 3.8), as in Murrells and Rose [179]. Also visualised are COPERT v5.5 curves for Euro 5 diesel passenger cars, both with (dashed) and without (solid) a 30% reduction factor to reflect post-dieselgate VW software updates[45].

dropeed to -0.19 g km^{-1}/-26%. The difference then reaches a local minima at 41 mph (-0.15 g km^{-1}/-24%), increases slightly to a local maxima at 57 mph (-0.17 g km^{-1}/-26%) and is at its lowest at 79 mph (-0.09 g km^{-1}/-9%). A literature search reveals a limited number of studies and technical reports across different version of COPERT that suggest that COPERT has historically underestimated NO_x emissions when compared to real-world emissions measurements[180–185].

There may be many reasons for this disparity. For example, in-lab measurements that feed into COPERT's emission factor calculations are commonly conducted at 20-30 °C[51,110]. As stated in Subsection 3.3.1, the average temperature at which the remote sensing measurements were conducted was 15.6 °C. Grange et al. [110] used 300,000 light-duty vehicle remote sensing measurements to explore the significance of temperature on NO_x emissions, and noted a "low temperature penalty" — NO_x emissions from light-duty diesel vehicles were higher at lower temperatures. The authors provided multipliers to apply to non-temperature adjusted NO_x emission data, such as the COPERT speed-emission curve. With the appropriate factor (×1.2) applied, the average difference between the uplifted COPERT curve and aggregated remote sensing curve drops to -0.084 g km^{-1}. At 6 mph the difference is -0.40 g km^{-1} (-34%) and at 30 mph -0.082 g km^{-1} (-11%), but by 70 mph the difference is effectively zero (to 3 decimal places). Another possibility may be emission deterioration of in-use passenger cars, which is a more complicated effect discussed in greater depth in Chapter 5.

An important insight from this analysis is that the greatest deviations between remote sensing and COPERT distance-specific emissions occur for low-speed driving, which can be interpreted as urban driving. While 6 mph is well below any signposted speed limit on UK roads, slow driving such as this is not uncommon in built-up, congested urban areas; for context, 6 mph represents the 15th percentile of speed in the instrumented vehicle data set. This is significant from an air quality and public health perspective, as built-up

urban areas almost by definition have a high density of people frequenting them who will be exposed to emissions. While accounting for temperature does close the gap between the COPERT and remote sensing curves, a significant 34% difference remains at the lowest vehicle speeds. This may be an intrinsic weakness of speed-emission curves more generally; they break down at the lowest speeds, despite an understanding of congested, low-speed conditions being particularly valuable from an air quality exposure perspective.

3.4.3 Journey-Average Emissions and Driver Behaviour

Journey-average emission factors were calculated for each sub-journey in the data set using Equation 3.7. An asymptotic effect is once again seen; as the total distance covered in the journey tends toward zero the overall emission factor tends towards infinity. The result of this is the calculation of unexpectedly high distance-specific emission factors for journeys where particularly short distances were covered (for example, a journey entirely comprised of moving slowly through traffic) and lower emission factors for long motorway journeys. This effect is visualised in Figure 3.3.

To avoid the extremely high values biasing results, very quick ($\leq$ 2 minutes) and short ($\leq$ 100 metres) sub-journeys were removed, leaving 24,931 distance-specific NO_x emission values between 0.24 and 11.6 g km^{-1}. The lower quartile was 0.67 g km^{-1}, the median 0.82 g km^{-1} and the upper quartile 0.99 g km^{-1}. Disaggregating to different speed limits, the median and interquartile ranges for the distance-specific NO_x factors were 0.88 (0.75–1.05) for 30 mph, 0.76 (0.60–0.94) for 40 mph, 0.69 (0.59–0.80) for 50 mph, 0.64 (0.57–0.74) for 60 mph and 0.76 (0.68–0.88) for 70 mph.

Having access to a high number of distance-specific emission factors allows for the influence of different driving conditions on emissions to be identified, such as the previously discussed issue of driver behaviour. The data set in this study contains real driving data for 79 different drivers, and the distributions

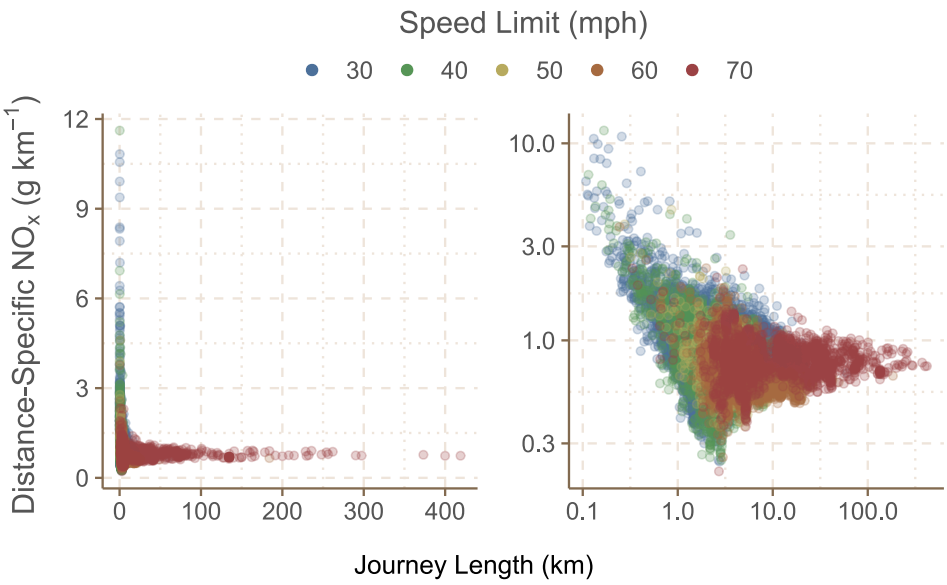

Figure 3.3: Distance specific NO_x (g km^{-1}) as a function of total journey distance. All journeys are over 2 minutes in duration and at least 100 metres in length. **Left:** Both axes on a linear scale, showing the asymptotic effect. **Right:** Both axes on logarithmic scales, more clearly indicating NO_x emission distribution as a function of journey length.

of their modelled distance-specific NO_x emissions may allow for the effect of behaviour to be quantified.

Figure 3.4 visualises the distributions of distance-specific NO_x emissions for each driver under each speed limit. Only drivers with at least 50 journeys under each speed limit are considered (all drivers regardless of their total numbers of journeys are visualised in Appendix B). The most apparent observation is that the whiskers of the boxplots for effectively all drivers are wide and overlap with one another. This is to be expected; drivers won't always drive consistently — a driver may drive more aggressively if they are running late, for example — and driving conditions (e.g., congestion) and journey characteristics (e.g., journey length) could vary radically between different journeys performed by the same driver.

Driver behaviour is difficult to isolate from external driving conditions. For

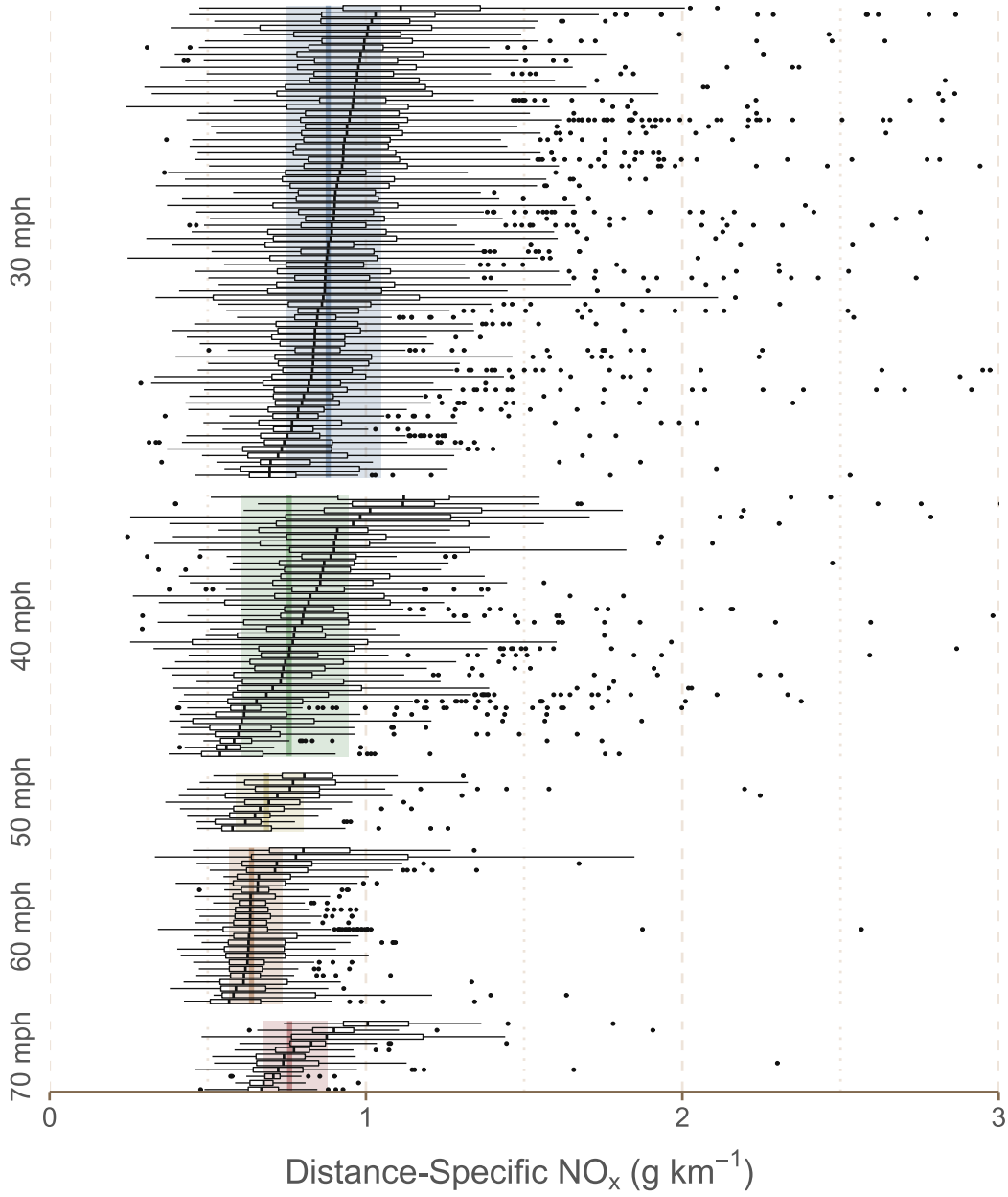

Figure 3.4: Distributions of journey-average distance-specific (g km^{-1}) NO_x emissions. Each boxplot represents an individual driver with 50 or greater journeys under the given speed limit. The hinges of each boxplot represent the first and third quartiles, and the hinges represent the largest/lowest value no greater than 1.5 times the interquartile range from the nearest hinge. Data beyond the whiskers are visualised as individual points. The vertical ribbons visualise the median and interquartile range of the whole speed limit. 68 observations greater than 3 g km^{-1} are not visualised.

example, a driver committed to "eco-driving" may still have higher journey-average emissions than a more aggressive driver if they happen to be travelling in more congested areas. Instead of full distributions, the *median* emission could instead be considered. The median is chosen over the mean to not be as influenced by the possible presence of atypically high emission factors owing to different journey lengths/times, as previously discussed, as well as "one-off" poor journeys a driver may have had. The range of median distance-specific NO_x emissions is 0.70–1.11 g km^{-1} for 30 mph driving, 0.54–1.12 g km^{-1} for 40 mph, 0.58–0.81 g km^{-1} for 50 mph, 0.57–0.80 g km^{-1} for 60 mph and 0.67–1.01 g km^{-1} for 70 mph. The range in values is the greatest in 40 mph zones, followed by 30 mph, 70 mph and finally 50 & 60 mph. This does suggest that there is *some* appreciable difference between drivers when it comes to emissions, particularly in urban areas.

Due to the large size of this data set, comment can be made as to whether drivers are *consistently* high emitting across multiple driving conditions. To assess this, drivers' median distance-specific NO_x emissions for each speed limit were taken and their correlation coefficients calculated. Only drivers with 10 or greater journeys under both speed limit conditions being correlated were considered for this analysis. However, not all of the 79 drivers had undertaken 10 or greater journeys under each speed limit. The number of drivers with at least 10 journeys under each speed limit are listed here: 30mph – all 79 drivers, 40 mph – 75 drivers, 50 mph – 49 drivers, 60 mph – 59 drivers, and 70 mph – 58 drivers. Table 3.1 shows correlation matrices using both the Pearson correlation (r) and Spearman's rank correlation (ρ) of the driver's median distance-specific NO_x emissions between the different speed limits.

Due to the many other factors which influence journey-average emissions, very high correlation coefficients are not expected. Still, the mean correlation coefficients between the different speed limits for both correlation methods ($r = 0.37, \rho = 0.42$) do indicate a moderate positive correlation. This suggests that a high-emitting driver in an urban area is somewhat likely to be a higher-

r	30	40	50	60	70
30	—	0.39	0.17	0.44	0.44
40	0.39	—	0.29	0.49	0.61
50	0.17	0.29	—	0.18	0.30
60	0.44	0.49	0.18	—	0.40
70	0.44	0.61	0.30	0.40	—

(a) Pearson

ρ	30	40	50	60	70
30	—	0.53	0.22	0.47	0.45
40	0.53	—	0.27	0.51	0.74
50	0.22	0.27	—	0.30	0.29
60	0.47	0.51	0.30	—	0.46
70	0.45	0.74	0.29	0.46	—

(b) Spearman (rank)

Table 3.1: Correlation matrices of median distance-specific NO_x emissions from the same drivers under different speed limits. Both the the pearson coefficient, r, and the spearman coefficient, ρ, are shown.

emitting driver on a motorway, and vice-versa. This reinforces the likelihood of a driver behaviour effect; under one kind of driving condition/speed limit it is possible a high emitting driver may unfortunately drive in predominantly congested areas, but it is unlikely that a driver is consistently experiencing congestion regardless of whether they are undertaking urban, rural or motorway driving.

The results from this section suggest that there is a driver behaviour effect, but it is important to put this effect in context. For example, at the end of Chapter 2, it was demonstrated that the range in distance-specific NO_x emissions from the studied Euro 5 diesel passenger cars on urban-rural journeys was 0.55-1.34 g km^{-1}. This corresponds to a roughly ±42% relative percentage range. Conversely, the relative percentage ranges for the median distance-specific emissions of different drivers average at ±22%. This appears to highlight that driver behaviour is a lower importance influence on emissions when compared to the difference between manufacturers.

3.5 Conclusion

Remote sensing is often used to examine real-world influences on emissions that are challenging to replicate in a laboratory, but only measuring "snapshots" of vehicle journeys limits the kinds of influences it can comment upon. Chapter 2 presented a method for calculating distance-specific emission factors using power-emission relationships from remote sensing and driving data from portable emission measurement system (PEMS) studies. The stated objective was to calculate emission factors that could be directly compared with those from commonly used on-road or in-lab measurement techniques, or used for inventory development. This chapter demonstrates that these methods are not restricted to use with short drive cycles or PEMS routes, but can be used flexibly with large driving databases of effectively any size. This enhances the ability for remote sensing to address sub-national, local-scale emissions.

The comprehensive modelled emission data allowed for the reproduction of COPERT-style speed-emission curves. The main benefit of this is the use of extensive real-world emissions data to critique the COPERT methodology that many European countries rely upon to calculate their emission inventories. There appears to be limited evidence that speed-emission curves vary drastically between different driving conditions, represented here as different speed limit zones. However, real Euro 5 NO_x emissions are demonstrated to be higher than predicted by COPERT v5.5, although adjusting for temperature closes the gap somewhat (reducing the average difference between the curves from -0.21 to -0.084 g km^{-1}). The apparent effect of ambient temperature reinforces the utility of local-scale emission measurements to refine international emission estimates like those used in COPERT.

Remote sensing data cannot usually easily comment on driver behaviour, but the diversity of drivers in the modelled data set allowed it to be considered. A key advantage of remote sensing data is also demonstrated in that the same data sets can address the relative importance of multiple influencing factors. In this

case, driver behaviour is suggested to be a second-order influence, around half as important as the differences between different vehicle manufacturers. Being able to rank influences in this way allows researchers to prioritise targeting the key sources of uncertainty in their emission estimates, and for policymakers to create effective strategies for road transport emission mitigation.

Chapter 4

Verification of a National Emission Inventory and Influence of On-road Vehicle Manufacturer-level Emissions

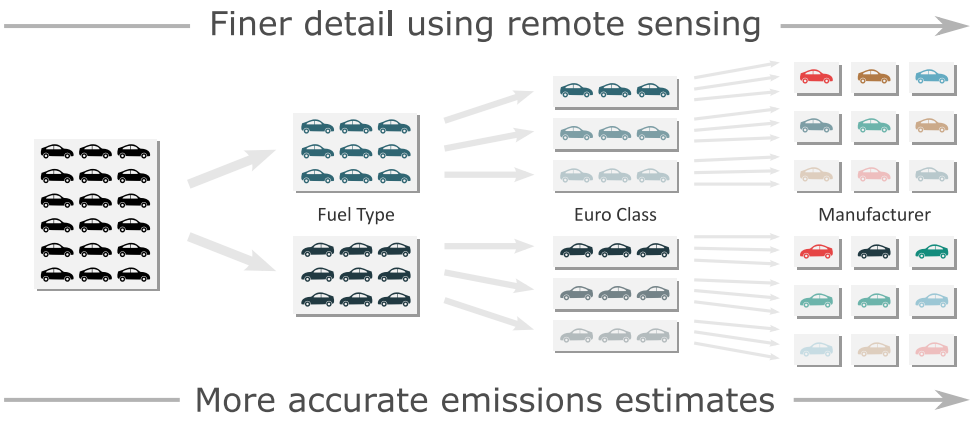

4.1 Abstract

Road vehicles make important contributions to a wide range of pollutant emissions from street level to global scales. The quantification of emissions from road vehicles is, however, highly challenging given the number of individual sources involved and the myriad factors that influence emissions such as fuel type, emission standard and driving behaviour. In this work, highly detailed and comprehensive vehicle emission remote sensing measurements made under real driving conditions were used to develop new bottom-up inventories that can be compared to official national inventory totals. It was found that total UK passenger car and light duty van emissions of nitrogen oxides (NO_x) are underestimated by 24–32%, and up to 47% in urban areas, compared with the UK national inventory, despite agreement within 1.5% for total fuel used. Emissions of NO_x at a country level are also shown to vary considerably depending on the mix of vehicle manufacturers in the fleet. Adopting the on-road mix of vehicle manufacturers for six European countries results in up to 13.4% range in total emissions of NO_x. Accounting for manufacturer-specific fleets at a country level could have a significant impact on emission estimates of NO_x and other pollutants across European countries, which are not currently reflected in emission inventories.

4.2 Introduction

Emission inventories are an important component of the management of air pollution and provide essential input to air quality models. Emission inventories are required and used at a range of scales from single sources and road sections through to quantifying national total emissions. At the local scale, estimating the emissions along individual road links is required to understand near-road exposures to air pollution. Equally, at a national scale, establishing total emissions is required to meet international obligations, such as the European National Emission Ceiling Directive (NECD)[186]. The accuracy of emission inventories is of central importance for many issues but in practice is difficult to establish.

The road transport sector is arguably a uniquely challenging sector for which to estimate emissions. In the UK alone, there are millions of individual vehicles that move in both space and time, representing a wide range of fuel types, emission standards, vehicle classes and technologies. Even nominally identical vehicles may behave differently based on driver behaviour, vehicle mileage and levels of maintenance[104,175]. Moreover, environmental conditions, such as the influence of ambient temperature, can also have an effect on road vehicle emissions[110,166].

Of particular recent interest has been the emission of NO_x from road transport vehicles. Given the wide ranging impacts of NO_x emissions into the atmosphere, it is important that emission estimates are robust and representative of the region being considered. In Europe over the past decade there has been a substantial focus on how road vehicle emissions of NO_x contribute to ambient nitrogen dioxide (NO_2) concentrations, which have often exceeded ambient air quality limits[144]. Emissions of NO_x also play a central role in the formation of O_3 and $PM_{2.5}$, both of which are important pollutants from a direct health impact perspective and in terms of wider environmental damage. Extensive evidence of considerable differences between emissions measured

in the laboratory for type approval purposes and real driving emissions has also been widely reported and is well-established[149,187]. However, the incorporation of increasingly available real driving emissions data to emission inventories has not been as extensive.

In the UK, the National Atmospheric Emissions Inventory (NAEI) is the primary inventory that categorises the emissions of many greenhouse gases and air quality pollutants. It covers multiple sectors, including industry, agriculture, land-use, energy generation, and transport[38]. In 2019, the NAEI indicated that the transport sector was responsible for 54% of the UK's NO_x emissions, with 33% coming from road transport[19]. The NAEI forms the basis of reporting total UK emissions as part of the National Emissions Ceiling Directive[186], as well as providing input to local and regional scale air quality models. It is important therefore that the inventory accurately represents the emissions from sectors such as road transport.

Like many European emission inventories, the UK NAEI relies heavily on the COPERT (COmputer Programme to calculate Emissions from Road Transport) emission factor approach for estimating road transport emissions[40,44], based on recommendations from the European Monitoring and Evaluation Programme (EMEP)/European Environment Agency (EEA) Emission Inventory Guidebook[45]. Initially, emission factor development was based entirely on laboratory measurements. More recently, portable emissions measurement systems (PEMS) have been incorporated into emission factor development. The 2019 EMEP/EEA guidebook notes that a combination of laboratory and on-board measurements are now typically used for emission factor development, with other methods such as vehicle emission remote sensing and tunnel studies being used for validation purposes. Indeed, the literature encompasses studies which have used PEMS[184,188], vehicle emission remote sensing[189,190] and even aircraft-based flux measurements[185] to independently validate emission inventory estimates.

Measuring relatively few vehicles using laboratory or on-board measure-

ment techniques such as PEMS can provide detailed single vehicle emissions information, but it is challenging to measure many vehicles using these methods due to cost and time constraints. It is known that emissions can vary significantly by vehicle manufacturer and model, but currently no account is taken of these differences in emission factor or inventory development[149]. Choosing a representative sample of a country's vehicle fleet from which to derive emission factors is therefore a potentially important issue. The advantage of remote sensing over other methods are the large sample sizes and comprehensive fleet coverage, which provides a better representation of in-use vehicle fleets.

A focus on the UK over other European countries for inventory verification is advantageous given that Great Britain is an island. In countries such as Germany, France and Belgium, gasoline and diesel fuel sold may not be used within the country itself, leading to some uncertainty in the allocation of fuel use (and hence emissions) to a specific country. Conversely, in the UK close to 100% of road transport fuel sold is used in the UK. This means that robust comparisons can be made between so-called 'bottom-up' and 'top-down' inventory methods. Specifically, there is high certainty in the top-down calculations that rely on total fuel sales data.

The primary focus of this work is to exploit the comprehensive fleet coverage provided by vehicle emission remote sensing to develop highly detailed and comprehensive bottom-up NO_x, CO and NH_3 emissions estimates at a UK scale for light duty vehicles. This aim is achieved through calculating distance-specific emission factors and making direct comparisons with the 2018 UK inventory. Additionally, calculations are made of CO_2 emissions to enable a direct comparison with fuel use statistics and provide a means of verifying the methods developed.

A specific focus is to estimate NO_x emissions, which have persistently been thought to be underestimated, and provide a national level quantification of total emissions. Finally, for the first time, the influence of different vehicle manufacturer fleet mixes is considered, which can be determined from remote

sensing data. By considering different measured vehicle manufacturer proportions in other European countries, it is established how these contrasting manufacturer proportions affect total emissions of NO_x and CO_2.

4.3 Materials and Methods

4.3.1 Vehicle Emission Remote Sensing

The development of and operating principles behind vehicle emission remote sensing has been described in considerable detail in the literature[79,145], but is summarised here. A remote sensing device (RSD) consists of a UV/IR source, multiple detectors, optical speed-acceleration bars and a number plate camera. A RSD is deployed such that vehicles drive past the set-up unimpeded, with the concentrations of gases in their exhaust plumes and their speed and acceleration being measured remotely via open path spectroscopy. Spectrometry is achieved using a collinear beam of IR and UV light which, after being absorbed by exhaust plumes, is separated into its two components within the detector. Non-dispersive infrared detectors measure CO, CO_2, hydrocarbons (HC) and a background reference. The UV component passes through a quartz fibre bundle and is used to measure NH_3, NO and NO_2.

One hundred measurements are taken in half a second for each vehicle plume exhaust when the rear of the vehicle is detected. From these measurements the ratio of a pollutant to CO_2 is calculated, from which fuel-specific (g kg^{-1}) emission factors can be calculated. The further transformation from fuel-specific to distance-specific (g km^{-1}) emission factors is described in detail in Chapter 2 and briefly in Subsection 4.3.2.

Vehicle number plates are recorded alongside emission and speed measurements and are used to obtain vehicle technical data, such as engine size, fuel type, Euro standard and vehicle manufacturer. In this study, the data were obtained from CDL Vehicle Information Services Ltd., a commercial supplier[85].

CDL retrieved the data from the Driver and Vehicle Licensing Agency and the Society of Motor Manufacturers and Traders Motor Vehicle Registration Information System. Data relating to the total mileage of each vehicle at its last annual technical inspection test was also obtained through CDL for vehicles greater than three years old.

Vehicle emission measurements were conducted between 2017 and 2020 at 37 sites across 14 regions in the United Kingdom using two remote sensing instruments — the majority with the Opus *AccuScan* RSD 5000[191], supplemented with data from the University of Denver Fuel Efficiency Automobile Test (FEAT) instrument[120]. A total of 304,039 measurements were collected of Euro 2–6 vehicles in three key classes of Light Duty Vehicles (LDV): diesel light commercial vehicles (LCVs) and diesel and gasoline passenger cars (PCs). A statistical summary of the data set is provided in Table 4.1.

4.3.2 Calculating Distance-Specific Emission Factors

The calculation of distance-specific (g km^{-1}) emission factors is required for the 'bottom-up' approach to estimating total UK emissions. The vehicle power-based approach used has been previously developed and evaluated[1,30], but is briefly outlined here. The principal steps include *(i)* the development of a vehicle power-based method to calculate g km^{-1} emissions from remote sensing data, *(ii)* development of relationships that enable the prediction of emissions over any 1-Hz drive cycle and *(iii)* the application of the g km^{-1} emissions to a UK national scale. Because vehicle emission remote sensing measurements tend to be made under higher engine load conditions than full drive cycle averages, their direct use would tend to overestimate mean exhaust emissions. The method provides a way in which to estimate emissions for typical real-world drive cycles that may have lower average engine loads, e.g., for typical urban driving.

A physics-based approach to calculating vehicle power is used, accounting

Characteristic	**Diesel LCV**	**Diesel PC**	**Gasoline PC**
# of Measurements	55,018	113,554	135,467
# of Manufacturers	34	51	61
(with ≥ 100 Measurements)	16	34	39
VSP[1] (kW t^{-1})	5.1 (7.4)	6.3 (8.1)	5.9 (7.5)
Speed[1] (km h^{-1})	34.2 (10.1)	35.2 (10.1)	35.0 (9.9)
Acceleration[1] (km h^{-1} s^{-1})	0.99 (2.25)	1.16 (2.40)	1.02 (2.29)
Temperature[1] (°C)	13.9 (5.1)	14.9 (5.3)	14.9 (5.2)
Mileage[1] (1000 km)	169.2 (102.1)	147.2 (105.7)	112.3 (72.9)
Euro standard[2]			
Euro 2	290 (0.5%)	488 (0.4%)	3,191 (2.4%)
Euro 3	3,912 (7.1%)	9,222 (8.1%)	23,272 (17%)
Euro 4	11,472 (21%)	22,743 (20%)	33,946 (25%)
Euro 5	27,985 (51%)	45,900 (40%)	39,691 (29%)
Euro 6	11,359 (21%)	35,201 (31%)	35,367 (26%)
Remote Sensing Device[2]			
Opus RSD 5000	47,140 (86%)	99,294 (87%)	118,379 (87%)
Denver FEAT	7,878 (14%)	14,260 (13%)	17,088 (13%)

Table 4.1: A statistical summary of the vehicle emission remote sensing data, split into diesel light commercial vehicles (LCV) and diesel and gasoline passenger cars (PC). Statistics presented: [1]Mean (Standard deviation); [2]Number of measurements (Percentage of the column total).

for all the main forces acting on a vehicle. First, instantaneous vehicle power is calculated as the total power to accelerate the vehicle, to overcome the road gradient, to resist both rolling and air resistance and to power auxiliary devices, adjusted for losses in the transmission. Vehicle specific power (VSP) is calculated as the instantaneous power divided by the vehicle mass (assumed to be the curb weight plus 150 kg to account for the weight of the driver, passengers and cargo). As none of the road load or aerodynamic drag coefficients were known, generic values taken from Chapter 2 were used. Fuel consumption is

straightforwardly calculated from VSP using a linear model relating VSP to fuel consumption using the Passenger Car and Heavy Duty Emissions Model[156]. As the parameters were based on Euro 5 and 6 vehicles, a 5% penalty was applied to Euro 2–4 vehicles to account for poorer fuel efficiency. Fuel-specific emission factors in g kg^{-1} can then be combined with fuel consumption in kg s^{-1} to produce instantaneous emission values (g s^{-1}).

Relationships between emissions in g s^{-1} and VSP for vehicles with different fuel types, vehicle types, Euro standards and pollutant species were established using Generalised Additive Models (GAMs), which are flexible enough to consider non-linear relationships between variables. The `mgcv` R package[134] was used to fit the models. These models were used to predict emissions for 1 Hz drive cycles from PEMS tests obtained from the UK *Department for Transport* (DfT)[159]. The PEMS data contained a total of 4,243 km of real-world driving over 58 PEMS routes which included urban, rural and motorway portions. The maximum VSP value across these drive cycles was 37.2 kW t^{-1} (equal to the 99.2 percentile VSP value of the remote sensing measurements), and GAMs were fit between 0 and 40 kW t^{-1}. Emissions from negative VSP conditions were assumed to be zero. The approach is flexible enough that it can be applied to any 1-Hz drive cycle for which VSP is available or can be calculated.

With 1 Hz modelled instantaneous emissions, distance-specific emission factors (g km^{-1}) can be calculated as the total of all instantaneous emissions divided by the total distance. The distance-specific emission factor used for the total UK emissions estimation was the mean of all the distance-specific factors from each of the 58 real-world drive cycles. Factors were calculated separately for each of the urban, rural and motorway conditions. The next step is to apply these emission factors to the corresponding driving activity data in the UK, thus providing a means of estimating total UK emissions.

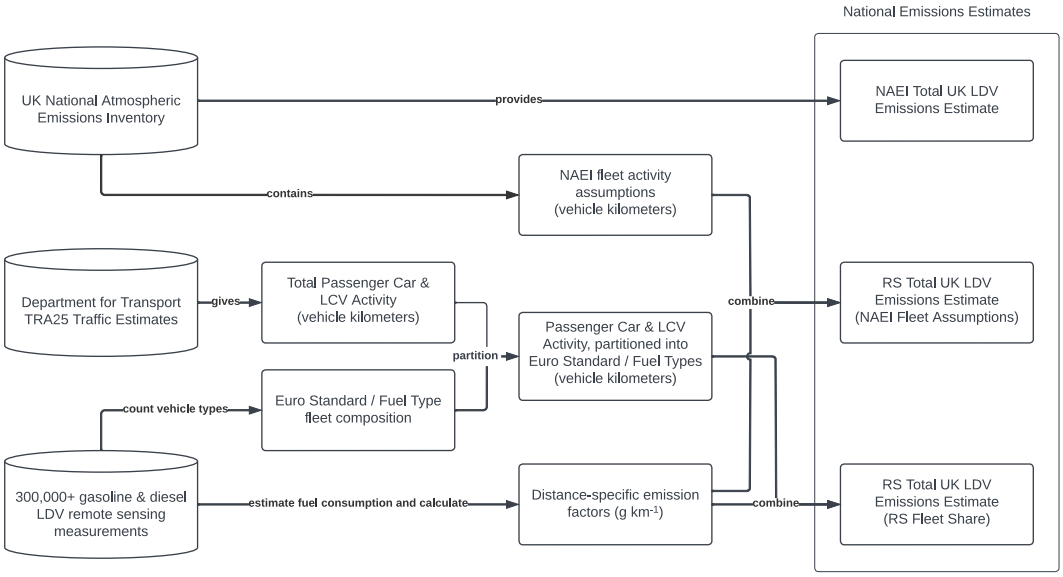

Figure 4.1: A flowchart showing the estimation of total UK LDV emissions using remote sensing (RS), using activity data sourced from, *i)*, the UK Department for Transport, partitioned using RS observations, and *ii)*, National Atmospheric Emissions Inventory fleet composition assumptions.

4.3.3 Estimating Total UK Emissions

A flowchart of the methods used to calculate total UK emissions in this chapter is provided in Figure 4.1.

Distance-specific emission factors for each vehicle type were used to calculate a bottom-up estimate of total UK emissions through multiplication with UK-wide mileage data. Estimates of the total distance travelled by UK passenger cars and light commercial vehicles per annum were obtained from a publicly available government database[192]. These activity data were obtained by the UK Department for Transport using a national network of around 180 automatic traffic counters, which used recorded physical properties of vehicles to segment these into vehicle types (passenger cars, vans, etc.). In order to apportion these vehicle mileage data into different fuel types, information available in the remote sensing data, such as average mileages by fuel type, was used, as provided in Table 4.1.

The vehicle mileages are already apportioned into urban, rural and motorway driving conditions, but not by fuel type or Euro standard. The data in Table 4.1 indicates that there is a 1:1.32 ratio of recorded mileage between gasoline and diesel passenger cars, but a 1.11:1 ratio of number of measurements. The number of measurements provides a direct measure of vehicle km driven under urban conditions, where remote sensing measurements are typically made. In other words, diesel vehicles drive further on an overall UK level compared with gasoline vehicles, but gasoline vehicles drive further than diesel vehicles in urban areas. The rural and motorway portions were adjusted proportionally such that the sum of the urban, rural and motorway portions summed to the total annual mileage reported in UK statistics. Only 0.71% of light commercial vehicles measured were gasoline, which have not been explicitly considered given their low numbers and minor contribution to emissions. However, overall LCV mileage data was reduced by this small amount to apply to diesel LCVs only.

Apportionment into Euro standards is straightforward, simply applying the ratio between the five Euro standards for each of the three vehicle categories — Diesel PC, Gasoline PC and Diesel LCV — given in Table 4.1. The fully apportioned mileages are provided in Table 4.2. To calculate UK totals for the exhaust pollutants, the g km^{-1} emission factors for each combination of pollutant species, vehicle category, Euro standard and driving condition (urban, rural or motorway) were multiplied by the corresponding apportioned mileage. While emission inventories themselves are often not reported with associated uncertainties, the estimates presented here are provided alongside the 95% confidence interval calculated from the original g kg^{-1} measurements.

The estimated UK totals can be directly compared with the NAEI. The comparison can be expressed through the use of a ratio between the bottom-up estimated emission and the emission reported in the NAEI, here labelled F. The value of F is therefore also the factor by which one would multiply the emission reported in the NAEI to arrive at the emission estimated using the

		Annual UK Mileage (billion km)							
		Gasoline				**Diesel**			
VT	**ES**	**Urban**	**Rural**	**Mway**	**Total**	**Urban**	**Rural**	**Mway**	**Total**
PC	2	1.89	1.78	0.57	4.24	0.28	0.43	0.22	0.93
	3	13.41	12.61	4.03	30.05	5.76	8.62	4.53	18.91
	4	19.72	18.54	5.93	44.19	14.22	21.28	11.19	46.68
	5	22.88	21.51	6.88	51.26	28.43	42.55	22.38	93.36
	6	20.51	19.28	6.17	45.96	22.03	32.98	17.34	72.36
	All	78.41	73.72	23.59	175.71	70.72	105.85	55.67	232.24
LCV	2	—	—	—	—	0.13	0.19	0.08	0.41
	3	—	—	—	—	1.90	2.69	1.19	5.78
	4	—	—	—	—	5.63	7.95	3.52	17.10
	5	—	—	—	—	13.68	19.30	8.56	41.53
	6	—	—	—	—	5.63	7.95	3.52	17.10
	All	—	—	—	—	26.98	38.07	16.89	81.93

Table 4.2: Annual UK passenger car (PC) and light commercial vehicle (LCV) mileage in billions of kilometers, rounded to two decimal places and dissagregated based on driving conditions and Euro standard (ES). The complete totals for each light-duty vehicle type (roughly 410 bn & 82 bn km for passenger cars and light commercial vehciles, respectively) is taken from Department for Transport quarterly traffic estimates (TRA25). Apportionment is based on fleet composition information obtained during vehicle emission remote sensing campaigns.

vehicle emission remote sensing data. $F = 1$ would mean that these two values were the same, $F > 1$ would mean the emission is under-reported in the NAEI and $F < 1$ would mean that the emission is over-reported.

Any disparity between the bottom-up remote sensing emission estimates and the NAEI reported values could be due to differences in emission factors and/or differences in fleet composition assumptions. While the focus of this study is on estimates using activity data partitioned using remote sensing observations, a second set of estimates are also made using the NAEI's fleet composition assumptions. This allows for a like-for-like comparison with identical activity data, which helps examine if disparities in emission estimates are sourced from differences in emission factors or in source activity.

The NAEI reports air quality pollutant sources from *four* driving conditions, those being urban, rural, motorway, and a separate cold start contribution. In common with most emission inventories, the increased emissions of some pollutants after engine start are considered as separate emissions from hot, stabilised emissions. For some pollutants, such as CO and hydrocarbons, the cold start emissions can be substantial. In the NAEI, cold start emissions are only considered in urban areas and reflect the estimated number of trips.

The potential importance of cold start emissions raises the question about the extent to which vehicle emission remote sensing includes a cold start contribution. Given the vast majority of emission measurements are made in urban areas, it might be expected that remote sensing data would include some fraction of elevated emissions due to cold starts. However, for gasoline vehicles, the three-way catalyst reaches effective operating temperature (called 'light-off') within 1 to 2 minutes of the engine starting[193]. This means that it is highly unlikely that remote sensing measurements include a significant proportion of cold start emissions given the proximity required of a cold start to the measurement location. Therefore, when urban comparisons are made, the estimates are compared with both the urban value from the NAEI *and* a combination of the urban and cold start contributions.

The NAEI is required to report road transport emissions of CO_2 from fossil fuels only, so the figures reported do not include the additional presence of bio-fuels. Assuming that diesel in the UK contains up to 3.7% bio-diesel and gasoline up to 4.6% bio-ethanol[194], an adjustment factor can be calculated through the multiplication of the bio-/fossil-fuel ratio by the ratio of fuel CO_2 emissions (kg) per litre of the bio-fuel and fossil fuel (1.52/2.31 for gasoline, 2.36/2.69 for diesel)[195]. The adjustments are therefore 1.032 for gasoline and 1.034 for diesel, and are used to uplift the reported NAEI CO_2 values.

4.3.4 Effects of Vehicle Fleet Composition

To investigate the importance of different fleet compositions in European countries, data from the CONOX project were analysed, which provides a database of European vehicle emission remote sensing measurements[98]. These data provide over 700,000 remote sensing measurements for the UK, Sweden, Switzerland, Belgium, France and Spain. The data usefully contain information on the breakdown of different manufacturers and vehicle models, which can be used to consider the effects on NO_x emissions due to different national fleet mixes. An advantage of these data is that they provide a direct, on-road measurement of the vehicle fleet, which accounts for the vehicle km driven by vehicles made by different manufacturers. These data are considered more representative of in-use vehicle fleets than, for example, statistics on new vehicle sales, which would not reflect actual distances travelled by different vehicle types. The data do show strong country-specific characteristics. For example, France is dominated by Renault and Peugeot-Citroen, Sweden by Volkswagen and Volvo, and Switzerland by Volkswagen and, to a lesser extent, Daimler and BMW (Figure 4.2).

The total emissions of CO_2 and NO_x based on UK mileage data for Euro 5 and Euro 6 diesel passenger cars are considered, but using the fleet mix for each country. In this respect, the analysis addresses the question of 'how

Figure 4.2: Treemaps showing the eight most popular manufacturer groups for Euro 5 and 6 diesel passenger cars in the six European countries contained within the CONOX remote sensing database. The area of each rectangle in relation to the overall square reflects the share of the fleet that the corresponding manufacturing group represents. Manufacturers are divided into engine sizes, labelled in cubic centimeters. Treemaps were visualised using the `treemapify` R package[126].

would UK emissions of NO_x change if the UK had the fleet of France, Spain, Belgium, Switzerland or Sweden?' The calculations keep the vehicle km the same between fuel type used and Euro standard, i.e., that of the UK, and simply considers different proportions of manufacturer families according to the fleets in other countries. Manufacturer and engine size-specific emission factors were developed for this purpose using the UK-based data set outlined in Subsection 4.3.1, using the same method as outlined in Subsection 4.3.2.

4.4 Results and Discussion

4.4.1 Total UK Light Duty Vehicle Emissions

The body of this chapter centres around emissions of NO_x and CO_2. Information for CO and NH_3, as well as emission factors for all four species, are provided in Appendix C.

The relationship between VSP and emission rate in g s^{-1} for NO_x and CO_2 is shown in Figure 4.3, based on the GAMs developed from the vehicle emission remote sensing data for each fuel type, vehicle type, and Euro standard. ANOVA testing of fitted GAMs confirmed the significance ($P < .05$) of VSP in modelling both CO_2 and NO_x in all three vehicle categories for all five Euro standards considered. Most of the relationships shown in Figure 4.3 are close to linear, particularly for CO_2, which highlights the benefit of expressing emissions as a function of vehicle power demand rather than vehicle speed. Indeed, an inherent problem with speed-dependent emission factors is that as the speed tends to zero, the emissions tend to infinity, which means fitting a model through the data is difficult. Some relationships are non-linear; this is particularly noticeable in the Euro 6 diesel LCV NO_x emission curve which appears to level off at around 20 kW t^{-1}. This can likely be attributed to modern after-treatment technologies effectively controlling NO_x emissions at high engine power conditions.

All predicted CO_2 and NO_x emissions and their associated *F* values (the ratio between the bottom-up estimate and the reported NAEI value) are tabulated in Table 4.3. Key values and implications are described here.

An important first step is to establish whether there is carbon / energy balance for the detailed bottom-up approach to estimate CO_2 at a national scale. The total estimated emissions from this method were 91.3 ± 0.9 Mt CO_2. This value is very similar to the NAEI value of 90.0 Mt, giving an *F* value equal to 1.01. The similarity extends when considering the two fuel

		Carbon Dioxide / CO_2		**Nitrogen Oxides** / NO_x	
Category	**Conditions**	**Pred. (Mt)**	**F**	**Pred. (kt)**	**F**
All LDV	All	91.3 ± 0.9	1.01	280 ± 6.3	1.24–1.32
	Urban	40.3 ± 0.4	1.17	103 ± 2.4	1.22–1.47
	Rural	34.6 ± 0.3	0.92	115 ± 2.5	1.27
	Motorway	16.4 ± 0.2	0.93	62.6 ± 1.3	1.21
Gasoline PC	All	35.2 ± 0.30	1.00	29.5 ± 1.5	1.82–1.95
	Urban	19.3 ± 0.2	1.23	15.0 ± 0.7	1.94–2.24
	Rural	11.9 ± 0.1	0.84	10.7 ± 0.5	1.71
	Motorway	4.01 ± 0.03	0.75	3.81 ± 0.2	1.77
Diesel LDV	All	56.1 ± 0.61	1.02	251 ± 5.0	1.19–1.27
	Urban	21.1 ± 0.2	1.12	87.8 ± 1.7	1.15–1.38
	Rural	22.6 ± 0.2	0.96	104 ± 2.0	1.24
	Motorway	12.4 ± 0.1	1.01	58.8 ± 1.1	1.18
Diesel PC	All	40.4 ± 0.4	1.14	169 ± 2.9	1.44–1.54
	Urban	15.0 ± 1.2	1.22	57.7 ± 1.5	1.22–1.46
	Rural	16.1 ± 1.1	1.07	70.0 ± 1.6	1.55
	Motorway	9.21 ± 1.1	1.15	41.7 ± 1.6	1.64
Diesel LCV	All	15.7 ± 0.2	0.81	81.2 ± 2.0	0.88–0.94
	Urban	5.99 ± 0.09	0.92	30.2 ± 0.7	1.03–1.26
	Rural	6.48 ± 0.10	0.76	34.0 ± 0.8	0.88
	Motorway	3.20 ± 0.05	0.74	17.0 ± 0.4	0.70

Table 4.3: Bottom-up vehicle emission remote sensing CO_2 and NO_x predictions for different vehicle categories and driving conditions, *pred*, and the ratio between the bottom-up estimate and the reported NAEI value, *F*. The *urban* and *total* driving condition ratios are given as a range, reflecting the difference between calculations using just hot urban emissions from the NAEI and a combination of hot urban and cold start emissions.

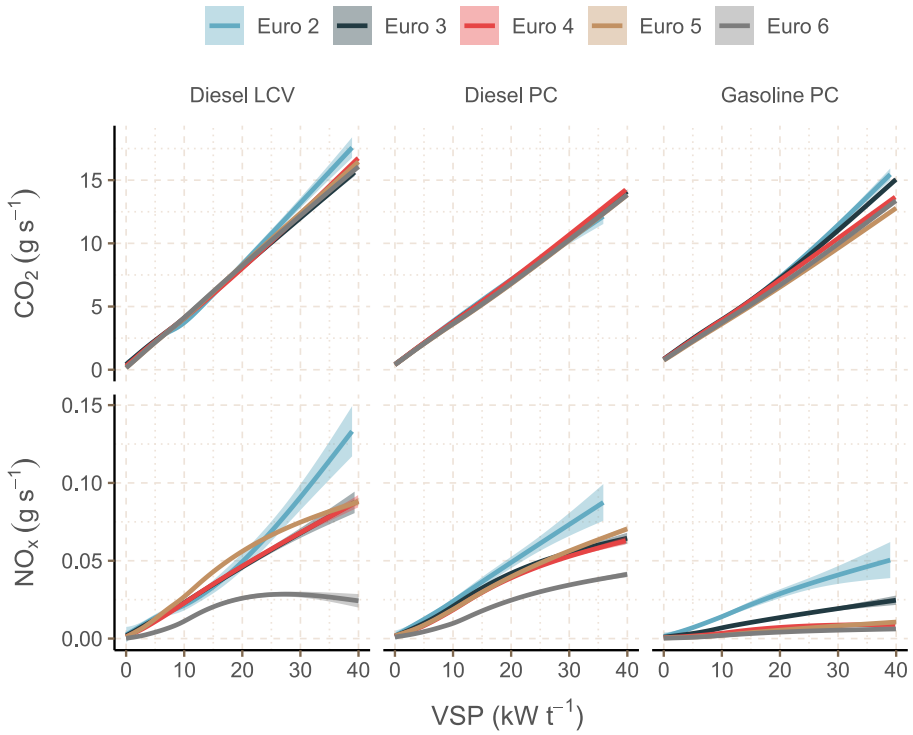

Figure 4.3: Generalised Additive Models (GAMs) fit using data from vehicle emission remote sensing relating vehicle CO_2 and NO_x g s^{-1} to VSP, coloured by Euro standard and faceted into three light duty vehicle categories. The shading shows the standard error of the GAM fit.

types independently — gasoline vehicles were shown to have an F value of 1.00 and diesel vehicles 1.02. When considering diesel passenger cars and light commercial vehicles separately, however, divergence from the NAEI is apparent, with the passenger cars having an associated F of 1.14 and the LCVs 0.81. The bottom-up calculations therefore suggest a different allocation of diesel fuel use (or CO_2 emissions) than is suggested by the NAEI, although the sum of passenger car and light commercial vehicle CO_2 is in good agreement. It should be noted that the comparison for gasoline is considered more robust than for diesel fuel because almost all gasoline use in the UK (97%) is for passenger cars, whereas diesel fuel is used in a wide range of vehicle types including passenger cars, light commercial vehicles, buses and other heavy duty vehicles,

which introduces some uncertainty in the allocation between diesel-fuelled vehicles[196].

With respect to NO_x, the total UK estimates were 280 ± 6.3 kt NO_x. On a UK scale, the NAEI underestimates NO_x emissions, with F between 1.24 and 1.32 depending on whether cold start emissions are included or excluded, respectively. These comparisons can be made at a more disaggregated level by considering the vehicle categories individually. Estimated gasoline PC emissions were higher than those reported in the NAEI, with NO_x emissions of 29.5 ± 1.5 kt ($1.82 < F < 1.95$). The NO_x predictions for light duty diesel vehicles were similarly under-reported in the NAEI, being 251 ± 5.0 kt NO_x ($1.19 < F < 1.27$). Of this diesel total, passenger cars contribute 169 ± 2.9 kt NO_x ($1.44 < F < 1.54$) and light commercial vehicles 81.2 ± 2.0 kt NO_x ($0.88 < F < 0.94$).

The comparison between the NAEI and the bottom-up remote sensing data estimations is made on a fully disaggregate level, including vehicle category and driving condition, in Figure 4.4. This analysis shows broad consistency between the the bottom-up estimates and NAEI reported values for CO_2, with F values between 0.77 to 1.27. Conversely, NO_x is shown to have F values between 0.70 to 2.24, with some important variability depending on driving conditions (urban, rural or motorway).

A specific interest is the quantification of NO_x emissions in urban areas where exposures to elevated concentrations of NO_2 are greatest. In total, the NAEI reports 84.0 kt NO_x from light duty vehicle activity in urban areas and from cold start emissions, with 70.1 kt coming from just urban emissions. Conversely, the new bottom-up estimates suggest total urban NO_x emissions of 103 ± 2.5 kt, a difference of 19 kt including cold start emissions or 32.9 kt excluding them. These results suggest the NAEI may be under-reporting urban emissions by 22–47%. As discussed previously, it is considered the remote sensing measurements comprise a very low proportion of enhanced emissions due to cold start effects. For this reason, the underestimate in urban NO_x

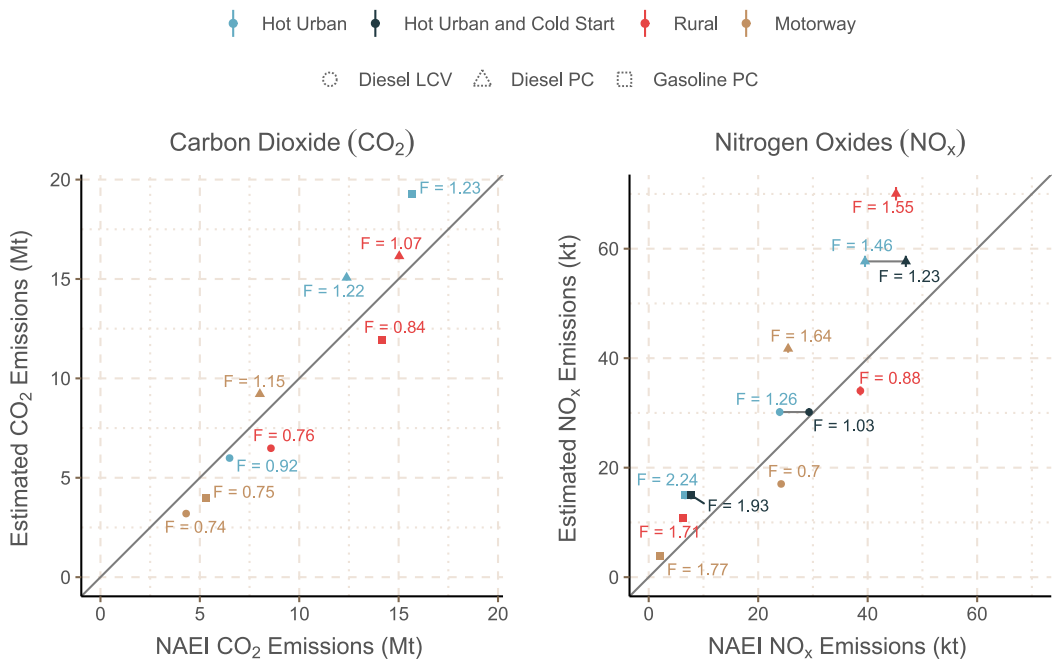

Figure 4.4: Total UK estimates for CO_2 and NO_x using vehicle emission remote sensing, in comparison with the 2018 emissions reported in the national inventory. *F* values, representing the ratio between the bottom-up estimate and the reported NAEI value, are provided. Urban bottom-up estimates are compared with both hot urban emissions from the NAEI and a combination of hot urban and cold start emissions, shown connected by a grey horizontal line. Error bars show the 95% confidence intervals projected from the fuel-specific (g kg^{-1}) emission factors. The grey diagonal line shows a 1:1 relationship.

emissions is considered to be closer to 47% than 22%.

It is important to consider the underlying reasons behind the disparity between the bottom-up estimates and the values reported in the NAEI, which could be associated with vehicle fleet assumptions *and/or* the emission factors. The bottom-up emissions were re-calculated based on the fleet composition assumptions used in the NAEI[19,197] and the NAEI allocations of gasoline and diesel fuel use in urban areas. The NAEI assumed a newer vehicle fleet compared with the observation-based values used for the bottom-up calculations. Using these NAEI assumptions resulted in UK-wide light duty vehicle emissions

with F values of 1.05 for CO_2 and 1.06–1.13 for NO_x, or 1.19 and 1.05–1.26 in only urban areas. However, there were some significant disparities on a disaggregated level when using NAEI fleet assumptions, for example, with $F = 1.20$ for gasoline CO_2 (compared with $F = 1.00$ using the bottom-up methods). These results strongly suggest that the use of the observation-based fleet information in the bottom-up emission calculations provide much better explanation of total UK emissions. On this basis, much of the discrepancy between the NAEI and the bottom-up methods is associated with vehicle fleet and vehicle activity assumptions rather than the emission factors. Nevertheless, even adopting the NAEI vehicle fleet assumptions still results in up to a 26% underestimate of NO_x emissions compared with the bottom-up calculation in urban areas.

4.4.2 Influence of Vehicle Fleet Composition

An inherent benefit of vehicle emission remote sensing data for use in emission factor and emission inventory development is the comprehensive coverage of a wide range of vehicle manufacturers and models, which is difficult to achieve through laboratory or PEMS studies owing to the large number of vehicles that would need to be tested. Vehicle fleets can vary from smaller city-wide to larger country-wide scales. For example, some cities may tend to have a higher than average proportion of vehicles from a certain manufacturer (e.g., taxis or local government vehicles).

Figure 4.5 provides an example of the variation in NO_x emissions between different manufacturer groups and engine sizes, revealing the considerable differences from the mean levels of emissions for each engine size (visualised as diamonds) and vehicle category (horizontal lines). In this case, manufacturer 'families' have been used, which groups similar engine types across different manufacturers[149]. For example, the Volkswagen group (VWG) consists of Volkswagen, Audi, Skoda and Seat. With large databases of vehicle emission remote sensing data, it is possible to disaggregate the data further. For example,

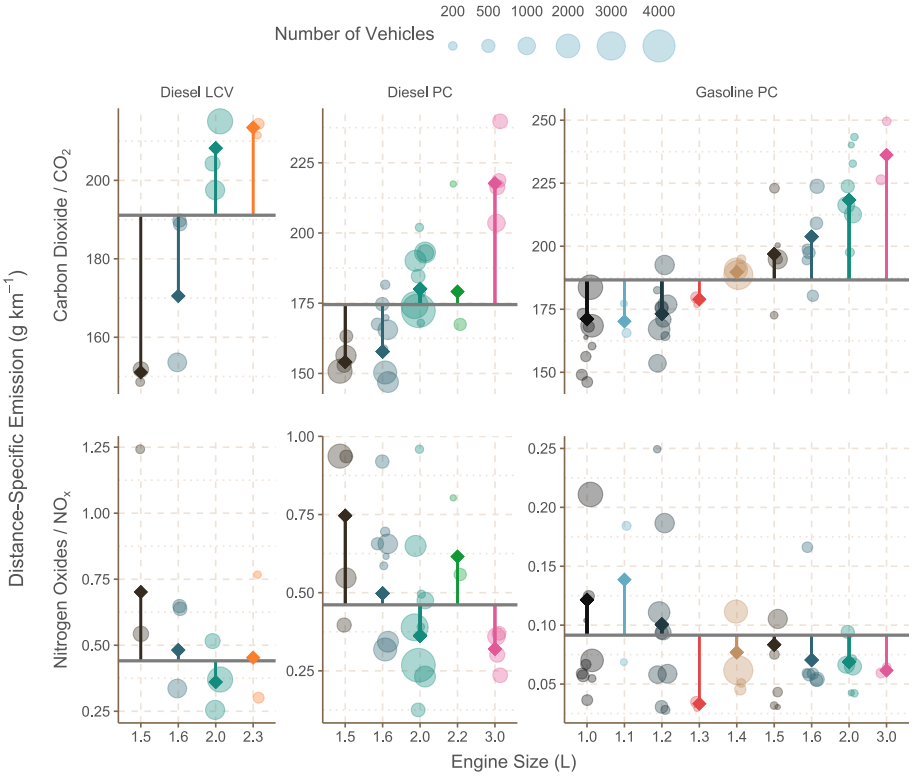

Figure 4.5: Distance-specific CO_2 and NO_x emissions (g km^{-1}) for Euro 6 light duty vehicles. Each dot represents a unique manufacturer group-engine size combination, with size proportional to the number of observations included in its calculation. The diamonds represent the weighted mean for each engine size, and the horizontal lines the weighted mean for each vehicle category (Diesel Light Commercial Vehicle, Diesel Passenger Car, Gasoline Passenger Car).

account can be taken of mandatory and voluntary software and hardware fixes applied to certain VWG vehicles following the dieselgate scandal, which have had an appreciable effect on reducing NO_x emissions from certain vehicle models; reducing emissions between 30 to 36%[101].

Emission factor models used throughout Europe do not account for manufacturer level differences in emissions and instead provide generic factors, e.g., for Euro 5 diesel passenger cars below 2.0 litre engine capacity. However, it is clear from Figure 4.5 that there can be large differences in emissions of

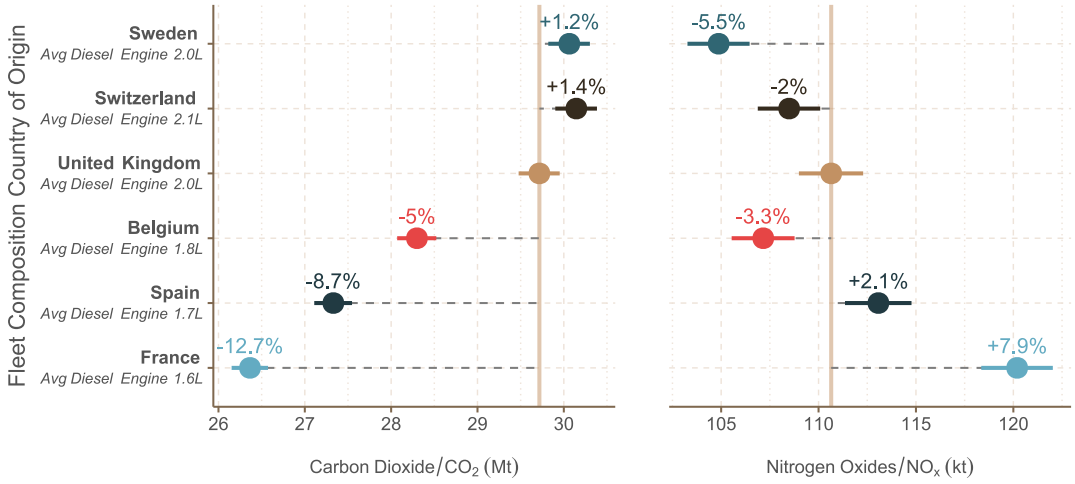

Figure 4.6: Total CO_2 and NO_x emissions from Euro 5 & 6 diesel passenger cars using UK activity data and the relative fleet composition of the UK and five other European countries. Estimations were made using manufacturer group and engine size-specific distance-specific emission factors. Each of the non-UK fleet compositions are shown relative to the UK fleet. The error bars correspond to the 95% confidence interval. Also provided are the average Euro 5 & 6 diesel car engine size.

NO_x between different manufacturers and vehicle models. Such differences would not be important if vehicle fleets were uniformly mixed throughout Europe. However, there are considerable differences between the compositions of vehicle fleets across different countries, which could have important effects on country-level emissions of different pollutants.

The results of the fleet composition analysis are shown in Figure 4.6 and demonstrate the impact of considering manufacturer-specific emissions representative of fleets in other countries. For example, estimates of NO_x from a French-like fleet of diesel cars are 7.9% higher than a UK-like fleet, despite the fact that CO_2 emission estimates decrease by 12.7%. Conversely, the NO_x estimate of a Swedish fleet mix is 5.5% lower despite a 1.2% increase in CO_2.

In general, Figure 4.6 highlights an overall trade-off at a country fleet level between CO_2 and NO_x in that as CO_2 emissions decrease, emissions of NO_x

tend to increase. The higher emissions of NO_x for a French fleet is attributable to two main factors. First, a higher proportion of small diesel engined passenger cars, which tend to have higher NO_x emissions (see Figure 4.5). In the CONOX database the average diesel passenger car engine size in the French fleet is 1695 cm^3, compared with 2152 cm^3 in Switzerland. Larger diesel-engined vehicles tend to use selective catalytic reduction for NO_x control, which has been shown to be a more effective approach when compared with lean NO_x traps[198]. Second, France has a higher proportion of manufacturers such as Renault that tend to have higher in-use emissions of NO_x compared with most other manufacturers[149].

4.5 Conclusion

With an appropriate methodology to model fuel consumption, vehicle emission remote sensing data can be used to calculate representative distance-based emission factors for a country's road transport fleet. Comparisons between emissions calculated using remote sensing and emissions inventories can lead to insightful observations and critiques of commonly used inventory development approaches, such as COPERT. For example, this study has shown that NO_x may be under-reported in the UK National Atmospheric Emissions Inventory by up to 47% in urban areas.

The size of remote sensing data sets allows for emissions to be considered on a more granular level than other approaches. This means that challenges to a national inventory can extend to what is *not* currently considered in calculations. This work highlights a significant effect between different manufacturers, which manifested in a 13.4% range in calculated NO_x emissions in the UK's Euro 5 & 6 diesel passenger car fleet purely by adopting the manufacturer compositions of different European countries. This "manufacturer effect" is not currently reflected in emission factors or inventories. This finding highlights the potential benefits of considering the fine details of vehicle fleets when at-

tempting to estimate emissions. Given the growing amount of detailed vehicle emission remote sensing data available in Europe and elsewhere[83,149,165,199], the methods adopted in the current work could be used in many other countries.

At a country level, increases or decreases in total NO_x emissions from current assumptions will likely have several implications. First, it would directly affect the evaluation of urban exposures to concentrations of NO_2, with potential impacts on meeting European Directive annual mean limits of 40 $\mu g\,m^{-3}$. Second, a country-level change in estimated NO_x emissions of around 10% compared with current assumptions would have wider air quality implications; especially for regional air quality modelling activities.

As well as influencing national-scale emissions, the effect of different manufacturers may also be important on a much more local scale. The manufacturer composition of a country is not uniform, and likely varies with wealth, culture and local geography. It will also be influenced by the preferences of businesses operating their own private fleets, such as taxi and delivery companies or public transport operators. A lack of an appreciation for the differences between manufacturers will affect the ability of local authorities to implement effective road transport emission mitigation strategies.

Chapter 5

Gasoline and Diesel Passenger Car Emissions Deterioration using On-Road Emission Measurements and Measured Mileage

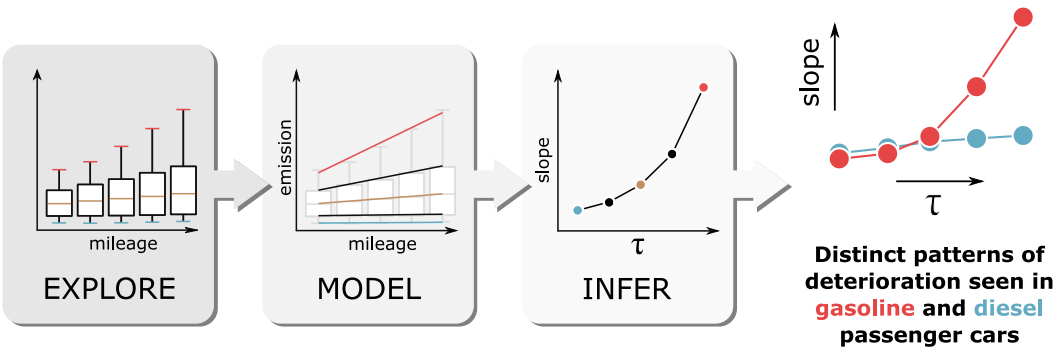

5.1 Abstract

Modern gasoline and diesel vehicles are equipped with highly effective emission control systems that result in low emissions of pollutants such as nitrogen oxides (NO_x) when new. However, with increasing age or mileage, the emissions performance of vehicles can deteriorate over time, leading to increased emissions. In this work comprehensive vehicle emission remote sensing measurements collected over a wide range of conditions is used, together with individual vehicle measured mileage to quantify vehicle emissions deterioration. A quantile regression modelling approach is used to provide a more complete understanding of the distribution of deterioration effects that is not captured by considering mean changes over time. The approach accounts for factors such as driving conditions and ambient temperature, as well as determining whether deterioration affects whole populations of vehicles or a smaller subset of them. Accounting for these factors, it was found that for most pollutants the rate of deterioration of emissions from pre-Euro 5 gasoline passenger cars is highly skewed. Between 5% and 10% of pre-Euro 5 gasoline passenger cars have emissions similar to a Euro 5 diesel car, suggesting that policies should be developed to accelerate their removal from the fleet. Furthermore, evidence is presented that there are differences between vehicle manufacturers in the way emissions of NO_x deteriorate.

5.2 Introduction

Worldwide, progressively more stringent vehicle emissions legislation has been developed to reduce the emissions of many important air pollutants from road vehicles. These developments have resulted in increasingly more sophisticated technologies being used to reduce emissions. The introduction and refinement of technologies such as the three way catalyst, particle filters and selective catalytic reduction (SCR) systems have led to considerable reductions in emission species such as nitrogen oxides (NO_x) and particulate matter[200–202]. While much of the focus of vehicle emission measurements is on newer vehicles with improved emission control technology, it is imperative to quantify the change in emissions from vehicles over their full lifetime, which can exceed 20 years. As a vehicle is driven, changes in emission behaviour can occur due to wear of engines, deterioration of emissions control systems and after-treatment technologies such as catalysts and particle filters. Moreover, with increasingly complex and sophisticated after-treatment technologies being adopted, it is important to ensure their effective performance throughout the lifetime of the vehicle.

In Europe, the legislation for the most recently regulated vehicles (Euro 6) specifies "Manufacturers' obligations", among which include an obligation that any technologies which limit tailpipe and evaporative emissions are effective "throughout the normal life of the vehicles under normal conditions of use"[47,203]. It is stipulated that, *a)*, in-service conformity testing eligibility continues until a vehicle is either 5 years old or has driven 100,000 km, and *b)*, manufacturers must conduct pollution control system durability tests to over 160,000 km of driving. Recently, the Consortium for ultra Low Vehicle Emissions (CLOVE) has suggested bringing future Euro 7 legislation in-line with US Tier 3, which defines a "normal life" for a vehicle as either 15 years or 150,000 miles (roughly 240,000 km)[55,204].

Emission factors and inventories recognise that emissions deterioration occurs and attempt to provide pragmatic approaches to account for such deteri-

oration. In Europe, the joint European Monitoring and Evaluation Programme (EMEP)/European Environment Agency (EEA) air pollutant emission inventory guidebook 2019 details the use of correction factors to account for emission deterioration due to vehicle age[45]. Importantly, deterioration factors are only applied to gasoline vehicles and it is assumed that the carbon monoxide (CO), nitrogen oxides (NO_x) and hydrocarbon emissions of Euro 3 and later gasoline cars and light commercial vehicles stop deteriorating at 160,000 km. The Handbook Emission Factors for Road Transport (HBEFA) version 4.1 updated its deterioration factors for CO, NO_x and hydrocarbon emissions[205] based on vehicle emission remote sensing data from the large European CONOX database[99]. The updated deterioration functions cover Euro 1 through to projected Euro 7 diesel and gasoline light duty vehicles within a mileage range of 0 to 200,000 km. They report that NO_x emissions are less than 1.5 times higher for all Euro standards of diesel vehicles at 200,000 km compared to 50,000 km. Gasoline vehicles, however, are found to be over 3 times as high for Euro 3 and 2.5 times as high for Euro 5, though the ratio for Euro 6 vehicles is only around 1.25.

Emission deterioration functions are typically based on a limited number of chassis dynamometer tests in a limited range of mileages[45,206]. An unavoidable aspect of in-lab and even on-board methods (e.g., Portable Emission Measurement Systems (PEMS)) is a small sample size owing to the time and cost requirements to measure a vehicle. Furthermore, these methods are typically used to measure newer vehicles, so there are sparse data for older or higher mileage vehicle emissions. Using these methods to get a broad sample of vehicles of different model years, meeting different Euro standards, and from different manufacturers, would be prohibitively expensive and time consuming.

Vehicle emission remote sensing has the potential to overcome some of these issues. The non-selective, real-world nature of remote sensing ensures that, with a sufficiently large sample size, the full spectrum of age, mileage and emission deterioration of a fleet will be captured. Furthermore, with the

large data sets obtained using remote sensing, multivariate statistical analysis can be conducted to isolate the effect of deterioration from other influences such as driving characteristics (e.g., instantaneous engine power) or ambient conditions. Indeed, much of the literature on emission deterioration focuses on the use of vehicle emission remote sensing[104,105,169–171,207], although a smaller number of studies using other methods such as PEMS[208,209] and chassis dynamometers[210–212] do feature. An important limitation of many of these remote sensing studies is that individual vehicle mileage is not available, leading to vehicle age being a frequent proxy. For example, in Borken-Kleefeld and Chen [169] and Chen and Borken-Kleefeld [170] the difference between the year of measurement and the year of first registration is taken to be a vehicle's age, which is then used to estimate mileage using statistics from the Swiss government.

Deterioration factors as used in emission factor development generally provide fleet-average linear relationships to correct an emission from a vehicle when assumed to be new. However, these factors do not capture potentially important information on the nature of deterioration, such as whether all vehicles tend to deteriorate similarly over time or whether the changes are dominated by significant deterioration from relatively few vehicles. These considerations are important from a policy perspective because different responses might be required depending on the nature of emissions deterioration. For example, it is arguably more efficient and cost effective to identify and fix (or remove) a small population of high emitters than it is to deal with a large population of vehicles that deteriorate by a more modest amount. To understand these issues, there is a need to consider large populations of vehicles and to establish the full distribution of effects rather than a mean response.

In this study, comprehensive vehicle emission remote sensing data are paired with measured vehicle mileage from individual vehicles using data from annual passenger car technical inspections. These paired data are used to study the deterioration of emissions from passenger cars, as well as consider the

appropriateness of vehicle age as a mileage proxy. This study uses measured mileage data from 197,000 gasoline and diesel passenger cars. The nature of any deterioration effects on emissions is complex and is not fully described by simple relationships that relate mileage and emissions. Therefore, this study adopts a quantile regression approach to consider the entire conditional distribution of effects. This approach allows for the control of other factors such as vehicle driving conditions and ambient temperature which also affect measured emissions. Finally, with large sample sizes available, manufacturer effects on how emissions deteriorate with mileage are considered.

5.3 Materials and Methods

5.3.1 Vehicle Emission Remote Sensing

The principles of vehicle emission remote sensing have been described in extensive detail elsewhere[79,145], so only a short summary is provided here. Remote sensing is a non-obtrusive, curbside method for measuring real-world vehicle emissions. A remote sensing device is typically deployed to be as unobstructive as possible, ensuring vehicles can drive through the set-up unimpeded. As a vehicle drives through, each individual module of the remote sensing device simultaneously activates. These are an ultraviolet/infrared (UV/IR) source and detector to measure exhaust emissions, optical speed-acceleration bars to capture instantaneous driving conditions, a camera to photograph number plates, and sensors to record ambient conditions such as temperature, pressure and relative humidity. As the triggering of all these modules is achieved in just a fraction of a second, remote sensing observations are often referred to as 'snapshots' of a vehicle's journey.

Spectrometry is achieved with a collinear beam of IR and UV light. Carbon monoxide (CO), carbon dioxide (CO_2), hydrocarbons and a background reference are measured using the IR component, and ammonia (NH_3), nitrogen

oxide (NO) and nitrogen dioxide (NO_2) by the UV component. 100 measurements are taken of each plume in just half a second. Pollutant concentrations are typically given as a ratio to CO_2, which is assumed to remain constant as the plume disperses. These ratios can be used to calculate fuel-specific (g kg^{-1}) emissions[79].

The photographed vehicle number plates can be cross-referenced with vehicle technical databases to obtain key information about the measured vehicles, such as fuel type, emissions standards and manufacturers. In this study, technical information was sourced from the Driver and Vehicle Licensing Agency and the Society of Motor Manufacturers and Traders Motor Vehicle Registration Information System. These data were obtained from the commercial supplier CDL Vehicle Information Services Ltd.[85].

An important aspect of the current work is the use of measured mileage information. While vehicle age is readily available, it is not an ideal metric for emissions deterioration. Data relating to the total mileage of each vehicle at its last annual "MOT" test was obtained through CDL for vehicles greater than three years old. Vehicles younger than three years do not require an annual technical inspection in the UK. As a result, the proportion of mileage information available for Euro 6 vehicles (introduced in 2016) is lower than that for older Euro standards (24% of Euro 6 observations have associated mileage information, compared to 63–76% for Euro 3–5). The date at which the mileage information is available and the emissions measurement date could be up to 12 months different, i.e., the measured mileages available would tend to underestimate the actual mileage at the time the emissions measurements were made.

Vehicle emission measurements were conducted between 2017 and 2020 at 39 sites across 14 regions in the United Kingdom mainly using the Opus *AccuScan* RSD 5000[76], augmented with a relatively small number of measurements using the Denver FEAT instrument[63]. Previous literature has shown good agreement between the two remote sensing devices, so the combination of

these data sets is appropriate[82]. Of interest to this study are measurements of diesel passenger cars or gasoline passenger cars. 197,000 of these measurements include mileage data from annual technical inspection "MOT" tests[100] and are therefore relevant to this study. Note that these are not 197,000 unique vehicles; available number plate data shows that around 13% of vehicles in the data set were measured twice, 4% three times, and 3% four or more times.

A statistical summary of these measurements is provided in Table 5.1. The speed ranges reflect that remote sensing is typically conducted in urban conditions, but this is not likely to be of detriment to the objectives of this study; it is unlikely that deterioration patterns would meaningfully differ under rural, motorway or any other driving conditions. Measurements being taken in urban areas may mean that a small proportion include cold start emissions, though this is unlikely as exhaust after-treatment technologies tend to reach effective operating temperatures in a few minutes[193]. The majority of emission measurements can therefore be assumed to be of hot, stabilised emissions.

5.3.2 Statistical Methods

While ordinary least squares (OLS) linear regression may provide some insight into emission deterioration, it is intuitively likely that different vehicles deteriorate at different rates. An important question to address is whether it is the case that there is a general deterioration in the emissions performance of all vehicles or whether there is a smaller population of much higher emitters that have a disproportionate effect. For this reason, a quantile regression-based approach was used, which can account for the full distribution of responses and not just the mean response that is considered by OLS.

Linear quantile regression can be understood in analogue to linear OLS regression; while an OLS regression line minimizes the sum of the squared differences between it and the data, a quantile regression line ensures that some proportion of the data are below and above it. For example, the quantile

Characteristic	Euro 3	Euro 4	Euro 5	Euro 6
Gasoline Passenger Cars				
# Measurements	22,952	36,327	38,855	10,776
# Manufacturer Groups	23	23	20	20
(with ≥ 100 Measurements)	18	18	15	13
Vehicle & Ambient Characteristics [1]				
VSP (kW t^{-1})	7.61 ±7.65	7.80 ±7.07	8.12 ±6.88	8.96 ±5.08
Speed (km h^{-1})	36.4 ±9.2	36.6 ±9.3	37.0 ±9.5	38.4 ±9.4
Acceleration (km h^{-1} s^{-1})	0.96 ±2.33	0.99 ±2.19	1.02 ±2.15	1.07 ±1.66
Ambient Temp. (K)	287.9 ±5.4	288.1 ±5.2	288.2 ±5.2	288.2 ±4.8
Cumulative Mileage (10^4 km)	15.7 ±6.9	12.2 ±5.6	7.1 ±3.9	4.6 ±2.5
Vehicle Age (years)	14.4 ±1.6	10.4 ±1.8	6.0 ±1.9	4.1 ±1.0
Remote Sensing Device [2]				
OPUS RSD 5000	20,387 (89%)	33,236 (91%)	36,181 (93%)	10,501 (97%)
Denver FEAT	2,565 (11%)	3,091 (8.5%)	2,674 (6.9%)	275 (2.6%)
Diesel Passenger Cars				
# Measurements	9,143	24,030	44,442	10,475
# Manufacturer Groups	22	22	21	18
(with ≥ 100 Measurements)	14	17	16	12
Vehicle & Ambient Characteristics [1]				
VSP (kW t^{-1})	8.26 ±8.38	8.09 ±7.70	8.23 ±7.56	8.72 ±6.14
Speed (km h^{-1})	36.3 ±9.4	36.5 ±9.8	36.6 ±9.8	37.1 ±9.8
Acceleration (km h^{-1} s^{-1})	1.06 ±2.38	1.07 ±2.26	1.14 ±2.27	1.19 ±1.79
Ambient Temp. (K)	288.2 ±5.5	288.1 ±5.4	287.9 ±5.2	287.8 ±4.9
Cumulative Mileage (10^4 km)	24 ±13	19 ±10	11 ±7	7 ±5
Vehicle Age (years)	14.0 ±1.5	10.2 ±1.8	5.7 ±1.8	3.9 ±1.2
Remote Sensing Device [2]				
OPUS RSD 5000	8,223 (90%)	21,894 (91%)	40,692 (92%)	10,146 (97%)
Denver FEAT	920 (10%)	2,136 (8.9%)	3,750 (8.4%)	329 (3.1%)

Table 5.1: A statistical summary of the vehicle emission remote sensing data, split into diesel and gasoline passenger cars. Statistics provided are only for measurements with an associated mileage value. Statistics presented: [1]Mean (Standard deviation); [2]Number of measurements (Percentage of the column total).

regression line for the median ($\tau = .50$) ensures that half of the data are above it and half below. For the 75th percentile ($\tau = .75$), 75% of the data would be found below the line and 25% would be above. A more thorough description of quantile regression can be found in Appendix D.

In this study, quantile regression — using the `quantreg` R package[136] — is used to explore the relationship, *a)*, between vehicle age, AGE, and cumulative vehicle mileage, MIL and, *b)*, between cumulative vehicle mileage and fuel-specific (g kg^{-1}) emissions. In the former case, a second-order polynomial was used. This is given in Equation 5.1, where $\hat{\mu}(\tau \mid AGE)$ represents the predicted quantile of vehicle mileage.

$$\hat{\mu}(\tau \mid AGE) = \hat{\beta}_0 + \hat{\beta}_1(\tau) \cdot AGE + \hat{\beta}_2(\tau) \cdot AGE^2 \tag{5.1}$$

When examining emissions, four air pollutants are initially explored: nitrogen oxides (NO_x), carbon monoxide (CO), ammonia (NH_3) and particulate matter (PM, measured by the OPUS remote sensing device using percentage UV opacity). Note that NH_3 is only pertinent to the gasoline vehicles and Euro 6 diesel vehicles, the latter of which have after-treatment systems that use SCR systems which can result in emissions of NH_3. When fitting models, multivariate analysis is used to predict fuel-specific emissions using vehicle mileage and additional covariates with known influences on vehicle emissions. The key covariate is vehicle specific power, VSP (Equation 5.2), though for diesel NO_x emissions ambient temperature, AT, is also included (Equation 5.3, [110]). B-splines, denoted using f, are used to smooth these covariates, both set to 3 degrees of freedom.

An interaction effect with some vehicle category, VC, is also included. The first category considered is Euro standard, to gain an understanding for the potential differences in deterioration as emission control technology has changed with legislation. The second category considered is vehicle manufacturer group, used to to examine the differences in deterioration between the varying techno-

logies employed by different vehicle manufacturers. In this second case, models are fit separately for each of Euro 3, 4 and 5; Euro 6 is excluded due to limited data and range of mileage.

$$\begin{aligned}\hat{\mu}(\tau \mid MIL, VSP, VC) &= \hat{\beta}_{0,VC}(\tau) + \hat{\beta}_{MIL,VC}(\tau) \cdot MIL \\ &\quad + f_{VSP,VC}(\tau, VSP) \qquad (5.2)\\ \hat{\mu}(\tau \mid MIL, VSP, AT, VC) &= \hat{\beta}_{0,VC}(\tau) + \hat{\beta}_{MIL,VC}(\tau) \cdot MIL \\ &\quad + f_{VSP,VC}(\tau, VSP) \\ &\quad + f_{AT,VC}(\tau, AT) \qquad (5.3)\end{aligned}$$

Data processing was carried out using the R programming language[121], with uncertainties calculated and term significance estimated using bootstrap resampling. The `tidymodels`[133,213] collection of R packages was used for the bootstrapping simulations. The `bootstrap()` function was used with 100 resamples with the sampling stratified (using the `strata` argument) by the relevant interaction term (Euro standard or manufacturer group) and otherwise default parameters. The stratification by the vehicle category ensures proportionally smaller categories (i.e. Euro 3 or 6 vehicles, or more niche manufacturers) are well represented in the bootstrap samples.

The "percentile" method was used to calculate 95% confidence intervals around the coefficients. If the 95% confidence interval of the bootstrapped mileage coefficients includes 0, the p-value is taken to be less than .05 and the term (and therefore the vehicle category's rate of deterioration) is judged to be insignificant. Furthermore, if the 95% confidence intervals of the *difference* between any given terms includes 0, it is taken that they are not significantly different from one another.

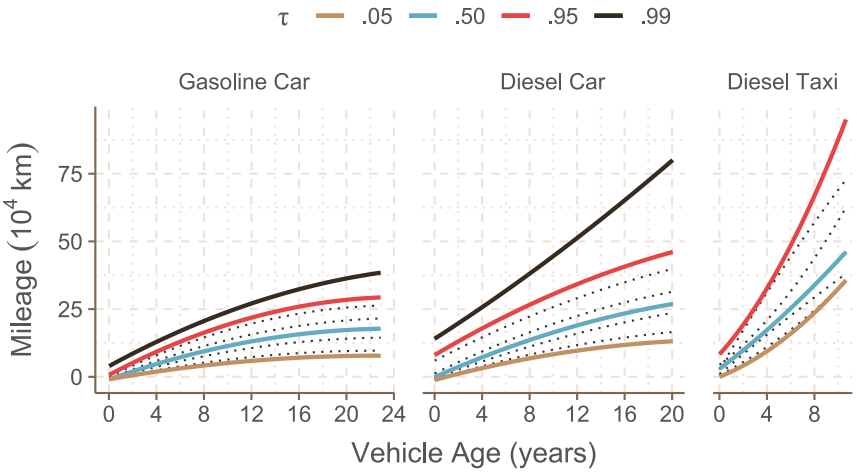

Figure 5.1: Second-order polynomial quantile regression fits for cumulative vehicle mileage as a function of vehicle age at the date of their MOT (Equation 5.1), where $\tau \in \{.05,.10,.30,.50,.70,.90,.95,.99\}$. $\tau \in \{.05,.50,.95,.99\}$ are solid and labelled; the dotted lines represent the unlabelled quantiles. $\tau = .99$ is not shown for the taxis due to the limited number of observations; the 99th percentile would represent just 5 vehicles.

5.4 Results and Discussion

5.4.1 Mileage and Age Characteristics for Light Duty Vehicles

In this section the potential drawbacks of using vehicle age as a measure of emissions deterioration are considered, highlighting the benefits of this study's use of measured mileage. Second-order polynomial quantile regression fits for measured cumulative vehicle mileage as a function of vehicle age from the remote sensing data are shown in Figure 5.1. Diesel London taxis ("black cabs", n = 556, 0.5% of the measured diesel passenger car fleet) have unique technical data relating to their body type so can be treated separately to the rest of the diesel passenger cars.

There is a clear distinction between the three vehicle types. Gasoline passenger cars are among the oldest of the three categories, but have the lowest maximum mileage. The maximum age decreases and maximum mileage increases progressing through the gasoline cars, the diesel vehicles, and finally

the taxis.

The quantile regression fits shown in Figure 5.1 highlight a weakness of using simple linear regression to derive mileage from vehicle age, in that it would not fully represent the underlying and significant distribution of cumulative vehicle mileages of vehicles of the same age. For example, the average age of a vehicle in the vehicle emission remote sensing data set is around 8 years. Using a second-order polynomial ordinary least squares (OLS) model, 8 year-old gasoline passenger cars have driven 98,000 km. This is similar to the median vehicle according to quantile regression, which has driven 94,300 km (−3.8% of the OLS). However, the lowest mileage 5% of these vehicles have only driven 41,700 km (−57.4% of the OLS), whereas the 5% highest mileage have driven 163,000 km (+66.3% of the OLS). The top 1% have driven 206,000 km (+110%). Similarly, an ordinary least squares approach indicates an 8 year-old diesel non-taxi passenger car has driven 148,000 km. The *median* vehicle from quantile regression has driven 136,000 km (−8.1% of the OLS), the bottom 5% have driven 68,100 km (−54.0%), the top 5% 266,000 km (+79.7%), and the top 1% 383,000 km (+157%).

While it could be argued that the "average" vehicle modelled using ordinary least squares is similar to the median vehicle modelled using quantile regression, relying on OLS regression ignores a significant distribution of vehicle mileage at any given vehicle age. A straightforward assumption that mileage increases linearly with age is useful in the absence of measured mileage data, but is not optimal in representing the inherent distributions of mileages that exist. This is particularly relevant if considering taxi fleets or other commercial vehicle fleets that may likely have a distinct mileage-age relationship, as clearly demonstrated in Figure 5.1. Moreover, if high mileage vehicles have emissions that are significantly different from average-age vehicles, then the estimated emissions response will also be erroneous.

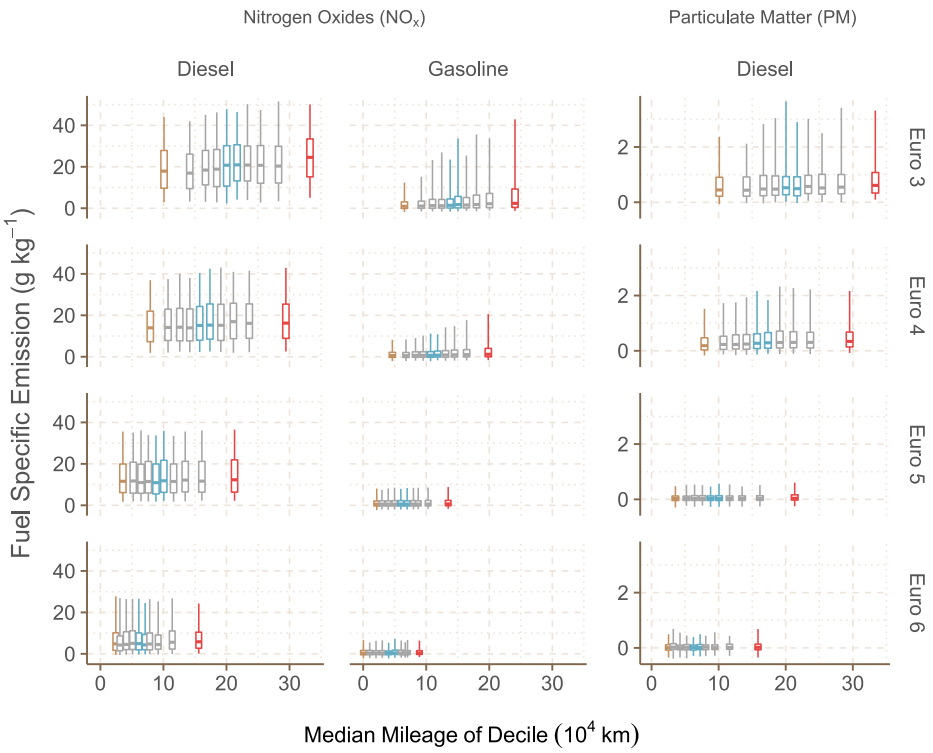

Figure 5.2: Fuel-specific emissions (g kg^{-1}) of NO_x and PM as a function of vehicle mileage. The box plots show the distribution of emissions per decile of mileage, with each decile plotted at its median mileage value. The lowest, highest and middle mileage deciles are coloured to aid in comparison between panels. The hinges of the boxplots represent the 25th and and 75th emission percentiles, and the whiskers the 5th and 95th percentiles.

5.4.2 Exploratory Analysis of Emission Deterioration

First, the relationship between vehicle mileage and emissions is explored without taking account of the influence of other factors such as ambient temperature and engine power demand. The distribution of vehicle NO_x, CO, NH_3 and PM emissions at different cumulative mileages are given in Figure 5.2 and Figure 5.3.

These distributions highlight the benefit of a quantile regression-based approach. The median intensity of emissions from the species typically increase at higher mileage deciles to various extents, which suggests the presence of

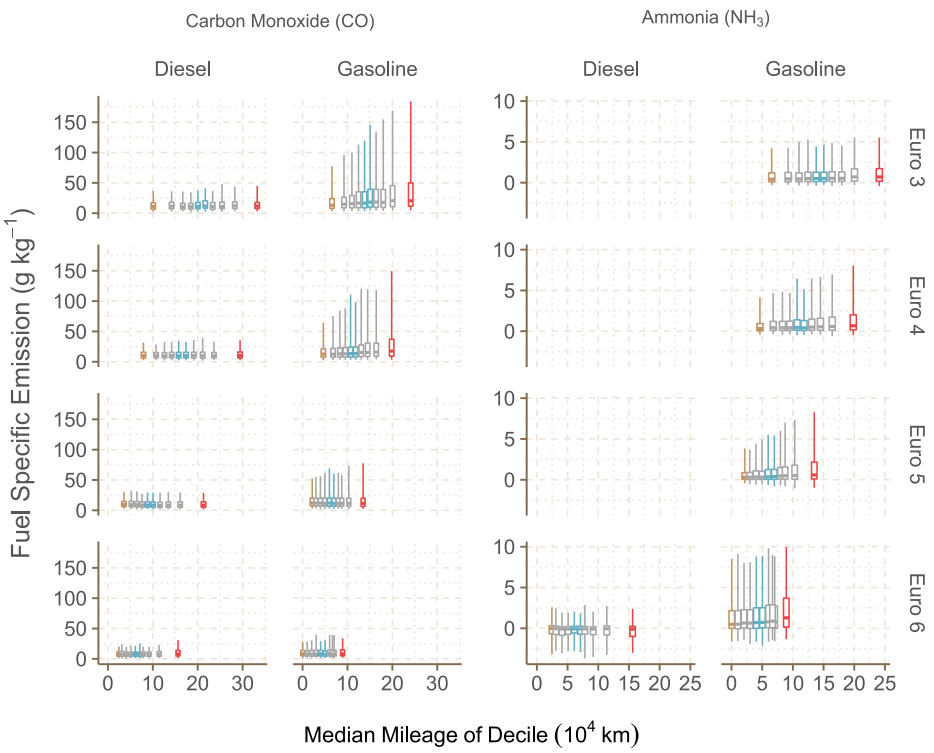

Figure 5.3: Fuel-specific emissions (g kg^{-1}) of CO and NH_3 as a function of vehicle mileage. The box plots show the distribution of emissions per decile of mileage, with each decile plotted at its median mileage value. The lowest, highest and middle mileage deciles are coloured to aid in comparison between panels. The hinges of the boxplots represent the 25th and and 75th emission percentiles, and the whiskers the 5th and 95th percentiles.

a mileage-based deterioration effect. More relevant for quantile regression, it also appears that for some species-fuel type combinations the spread of emission values (seen in both ranges between the 25th and 75th, and the 5th and 95th percentiles) appears to increase at higher deciles of mileage. This suggests that the *rate* of increase in emissions is itself greater at higher emission quantiles, indicating that an ordinary least squares linear regression may not fully represent the true range of responses different emitters have to increasing cumulative mileage.

From this exploratory analysis, it is clear that the species behave distinctively

from one another with respect to mileage deterioration. The four species, NO_x, PM, CO and NH_3, will now be discussed in turn.

NO_x emissions show clear differences between the two vehicle types. The five visualised quantiles of fuel-specific NO_x in diesel vehicles all appear to show a gentle increase from the lowest to highest mileage deciles across all Euro standards, with the exception of the 95th percentile of Euro 6. The large interquartile ranges seen in the diesel passenger cars (6.9–19.5 g kg^{-1} across all Euro standards) are consistent with the wide range of NO_x performance in diesel vehicles widely reported in the literature[1,83,112,199].

The distributions of the gasoline passenger car NO_x emissions differ considerably from the diesel passenger cars and between the Euro standards. Euro 5 and 6 gasoline vehicles show a flat trend across the mileage deciles, and very small interquartile ranges (2.4–2.7 and 1.8–2.2 g kg^{-1} respectively). Conversely, the Euro 3 and 4 gasoline vehicles show relatively larger interquartile ranges (3.2–8.8 and 2.4–4.0 g kg^{-1}), flatter trends for the lower NO_x quantiles and much steeper trends in the higher NO_x quantiles. The differences in the 95th percentile of fuel-specific NO_x between the first and tenth mileage deciles are +30.5 g kg^{-1} in Euro 3, +12.3 g kg^{-1} for Euro 4, +0.7 g kg^{-1} for Euro 5 and -0.3 g kg^{-1} for Euro 6. For comparison, the highest equivalent value for the diesel vehicles is seen in Euro 3 at +6.11 g kg^{-1}. All of this suggests a small proportion of high NO_x emitters among the Euro 3 and 4 gasoline fleets that are particularly sensitive to deterioration.

An unavoidable aspect of the data when making comparisons between Euro standards is that Euro 5 and 6 data are for a much lower range of cumulative mileage than the Euro 3 and 4 data, owing to the former vehicles being much younger. It is therefore possible that at higher cumulative mileages that are present in the remote sensing data set, Euro 5 and 6 gasoline passenger cars may show similar patterns of deterioration to the Euro 3 and 4 vehicles. However, it should be noted that there is overlap between the cumulative mileages of the four gasoline Euro standards. Even up to 135,000 km of cumulative mileage

(representing the tenth mileage decile of Euro 5 and fifth decile of Euro 3), the Euro 3 and 4 distributions are widening, suggesting a deterioration effect, whereas the Euro 5 and 6 distributions remain flat, suggesting well controlled emissions.

A limited number of recent remote sensing studies focus on particulate matter emissions[59,89], with Chen et al. [59] noting that black smoke emissions have been following PM legislation limits, unlike many gaseous tailpipe emissions which have continued to exceed their respective limits. Gautam et al. [118] notes that measuring exhaust PM close to zero is difficult, and that "the focus of using [remote sensing] should be to detect failing or missing DPFs with high confidence." To this end, Gautam et al. [118] sets a threshold of 1.5 g kg^{-1} of PM as a flag for a compromised diesel particulate filter (DPF), which is well outside of the distributions of the DPF-equipped Euro 5 and 6 vehicles in Figure 5.2. The fuel-specific PM emissions of Euro 5 and 6 diesel passenger cars appear to be well controlled overall, with a flat trend across mileage deciles at most PM quantiles. However, there does appear to be evidence of deterioration at higher quantiles for Euro 3 and 4 vehicles, which were not required to be equipped with a DPF (although some Euro 4 vehicles were[59]).

Carbon monoxide is generally understood to be well controlled and CO emissions are typically comfortably below emission limits[214]. Both gasoline and diesel vehicles appear to show similar trends in Figure 5.3 — the five fuel-specific CO quantiles all increase at higher mileage deciles, with the difference between the lowest and highest deciles being greatest at $\tau = .95$, not unlike the trends seen in Euro 3 and 4 gasoline NO_x emissions. The key difference between the gasoline and diesel passenger cars is the lower absolute emissions of CO for diesel vehicles, particularly in the older Euro standards.

Recently, more attention has been paid toward ammonia emissions using remote sensing[30,215], including limited analysis on their deterioration[31]. There is some evidence of the deterioration of ammonia emissions for gasoline vehicles which is most pronounced in Euro 4 and 5. The gasoline vehicles tend to show

a relatively low median but high 95th percentile fuel-specific NH_3 emission, reflecting the skewed nature of NH_3 emissions seen in Zhang et al. [215]. There appears to be no significant deterioration effect for the Euro 6 diesel passenger cars, suggesting that SCR-equipped vehicles are robust as far as NH_3 emissions are concerned.

Statistical modelling has some clear advantages over this sort of exploratory and visual analysis as it can be difficult to make real-world inferences from simple statistical tools like box plots. Firstly, there is arbitrariness that often comes with binning continuous data like vehicle mileage. More importantly, a key limitation is the inability to easily isolate the influences of other variables known to be important — in this case the instantaneous driving condition of the vehicle and ambient conditions. A modelling framework removes some of this arbitrariness and allows for the control of other covariates, as well as providing what could be described as a "rate of deterioration" as a function of vehicle mileage.

5.4.3 Multivariate Statistical Modelling

The introduction of new Euro standards tends to be associated with improvements in emissions control technologies and it is therefore important to consider how emissions deteriorate within a single Euro standard. Two pollutants were chosen to be further examined in a multivariate framework; NO_x due to being of significant interest owing to its air pollution impacts, and PM due to the considerable health effects associated with fine particulate matter.

Deterioration effects over the normal lifetime of a vehicle are first considered, i.e., after 160,000 km of driving under Euro 6 legislation[47]. The models given in Equation 5.2 for gasoline NO_x and diesel PM and Equation 5.3 for diesel NO_x were fit with $\tau \in \{.05,.10,.30,.50,.70,.90,.95\}$ and used to predict emissions at 0 and 160,000 km of cumulative mileage. VSP and ambient temperature were taken to be 7 kW t^{-1} and 288 K respectively, equal to the mean value of the

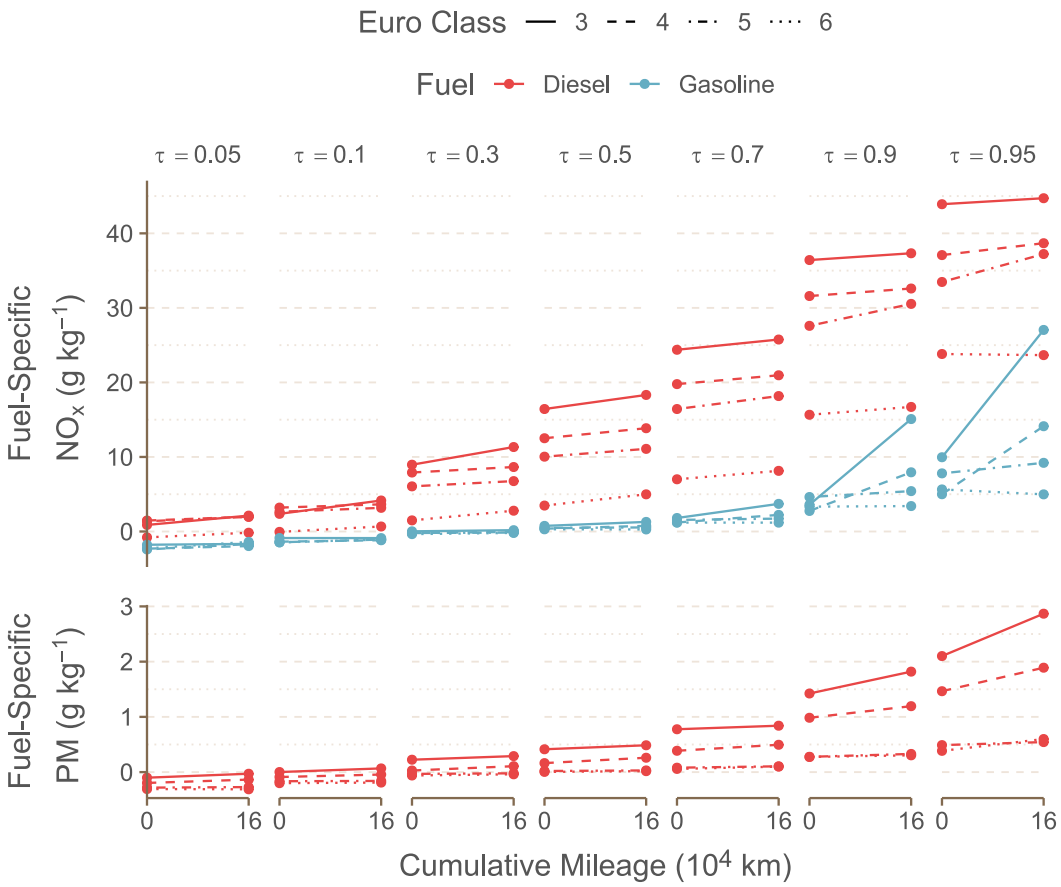

Figure 5.4: Plot showing the modelled linear deterioration of passenger cars from 0 to 160,000 km of cumulative mileage (a vehicle's "normal life" under Euro 6 legislation[47]).

variables in the remote sensing data set. Figure 5.4 presents the predicted absolute deterioration of the fuel-specific NO_x and PM emissions for different quantiles for gasoline and diesel passenger cars. These values are also tabulated in Table 5.2.

The highest quantiles of Euro 3 and 4 gasoline vehicles increase by 17.1 and 9.1 g kg^{-1}, respectively. To put these values in context, the mean emissions of NO_x from Euro 3, 4, 5 and 6 passenger cars are 5.3, 2.9, 1.9 and 1.5 g kg^{-1} for gasoline and 21.0, 17.1, 15.9 and 8.2 g kg^{-1} for diesel. This analysis of absolute deterioration reveals some important characteristics for NO_x emissions. First,

Pollutant	Fuel	τ	Euro 3	Euro 4	Euro 5	Euro 6
NO_x	Diesel	.05	+1.25	+0.52	+0.58	+0.62
		.10	+1.79	+0.44	+0.53	+0.72
		.30	+2.37	+0.74	+0.71	+1.30
		.50	+1.89	+1.34	+1.05	+1.51
		.70	+1.37	+1.18	+1.74	+1.13
		.90	+0.91	+1.01	+2.94	+1.05
		.95	+0.80	+1.59	+3.75	−0.15
	Gasoline	.05	+0.12	+0.35	+0.72	+0.86
		.10	−0.01	+0.19	+0.36	+0.38
		.30	+0.15	+0.18	+0.06	+0.16
		.50	+0.54	+0.38	+0.06	−0.02
		.70	+1.90	+1.02	+0.18	−0.01
		.90	+11.5	+5.19	+0.79	+0.08
		.95	+17.1	+9.12	+1.41	−0.66
PM	Diesel	.05	+71.2	+60.1	+10.0	−4.58
		.10	+65.7	+45.0	+5.56	+10.5
		.30	+65.3	+78.1	+10.5	+21.8
		.50	+72.3	+97.3	+10.5	+13.4
		.70	+64.2	+108	+25.1	+41.5
		.90	+396	+210	+52.5	+29.4
		.95	+767	+425	+54.8	+214

Table 5.2: The absolute change in passenger car g kg^{-1} NO_x and mg kg^{-1} PM as cumulative mileage increases from 0 to 160,000 km for different emission quantiles, fuel types, and Euro standards.

that the rate of deterioration of NO_x emissions is greater for a population of high-emitting gasoline passenger cars compared to diesel passenger cars. Second, Euro 5 and 6 gasoline passenger cars appear to have much better NO_x control than Euro 3 or 4 vehicles over the same range of cumulative mileage.

The trends in particulate matter for diesel vehicles reveal some interesting characteristics. For context, Euro 3 legislation did not require the use of a diesel particulate filters (DPF) whereas Euro 5 onward did. DPF technology became more widespread for Euro 4 vehicles even though they were not necessary, so the Euro 4 observations in the remote sensing data will contain a mixture of DPF and non-DPF-equipped vehicles[59]. The results show that there are small populations of Euro 3 and Euro 4 diesel passenger cars where there is evidence of increased emissions of PM due to deterioration. However, Euro 5 and 6 vehicles appear to be well-controlled, suggesting that DPF technology provides a robust way of controlling particulate emissions over the lifetime of a vehicle.

One benefit of a statistical modelling approach is being able to comment directly on the magnitude and statistical significance of the rates of deterioration (represented by the models' mileage coefficients), which can provide a more comprehensive assessment of deterioration than is shown in Figure 5.4. The magnitudes and bootstrapped confidence intervals of these rates of deterioration are tabulated in Table 5.3 and Table 5.4, and are briefly discussed below. When tabulated and presented in-text, deterioration rates are provided with their 95% confidence interval in parentheses and are expressed in the units of g kg^{-1} per 10^4 km driven for NO_x and mg kg^{-1} per 10^4 km driven for PM.

Gasoline passenger cars can be considered in two groups. First, Euro 3 and 4 gasoline vehicles show an exponential increase in their rates of deterioration as a function of τ. All terms are significant with the exception of $\tau \in \{.05,.10\}$ for Euro 3 vehicles. These Euro standards both reach maxima at $\tau = .95$, at 1.06 (0.87–1.3) and 0.57 (0.49–0.67), respectively. Second, the Euro 5 and 6 gasoline vehicles show a relatively flat trend in rates of deterioration that are almost all insignificant. At higher quantiles ($\tau \geq .50$), Euro 5 and 6 are the only Euro

τ		Euro 3		Euro 4		Euro 5		Euro 6
Diesel Passenger Cars								
.05	*	0.075	*	0.032	*	0.037	*	0.037
		(0.054–0.12)		(0.014–0.047)		(0.027–0.058)		(0.007–0.065)
.10	*	0.12	*	0.025	*	0.033	*	0.046
		(0.08–0.15)		(0.013–0.036)		(0.019–0.043)		(0.019–0.071)
.30	*	0.15	*	0.046	*	0.043	*	0.08
		(0.12–0.18)		(0.024–0.068)		(0.027–0.063)		(0.053–0.1)
.50	*	0.12	*	0.087	*	0.063	*	0.094
		(0.097–0.15)		(0.064–0.11)		(0.039–0.093)		(0.054–0.12)
.70	*	0.085	*	0.079	*	0.11	*	0.07
		(0.053–0.12)		(0.048–0.11)		(0.07–0.15)		(0.0052–0.11)
.90		0.054	*	0.06	*	0.19		0.039
		(-0.01–0.12)		(0.011–0.12)		(0.14–0.24)		(-0.11–0.25)
.95		0.021		0.082	*	0.24		-0.012
		(-0.085–0.099)		(-0.034–0.16)		(0.18–0.34)		(-0.3–0.22)
Gasoline Passenger Cars								
.05		0.0066	*	0.021	*	0.046	*	0.056
		(-0.004–0.017)		(0.013–0.033)		(0.03–0.058)		(0.033–0.079)
.10		-0.00046	*	0.012	*	0.024	*	0.024
		(-0.006–0.005)		(0.005–0.021)		(0.013–0.033)		(0.011–0.046)
.30	*	0.0099	*	0.011		0.0043		0.0091
		(0.005–0.014)		(0.008–0.015)		(0.000–0.007)		(-0.002–0.019)
.50	*	0.034	*	0.023		0.0039		-0.0013
		(0.023–0.044)		(0.018–0.029)		(-0.002–0.010)		(-0.013–0.015)
.70	*	0.12	*	0.064		0.013		-0.00076
		(0.094–0.14)		(0.053–0.073)		(-0.003–0.022)		(-0.022–0.019)
.90	*	0.71	*	0.32	*	0.052		0.0041
		(0.6–0.83)		(0.28–0.36)		(0.001–0.09)		(-0.083–0.081)
.95	*	1.1	*	0.56	*	0.087		-0.034
		(0.87–1.3)		(0.49–0.67)		(0.029–0.17)		(-0.19–0.17)

Table 5.3: Mileage coefficients for NO_x (g kg^{-1} per 10^4 km driven) from the quantile regression emission models. 95% confidence intervals are shown in parentheses beneath each coefficient. Significant coefficients, for which 0 is not within the 95% confidence interval, are highlighted with an asterisk (∗).

τ		Euro 3		Euro 4		Euro 5		Euro 6
Diesel Passenger Cars								
.05	*	4.5	*	3.7		0.7		0.011
		(2.9–6.6)		(2–5)		(-1.6–2)		(-4.4–5.9)
.10	*	4.3	*	2.8		0.38		0.87
		(2.7–5.9)		(2.4–3.9)		(-0.87–1.2)		(-2.5–3.4)
.30	*	4	*	5.1	*	0.68		1.4
		(2.8–5.2)		(4.3–5.8)		(0.38–1)		(-0.055–2.3)
.50	*	4.9	*	6.1	*	0.65	*	0.9
		(2.7–6.8)		(4.9–7.4)		(0.38–0.9)		(0.075–1.5)
.70		4.4	*	6.8	*	1.6	*	2.5
		(-0.45–8.3)		(5–8.6)		(1.1–2)		(0.83–3.7)
.90	*	25	*	14	*	3.2		2.2
		(9.5–41)		(7.1–21)		(1.2–4.7)		(-1.5–8.4)
.95	*	53	*	30		3		12
		(27–86)		(16–46)		(-0.18–6.3)		(-0.8–24)

Table 5.4: Mileage coefficients for PM (mg kg^{-1} per 10^4 km driven) from the quantile regression emission models. 95% confidence intervals are shown in parentheses beneath each coefficient. Significant coefficients, for which 0 is not within the 95% cofidence interval, are highlighted with an asterisk ($*$).

standards where the differences are insignificant from one another, confirming well-controlled emissions for these vehicles.

For NO_x emissions from diesel passenger cars there is no consistent pattern of rates of deterioration changing with τ. The rates of Euro 3, 4 and 6 diesel cars reach maxima of 0.15 (0.12–0.18) at $\tau = .30$, 0.087 (0.064–0.11) at $\tau = .50$ and 0.094 (0.054–0.12) at $\tau = .50$ respectively, suggesting that the highest emitting vehicles are not necessarily any more sensitive to mileage-based deterioration than average emitters. Conversely, the deterioration rates of Euro 5 diesel cars reach a maxima of 0.24 (0.18–0.34) at $\tau = .95$, with rates increasing roughly linearly with τ ($R^2 = .91$). This pattern of behaviour is consistent with diesel passenger cars having a wide range of NO_x emissions, but emissions that do not show evidence of increases with mileage.

Across all four studied Euro standards, the rates of deterioration of diesel PM emissions possess a slight positive gradient with respect to τ up to $\tau = .70$. After this point the Euro standards deviate; the deterioration rates of the high emitting ($\tau > .70$) Euro 3 and 4 vehicles increase rapidly, reaching maxima of 53 (27–86) and 30 (16–46) mg kg^{-1} respectively, whereas the rates for Euro 5 and 6 remain low. Importantly, all but one of the deterioration rates for Euro 3 and 4 are seen to be significant, whereas the majority of the rates for Euro 5 and 6 are insignificant. This reinforces the insight from Figure 5.4 that the PM emissions of DPF-equipped vehicles are well controlled.

5.4.4 Vehicle Manufacturer Effects

The differences between the real driving emissions of vehicles from different manufacturers is well reported[1,2,83,101,110–112], but little has been reported on the differences in emission *deterioration* between manufacturers. Gasoline vehicles are of particular interest in this study due to the evidence of deterioration effects for some Euro standards. The exponential increase in the rate of deterioration seen in Euro 3 and 4 vehicles may be driven by only certain man-

ufacturers, for example. Conversely, some manufacturers of gasoline vehicles may have a significant deterioration effect for Euro 5 and 6 cars, despite no strong effect being present when considered on a bulk level.

The density functions of the bootstrapped deterioration rates from Equation 5.2 using vehicle manufacturer group as the interaction effect are visualised in Figure 5.5. The 8 most common manufacturer groups are shown for each Euro standard, each with at least 1000 observations. The distribution of cumulative mileage for each of these manufacturers are similar, although not identical (Figure 5.6).

There are clear differences between gasoline car manufacturers within each Euro standard. The influence of mileage on NO_x emissions from almost all Euro 5 vehicles is insignificant; the confidence intervals includes 0 for most manufacturers and values of τ. The only Euro 5 manufacturers with a significant mileage effect are Ford with 0.0294 and General Motors with 0.0255 g kg^{-1} NO_x per 10^4 at $\tau = .50$, and General Motors with 0.373 g kg^{-1} NO_x per 10^4 at $\tau = .95$. For Euro 3 and 4 manufacturers there is more evidence of diverging behaviours with some manufacturers demonstrating good NO_x control across a range of quantiles and others showing much stronger deterioration effects, especially at higher quantiles.

The analysis reveals that the progressive improvement of vehicle technology through Euro 3 to Euro 6 vehicles demonstrably led to improvements in vehicle emissions control. This finding is supported by the availability of vehicle-specific mileage information which shows that at 160,000 km, Euro 5 and Euro 6 gasoline passenger cars have much improved emissions control than Euro 3 and 4 vehicles for the *same* mileage.

The analysis of emissions deterioration of gasoline passenger cars shows that there exist small fractions of older vehicles in the fleet (Euro 4 and older) that have emissions that are similar to Euro 5 diesel cars for NO_x. From a policy perspective, it would be beneficial to target those vehicles for replacement or scrappage, given that there are relatively few of them. The current work

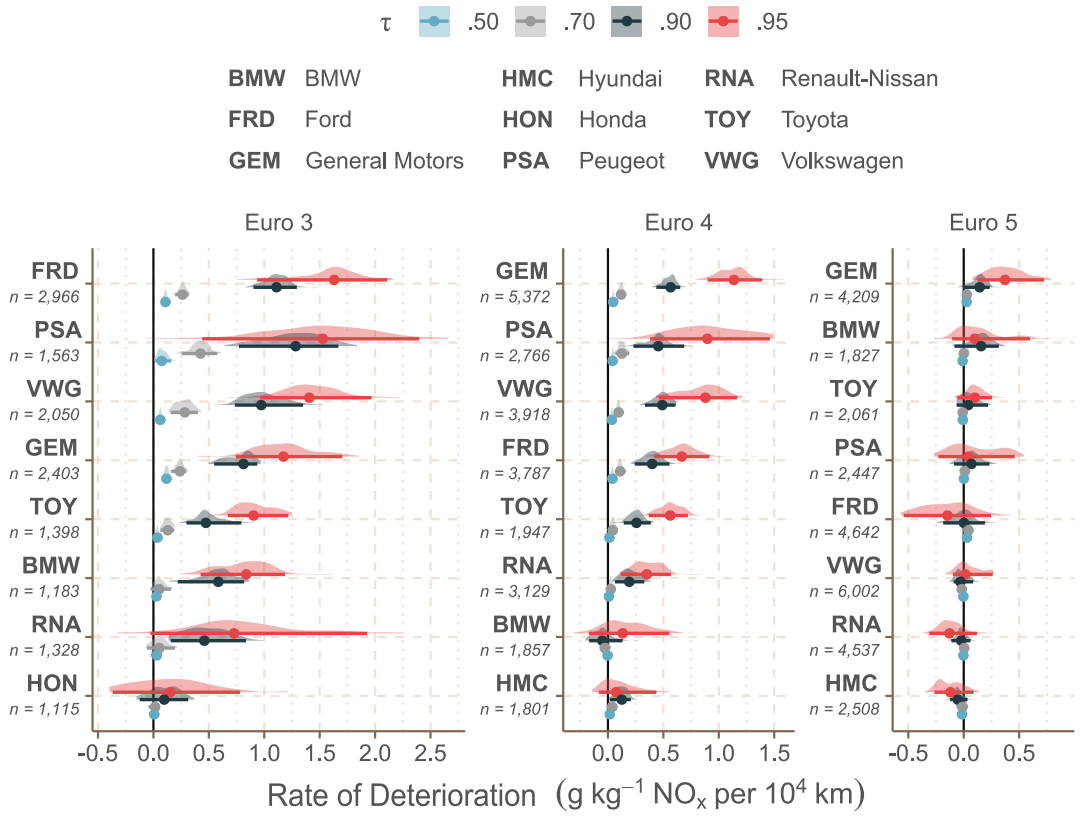

Figure 5.5: Density functions of bootstrapped rates of deterioration from multivariate linear quantile regression fits ($\tau \in \{.50,.70,.90,.95\}$) predicting NO_x as a function of vehicle mileage and vehicle specific power for gasoline passenger car manufacturers (Equation 5.2). Density functions are normalised per individual function, so their peak heights should not be directly compared. Manufacturers are ordered by the magnitude of their 95th percentile deterioration effect. The number of observations for each manufacturer, n, is shown. $x = 0$ is indicated with a solid black vertical line. The median value and the 95% confidence intervals are shown beneath each density function as circles and horizontal lines, respectively. Distribution functions and confidence intervals were calculated and visualised using the `ggdist` R package[127].

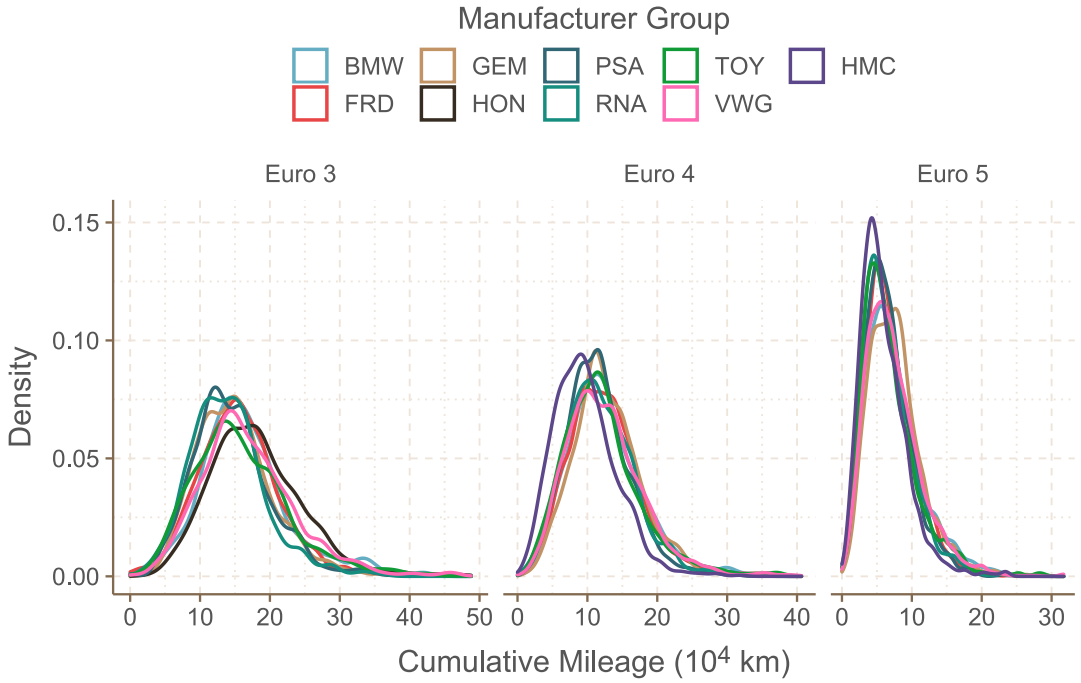

Figure 5.6: Density functions of cumulative mileage for the 8 most common Euro 3, 4 and 5 gasoline passenger car manufacturers in the remote sensing data set.

broadly supports recent Low Emission Zone developments such as the ULEZ (Ultra Low Emission Zone) in London[216], which prohibits gasoline passenger cars older than Euro 4 and pre-Euro 6 diesel cars. However, the analysis suggests that restricting pre-Euro 5 gasoline cars would be advantageous given the consistently low emissions of Euro 5 and 6 gasoline cars, even with high mileage.

5.5 Conclusion

The large data sets that can be acquired by vehicle emission remote sensing measurements provide many opportunities to develop a good understanding of vehicle emission characteristics. Such data also offers the potential to adopt more sophisticated analysis approaches that extend beyond simple aggregations such as mean emissions by Euro standard. By adopting statistical modelling

approaches, inferences drawn from the data will be stronger, with valuable information provided on uncertainties. An important advantage of this approach is that in determining vehicle mileage effects on emissions, other influences such as ambient temperature and vehicle power demand can be controlled for.

In the current work, the adoption of quantile regression as a technique fits well with the characteristics of the data being studied. The main benefit is the determination of whether all vehicles deteriorate similarly with increased mileage, or whether deterioration is controlled differently by different strata of a vehicle fleet. For gasoline passenger cars, where deterioration effects are most apparent, the results show that NO_x emission deterioration is significantly greater in a small population of vehicles.

In contrast to most other studies on vehicle emissions deterioration, the availability of measured mileage for individual vehicles in the current study is a considerable benefit, which avoids the use of proxy vehicle age-based data. For particulate matter, only pre-DPF vehicles show evidence of increasing emissions at higher mileages, and DPF-equipped vehicles retain effective PM control even at high mileages. The results also show that while there is evidence of different deterioration behaviour depending on vehicle manufacturer for pre-Euro 5 vehicles, post-Euro 4 vehicles show no such evidence.

Chapter 6

Conclusion

6.1 Contribution of Current Work

Vehicle emission remote sensing (RS) is different to the measurement techniques typically employed for type approval and emission factor development. While possessing obvious differences, chassis dynamometers and portable emission measurement systems (PEMS) share a common approach to measuring vehicle emissions; a whole journey (or drive cycle) is measured for a few representative vehicles. This approach allows researchers to understand emission behaviour under effectively any driving condition, from idling in traffic to speeding down a motorway. Conversely, remote sensing takes an approach to measure a single snapshot of many vehicles' journeys (commonly urban journeys). This allows for an appreciation of the distribution of emission behaviour across an in-use fleet. In short, chassis dynamometers/PEMS give good journey but poor fleet coverage, whereas RS gives good fleet but poor journey coverage. In isolation, none of these methods individually provide a comprehensive treatment of emissions. Remote sensing is well positioned to capture the myriad of factors influencing tailpipe emissions across a fleet — different fuels, emission standards, vehicle types, manufacturers, etc. — but has several fundamental features which limits its applicability in emission factor and inventory calculation.

Being restricted to snapshot measurements is a valid criticism of remote sensing as a technique; a single measurement of a vehicle does not necessarily represent its average emissions; a momentary high engine-demand condition, such as a sharp acceleration, during the triggering of the remote sensing device may lead to the mischaracterisation of a vehicle as "dirty" when it is otherwise "clean". Furthermore, being a roadside technique with relatively limited information on the vehicles being measured — at least compared to PEMS or in-lab studies — there are several assumptions that need to be made when working up remote sensing data (assumptions related to combustion chemistry, fuel composition, the amount of cargo in a vehicle, etc.). A fundamental aspect of

remote sensing is that emissions are reported as ratios to CO_2 rather than as absolute emissions in g km^{-1} as exhaust flow rate cannot be measured.

This thesis set out to overcome several of these limitations of remote sensing through the development of new approaches in the way RS data is handled. In the literature, one of the most common ways to report remote sensing data is average fuel-specific emissions for specific vehicle categories, which may be fuel types, vehicle types (car, van, bus, etc.), legislative categories like Euro standards, years of manufacture, vehicle make and model, and so on. In this work, remote sensing data is instead exploited to fit statistical models to predict emissions. In Chapter 2, 3 and 4, these are models to predict instantaneous emissions using vehicle specific power, which are used to predict emissions over real-world driving data. This approach allows for comprehensive assessments of emissions — good fleet *and* journey coverage. In Chapter 5, fuel-specific emissions are predicted using measured mileage data, with the statistical modelling framework itself allowing for the significance of emission deterioration to be quantitatively assessed.

The four research chapters of this thesis demonstrate the capability of remote sensing to assess emissions at different scales when the outlined new approaches are employed; from individual vehicles, to sub-national/local-scale emissions, to national estimates, to projected trends across the entire fleet.

- Chapter 2 first presents the emission-engine power modelling approach, but effectively concludes with the individual assessment of vehicles — 'what are the distance-specific emissions of vehicles of a specific fuel type, Euro standard, engine size, and manufacturer?' This question can be answered using chassis dynamometer- or PEMS-based studies, but with much smaller sample sizes of vehicles. The work in this chapter is a new approach to calculate comprehensive emission factors from remote sensing data, which are likely to more accurately reflect real-world fleet emissions than factors achievable with other approaches.

- Chapter 3 makes a wider examination of emissions; instead of being concerned with individual vehicles, the question asked is on broader, sub-national scale — 'how does the average diesel passenger car (and its driver) behave while moving in and around UK cities?' Traditionally, remote sensing would struggle to provide a thorough answer to this question; snapshots of journeys do not address how drivers behave when stuck in traffic, for example. Here, for the first time, an expansive data set of over 100,000 km of continuous driving was combined with a large database of over 60,000 RS measurements, allowing for a comprehensive examination of local-scale emissions. These modelled emissions permit the assessment of effectively any driving condition, the critique of methodologies like COPERT, and the de-coupling of the effects of different driver behaviours from the also varying emissions of their individual vehicles. Driver behaviour was demonstrated to induce a range of NO_x emissions of around ±22%; this suggests that emissions could be partially mitigated through driver training and/or speed adaptation technology, which may be cheaper and more straightforward than advances in exhaust after-treatment. Potentially more significant was the observation that COPERT speed-emission curves appear to underestimate NO_x emissions — particularly in low-speed conditions — which could have serious ramifications for inventory development and atmospheric modelling.

- Chapter 4 increases the scale a step further by examining national emissions through, for the first time, constructing a highly detailed remote sensing-based national emission inventory for light-duty road transport. Remote sensing data could already construct a top-down fuel-based inventory, but these are more uncertain for nations with land borders and do not scale nearly as well as bottom-up distance-based inventories. For the first time, evidence from vehicle emission remote sensing could be compared, like-for-like, with a national emissions inventory. Excellent

carbon balance was achieved (within 1% of CO_2 when compared to the NAEI) but NO_x was underestimated in the NAEI by 24–32%, or up to 47% in urban areas. An underestimation of NO_x in a national inventory has many important knock-on effects; inventories are used to establish whether a country is meeting international obligations and are inputs into air quality models. Inaccuracies in inventories will affect both of these activities and, ultimately, diminish the ability to create effective strategies to combat poor air quality.

- Chapter 5 instead considered fleet *trends*, examining the significance of emission deterioration with increasing mileage. Remote sensing is uniquely positioned to examine the distribution of emission deterioration within a vehicle fleet, adjusted for other emission-influencing covariates. The work in this chapter indicates that emissions are broadly well controlled in Euro 5 and 6 gasoline and diesel vehicles, even at cumulative mileages where Euro 3 and 4 emissions had started to deteriorate. However, a small proportion of pre-Euro 5 gasoline vehicles were revealed to have higher emissions than modern diesel vehicles, so it is suggested that these vehicles should be restricted in clean-air zones and their removal from the fleet be accelerated.

As discussed briefly in Chapter 3, remote sensing can examine the relative importance of different influences on vehicle emissions. Three key influencing factors were discussed in this thesis; manufacturers, driver behaviour, and deterioration. Of these three, the difference between manufacturer groups is seen to be the most consistently significant. The preliminary results in Chapter 2 identified relative percentage ranges of between ±42% and ±70% in distance-specific NO_x emissions from Euro 5 and 6 cars and vans. This manufacturer effect on emissions was shown in Chapter 4 to be significant even on a national level, inducing a 13.4% range in total emissions of NO_x when considering the different manufacturer fleet compositions of different European

countries. It even factors into emission deterioration; Chapter 5 shows that certain manufacturers have much better control over NO_x emissions at high mileages than others. For comparison, driver behaviour could be described as a second-order influence, with distance-specific NO_x emission ranges of around ±22%, and the importance of emission deterioration is shown to vary widely between different vehicle categories, with little strong evidence of deterioration identified in the newest (Euro 5+) passenger cars.

The difference between manufacturers is significant at almost all scales at which road transport emissions are considered. On a per-vehicle scale, the distribution between different manufacturers can explain how emissions may differ if all vehicles of a given category were emitting the same as those designed by the "best-in-class" manufacturer. On a national scale, evidence from this thesis suggests that the manufacturer composition of a country's fleet could have a significant effect on total estimated pollutant emissions in inventories. This latter point is important as no European emissions inventory currently takes account of manufacturers. Consequently, it is possible that some countries are underestimating or overestimating the contribution of their road transport fleets to their total NO_x emissions. This will create downstream issues, such as affecting urban air quality source apportionment and air quality modelling of NO_x, O_3 and secondary PM. Strategies to mitigate this are briefly outlined in Section 6.2.

6.2 Future Directions

As mentioned in Chapter 1, the most recent WHO guidelines have significantly decreased suggested air quality limits, with annual limits for NO_2 decreasing from 40 to 5 $\mu g\,m^{-3}$, $PM_{2.5}$ from 10 to 5 $\mu g\,m^{-3}$, and PM_{10} from 20 to 15 $\mu g\,m^{-3}$. Consequently, air quality must continue to improve past where it is today to mitigate its negative public health impacts. The road transport sector, being an important source of NO_x and PM, must control its emissions better than it is

presently doing. Remote sensing could continue to have a prominent role in monitoring the evolution of vehicle emissions, and understanding the sources of these emissions in greater detail.

This thesis presents new approaches for understanding vehicle emissions using remote sensing data. The key output of this research is the framework of expressing remote sensing emission data as a function of engine power, which can go on to be used to calculate distance-specific emissions, calculate emission inventories, comment on the influences of driving conditions, and so on. The applications of this approach extend well beyond the work presented in this thesis, however.

A natural extension would be the estimation of distance-specific emissions for species other than those typically measured using remote sensing. Hydrocarbon emission analysis was not a feature of this thesis, owing to the uncertainty surrounding hydrocarbon measurements by remote sensing and their treatment as bulk hydrocarbons rather than individual chemical species. The co-location of a remote sensing device and a device better suited for the measurement of discrete volatile organic species (e.g., an online mass spectrometer) could allow for distance-specific emission factors of individual hydrocarbon species to be calculated. Equally, distance-specific particulate emissions could be better calculated with the co-location of an RSD with a system better suited for PM measurements (e.g., a condensation particle counter or aethalometer). There is nothing to limit this method purely to air quality pollutants either — non-CO_2 greenhouse gas emissions from road transport could also be quantified, such a methane and N_2O.

The work presented in this thesis focuses entirely on light-duty vehicles — passenger cars and vans. While light-duty vehicles comprise the majority of the road transport fleet in the UK, heavy-duty vehicles are still of significant importance. HGVs, for example, are commercial vehicles which do a large amount of driving. Buses are few in number, but most commonly operate in urban areas where passengers and pedestrians will be exposed to their

emissions. While the same broad approach as in Chapter 2 can likely be employed, there will be extra work required to estimate emissions from heavy-duty vehicles. Vehicle weight will likely be a large source of uncertainty; heavy goods vehicles which could be fully laden with cargo or totally empty, and buses could have any number of passengers depending on location and time of day. Furthermore, appropriate drive cycles would have to be sourced as the real-world behaviour of heavy vehicles will be different to that of light vehicles. An obvious example of this is buses, which by necessity regularly come to complete stops for passengers to board and alight.

As previously mentioned, this thesis presents evidence that the variance in emissions between manufacturers is significant even on a national level, and that it should start being accounted for in European emission inventory calculations. This could be achieved in a few ways, all of which could incorporate remote sensing as the key technique for data collection. It could be accomplished through separate emission factors per manufacturer — this thesis and other remote sensing studies demonstrate that this can be achieved straightforwardly. In practice, however, having per-manufacturer factors built-in to COPERT, HBEFA or other models may be opposed by the manufacturer groups who are assigned the highest emission factors. As an alternative, focus could shift to using local data to complement the current COPERT approach for emission factor development, i.e., measuring the UK fleet to develop UK-specific emission factors, the French fleet for France, the Spanish fleet for Spain, and so forth. Vehicle emission remote sensing, with its portability and excellent fleet coverage, is well suited for the task of cheaply and quickly obtaining country-specific data. Furthermore, the use of local remote sensing data will also help capture the effects of other emissions influences which vary with country, such as ambient temperature.

In Chapter 2 the treatment of hybrid vehicles is briefly discussed, but hybrid vehicles are not a major focus of this thesis. The remote sensing publication Farren et al. [31] does address hybrid vehicles, using the proportion of invalid

remote sensing measurements to identify how often hybrid vehicles are in battery-on mode (and are therefore not emitting anything from their tailpipes) at different values of VSP. Utility factors were estimated and then applied to downscale emission factors to more accurately represent trip-average emissions. While a useful initial application to hybrid vehicles, there are potential improvements to be made — particularly with respect to distance-specific emissions. Applying a flat reduction may not be appropriate, as battery-on conditions are not consistent across different driving conditions. A relationship between VSP and battery-use percentage may itself have inherent uncertainty, as the proportion of time a plug-in hybrid vehicle will be using its battery will be affected by how frequently it is charged. Remote sensing may be able to provide underpinning evidence on unimpeded urban-type conditions (as in Farren et al. [31]), but external data sets will be required to understand the battery modes of hybrid vehicles under different conditions.

Two key targets in this area could be, *i)*, the development of a hybrid vehicle VSP-based drive cycle which contains battery on/off information, which could then be straightforwardly predicted over, and/or, *ii)*, a refined VSP-battery percentage relationship which includes data from rural and motorway driving (likely from non-RS sources). At time of writing, the UK Government intends to ban the sale of new petrol and diesel vehicles in 2030 and new hybrid vehicles from 2035[217]. The importance of accurate estimates of hybrid vehicle emissions will therefore increase as conventionally powered vehicles are phased out of road transport fleets. Furthermore, the deterioration of hybrid vehicles will be an important consideration as, if the last hybrid vehicles are sold in 2035, hybrid vehicles will likely remain in the UK fleet till the 2050s. As hybrid vehicles become more popular and a greater number of remote sensing measurements of hybrid vehicles are made, the framework set out in Chapter 5 could easily be re-applied to examine the distribution of their emission deterioration.

6.3 Closing Thoughts

Air quality is one of the biggest public health issues of the modern age, and much of the blame can be attributed to the ubiquity of combustion-fuelled road transport. Despite increasingly strict legislation and improvements in vehicle technology, health evidence continues to demand that lower and lower amounts of air quality pollutants be emitted. The future is uncertain with respect to road transport; at the time of writing, the UK Government appears to be pushing toward fleet electrification, but this has economic and political consequences as well as needing a large investment in infrastructure. It is possible that the world's issues with road transport will not exclusively be solved by new technologies, but also with changes to urban planning and public attitudes to prioritise the use of active and public transport over private road transport. Regardless of what the future of mass transportation will hold, for the time being the internal combustion engine isn't going anywhere — and vehicle emission remote sensing is in prime position to further understand its effect on the air we breathe.

Appendix A

`gramsper` – An R Package for Absolute Emission Estimates Using Remote Sensing

While arguably simple to understand, the method to calculate distance-specific emission factors from a remote sensing data set is long with much scope for errors. To streamline the method for other researchers and air quality professionals, the `gramsper` package was developed (named after the common emissions factor unit prefix of *grams per* kilogram, second, kilometer, etc.).

This appendix is intended to give a brief demonstration of a `gramsper` workflow in R[121] and some of the functionality that it provides. Note that `gramsper` is in development so the information in this appendix is subject to change before public release.

Style & Scope

`gramsper` follows the "tidyverse" style guide as closely as possible. It also makes heavy use of "tidy evaluation" set out in the `rlang` package[218], meaning that column names given as function arguments are provided unquoted. These two style choices allow for easy integration with "tidyverse" functions in `magrittr`[219] pipelines.

`gramsper` has been written for use with the OPUS RSD which has been joined with technical information obtained from the UK "Motor Vehicle Registration Information System" (MVRIS). Therefore much of its functionality will not readily work with data from other RSD systems (FEAT, EDAR, etc.) or with technical data from other countries at time of writing.

Emission Factor Calculations

The main objective of `gramsper` is to calculate emission factors from remote sensing data.

The most straightforward emission factor to calculate is the fuel-specific (g kg^{-1}) factor, as this only requires pollutant concentrations in PPM which are provided by default in "raw" remote sensing data. `calculate_gpkg()` takes a data frame of raw remote sensing data as its only argument and uses the concentration columns contained within to add g kg^{-1} columns for CO_2, CO, NO, NO_2, HC, and NH_3.

More complicated is the calculation of distance-specific (g km^{-1}) factors. To calculate these emissions, `gramsper` uses the methods outlined in Chapter 2 and demonstrated in Chapter 3 and Chapter 4. The first step is the calculation of VSP and fuel consumption, which `gramsper` automates with `calculate_power_fuel()`. This function automates the segmentation of vehicles through the use of the MVRIS technical data, assigns estimates of C_dA, R_0 and R_1, and uses these to calculate VSP and fuel consumption. Additional

arguments allow for control over the adjustment of vehicle kerb weight (defaulting to +150 kg) and the automatic calculation of instantaneous emissions (g s^{-1}) for all available fuel-specific emissions in the data set.

The second step to calculating distance-specific emissions is mapping the instantaneous emissions to a drive cycle using an emission-power generalised additive model (GAM). This step is achieved with the `rs_to_drive_cycle()` function. The key arguments it takes are:

- **df**: A data frame of remote sensing data which includes estimated instantaneous emissions.
- **pollutant**: A column of instantaenous emissions.
- **drive_cycle**: A data frame of VSP-based drive cycles. `gramsper` contains some in-built drive cycles, including the PEMS cycles from Chapter 2, but external cycles can also be used. The minimum required of a drive cycle data frame is a column of VSP values, although any additional data from the drive cycle will be retained in the function output.
- **...**: Any number of columns from the remote sensing data frame to group the output by, for example any columns pertaining to Euro Standard, fuel type, engine size, etc.
- **min**: The minimum number of measurements required to fit the GAM. This avoids having to pre-filter remote sensing data to remove niche vehicle categories (e.g., unpopular manufacturer groups)

Without any grouping columns specified, `rs_to_drive_cycle()` returns the drive cycle data augmented with an additional column of predictions for whatever pollutant has been modelled. With grouping columns specified, the grouping columns are retained and predictions are made per-group, meaning that the data frame returned has n times as many rows as the drive cycle data, where n is the number of unique groups. From this point, users can manually calculate a distance-specific emission (see ***Example Workflow*** below).

Remote Sensing Utilities

There are numerous other utility functions in `gramsper` to make using remote sensing data easier in `R`. These are not necessarily directly related to emission factor calculation, but may form part of a complete `gramsper` workflow. Examples include:

- `cop_create_type()`: Adds columns to a remote sensing data frame which label vehicles with their COPERT assignments. These are more evocative and easy to work with than some of the MVRIS assignments. For example, a "vehicle type" of "Car" is easier to understand than a "type approval category" of "M1".
- `estimate_missing()`: Sets invalid speed and acceleration measurements to the average speed and acceleration for the measurement site, and predicts missing vehicle weights using vehicle volume and engine size. These estimations allow for value to be extracted from incomplete remote sensing observations.
- `summarise_se_curve()`: Takes the output of `rs_to_drive_cycle()` and returns a COPERT speed-emission curve-style reference table of distance-specific emission averages at user-defined speed intervals. This is a similar output to the COPERT-style curve produced in Chapter 3, although uses binned speed intervals rather than fitting a polynomial model.
- `naei_road_airquality()`: Uses the `rvest`[220] package to scrape the NAEI website for total UK road transport air quality emissions. Its sister function, `naei_road_greenhouse()`, scrapes NAEI greenhouse gas emissions. While not directly related to the use of remote sensing data, more efficient analysis can be facilitated by having ready access to the most recent official NAEI estimates (as in Chapter 4).
- Unit conversion functions allow for quick conversions between units. For example, `kmh_to_ms()` will convert vehicle speeds in km h^{-1} to m s^{-1}.

Example Workflow

Listing A.1 provides an example workflow for the use of `gramsper`. In this case, NO_x g km^{-1} values are calculated over London-based LDV drive cycles (included in `gramsper` as `cycles_tfl`).

Listing A.1: An example `gramsper` workflow.

```
library(gramsper)
library(dplyr)

# read in RS data
rs_raw = readRDS("rs_data.rds")

# prep data - get COPERT classes, recover data,
# calculate VSP, FC and g/s values
rs_prepped = rs_raw %>%
    calculate_gpkg() %>%
    cop_create_type() %>%
    estimate_missing() %>%
    calculate_power_fuel(data, ldv_adj = 150,
                         calc_gs = TRUE)

# map nox g/s values to TFL drive cycles
tfl_pred = rs_prepped %>%
    rs_to_drive_cycle(drive_cycle = cycles_tfl,
                      pollutant = NOx_gps,
                      cop_eu_class, cop_veh_type,
                      min = 200)

# use dplyr to calculate g/km - sum of predicted
# values divide by sum of distance covered
tfl_gkm = tfl_pred %>%
    summarise(nox_gkm = sum(pred, na.rm = T) /
                        sum(dist_hz, na.rm = T)
```

Appendix B

Supporting Information for Chapter 3

In Chapter 3, Figure 3.4 and the associated analysis considered drivers who had performed at least 50 journeys in each speed limit zone. This was chosen as drivers who had only undertaken a small number of journeys may have journeys more effected by external influences (e.g., congestion) or transitory factors (e.g., driver mood/personal circumstance) rather than their individual consistent driving style. The limit of 50 is somewhat arbitrary, and was chosen in part due to the appearance in an "elbow" in the trend of relative percentage range against the chosen journey limit at around a limit of 50 journeys.

The purpose of this appendix is for transparency; *all* drivers are visualised regardless of the number of journeys they had taken. Due to the amount of data being visualised, each speed limit zone is presented in its own figure.

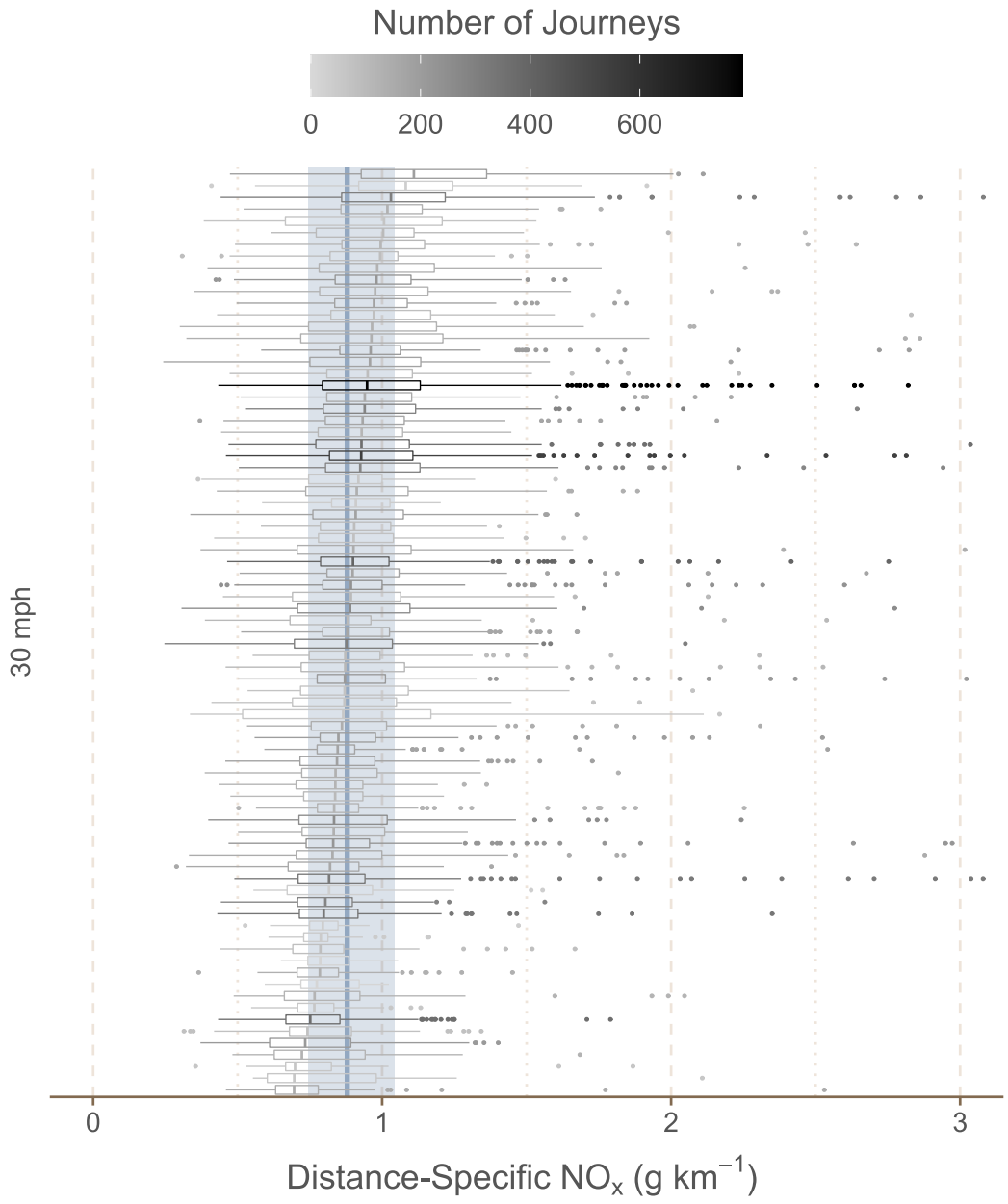

Figure B.1: Distributions of journey-average distance-specific (g km^{-1}) NO_x emissions in 30 mph speed zones. Each boxplot represents an individual driver, with the intensity of the line colour proportionate to the number of journeys the driver undertook under that speed limit.

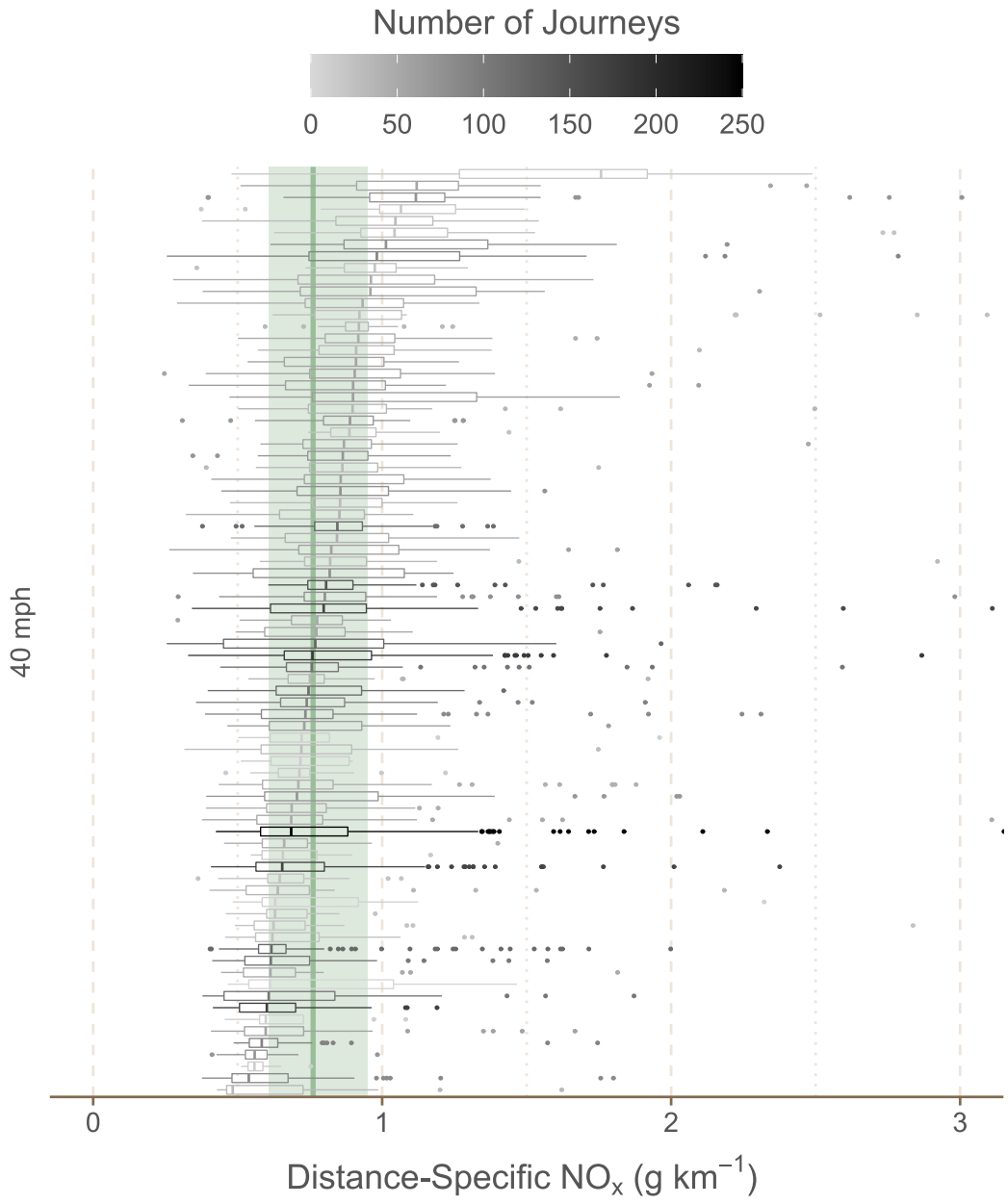

Figure B.2: Distributions of journey-average distance-specific (g km^{-1}) NO_x emissions in 40 mph speed zones. Each boxplot represents an individual driver, with the intensity of the line colour proportionate to the number of journeys the driver undertook under that speed limit.

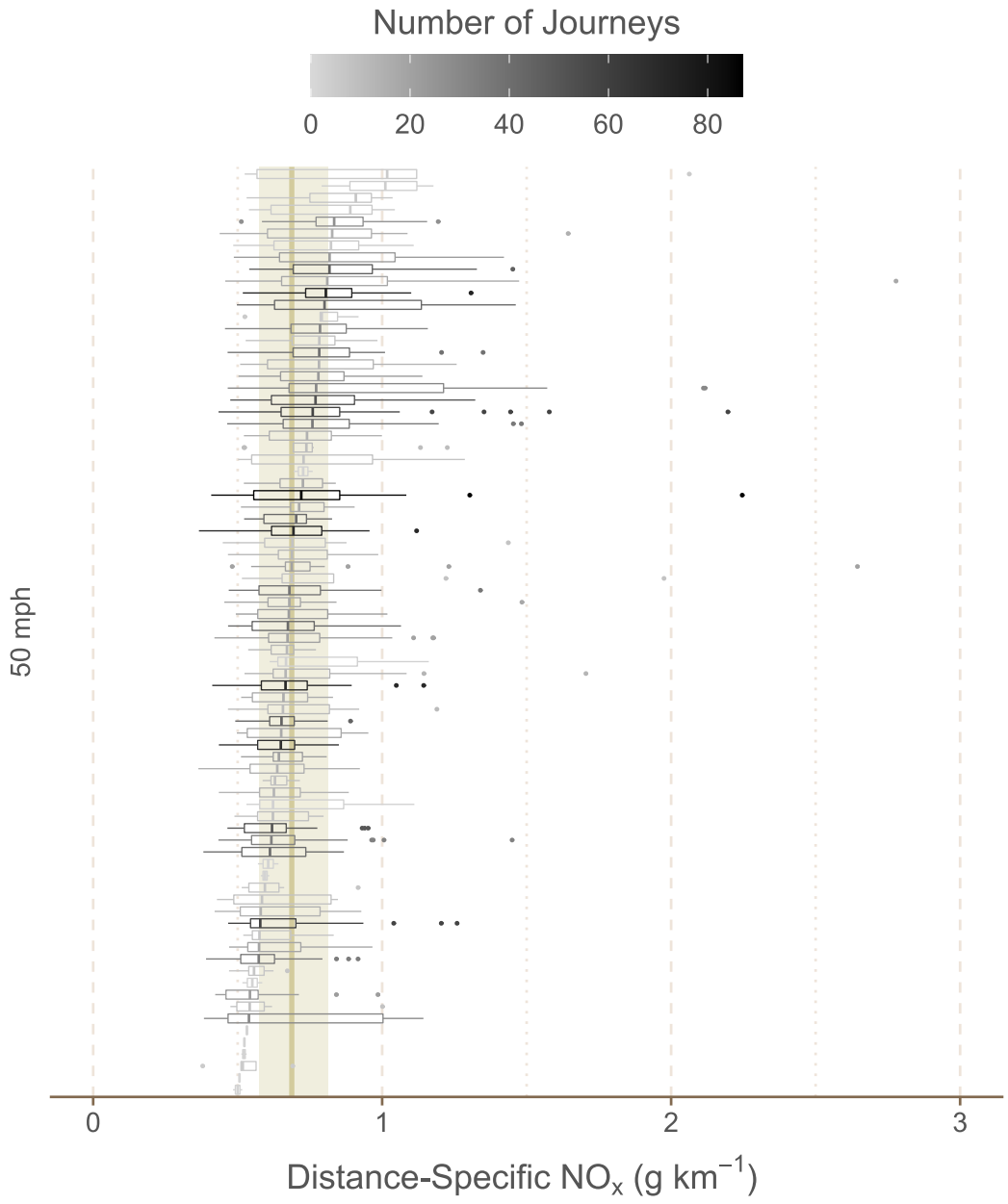

Figure B.3: Distributions of journey-average distance-specific (g km^{-1}) NO_x emissions in 50 mph speed zones. Each boxplot represents an individual driver, with the intensity of the line colour proportionate to the number of journeys the driver undertook under that speed limit.

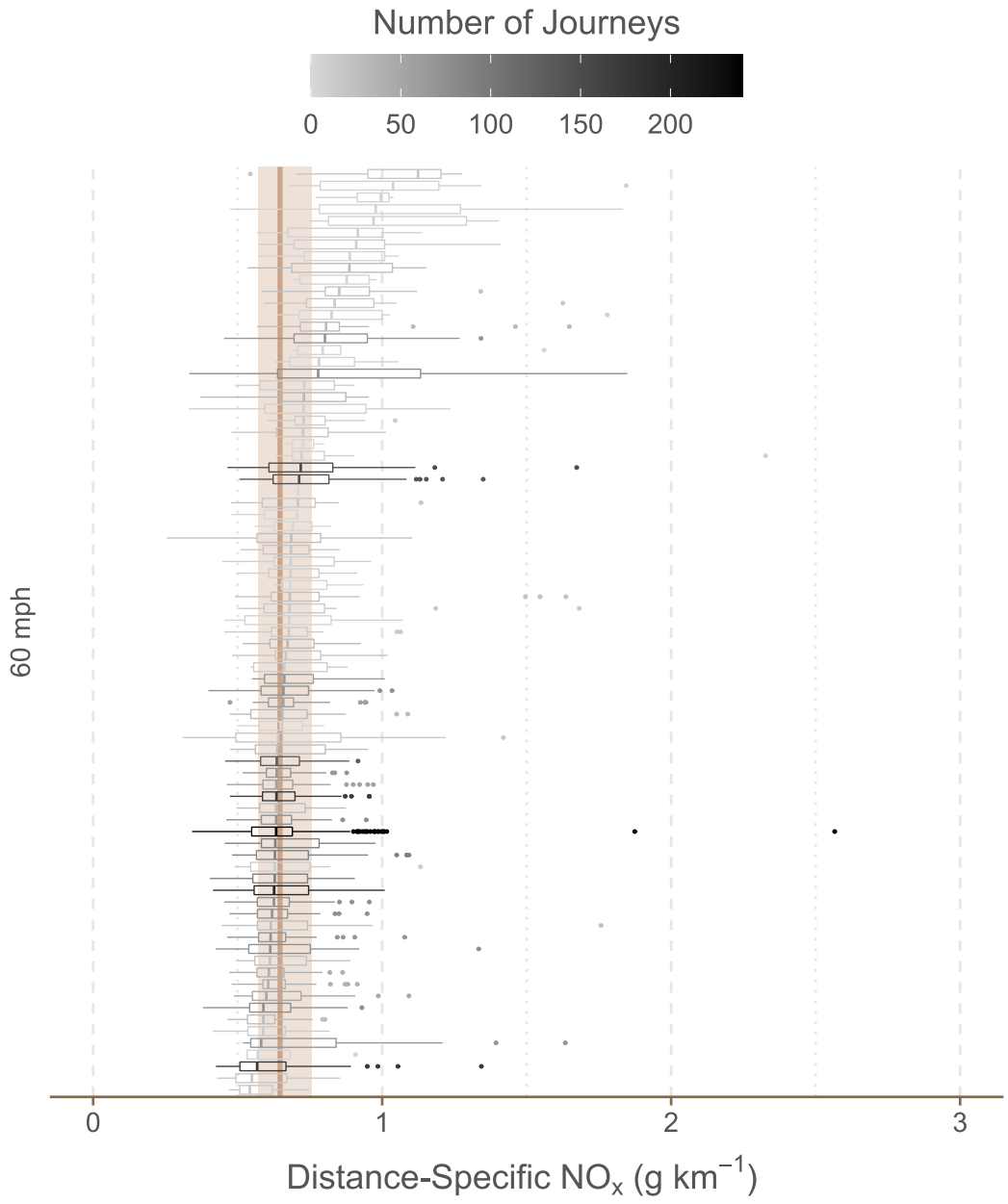

Figure B.4: Distributions of journey-average distance-specific (g km^{-1}) NO_x emissions in 60 mph speed zones. Each boxplot represents an individual driver, with the intensity of the line colour proportionate to the number of journeys the driver undertook under that speed limit.

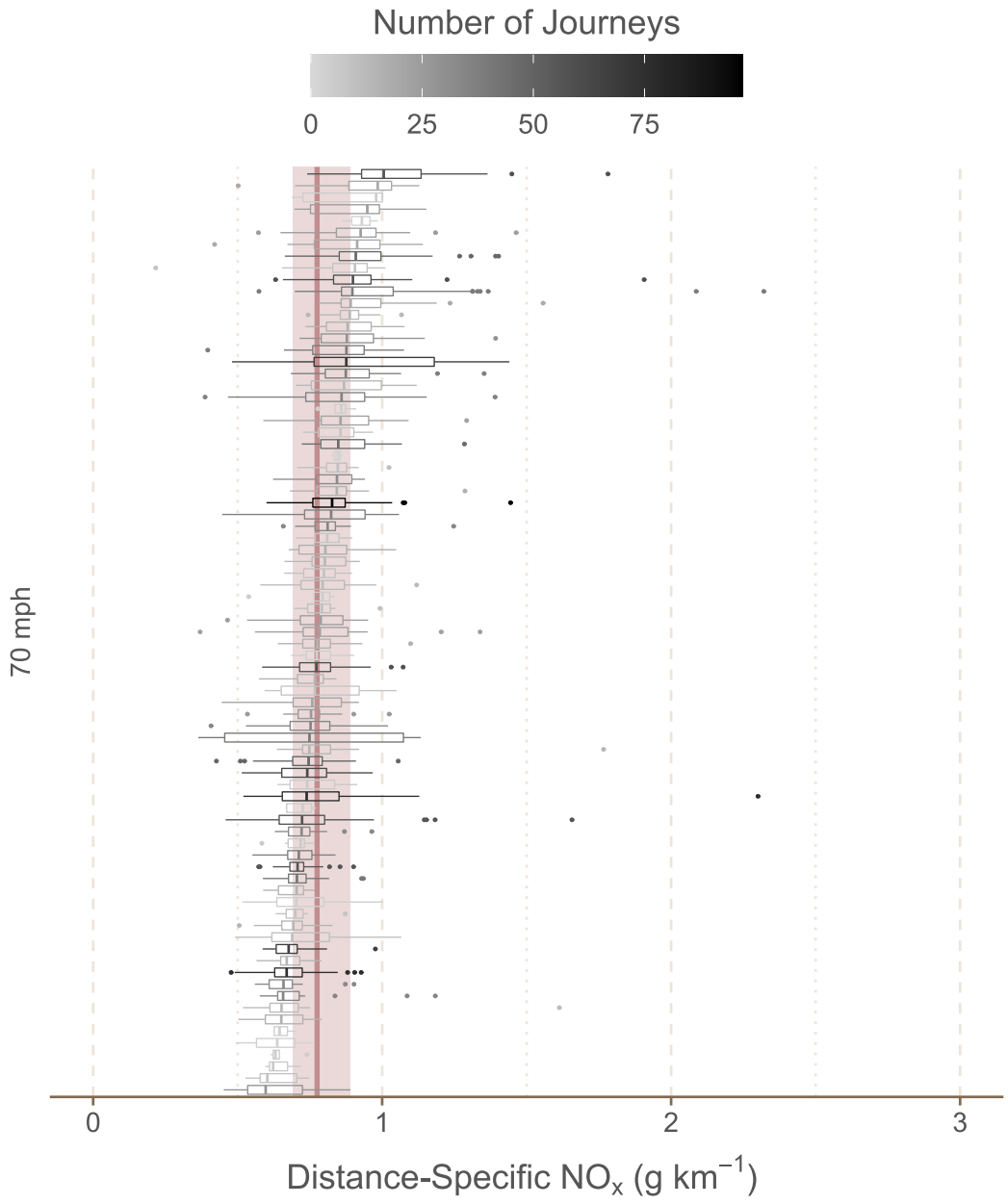

Figure B.5: Distributions of journey-average distance-specific (g km^{-1}) NO_x emissions in 70 mph speed zones. Each boxplot represents an individual driver, with the intensity of the line colour proportionate to the number of journeys the driver undertook under that speed limit.

Appendix C

Supporting Information for Chapter 4

This section provides further research outputs, mainly those originally provided as the supplementary information of Davison et al. [2], in part including the carbon monoxide and ammonia estimates. The total UK bottom-up estimates for these air quality pollutants were 537 ± 25.4 kt CO and 9.1 kt ± 0.5 NH_3. At a UK scale, the NAEI is seen to consistently underestimate these emissions, with $F = 2.86$ for CO and $F = 2.23$ for NH_3.

The equivalent visualisations to Figure 4.3 and Figure 4.4 inclusive of CO and NH_3 are provided as Figure C.1 and Figure C.2, respectively. The distance-based emission factors calculated in this study are provided in Table C.1, Table C.2, Table C.3 and Table C.4.

The bottom-up approach given in Chapter 4 was first demonstrated in Farren et al. [30], which focused exclusively on NH_3 emissions and where it was compared with a top-down approach also using vehicle emission remote sensing data. Excellent agreement was found between the two approaches, both in terms of carbon balance and estimated total UK NH_3 road transport emissions.

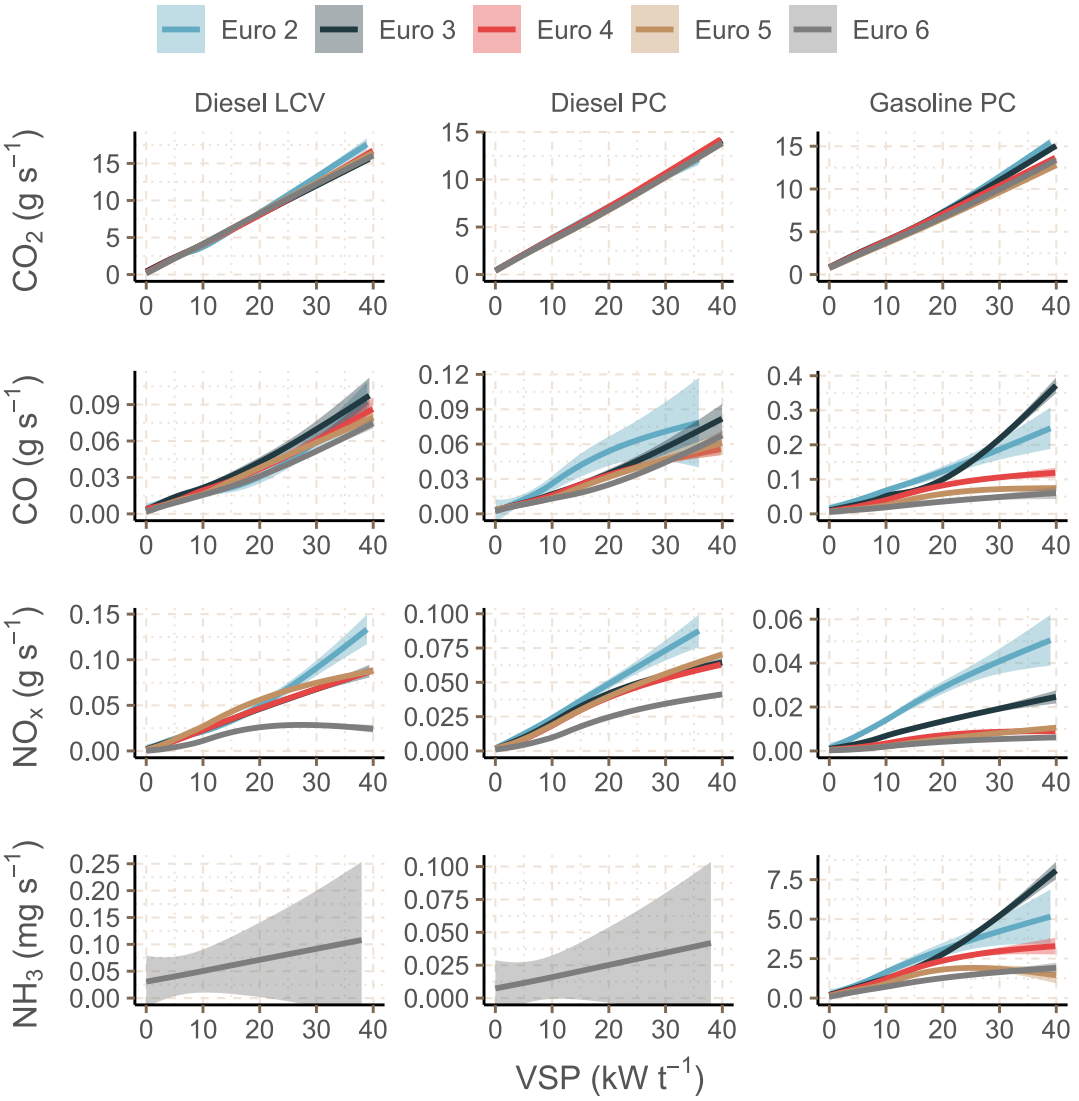

Figure C.1: Generalised Additive Models (GAMs) relating passenger car CO_2, NO_x and CO g s^{-1} and NH_3 mg s^{-1} to VSP, coloured by Euro classification and faceted into three light duty vehicle categories. The shading shows the standard error of the GAM fit.

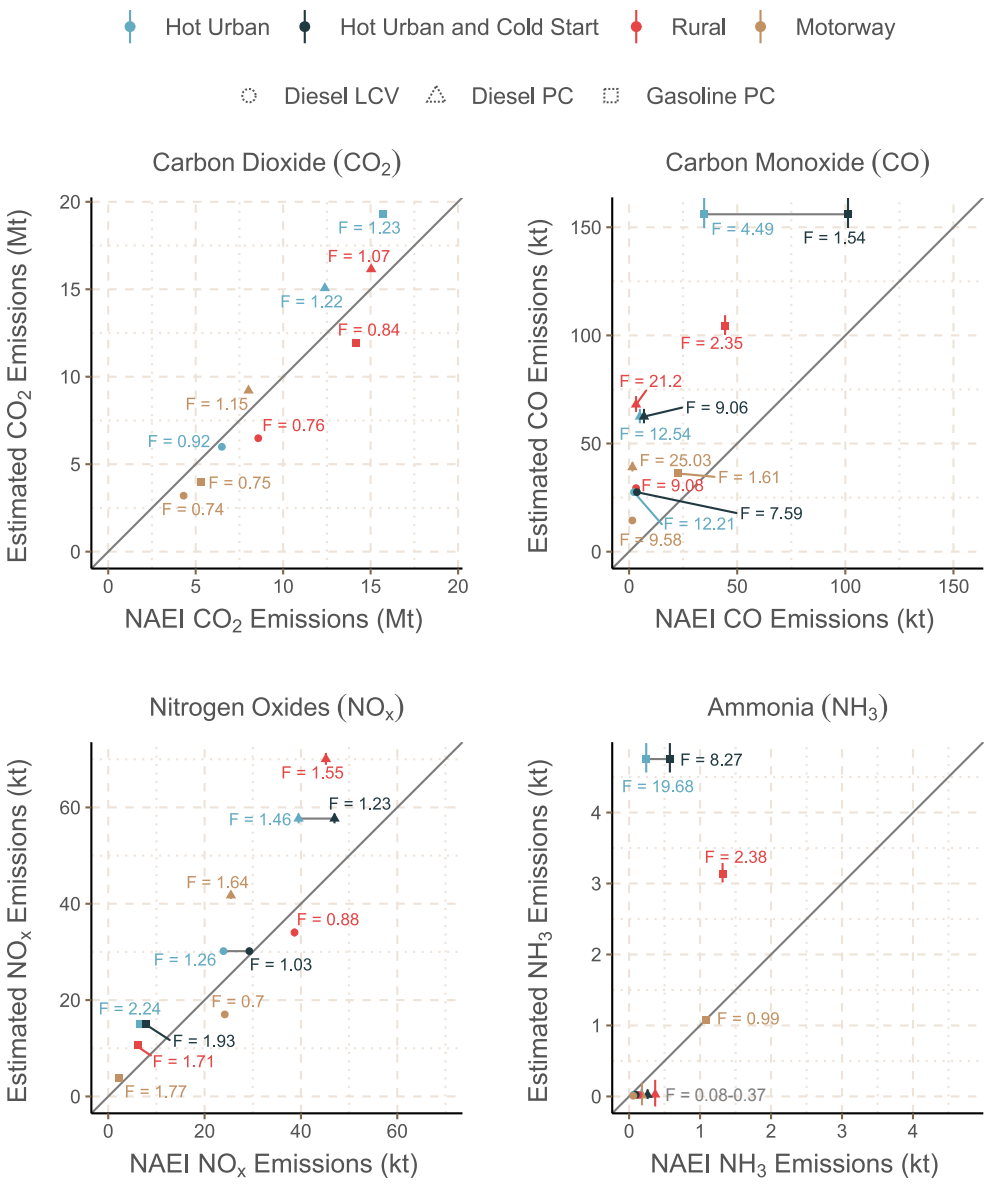

Figure C.2: Total UK estimates for CO_2, NO_x, CO and NH_3 using vehicle emission remote sensing, in comparison with the 2018 emissions reported in the National Atmospheric Emissions Inventory. *F* values, representing the ratio between the VERS estimate and the reported NAEI value, are provided. Urban VERS estimates are compared with both hot urban emissions from the NAEI and a combination of hot urban and cold start emissions, shown connected by a grey horizontal line. Error bars show the 95% confidence intervals projected from the fuel-specific (g kg^{-1}) emission factors. The grey diagonal line shows a 1:1 relationship.

		Urban			Rural			Motorway		
	ES	**Low.**	**Avg.**	**High.**	**Low.**	**Avg.**	**High.**	**Low.**	**Avg.**	**High.**
Gasoline PC	2	244.5	251.6	258.8	163.8	168.6	173.4	173.1	178.2	183.3
	3	257.2	259.8	262.3	169.3	171.0	172.7	177.6	179.4	181.1
	4	252.8	254.7	256.5	166.0	167.2	168.4	173.9	175.2	176.4
	5	232.6	234.2	235.9	153.2	154.2	155.3	160.8	161.9	163.0
	6	239.2	241.1	242.9	157.4	158.6	159.8	165.1	166.4	167.7
Diesel PC	2	202.9	219.8	238.8	144.9	157.1	170.6	157.1	170.2	184.9
	3	212.2	216.2	220.1	152.4	155.2	158.0	165.5	168.6	171.6
	4	217.0	219.1	221.4	155.4	157.0	158.6	168.7	170.3	172.1
	5	208.6	210.1	211.6	149.3	150.4	151.5	162.0	163.1	164.3
	6	210.0	211.8	213.7	150.3	151.6	152.9	163.0	164.4	165.9
Diesel LCV	2	206.4	228.8	255.7	156.6	173.6	194.1	173.5	192.4	215.0
	3	231.4	237.8	244.6	168.7	173.3	178.3	184.2	189.2	194.7
	4	224.6	228.4	232.5	168.5	171.3	174.4	185.9	189.1	192.5
	5	215.5	218.0	220.5	167.7	169.7	171.6	187.5	189.6	191.8
	6	216.0	220.2	224.3	166.6	169.8	173.0	185.6	189.2	192.8

Table C.1: Distance-based emission factors in g km^{-1} for carbon dioxide (CO_2). "ES" refers to the Euro Status of the vehicle. The *Low.* and *High.* values represent the 95% confidence interval.

		Urban			Rural			Motorway		
	ES	**Low.**	**Avg.**	**High.**	**Low.**	**Avg.**	**High.**	**Low.**	**Avg.**	**High.**
Gasoline PC	2	3.94	4.30	4.73	2.63	2.87	3.16	2.78	3.03	3.34
	3	2.77	2.88	2.99	2.15	2.23	2.32	2.40	2.49	2.59
	4	2.33	2.40	2.48	1.64	1.69	1.74	1.77	1.82	1.88
	5	1.50	1.55	1.60	1.08	1.11	1.15	1.17	1.20	1.24
	6	1.21	1.29	1.44	0.78	0.83	0.92	0.81	0.86	0.96
Diesel PC	2	1.03	1.34	1.69	0.81	1.05	1.33	0.91	1.18	1.49
	3	0.87	0.97	1.05	0.66	0.74	0.80	0.74	0.82	0.88
	4	0.94	0.98	1.01	0.67	0.69	0.72	0.72	0.75	0.77
	5	0.81	0.87	0.94	0.60	0.64	0.69	0.66	0.70	0.75
	6	0.79	0.82	0.85	0.57	0.59	0.61	0.62	0.64	0.66
Diesel LCV	2	1.11	1.29	1.47	0.73	0.85	0.97	0.77	0.89	1.02
	3	1.28	1.38	1.49	0.90	0.97	1.05	0.98	1.05	1.13
	4	1.05	1.10	1.17	0.77	0.81	0.86	0.85	0.89	0.94
	5	0.95	0.98	1.01	0.74	0.76	0.79	0.83	0.85	0.88
	6	0.88	0.91	0.95	0.66	0.69	0.71	0.73	0.76	0.78

Table C.2: Distance-based emission factors in g km^{-1} for carbon monoxide (CO). "ES" refers to the Euro Status of the vehicle. The *Low.* and *High.* values represent the 95% confidence interval.

		Urban			Rural			Motorway		
	ES	**Low.**	**Avg.**	**High.**	**Low.**	**Avg.**	**High.**	**Low.**	**Avg.**	**High.**
Gasoline PC	2	0.70	0.77	0.84	0.53	0.58	0.63	0.59	0.65	0.70
	3	0.36	0.37	0.39	0.27	0.28	0.29	0.29	0.31	0.32
	4	0.18	0.19	0.20	0.13	0.14	0.15	0.15	0.15	0.16
	5	0.11	0.12	0.12	0.09	0.10	0.10	0.10	0.11	0.11
	6	0.10	0.10	0.11	0.08	0.08	0.08	0.08	0.09	0.09
Diesel PC	2	1.15	1.29	1.44	0.89	1.00	1.11	0.99	1.11	1.24
	3	1.06	1.09	1.12	0.81	0.83	0.85	0.89	0.92	0.94
	4	0.91	0.92	0.94	0.73	0.74	0.76	0.82	0.84	0.85
	5	0.94	0.95	0.96	0.76	0.77	0.78	0.85	0.87	0.88
	6	0.48	0.49	0.50	0.42	0.43	0.44	0.48	0.49	0.51
Diesel LCV	2	1.12	1.31	1.54	0.91	1.06	1.24	1.02	1.20	1.40
	3	1.22	1.27	1.33	0.92	0.96	1.00	1.01	1.06	1.11
	4	1.12	1.15	1.18	0.90	0.92	0.95	1.01	1.04	1.07
	5	1.32	1.34	1.36	1.05	1.07	1.09	1.18	1.20	1.22
	6	0.46	0.48	0.51	0.39	0.42	0.44	0.45	0.48	0.51

Table C.3: Distance-based emission factors in g km^{-1} and mg km^{-1} for nitrogen oxides (NO_x). "ES" refers to the Euro Status of the vehicle. The *Low.* and *High.* values represent the 95% confidence interval.

		Urban			Rural			Motorway		
	ES	**Low.**	**Avg.**	**High.**	**Low.**	**Avg.**	**High.**	**Low.**	**Avg.**	**High.**
Gasoline PC	2	83.71	93.11	106.16	59.78	66.50	75.82	64.78	72.06	82.15
	3	70.25	73.16	75.90	54.73	57.00	59.14	61.18	63.72	66.11
	4	67.36	70.36	73.17	47.60	49.72	51.70	51.37	53.66	55.80
	5	54.48	56.66	59.57	36.35	37.80	39.75	38.35	39.88	41.93
	6	42.77	44.48	46.30	28.35	29.48	30.69	29.82	31.02	32.28
Diesel PC	6	0.08	0.94	2.03	0.07	0.77	1.66	0.07	0.88	1.88
Diesel LCV	6	1.34	3.88	7.52	0.87	2.52	4.88	0.91	2.63	5.09

Table C.4: Distance-based emission factors in g km^{-1} and mg km^{-1} for ammonia (NH_3). "ES" refers to the Euro Status of the vehicle. The *Low.* and *High.* values represent the 95% confidence interval.

Appendix D

Description of Quantile Regression for Chapter 5

The purpose of this appendix is to give an more thorough overview of quantile regression to aid with the interpretation of results in Chapter 5. This text was originally included in the supplementary information of Davison et al. [3].

Quantile regression can be understood in relation to ordinary least squares (OLS) regression. An example of an OLS equation is given in Equation D.1. $\hat{y}_i$ is the predicted value of the response variable y_i, and x_{ik} is the predictor variable associated with the covariate k, of which there are p. In OLS regression, the β coefficients are constant.

$$\hat{y}_i = \beta_0 + \sum_{k=1}^{p} \beta_k \cdot x_{ik} \tag{D.1}$$

The "best" OLS regression equation is found my minimising a loss function. This is typically the *Mean Squared Error* (MSE), found by summing the sqare of the difference between the real and predicted values of y_i, of which there are n, and dividing through by n. This equation is shown as Equation D.2.

$$MSE = \frac{1}{n} \sum_{i=1}^{n} (y_i - \hat{y}_i)^2 \tag{D.2}$$

A generic quantile regression equation is given in Equation D.3. The key difference between Equation D.3 and Equation D.1 is that the β coefficients are

now functions of the quantile, τ.

$$Q_\tau(\hat{y}_i) = \beta_0(\tau) + \sum_{k=1}^{p} \beta_k(\tau) \cdot x_{ik} \tag{D.3}$$

The "best" quantile regression equation is also found my minimising a loss function – this time the *Median Absolute Deviation* (MAD). The MAD function (Equation D.4) is analogous to the MSE function (Equation D.2), but now has the addition of a check function, ρ_τ, defined in Equation D.5, where I is an indicator function that is equal to 1 if true and 0 if false.

$$MAD = \frac{1}{n} \sum_{i=1}^{n} \rho_\tau(y_i - Q_\tau(\hat{y}_i)) \tag{D.4}$$

$$\rho_\tau(u) = |u|\{\tau \cdot I(u > 0) + (1 - \tau) \cdot I(u < 0)\} \tag{D.5}$$

To illustrate some use-cases of quantile regression, Figure D.1-Scatter shows some example data with quantile regression lines fit, $\tau \in \{.10, \ldots, .90\}$. Figure D.1-Model shows the intercept and slope term. In these latter plots, the intercept and slope terms for the equivalent ordinary least squares regressions, along with their 95% confidence intervals, are shown as horizontal lines. Three distinct cases are presented.

- **Case A**: The points are in a near-perfect 1:1 line, meaning that all of the fits at different quantiles are effectively the same. This is reflected in the model plots; in both cases, the points effectively form a straight horizontal line. In this case, quantile regression is unnecessary - an ordinary least squares linear regression would explain this relationship adequately.

- **Case B**: There is still a linear correlation between x and y, but there is much greater spread in y. The quantile regression fits are therefore nearly parallel, but are transformed in the y axis. Notice that, in the model plots, the intercept increases near-linearly with τ, whereas the slope term remains similar to that seen in Case A. As all of the slope terms are contained within the confidence interval of the OLS slope term, it can be

said that the rate at which y increases as a function of x is not significantly different at different quantiles.

  - In emissions science, this would reflect a situation in which the "high-emitters" of a pollutant are no more or less influenced by some covariate than the lower or average emitters.

- **Case C**: The spread in y increases as x increases, giving the quantile regression lines a fan-like appearance. The model plots are the opposite of those seen in Case B; the model intercepts are not significantly different from the OLS, but the slope terms are. In this case, the rate at which y increases as a function of x would be inadequately explained by an OLS model.

  - In emissions science, this would reflect a situation in which the "high-emitters" of a pollutant are influenced more by some covariate than other emitters. This is not to say that the model term will always increase with τ; the situation could arise whereby lower emitters is greatly influenced by Covariate A but not B, while high emitters are influenced by B but not A.

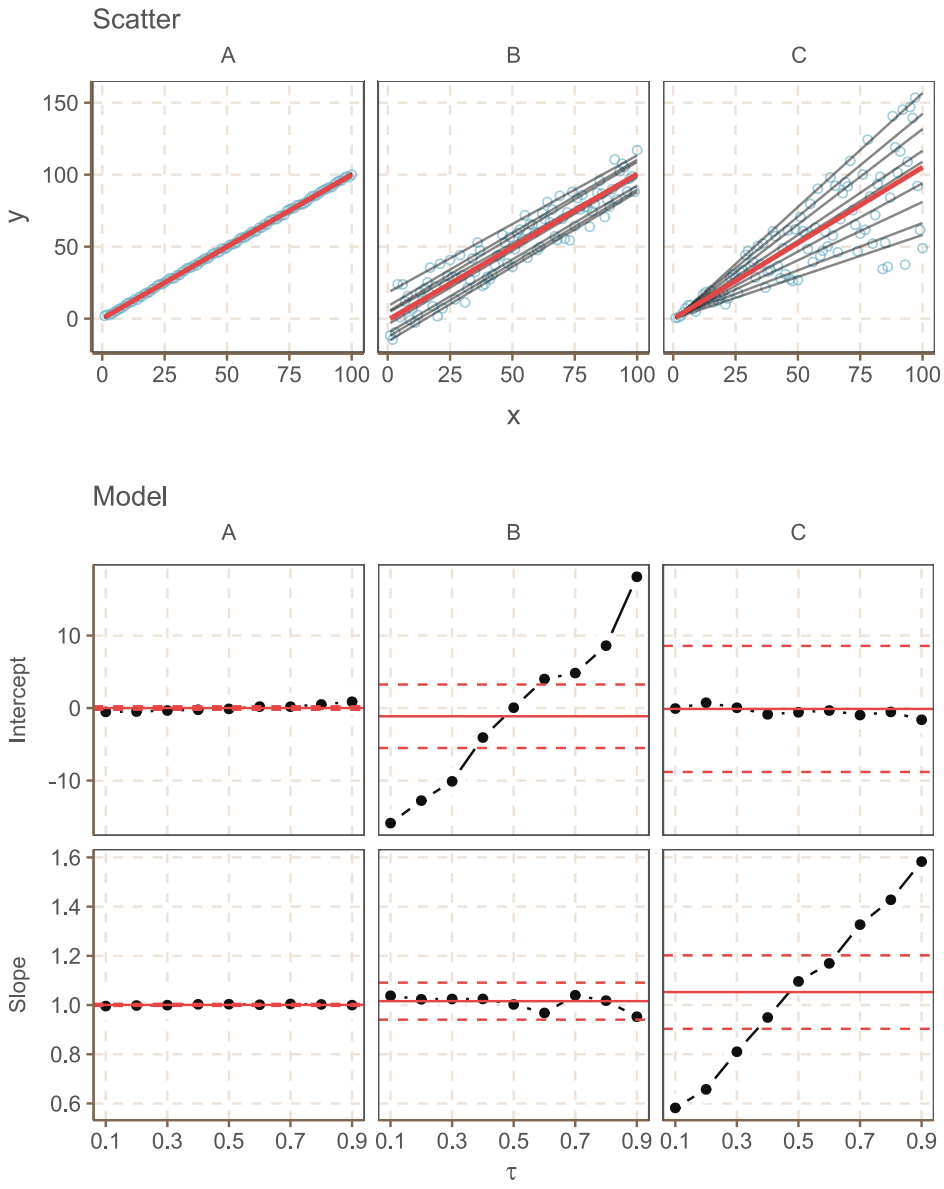

Figure D.1: Three data sets to illustrate quantile regression. Case A effectively shows a 1:1 relationship, Case B shows a linear relationship with a wider distribution in the y axis, and Case C shows an increase in the distribution of y as a function of x. **Scatter**: A scatter plot showing the raw data (blue), linear quantile regression fits (black) and a linear ordinary least squares (OLS) fit (red). **Model**: Line plots showing quantile regression model intercept and slope terms as a function of the quantile (black), and the equivalent ordinary least squares model term estimates and 95% confidence intervals (red).

Bibliography

[1] Davison, J., Bernard, Y., Borken-Kleefeld, J., Farren, N. J., Hausberger, S., Sjödin, Å., Tate, J. E., Vaughan, A. R. and Carslaw, D. C. Distance-based emission factors from vehicle emission remote sensing measurements. *Science of the Total Environment* 739 (2020), p. 139688. DOI: 10.1016/j.scitotenv.2020.139688 (cit. on pp. 22, 96, 100, 120, 154, 162).

[2] Davison, J., Rose, R. A., Farren, N. J., Wagner, R. L., Murrells, T. P. and Carslaw, D. C. Verification of a National Emission Inventory and Influence of On-road Vehicle Manufacturer-Level Emissions. *Environmental Science and Technology* 55.8 (2021), pp. 4452–4461. DOI: 10.1021/acs.est.0c08363. URL: https://doi.org/10.1021/acs.est.0c08363 (cit. on pp. 22, 98, 162, 188).

[3] Davison, J., Rose, R. A., Farren, N. J., Wagner, R. L., Wilde, S. E., Wareham, J. V. and Carslaw, D. C. Gasoline and diesel passenger car emissions deterioration using on-road emission measurements and measured mileage. *Atmospheric Environment: X* 14 (2022), p. 100162. DOI: 10.1016/J.AEAOA.2022.100162. URL: https://linkinghub.elsevier.com/retrieve/pii/S2590162122000168 (cit. on pp. 22, 194).

[4] Department for Transport. *Vehicle Licensing Statistics: July to September 2021*. 2022. URL: https://assets.publishing.service.gov.uk/government/uploads/system/uploads/attachment_data/file/1045962/vehicle-licensing-statistics-july-to-september-2021.pdf (cit. on p. 24).

[5] Office for National Statistics. *Population estimates*. 2021. URL: https://www.ons.gov.uk/peoplepopulationandcommunity/populationandmigration/populationestimates (cit. on p. 24).

[6] Department for Transport. *Reported road casualties in Great Britain, provisional estimates: year ending June 2021*. 2021. URL: https://www.gov.uk/government/statistics/reported-road-casualties-in-great-britain-provisional-estimates-year-ending-june-2021/reported-road-casualties-in-great-britain-provisional-estimates-year-ending-june-2021 (cit. on p. 24).

[7] Avila-Palencia, I., Int Panis, L., Dons, E., Gaupp-Berghausen, M., Raser, E., Götschi, T., Gerike, R., Brand, C., Nazelle, A. de, Orjuela, J. P., Anaya-Boig, E., Stigell, E., Kahlmeier, S., Iacorossi, F. and Nieuwenhuijsen, M. J. The effects of transport mode use on self-perceived health, mental health, and social contact measures: A cross-sectional and longitudinal study. *Environment International* 120 (2018), pp. 199–206. DOI: 10.1016/J.ENVINT.2018.08.002 (cit. on p. 24).

[8] Yang, X., McCoy, E., Anaya-Boig, E., Avila-Palencia, I., Brand, C., Carrasco-Turigas, G., Dons, E., Gerike, R., Goetschi, T., Nieuwenhuijsen, M., Pablo Orjuela, J., Int Panis, L., Standaert, A. and Nazelle, A. de. The effects of traveling in different transport modes on galvanic skin response (GSR) as a measure of stress: An observational study. *Environment International* 156 (2021), p. 106764. DOI: 10.1016/J.ENVINT.2021.106764 (cit. on p. 24).

[9] Dons, E., Rojas-Rueda, D., Anaya-Boig, E., Avila-Palencia, I., Brand, C., Cole-Hunter, T., Nazelle, A. de, Eriksson, U., Gaupp-Berghausen, M., Gerike, R., Kahlmeier, S., Laeremans, M., Mueller, N., Nawrot, T., Nieuwenhuijsen, M. J., Orjuela, J. P., Racioppi, F., Raser, E., Standaert, A., Int Panis, L. and Götschi, T. Transport mode choice and body mass index: Cross-sectional and longitudinal evidence from a European-wide study. *Environment International* 119 (2018), pp. 109–116. DOI: 10.1016/J.ENVINT.2018.06.023 (cit. on p. 24).

[10] Department for Transport. *Transport and Environment Statistics: 2021 Annual report*. 2021. URL: https://assets.publishing.service.gov.uk/government/uploads/system/uploads/attachment_data/file/984685/transport-and-environment-statistics-2021.pdf (cit. on p. 25).

[11] Royal College of Physicians. *Every breath we take: the lifelong impact of air pollution*. 2016. URL: https://www.rcplondon.ac.uk/projects/outputs/every-breath-we-take-lifelong-impact-air-pollution (cit. on p. 25).

[12] NHS. *Carbon monoxide poisoning*. URL: https://www.nhs.uk/conditions/carbon-monoxide-poisoning/ (cit. on p. 28).

[13] National Atmospheric Emissions Inventory. *Pollutant information: Carbon Monoxide*. 2018. URL: https://naei.beis.gov.uk/overview/pollutants?pollutant_id=4 (cit. on p. 28).

[14] Donaldson, K., Mills, N., MacNee, W., Robinson, S. and Newby, D. Role of inflammation in cardiopulmonary health effects of PM. *Toxicology and Applied Pharmacology* 207.2 (2005), pp. 483–488. DOI: 10.1016/J.TAAP.2005.02.020 (cit. on p. 29).

[15] Pope, C. A. and Dockery, D. W. Health Effects of Fine Particulate Air Pollution: Lines that Connect. *https://doi.org/10.1080/10473289.2006.10464485* 56.6 (2012), pp. 709–742. DOI: 10.1080/10473289.2006.10464485. URL: https://www.tandfonline.com/doi/abs/10.1080/10473289.2006.10464485 (cit. on p. 29).

[16] An, Z., Jin, Y., Li, J., Li, W. and Wu, W. *Impact of Particulate Air Pollution on Cardiovascular Health*. 2018. DOI: 10.1007/s11882-018-0768-8 (cit. on pp. 29, 63).

[17] Reşitotlu, I. A., Altinişik, K. and Keskin, A. *The pollutant emissions from diesel-engine vehicles and exhaust aftertreatment systems*. 2015. DOI: 10.1007/s10098-014-0793-9 (cit. on pp. 29, 30, 74).

[18] Zeldvich, Y. B. The oxidation of nitrogen in combustion and explosions. *J. Acta Physicochimica* 21 (1946), p. 577 (cit. on p. 30).

[19] National Atmospheric Emissions Inventory. *Pollutant Information: Nitrogen Oxides*. 2018. URL: https://naei.beis.gov.uk/overview/pollutants?pollutant_id=6 (cit. on pp. 30, 41, 117, 133).

[20] National Atmospheric Emissions Inventory. *Pollutant information: Sulphur Dioxide*. 2018. URL: https://naei.beis.gov.uk/overview/pollutants?pollutant_id=8 (cit. on p. 31).

[21] De Serio, D., Oliveira, A. de and Sodré, J. R. Effects of EGR rate on performance and emissions of a diesel power generator fueled by B7. *Journal of the Brazilian Society of Mechanical Sciences and Engineering* 39.6 (2017), pp. 1919–1927. DOI: 10.1007/S40430-017-0777-X/FIGURES/10. URL: https://link.springer.com/article/10.1007/s40430-017-0777-x (cit. on p. 31).

[22] Li, X., Xu, Z., Guan, C. and Huang, Z. Impact of exhaust gas recirculation (EGR) on soot reactivity from a diesel engine operating at high load. *Applied Thermal Engineering* 68.1-2 (2014), pp. 100–106. DOI: 10.1016/J.APPLTHERMALENG.2014.04.029 (cit. on p. 31).

[23] Abd-Alla, G. H. Using exhaust gas recirculation in internal combustion engines: a review. *Energy Conversion and Management* 43.8 (2002), pp. 1027–1042. DOI: 10.1016/S0196-8904(01)00091-7 (cit. on p. 31).

[24] Kašpar, J., Fornasiero, P. and Hickey, N. Automotive catalytic converters: current status and some perspectives. *Catalysis Today* 77.4 (2003), pp. 419–449. DOI: 10.1016/S0920-5861(02)00384-X (cit. on p. 32).

[25] National Atmospheric Emissions Inventory. *Pollutant Information: Ammonia*. 2018. URL: https://naei.beis.gov.uk/overview/pollutants?pollutant_id=21 (cit. on p. 32).

[26] Umicore Automotive Catalysts. *Three-way Catalyst L Umicore Automotive catalysts*. 2017. URL: https://ac.umicore.com/en/technologies/three-way-catalyst/ (cit. on p. 33).

[27] Wang, Y., Raman, S. and Grizzle, J. W. Dynamic Modeling of a Lean NOx Trap for Lean Burn Engine Control. 1999 (cit. on p. 33).

[28] Amiridis, M. D., Zhang, T. and Farrauto, R. J. Selective catalytic reduction of nitric oxide by hydrocarbons. *Applied Catalysis B: Environmental* 10.1-3 (1996), pp. 203–227. DOI: 10.1016/0926-3373(96)00031-8 (cit. on p. 34).

[29] Han, L., Cai, S., Gao, M., Hasegawa, J. Y., Wang, P., Zhang, J., Shi, L. and Zhang, D. Selective Catalytic Reduction of NOx with NH3 by Using Novel Catalysts: State of the Art and Future Prospects. *Chemical Reviews* 119.19 (2019), pp. 10916–10976. DOI: 10.1021/ACS.CHEMREV.9B00202. URL: https://pubs.acs.org/doi/full/10.1021/acs.chemrev.9b00202 (cit. on p. 34).

[30] Farren, N. J., Davison, J., Rose, R. A., Wagner, R. L. and Carslaw, D. C. Underestimated ammonia emissions from road vehicles. *Environmental Science and Technology* 54.24 (2020), pp. 15689–15697. DOI: 10.1021/acs.est.0c05839. URL: https://pubs.acs.org/doi/abs/10.1021/acs.est.0c05839 (cit. on pp. 35, 120, 155, 188).

[31] Farren, N. J., Davison, J., Rose, R. A., Wagner, R. L. and Carslaw, D. C. Characterisation of ammonia emissions from gasoline and gasoline hybrid passenger cars. *Atmospheric Environment: X* 11 (2021). DOI: 10.1016/J.AEAOA.2021.100117 (cit. on pp. 35, 54, 57, 155, 174, 175).

[32] Air quality expert group. *Non-Exhaust Emissions from Road Traffic*. 2019. URL: https://uk-air.defra.gov.uk/assets/documents/reports/cat09/1907101151_20190709_Non_Exhaust_Emissions_typeset_Final.pdf (cit. on p. 37).

[33] Timmers, V. R. and Achten, P. A. Non-exhaust PM emissions from electric vehicles. *Atmospheric Environment* 134 (2016), pp. 10–17. DOI: 10.1016/J.ATMOSENV.2016.03.017 (cit. on p. 37).

[34] Organization, W. H. *WHO global air quality guidelines: particulate matter (PM2.5 and PM10), ozone, nitrogen dioxide, sulfur dioxide and carbon monoxide*. World Health Organization, 2021, xxi, 273 p. (Cit. on pp. 39, 40).

[35] Department for Environment, Food & Rural Affairs. *UK Air Quality Limits*. 2010. URL: https://uk-air.defra.gov.uk/air-pollution/uk-eu-limits (cit. on pp. 39, 40).

[36] Organization, W. H. *Air quality guidelines. Global update 2005. Particulate matter, ozone, nitrogen dioxide and sulfur dioxide*. World Health Organization, 2006, ix, 484 p. (Cit. on p. 40).

[37] Breeze Technologies. *The new 2021 WHO air quality guideline limits*. 2021. URL: https://www.breeze-technologies.de/blog/new-2021-who-air-quality-guideline-limits/ (cit. on p. 40).

[38] National Atmospheric Emissions Inventory. *NAEI, UK National Atmospheric Emissions Inventory*. 2014. URL: https://naei.beis.gov.uk/ (cit. on pp. 41, 117).

[39] Ntziachristos, L., Gkatzoflias, D., Kouridis, C. and Samaras, Z. COPERT: A European Road Transport Emission Inventory Model. *Information Technologies in Environmental Engineering*. Ed. by I. N. Athanasiadis, A. E. Rizzoli, P. A. Mitkas and J. M. Gómez. Berlin, Heidelberg: Springer Berlin Heidelberg, 2009, pp. 491–504 (cit. on p. 42).

[40] EMISIA SA. *COPERT | EMISIA SA*. 2018. URL: https://www.emisia.com/utilities/copert/ (cit. on pp. 42, 97, 117).

[41] INFRAS. *The Handbook Emission Factors for Road Transport (HBEFA)*. 2022. URL: https://www.hbefa.net/e/index.html (cit. on p. 42).

[42] The ERMES Group. *European Research for Mobile Emission Sources*. 2021. URL: https://www.ermes-group.eu/ (cit. on p. 42).

[43] Franco, V., Fontaras, G. and Dilara, P. Towards Improved Vehicle Emissions Estimation in Europe. *Procedia - Social and Behavioral Sciences* 48 (2012), pp. 1304–1313. DOI: 10.1016/J.SBSPRO.2012.06.1106 (cit. on p. 42).

[44] Brown, P., Wakeling, D., Pang, Y. and Murrells, T. *Methodology for the UK's Road Transport Emissions Inventory*. Tech. rep. Didcot: Ricardo Energy & Environment, 2018. URL: https://uk-air.defra.gov.uk/assets/documents/reports/cat07/1804121004_Road_transport_emissions_methodology_report_2018_v1.1.pdf (cit. on pp. 42, 97, 117).

[45] Ntziachristos, L. and Samaras, Z. *1.A.3.b.i-iv Road transport 2019*. Tech. rep. European Environment Agency, 2019. URL: https://www.eea.europa.eu/publications/emep-eea-guidebook-2019/part-b-sectoral-guidance-chapters/1-energy/1-a-combustion/1-a-3-b-i/view (cit. on pp. 42, 99, 101, 104, 105, 117, 142).

[46] Gieseke, J. and Gerbrandy, G.-J. *Committee of Inquiry into Emission Measurements in the Automotive Sector, WORKING DOCUMENT No. 11, Appendix D: Timeline*. 2014. URL: https://www.europarl.europa.eu/doceo/document/EMIS-DT-594081_EN.pdf?redirect (cit. on p. 43).

[47] Council of European Union. *Council regulation (EU) no 715/2007*. https://eur-lex.europa.eu/legal-content/EN/ALL/?uri=celex%3A32007R0715. 2014 (cit. on pp. 44, 141, 156, 157).

[48] Demuynck, J., Favre, C., Bosteels, D., Hamje, H. and Andersson, J. *Real-world emissions measurements of a gasoline direct injection vehicle without and with a gasoline particulate filter*. Tech. rep. 2017 (cit. on p. 45).

[49] Giechaskiel, B., Valverde, V., Kontses, A., Melas, A., Martini, G., Balazs, A., Andersson, J., Samaras, Z. and Dilara, P. Particle Number Emissions of a Euro 6d-Temp Gasoline Vehicle under Extreme Temperatures and Driving Conditions. *Catalysts 2021, Vol. 11, Page 607* 11.5 (2021), p. 607. DOI: 10.3390/CATAL11050607. URL: https://www.mdpi.com/2073-4344/11/5/607/htm%20https://www.mdpi.com/2073-4344/11/5/607 (cit. on p. 45).

[50] Lähde, T., Giechaskiel, B., Pavlovic, J., Suarez-Bertoa, R., Valverde, V., Clairotte, M. and Martini, G. Solid particle number emissions of 56 light-

duty Euro 5 and Euro 6 vehicles. *Journal of Aerosol Science* 159 (2022), p. 105873. DOI: 10.1016/J.JAEROSCI.2021.105873 (cit. on p. 45).

[51] Degraeuwe, B. and Weiss, M. Does the New European Driving Cycle (NEDC) really fail to capture the NOx emissions of diesel cars in Europe? *Environmental Pollution* 222 (2017), pp. 234–241. URL: http://www.sciencedirect.com/science/article/pii/S0269749116327476 (cit. on pp. 45, 106).

[52] Puškár, M., Jahnátek, A., Kádárová, J., Šoltésová, M., Kovanič, Ľ. and Krivosudská, J. Environmental study focused on the suitability of vehicle certifications using the new European driving cycle (NEDC) with regard to the affair "dieselgate" and the risks of NO x emissions in urban destinations. *Air Quality, Atmosphere and Health* 12.2 (2019), pp. 251–257. DOI: 10.1007/S11869-018-0646-5/FIGURES/5. URL: https://link.springer.com/article/10.1007/s11869-018-0646-5 (cit. on p. 45).

[53] European Commission. *The European Green Deal*. 2019. URL: https://eur-lex.europa.eu/resource.html?uri=cellar:b828d165-1c22-11ea-8c1f-01aa75ed71a1.0002.02/DOC_1&format=PDF (cit. on p. 46).

[54] AGVES. *Study on post-EURO 6/VI emission standards in Europe. Presentation to the Advisory Group on Vehicle Emission Standards (AGVES) Brussels, October 18, 2019*. 2019 (cit. on p. 46).

[55] ICCT. *Comments and Technical Recommendations On Future Euro 7/Vii Emission Standards*. Tech. rep. Berlin: International Council on Clean Transportation, 2021. URL: https://theicct.org/sites/default/files/eu-commission-euro-7-and-VI-may2021.pdf (cit. on pp. 46, 141).

[56] European Commission. *European vehicle emissions standards – Euro 7 for cars, vans, lorries and buses*. URL: https://ec.europa.eu/info/law/better-regulation/have-your-say/initiatives/12313-European-vehicle-emissions-standards-Euro-7-for-cars-vans-lorries-and-buses_en (cit. on p. 46).

[57] European Federation for Transport and Environment. *Euro 7: Europe's chance to have clean air*. Tech. rep. 2021. URL: https://www.transportenvironment.org/wp-content/uploads/2021/09/2021_09_Euro_7_cars_vans_policy_paper.pdf (cit. on p. 46).

[58] European Federation for Transport and Environment. *The seven (dirty) air pollution tricks of the auto industry*. Tech. rep. 2021. URL: https://www.transportenvironment.org/wp-content/uploads/2021/09/2021_09_dirty_air_pollution_tricks.pdf (cit. on p. 46).

[59] Chen, Y., Sun, R. and Borken-Kleefeld, J. On-Road NOx and Smoke Emissions of Diesel Light Commercial Vehicles–Combining Remote Sensing Measurements from across Europe. *Environmental Science & Technology* 54.19 (2020), pp. 11744–11752. DOI: 10.1021/ACS.EST.9B07856. URL: https://pubs.acs.org/doi/full/10.1021/acs.est.9b07856 (cit. on pp. 46, 55, 155, 159).

[60] Jonson, J. E., Borken-Kleefeld, J., Simpson, D., Nyíri, A., Posch, M. and Heyes, C. Impact of excess NOx emissions from diesel cars on air quality, public health and eutrophication in Europe. *Environmental Research Letters* 12.9 (2017), p. 94017. URL: http://stacks.iop.org/1748-9326/12/i=9/a=094017 (cit. on pp. 46, 63).

[61] Chossière, G. P., Malina, R., Ashok, A., Dedoussi, I. C., Eastham, S. D., Speth, R. L. and Barrett, S. R. H. Public health impacts of excess NOx emissions from Volkswagen diesel passenger vehicles in Germany. *Environmental Research Letters* 12.3 (2017), p. 34014. URL: http://stacks.iop.org/1748-9326/12/i=3/a=034014 (cit. on pp. 46, 63).

[62] Chossière, G. P., Malina, R., Allroggen, F., Eastham, S. D., Speth, R. L. and Barrett, S. R. Country- and manufacturer-level attribution of air quality impacts due to excess NOx emissions from diesel passenger vehicles in Europe. *Atmospheric Environment* 189 (2018), pp. 89–97. DOI: 10.1016/j.atmosenv.2018.06.047 (cit. on pp. 46, 63).

[63] University of Denver. *What's a FEAT?* 2011. URL: http://www.feat.biochem.du.edu/whatsafeat.html (cit. on pp. 47, 145).

[64] Stedman, D. H., Bishop, G. A., Armstrong, J. A. and Maddox, J. *Fuel Efficiency Automobile Testing (F. E. A. T.), Final Report to the Colorado Office of Energy Conservation*. 1988. URL: https://digitalcommons.du.edu/cgi/viewcontent.cgi?article=1218&context=feat_publications (cit. on p. 47).

[65] Stedman, D. H. Automobile carbon monoxide emission. *Environmental Science and Technology* 23.2 (1989), pp. 147–149. DOI: 10.1021/ES00179A002. URL: https://pubs.acs.org/doi/abs/10.1021/es00179a002 (cit. on p. 47).

[66] Bishop, G. A., Starkey, J. R., Ihlenfeldt, A., Williams, W. J. and Stedman, D. H. IR Long-Path Photometry: A Remote Sensing Tool for Automobile Emissions. *Analytical Chemistry* 61.10 (1989). DOI: 10.1021/AC00185A746. URL: https://pubs.acs.org/doi/abs/10.1021/ac00185a746 (cit. on p. 47).

[67] Bishop, G. A. and Stedman, D. H. On-road carbon monoxide emission measurement comparisons for the 1988-1989 Colorado oxy-fuels programs. *Environmental Science and Technology; (United States)* 24.6 (1990). DOI: 10.1021/es00076a008. URL: https://www.osti.gov/biblio/5455737 (cit. on p. 48).

[68] Lawson, D. R., Groblicki, P. J., Stedman, D. H., Bishop, G. A. and Guenther, P. L. Emissions from lit-use Motor Vehicles in Los Angeles: A Pilot Study of Remote Sensing and the Inspection and Maintenance Program. *Journal of the Air & Waste Management Association* 40.8 (1990), pp. 1096–1105. DOI: 10.1080/10473289.1990.10466754. eprint: https://doi.org/10.1080/10473289.1990.10466754. URL: https://doi.org/10.1080/10473289.1990.10466754 (cit. on p. 48).

[69] Guenther, P. L., Stedman, D. H., Bishop, G. A., Beaton, S. P., Bean, J. H. and Quine, R. W. A hydrocarbon detector for the remote sensing of vehicle exhaust emissions. *Review of Scientific Instruments* 66.4 (1995), p. 3024. DOI:

10.1063/1.1146498. URL: https://aip.scitation.org/doi/abs/10.1063/1.1146498 (cit. on p. 48).

[70] Beaton, S., Bishop, G. and Stedman, D. Emission Characteristics of Mexico City Vehicles. *Journal of the Air & Waste Management Association* 42.11 (1992), pp. 1424–1429. DOI: 10.1080/10473289.1992.10467088. URL: https://doi.org/10.1080/10473289.1992.10467088 (cit. on p. 48).

[71] Stedman, D. and Bishop, G. *Apparatus for remote analysis of vehicle emissions*. 1993 (cit. on p. 48).

[72] Butler, J. W., Gierczak, C. A., Jesion, G., Stedman, D. H. and Lesko, J. M. *On-road NOx emissions intercomparison of on-board measurements and remote sensing. Final report*. 1994. URL: https://www.osti.gov/biblio/7105457 (cit. on p. 48).

[73] Bishop, G. A., Beaton, S. P., Guenther, P. L., McVey, l. F. and Zhang, Y. Enhancement of Remote Sensing for Mobile Source Nitric Oxide. *https://doi.org/10.1080/10473289.1996.10467437* 46.1 (2012), pp. 25–29. DOI: 10.1080/10473289.1996.10467437. URL: https://www.tandfonline.com/doi/abs/10.1080/10473289.1996.10467437 (cit. on p. 48).

[74] Carslaw, D. C. and Beevers, S. D. New Directions: Should road vehicle emissions legislation consider primary NO2? *Atmospheric Environment* 38.8 (2004), pp. 1233–1234. DOI: 10.1016/J.ATMOSENV.2003.12.008 (cit. on p. 48).

[75] Burgard, D. A., Bishop, G. A. and Stedman, D. H. Remote Sensing of Ammonia and Sulfur Dioxide from On-Road Light Duty Vehicles. *Environmental Science and Technology* 40.22 (2006), pp. 7018–7022. DOI: 10.1021/ES061161R. URL: https://pubs.acs.org/doi/abs/10.1021/es061161r (cit. on p. 48).

[76] OPUS. *Remote Sensing*. 2018. URL: https://www.opus.global/vehicle-inspection/remote-sensing/ (cit. on pp. 48, 58, 145).

[77] Hager Environmental & Atmospheric Technologies. *EDAR: A Touchless Emissions Testing Solution*. 2019. URL: https://www.heatremotesensing.com/edar (cit. on pp. 48, 88).

[78] Ropkins, K., DeFries, T. H., Pope, F., Green, D. C., Kemper, J., Kishan, S., Fuller, G. W., Li, H., Sidebottom, J., Crilley, L. R., Kramer, L., Bloss, W. J. and Stewart Hager, J. Evaluation of EDAR vehicle emissions remote sensing technology. *Science of the Total Environment* 609 (2017), pp. 1464–1474. DOI: 10.1016/j.scitotenv.2017.07.137 (cit. on pp. 48, 88, 91).

[79] Burgard, D. A., Bishop, G. A., Stadtmuller, R. S., Dalton, T. R. and Stedman, D. H. Spectroscopy Applied to On-Road Mobile Source Emissions. *Applied Spectroscopy* 60.5 (2006), 135A–148A. DOI: 10.1366/00037020677741218 5. URL: http://journals.sagepub.com/doi/10.1366/00037020677 7412185 (cit. on pp. 49, 54, 65, 76, 119, 144, 145).

[80] Singer, B. C., Harley, R. A., Littlejohn, D., Ho, J. and Vo, T. Scaling of infrared remote sensor hydrocarbon measurements for motor vehicle emission inventory calculations. *Environmental Science & Technology* 32.21 (1998), pp. 3241–3248 (cit. on pp. 51, 71).

[81] Bernard, Y., Dallmann, T., Lee, K., Rintanen, I. and Tietge, U. *Evaluation of real-world vehicle emissions in Brussels*. Tech. rep. TRUE - The Real Urban Emissions Initiative, 2021 (cit. on p. 51).

[82] Rushton, C. E., Tate, J. E., Shepherd, S. P. and Carslaw, D. C. Interinstrument comparison of remote-sensing devices and a new method for calculating on-road nitrogen oxides emissions and validation of vehicle-specific power. *Journal of the Air and Waste Management Association* 68.2 (2018). DOI: 10.1080/10962247.2017.1296504 (cit. on pp. 51, 53, 83, 146).

[83] Dallmann, T., Bernard, Y., Tietge, U. and Muncrief, R. *Remote sensing of motor vehicle exhaust emissions in London*. Tech. rep. December. Washington DC: International Council on Clean Transportation, 2018. URL: https://theicct.org/publications/true-london-dec2018 (cit. on pp. 52, 57, 138, 154, 162).

[84] Jiménez-Palacios, J. L. Understanding and quantifying motor vehicle emissions with vehicle specific power and TILDAS remote sensing. PhD thesis. Massachusetts Institute of Technology, 1999. URL: https://dspace.mit.edu/handle/1721.1/44505 (cit. on pp. 52, 56, 67, 83).

[85] Cheshire Datasystems Limited. *CDL Vehicle Information Services (CDL VIS)*. 2018. URL: https://www.cdl.co.uk/ (cit. on pp. 52, 77, 98, 119, 145).

[86] Franco, V., Kousoulidou, M., Muntean, M., Ntziachristos, L., Hausberger, S. and Dilara, P. Road vehicle emission factors development: A review. *Atmospheric Environment* 70 (2013), pp. 84–97. DOI: 10.1016/J.ATMOSENV.2013.01.006 (cit. on p. 53).

[87] Carslaw, D. C. and Rhys-Tyler, G. New insights from comprehensive on-road measurements of NOx, NO2 and NH3 from vehicle emission remote sensing in London, UK. *Atmospheric Environment* 81.0 (2013), pp. 339–347. DOI: http://dx.doi.org/10.1016/j.atmosenv.2013.09.026 (cit. on pp. 54, 77).

[88] Chen, Y., Zhang, Y. and Borken-Kleefeld, J. When is Enough? Minimum Sample Sizes for On-Road Measurements of Car Emissions. *Environmental Science and Technology* 53.22 (2019), pp. 13284–13292. DOI: 10.1021/ACS.EST.9B04123/ASSET/IMAGES/ACS.EST.9B04123.SOCIAL.JPEG{_}V03. URL: https://pubs.acs.org/doi/full/10.1021/acs.est.9b04123 (cit. on p. 54).

[89] Smit, R., Bainbridge, S., Kennedy, D. and Kingston, P. A decade of measuring on-road vehicle emissions with remote sensing in Australia. *Atmospheric Environment* 252 (2021), p. 118317. DOI: 10.1016/J.ATMOSENV.2021.118317 (cit. on pp. 55, 155).

[90] Bishop, G. A. and Stedman, D. H. Reactive Nitrogen Species Emission Trends in Three Light-/Medium-Duty United States Fleets. *Environmental Science and Technology* 49 (2015), pp. 11234–11240. DOI: 10.1021/acs.est.5b02392 (cit. on pp. 55, 64).

[91] Bishop, G. A. Three decades of on-road mobile source emissions reductions in South Los Angeles. *Journal of the Air and Waste Management Association* 69.8 (2019), pp. 967–976. DOI: 10.1080/10962247.2019.1611677/SUPPL{_}FILE/UAWM{_}A{_}1611677{_}SM4781.DOCX. URL: https://www.tandfonline.com/doi/abs/10.1080/10962247.2019.1611677 (cit. on p. 55).

[92] Burgard, D. A., Bishop, G. A., Stedman, D. H., Gessner, V. H. and Daeschlein, C. Remote Sensing of In-Use Heavy-Duty Diesel Trucks. *Environmental Science and Technology* 40.22 (2006), pp. 6938–6942. DOI: 10.1021/ES060989A. URL: https://pubs.acs.org/doi/full/10.1021/es060989a (cit. on pp. 55, 56).

[93] Bishop, G. A., Schuchmann, B. G. and Stedman, D. H. Heavy-duty truck emissions in the south coast air basin of California. *Environmental Science and Technology* 47.16 (2013), pp. 9523–9529. DOI: 10.1021/ES401487B (cit. on p. 55).

[94] Bishop, G. A., Hottor-Raguindin, R., Stedman, D. H., McClintock, P., Theobald, E., Johnson, J. D., Lee, D. W., Zietsman, J. and Misra, C. On-road heavy-duty vehicle emissions monitoring system. *Environmental Science and Technology* 49.3 (2015), pp. 1639–1645. DOI: 10.1021/ES505534E/SUPPL{_}FILE/ES505534E{_}SI{_}001.PDF. URL: https://pubs.acs.org/doi/full/10.1021/es505534e (cit. on p. 55).

[95] Haugen, M. J. and Bishop, G. A. Repeat Fuel Specific Emission Measurements on Two California Heavy-Duty Truck Fleets. *Environmental Science and Technology* 51.7 (2017), pp. 4100–4107. DOI: 10.1021/ACS.EST.6B06172/SUPPL{_}FILE/ES6B06172{_}SI{_}001.PDF. URL: https://pubs.acs.org/doi/full/10.1021/acs.est.6b06172 (cit. on p. 55).

[96] Haugen, M. J., Bishop, G. A., Thiruvengadam, A. and Carder, D. K. Evaluation of Heavy- and Medium-Duty On-Road Vehicle Emissions in California's South Coast Air Basin. *Environmental Science and Technology* 52.22 (2018), pp. 13298–13305. DOI: 10.1021/ACS.EST.8B03994/SUPPL{_}FILE/

ES8B03994{_}SI{_}001.PDF. URL: https://pubs.acs.org/doi/full/10.1021/acs.est.8b03994 (cit. on p. 55).

[97] Haugen, M. J. and Bishop, G. A. Long-Term Fuel-Specific NOx and Particle Emission Trends for In-Use Heavy-Duty Vehicles in California. *Environmental Science and Technology* 52.10 (2018), pp. 6070–6076. DOI: 10.1021/ACS.EST.8B00621/SUPPL{_}FILE/ES8B00621{_}SI{_}001.PDF. URL: https://pubs.acs.org/doi/abs/10.1021/acs.est.8b00621 (cit. on p. 55).

[98] Borken-Kleefeld, J., Hausberger, S., Mcclintock, P., Tate, J., Carslaw, D., Bernard, Y., Sjödin, Å., Jerksjö, M., Gentala, R., Alt, G.-M., Tietge, U. and De La Fuente, J. *Comparing emission rates derived from remote sensing with PEMS and chassis dynamometer tests - CONOX Task 1 Report*. Tech. rep. IVL Swedish Environmental Research Institute, 2018. URL: www.ivl.se (cit. on pp. 55, 67, 69, 70, 127).

[99] Sjödin, Å., Borken-Kleefeld, J., Carslaw, D., Tate, J., Alt, G.-M., De La Fuente, J. and Bernard, Y. *Real-driving emissions from diesel passenger cars measured by remote sensing and as compared with PEMS and chassis dynamometer measurements-CONOX Task 2*. Tech. rep. IVL Swedish Environmental Research Institute, 2018. URL: www.ivl.se (cit. on pp. 55, 142).

[100] Carslaw, D., Farren, N., Borken-Kleefeld, J. and Sjödin, Å. *Study on the durability of European passenger car emission control systems utilizing remote sensing data Commissioned by the Federal Office for the Environment (FOEN), Switzerland*. Tech. rep. IVL Swedish Environmental Research Institute, 2019. URL: www.ivl.se (cit. on pp. 55, 77, 146).

[101] Grange, S. K., Farren, N. J., Vaughan, A. R., Davison, J. and Carslaw, D. C. Post-Dieselgate: Evidence of NOx Emission Reductions Using On-Road Remote Sensing. *Environmental Science & Technology Letters* 7.6 (2020), pp. 382–387. DOI: 10.1021/ACS.ESTLETT.0C00188. URL: https://pubs.acs.org/doi/abs/10.1021/acs.estlett.0c00188 (cit. on pp. 56, 57, 99, 135, 162).

[102] Bishop, G. A. On-Road NOx Emissions Evaluation of the Repair Effectiveness for Recalled Volkswagen Group Light-Duty Diesel Vehicles in the United States. *Environmental Science and Technology* 55.24 (2021), pp. 16581–16585. DOI: 10.1021/ACS.EST.1C06826/SUPPL{_}FILE/ES1C06826{_}SI{_}001.PDF. URL: https://pubs.acs.org/doi/full/10.1021/acs.est.1c06826 (cit. on p. 56).

[103] Bishop, G. A. and Stedman, D. H. The recession of 2008 and its impact on light-duty vehicle emissions in three western United States cities. *Environmental Science and Technology* 48.24 (2014), pp. 14822–14827. DOI: 10.1021/ES5043518/SUPPL{_}FILE/ES5043518{_}SI{_}001.PDF. URL: https://pubs.acs.org/doi/full/10.1021/es5043518 (cit. on p. 56).

[104] Bishop, G. A., Stedman, D. H., Burgard, D. A. and Atkinson, O. High-Mileage Light-Duty Fleet Vehicle Emissions: Their Potentially Overlooked Importance. *Environmental Science and Technology* 50.10 (2016), pp. 5405–5411. DOI: 10.1021/ACS.EST.6B00717. URL: https://pubs.acs.org/doi/full/10.1021/acs.est.6b00717 (cit. on pp. 56, 95, 116, 143).

[105] Zhan, T., Ruehl, C. R., Bishop, G. A., Hosseini, S., Collins, J. F., Yoon, S. and Herner, J. D. An analysis of real-world exhaust emission control deterioration in the California light-duty gasoline vehicle fleet. *Atmospheric Environment* 220 (2020), p. 117107. DOI: 10.1016/J.ATMOSENV.2019.117107 (cit. on pp. 56, 95, 143).

[106] Bishop, G. A. Does California's EMFAC2017 vehicle emissions model underpredict California light-duty gasoline vehicle NOx emissions? *Journal of the Air and Waste Management Association* 71.5 (2021), pp. 597–606. DOI: 10.1080/10962247.2020.1869121/SUPPL{_}FILE/UAWM{_}A{_}1869121{_}SM6311.DOCX. URL: https://www.tandfonline.com/doi/abs/10.1080/10962247.2020.1869121 (cit. on p. 56).

[107] Carslaw, D. C., Williams, M. L., Tate, J. E. and Beevers, S. D. The importance of high vehicle power for passenger car emissions. *Atmospheric Environment*

68 (2013), pp. 8–16. DOI: 10.1016/J.ATMOSENV.2012.11.033 (cit. on p. 56).

[108] Bishop, G. A., Morris, J. A., Stedman, D. H., Cohen, L. H., Countess, R. J., Countess, S. J., Maly, P. and Scherer, S. The Effects of Altitude on Heavy-Duty Diesel Truck On-Road Emissions. *Environmental Science & Technology* 35.8 (2001), pp. 1574–1578. DOI: 10.1021/es001533a. URL: https://pubs.acs.org/doi/10.1021/es001533a (cit. on pp. 56, 64).

[109] Bishop, G. A., Haugen, M. J., Mcdonald, B. C. and Boies, A. M. Utah Wintertime Measurements of Heavy-Duty Vehicle Nitrogen Oxide Emission Factors. *Environmental Science and Technology* 56.3 (2022), pp. 1885–1893. DOI: 10.1021/ACS.EST.1C06428/SUPPL{_}FILE/ES1C06428{_}SI{_}001.PDF. URL: https://pubs.acs.org/doi/full/10.1021/acs.est.1c06428 (cit. on p. 56).

[110] Grange, S. K., Farren, N. J., Vaughan, A. R., Rose, R. A. and Carslaw, D. C. Strong Temperature Dependence for Light-Duty Diesel Vehicle NOx Emissions. *Environmental Science & Technology* 53 (2019), pp. 6587–6596. DOI: 10.1021/acs.est.9b01024. URL: https://pubs.acs.org/doi/10.1021/acs.est.9b01024. (cit. on pp. 56, 57, 64, 95, 106, 116, 148, 162).

[111] Borken-Kleefeld, J. and Dallmann, T. *Remote sensing of motor vehicle exhaust emissions*. Tech. rep. September. Washington: International Council on Clean Transportation, 2018. URL: www.theicct.org (cit. on pp. 57, 64, 162).

[112] Bernard, Y., Tietge, U. and Pniewska, I. *Remote sensing of motor vehicle exhaust emissions in Krakow*. Tech. rep. September. Washington DC: International Council on Clean Transportation, 2018. URL: https://theicct.org/publications/remote-sensing-krakow-sept2020 (cit. on pp. 57, 154, 162).

[113] Huang, Y., Organ, B., Zhou, J. L., Surawski, N. C., Hong, G., Chan, E. F. and Yam, Y. S. Remote sensing of on-road vehicle emissions: Mechanism, applications and a case study from Hong Kong. *Atmospheric Environment* 182 (2018), pp. 58–74. DOI: 10.1016/J.ATMOSENV.2018.03.035. URL: https:

//www.sciencedirect.com/science/article/pii/S1352231018301870 (cit. on pp. 57, 64).

[114] Rushton, C. E., Tate, J. E. and Shepherd, S. P. A novel method for comparing passenger car fleets and identifying high-chance gross emitting vehicles using kerbside remote sensing data. *Science of The Total Environment* 750 (2021), p. 142088. DOI: 10.1016/J.SCITOTENV.2020.142088 (cit. on p. 57).

[115] Qiu, M. and Borken-Kleefeld, J. Using snapshot measurements to identify high-emitting vehicles. *Environmental Research Letters* (2022). DOI: 10.1088/1748-9326/AC5C9E. URL: https://iopscience.iop.org/article/10.1088/1748-9326/ac5c9e%20https://iopscience.iop.org/article/10.1088/1748-9326/ac5c9e/meta (cit. on p. 57).

[116] Yang, Z., Tate, J. E., Rushton, C. E., Morganti, E. and Shepherd, S. P. Detecting candidate high NOx emitting light commercial vehicles using vehicle emission remote sensing. *Science of The Total Environment* 823 (2022), p. 153699. DOI: 10.1016/J.SCITOTENV.2022.153699 (cit. on p. 57).

[117] Opus Remote Sensing Europe. *Spanish Guardia Civil publishes its investigation of manipulated trucks thanks to the collaboration with Opus RSE*. 2019. URL: https://www.opusrse.com/2019/03/27/spanish-guardia-civil-publishes-its-investigation-of-manipulated-trucks-thanks-to-the-collaboration-with-opus-rse/ (cit. on pp. 57, 64).

[118] Gautam, M., Stedman, D., Carder, D., Shade, B., Clark, N., Thompson, G., Wayne, S., Bishop, G., Schuchmann, B., Pope, D., Vescio, N., Full, G., McClintock, P., Rau, D., Collins, J. and Stedman, D. H. *Correlation of the Real-Time Particulate Matter Emissions Measurements of a ESP Remote Sensing Device (RSD) and a Dekati Electronic Tailpipe Sensor (ETaPS) with Gravimetrically Measured PM from a Total Exhaust Dilution Tunnel System*. Tech. rep. Sacramento: California Air Resources Board, 2010. URL: https://ww2.arb.ca.gov/sites/default/files/classic//research/apr/past/icat06-02.pdf (cit. on pp. 58, 155).

[119] Bishop, G. A., Defries, T. H., Sidebottom, J. A. and Kemper, J. M. Vehicle Exhaust Remote Sensing Device Method to Screen Vehicles for Evaporative Running Loss Emissions. *Environmental science & technology* 54.22 (2020), pp. 14627–14634. DOI: 10.1021/ACS.EST.0C05433. URL: https://pubmed.ncbi.nlm.nih.gov/33156619/ (cit. on p. 58).

[120] Bishop, G. A. *Fuel Efficiency Automobile Test Data Center: What's a FEAT?* 2011. URL: http://www.feat.biochem.du.edu/whatsafeat.html (cit. on pp. 58, 120).

[121] R Core Team. *R: A Language and Environment for Statistical Computing*. R Foundation for Statistical Computing. Vienna, Austria, 2020. URL: https://www.R-project.org/ (cit. on pp. 60, 74, 149, 177).

[122] RStudio Team. *RStudio: Integrated Development Environment for R*. RStudio, PBC. Boston, MA, 2020. URL: http://www.rstudio.com/ (cit. on p. 60).

[123] Wickham, H., Averick, M., Bryan, J., Chang, W., McGowan, L. D., François, R., Grolemund, G., Hayes, A., Henry, L., Hester, J., Kuhn, M., Pedersen, T. L., Miller, E., Bache, S. M., Müller, K., Ooms, J., Robinson, D., Seidel, D. P., Spinu, V., Takahashi, K., Vaughan, D., Wilke, C., Woo, K. and Yutani, H. Welcome to the tidyverse. *Journal of Open Source Software* 4.43 (2019), p. 1686. DOI: 10.21105/joss.01686 (cit. on p. 60).

[124] Dowle, M. and Srinivasan, A. *data.table: Extension of 'data.frame'*. R package version 1.14.0. 2021. URL: https://CRAN.R-project.org/package=data.table (cit. on p. 60).

[125] Wickham, H. *ggplot2: Elegant Graphics for Data Analysis*. Springer-Verlag New York, 2016. URL: https://ggplot2.tidyverse.org (cit. on p. 60).

[126] Wilkins, D. *treemapify: Draw Treemaps in 'ggplot2'*. R package version 2.5.5. 2021. URL: https://CRAN.R-project.org/package=treemapify (cit. on pp. 60, 128).

[127] Kay, M. *ggdist: Visualizations of Distributions and Uncertainty*. R package version 2.4.0. 2021. DOI: 10.5281/zenodo.3879620. URL: https://mjskay.github.io/ggdist/ (cit. on pp. 60, 164).

[128] Wilke, C. O. *ggtext: Improved Text Rendering Support for 'ggplot2'*. R package version 0.1.1. 2020. URL: https://CRAN.R-project.org/package=ggtext (cit. on p. 60).

[129] Wilke, C. O. *cowplot: Streamlined Plot Theme and Plot Annotations for 'ggplot2'*. R package version 1.1.1. 2020. URL: https://CRAN.R-project.org/package=cowplot (cit. on p. 60).

[130] Pedersen, T. L. *patchwork: The Composer of Plots*. R package version 1.1.1. 2020. URL: https://CRAN.R-project.org/package=patchwork (cit. on p. 60).

[131] Tobin, C. *ggthemr: Themes for 'ggplot2'*. R package version 1.1.0. 2020 (cit. on p. 60).

[132] Inkscape Project. *Inkscape*. Version 1.00.0. 2020. URL: https://inkscape.org (cit. on p. 60).

[133] Kuhn, M. and Wickham, H. *Tidymodels: a collection of packages for modeling and machine learning using tidyverse principles.* 2020. URL: https://www.tidymodels.org (cit. on pp. 60, 149).

[134] Wood, S. N. *Generalized Additive Models: An Introduction with R*. 2nd ed. Chapman and Hall/CRC, 2017 (cit. on pp. 60, 72, 122).

[135] Therneau, T. and Atkinson, B. *rpart: Recursive Partitioning and Regression Trees*. R package version 4.1-15. 2019. URL: https://CRAN.R-project.org/package=rpart (cit. on pp. 60, 78).

[136] Koenker, R. *quantreg: Quantile Regression*. R package version 5.86. 2021. URL: https://CRAN.R-project.org/package=quantreg (cit. on pp. 60, 148).

[137] Iannone, R., Cheng, J. and Schloerke, B. *gt: Easily Create Presentation-Ready Display Tables*. R package version 0.3.1. 2021. URL: https://CRAN.R-project.org/package=gt (cit. on p. 60).

[138] Sjoberg, D. D., Curry, M., Hannum, M., Larmarange, J., Whiting, K. and Zabor, E. C. *gtsummary: Presentation-Ready Data Summary and Analytic Result Tables*. R package version 1.4.2. 2021. URL: https://CRAN.R-project.org/package=gtsummary (cit. on p. 60).

[139] European Environment Agency. *Air quality in Europe - 2019 Report*. Tech. rep. European Environment Agency, 2019. URL: https://op.europa.eu/en/publication-detail/-/publication/7d42ac97-faca-11e9-8c1f-01aa75ed71a1/language-en (cit. on p. 63).

[140] Mannucci, P. M., Harari, S., Martinelli, I. and Franchini, M. Effects on health of air pollution: a narrative review. *Internal and Emergency Medicine* 10.6 (2015), pp. 657–662. DOI: 10.1007/s11739-015-1276-7 (cit. on p. 63).

[141] Kar Kurt, O., Zhang, J. and Pinkerton, K. E. Pulmonary Health Effects of Air Pollution. *Current opinion in pulmonary medicine* 22.2 (2016), p. 138. DOI: 10.1097/MCP.0000000000000248 (cit. on p. 63).

[142] Schraufnagel, D. E., Balmes, J. R., Cowl, C. T., De Matteis, S., Jung, S. H., Mortimer, K., Perez-Padilla, R., Rice, M. B., Riojas-Rodriguez, H., Sood, A., Thurston, G. D., To, T., Vanker, A. and Wuebbles, D. J. Air Pollution and Noncommunicable Diseases: A Review by the Forum of International Respiratory Societies' Environmental Committee, Part 1: The Damaging Effects of Air Pollution. *Chest* 155.2 (2019), pp. 409–416. DOI: 10.1016/j.chest.2018.10.042 (cit. on p. 63).

[143] Mock, P. *Real-driving emissions test procedure for exhaust gas pollutant emissions of cars and light commercial vehicles in Europe*. Tech. rep. International Council on Clean Transportation, 2017, pp. 1–10 (cit. on p. 64).

[144] Carslaw, D. C., Murrells, T. P., Andersson, J. and Keenan, M. Have vehicle emissions of primary NO2 peaked? *Faraday Discuss.* 189 (2016), pp. 439–454. DOI: 10.1039/C5FD00162E. URL: http://xlink.rsc.org/?DOI=C5FD00162E (cit. on pp. 64, 116).

[145] Bishop, G. A. and Stedman, D. H. Measuring the Emissions of Passing Cars. *Accounts of Chemical Research* 29.10 (1996), pp. 489–495. DOI: 10.1021/ar950240x (cit. on pp. 65, 76, 119, 144).

[146] Singer, B. C. and Harley, R. A. A Fuel-Based Motor Vehicle Emission Inventory. *Journal of the Air & Waste Management Association* 46.6 (1996), pp. 581–593. DOI: 10.1080/10473289.1996.10467492. URL: https://www.tandfonline.com/action/journalInformation?journalCode=uawm20 (cit. on p. 65).

[147] Lee, T. and Frey, H. C. Evaluation of representativeness of site-specific fuel-based vehicle emission factors for route average emissions. *Environmental Science and Technology* 46.12 (2012), pp. 6867–6873. DOI: 10.1021/es204451z (cit. on p. 65).

[148] Carslaw, D. C., Beevers, S. D., Tate, J. E., Westmoreland, E. J. and Williams, M. L. Recent evidence concerning higher NOx emissions from passenger cars and light duty vehicles. *Atmospheric Environment* 45.39 (2011). DOI: 10.1016/j.atmosenv.2011.09.063 (cit. on p. 65).

[149] Bernard, Y., Tietge, U., German, J. and Muncrief, R. *Determination of real-world emissions from passenger vehicles using remote sensing data*. 2018. URL: https://www.theicct.org/publications/real-world-emissions-using-remote-sensing-data (cit. on pp. 65, 71, 117, 118, 134, 137, 138).

[150] Andrés Aguilar-Gómez, J., Garibay-Bravo, V., Tzintzun-Cervantes, G., Cruz-Jimate, I. and Echániz-Pellicer, G. *Mobile Source Emission Estimates using Remote Sensing Data from Mexican Cities*. Tech. rep. Instituto Nacional de Ecología, 2009 (cit. on p. 65).

[151] Zhou, Y., Wu, Y., Zhang, S., Fu, L. and Hao, J. Evaluating the emission status of light-duty gasoline vehicles and motorcycles in Macao with real-world remote sensing measurement. *Journal of Environmental Sciences (China)* 26.11 (2014), pp. 2240–2248. DOI: 10.1016/j.jes.2014.09.009 (cit. on p. 66).

[152] Wang, Z., Wu, Y., Zhou, Y., Li, Z., Wang, Y., Zhang, S. and Hao, J. Real-world emissions of gasoline passenger cars in Macao and their correlation with driving conditions. *International Journal of Environmental Science and Technology* 11.4 (2014), pp. 1135–1146. DOI: 10.1007/s13762-013-0276-2 (cit. on pp. 66, 75).

[153] Chan, T. L. and Ning, Z. On-road remote sensing of diesel vehicle emissions measurement and emission factors estimation in Hong Kong. *Atmospheric Environment* 39.36 (2005), pp. 6843–6856. DOI: 10.1016/j.atmosenv.2005.07.048 (cit. on p. 66).

[154] Tong, H. Y., Hung, W. T. and Cheung, C. S. On-road motor vehicle emissions and fuel consumption in urban driving conditions. *Journal of the Air and Waste Management Association* 50.4 (2000), pp. 543–554. DOI: 10.1080/10473289.2000.10464041 (cit. on p. 66).

[155] Zhou, Y., Fu, L. and Cheng, L. Characterization of in-use light-duty gasoline vehicle emissions by remote sensing in Beijing: Impact of recent control measures. *Journal of the Air and Waste Management Association* 57.9 (2007), pp. 1071–1077. DOI: 10.3155/1047-3289.57.9.1071 (cit. on p. 66).

[156] Hausberger, S. *Simulation of Real World Vehicle Exhaust Emissions*. Vol. 82. Austria: Technische Universität Graz, 2003 (cit. on pp. 67, 69, 70, 122).

[157] European Commission. *REGULATION (EEC) No 4064/89 MERGER PROCEDURE Article 6(1)(b) NON-OPPOSITION*. Tech. rep. European Commission, 1999 (cit. on p. 69).

[158] Keller, M., Hausberger, S., Matzer, C., Wüthrich, P. and Notter, B. *A novel approach for NOx emission factors of diesel cars in HBEFA (Version 3.3)*. Tech. rep. IVT Institute for internal combustion engines and thermodynamics, 2017 (cit. on pp. 69, 70).

[159] Department for Transport. *Vehicle Emissions Testing Programme*. London, 2016. URL: https://www.gov.uk/government/publications/vehicle-emissions-testing-programme-conclusions (cit. on pp. 73, 122).

[160] Driver & Vehicle Standards Agency. *Vehicle Market Surveillance Unit*. Tech. rep. London: Driver & Vehicle Standards Agency, 2017, p. 39. URL: https://assets.publishing.service.gov.uk/government/uploads/system/uploads/attachment_data/file/691601/vehicle-market-surveillance-unit-programme-results-2017.pdf (cit. on p. 73).

[161] Carslaw, D. C. and Ropkins, K. openair — An R package for air quality data analysis. *Environmental Modelling & Software* 27-28 (2012), pp. 52–61. DOI: 10.1016/J.ENVSOFT.2011.09.008. URL: https://www.sciencedirect.com/science/article/pii/S1364815211002064 (cit. on p. 80).

[162] Carlson, R. B., Wishart, J. and Stutenberg, K. On-Road and Dynamometer Evaluation of Vehicle Auxiliary Loads. *SAE International Journal of Fuels and Lubricants* 9.1 (2016), pp. 260–268. DOI: 10.4271/2016-01-0901 (cit. on p. 83).

[163] Baldino, C., Tietge, U., Muncrief, R., Bernard, Y. and Mock, P. *Road Tested: Comparative Overview of Real-world Versus Type-approval NOx and CO2 Emissions from Diesel Cars in Europe*. 2017. URL: https://www.theicct.org/publications/road-tested-comparative-overview-real-world-versus-type-approval-nox-and-co2-emissions (cit. on p. 88).

[164] TRUE. *Data | TRUE - The Real Urban Emissions Initiative - The Real Urban Emissions*. 2020. URL: https://www.trueinitiative.org/data (cit. on p. 91).

[165] Bernard, Y., German, J. and Muncrief, R. *Worldwide Use of Remote Sensing to Measure Motor Vehicle Emissions*. Washington DC, 2019. URL: https://theicct.org/publications/worldwide-use-remote-sensing-measure-motor-vehicle-emissions (cit. on pp. 91, 138).

[166] Suarez-Bertoa, R. and Astorga, C. Impact of cold temperature on Euro 6 passenger car emissions. *Environmental Pollution* 234 (2018), pp. 318–329. DOI: 10.1016/j.envpol.2017.10.096 (cit. on pp. 95, 116).

[167] Weber, C., Sundvor, I. and Figenbaum, E. Comparison of regulated emission factors of Euro 6 LDV in Nordic temperatures and cold start conditions: Diesel- and gasoline direct-injection. *Atmospheric Environment* 206 (2019), pp. 208–217. DOI: 10.1016/J.ATMOSENV.2019.02.031 (cit. on p. 95).

[168] Hall, D. L., Anderson, D. C., Martin, C. R., Ren, X., Salawitch, R. J., He, H., Canty, T. P., Hains, J. C. and Dickerson, R. R. Using near-road observations of CO, NOy, and CO2 to investigate emissions from vehicles: Evidence for an impact of ambient temperature and specific humidity. *Atmospheric Environment* 232 (2020), p. 117558. DOI: 10.1016/J.ATMOSENV.2020.117558 (cit. on p. 95).

[169] Borken-Kleefeld, J. and Chen, Y. New emission deterioration rates for gasoline cars - Results from long-term measurements. *Atmospheric Environment* 101 (2015), pp. 58–64. DOI: 10.1016/j.atmosenv.2014.11.013 (cit. on pp. 95, 143).

[170] Chen, Y. and Borken-Kleefeld, J. NO x Emissions from Diesel Passenger Cars Worsen with Age. *Environ. Sci. Technol* 50 (2016), p. 3332. DOI: 10.1021/acs.est.5b04704. URL: https://pubs.acs.org/doi/10.1021/acs.est.5b04704. (cit. on pp. 95, 143).

[171] Sjödin, Å. and Andréasson, K. Multi-year remote-sensing measurements of gasoline light-duty vehicle emissions on a freeway ramp. *Atmospheric Environment* 34.27 (2000), pp. 4657–4665. DOI: 10.1016/S1352-2310(00)00158-8 (cit. on pp. 95, 143).

[172] Hari, D., Brace, C. J., Vagg, C., Poxon, J. and Ash, L. Analysis of a driver behaviour improvement tool to reduce fuel consumption. *Proceedings - 2012 International Conference on Connected Vehicles and Expo, ICCVE 2012* (2012), pp. 208–213. DOI: 10.1109/ICCVE.2012.46 (cit. on p. 95).

[173] Samaras, Z., Ntziachristos, L., Burzio, G., Toffolo, S., Tatschl, R., Mertz, J. and Monzon, A. Development of a Methodology and Tool to Evaluate the Impact of ICT Measures on Road Transport Emissions. *Procedia - Social and*

Behavioral Sciences 48 (2012), pp. 3418–3427. DOI: 10.1016/J.SBSPRO.2012.06.1306 (cit. on p. 95).

[174] Tran, M. and Brand, C. Smart urban mobility for mitigating carbon emissions, reducing health impacts and avoiding environmental damage costs. *Environmental Research Letters* 16.11 (2021), p. 114023. DOI: 10.1088/1748-9326/AC302E. URL: https://iopscience.iop.org/article/10.1088/1748-9326/ac302e%20https://iopscience.iop.org/article/10.1088/1748-9326/ac302e/meta (cit. on p. 95).

[175] Zheng, F., Li, J., Van Zuylen, H. and Lu, C. Influence of driver characteristics on emissions and fuel consumption. *Transportation Research Procedia*. Vol. 27. Elsevier B.V., 2017, pp. 624–631. DOI: 10.1016/j.trpro.2017.12.142 (cit. on pp. 95, 116).

[176] Xu, J., Saleh, M. and Hatzopoulou, M. A machine learning approach capturing the effects of driving behaviour and driver characteristics on trip-level emissions. *Atmospheric Environment* 224 (2020), p. 117311. DOI: 10.1016/J.ATMOSENV.2020.117311 (cit. on p. 96).

[177] Huang, Y., Ng, E. C., Zhou, J. L., Surawski, N. C., Lu, X., Du, B., Forehead, H., Perez, P. and Chan, E. F. Impact of drivers on real-driving fuel consumption and emissions performance. *Science of The Total Environment* 798 (2021), p. 149297. DOI: 10.1016/J.SCITOTENV.2021.149297 (cit. on p. 96).

[178] Carsten, O. M. and Tate, F. N. Intelligent speed adaptation: accident savings and cost–benefit analysis. *Accident Analysis & Prevention* 37.3 (2005), pp. 407–416. DOI: 10.1016/J.AAP.2004.02.007 (cit. on p. 98).

[179] Murrells, T. and Rose, R. *Production of Updated Emission Curves for Use in the NTM and WebTAG*. Tech. rep. Didcot: Ricardo Energy & Environment, 2019. URL: https://assets.publishing.service.gov.uk/government/uploads/system/uploads/attachment_data/file/942830/Production_of_Updated_Emission_Curves_for_Use_in_the_NTM_and_WebTAG-document.pdf (cit. on pp. 101, 105).

[180] Sjodin, A. and Jerksjo, M. Evaluation of European road transport emission models against on-road emission data as measured by optical remote sensing. *17th International Conference 'Transport and Air Pollution'*. Graz, 2008 (cit. on p. 106).

[181] Kousoulidou, M., Ntziachristos, L., Gkeivanidis, S. and Samaras, Z. Validation of the COPERT road emission inventory model with real-use data. 2010 (cit. on p. 106).

[182] Carslaw, D., Beevers, S., Westmoreland, E., Williams, M., Tate, J., Murrells, T., Stedman, J., Li, Y., Grice, S., Kent, A. and Tsagatakis, I. *Trends in NOx and NO2 emissions and ambient measurements in the UK*. Tech. rep. Defra, 2011. URL: https://uk-air.defra.gov.uk/assets/documents/reports/cat05/1108251149_110718_AQ0724_Final_report.pdf (cit. on p. 106).

[183] Shen, X., Yao, Z., Zhang, Q., Wagner, D. V., Huo, H., Zhang, Y., Zheng, B. and He, K. Development of database of real-world diesel vehicle emission factors for China. *Journal of Environmental Sciences* 31 (2015), pp. 209–220. DOI: 10.1016/J.JES.2014.10.021 (cit. on p. 106).

[184] O'Driscoll, R., ApSimon, H. M., Oxley, T., Molden, N., Stettler, M. E. and Thiyagarajah, A. A Portable Emissions Measurement System (PEMS) study of NOx and primary NO2 emissions from Euro 6 diesel passenger cars and comparison with COPERT emission factors. *Atmospheric Environment* 145 (2016), pp. 81–91. DOI: 10.1016/j.atmosenv.2016.09.021 (cit. on pp. 106, 117).

[185] Vaughan, A. R., Lee, J. D., Misztal, P. K., Metzger, S., Shaw, M. D., Lewis, A. C., Purvis, R. M., Carslaw, D. C., Goldstein, A. H., Hewitt, C. N., Davison, B., Beevers, S. D. and Karl, T. G. Spatially resolved flux measurements of NOX from London suggest significantly higher emissions than predicted by inventories. *Faraday Discussions* 189.0 (2016), pp. 455–472. DOI: 10.1039/c5fd00170f. URL: https://pubs.rsc.org/en/content/articlehtml/2016/fd/c5fd00170f%20https://pubs.rsc.org/en/content/articlelanding/2016/fd/c5fd00170f (cit. on pp. 106, 117).

[186] European Environment Agency. *National Emission Ceilings Directive*. 2016. URL: https://www.eea.europa.eu/themes/air/air-pollution-sources-1/national-emission-ceilings (cit. on pp. 116, 117).

[187] Weiss, M., Bonnel, P., Hummel, R., Provenza, A. and Manfredi, U. On-road emissions of light-duty vehicles in Europe. *Environmental Science and Technology* 45.19 (2011), pp. 8575–8581. DOI: 10.1021/es2008424. URL: https://pubs.acs.org/doi/abs/10.1021/es2008424 (cit. on p. 117).

[188] Kousoulidou, M., Fontaras, G., Ntziachristos, L., Bonnel, P., Samaras, Z. and Dilara, P. Use of portable emissions measurement system (PEMS) for the development and validation of passenger car emission factors. *Atmospheric Environment* 64 (2013), pp. 329–338. DOI: 10.1016/j.atmosenv.2012.09.062 (cit. on p. 117).

[189] Ekström, M., Sjödin, Å. and Andreasson, K. Evaluation of the COPERT III emission model with on-road optical remote sensing measurements. *Atmospheric Environment* 38.38 (2004), pp. 6631–6641. DOI: 10.1016/j.atmosenv.2004.07.019 (cit. on p. 117).

[190] Guo, H., Zhang, Q. y., Shi, Y. and Wang, D. h. Evaluation of the International Vehicle Emission (IVE) model with on-road remote sensing measurements. *Journal of Environmental Sciences* 19.7 (2007), pp. 818–826. DOI: 10.1016/S1001-0742(07)60137-5 (cit. on p. 117).

[191] Opus Inspection. *Remote Sensing Technology*. 2018. URL: http://opusinspection.com/remote-sensing-device-technology (cit. on p. 120).

[192] Department for Transport. *Quarterly traffic estimates (TRA25)*. 2020. URL: https://www.gov.uk/government/statistical-data-sets/tra25-quarterly-estimates (cit. on p. 123).

[193] Han, D., E, J., Deng, Y., Chen, J., Leng, E., Liao, G., Zhao, X., Feng, C. and Zhang, F. A review of studies using hydrocarbon adsorption material for reducing hydrocarbon emissions from cold start of gasoline engine. *Renewable and Sustainable Energy Reviews* 135 (2021), p. 110079. DOI: 10.1016/j.rser.2020.110079 (cit. on pp. 126, 146).

[194] BEIS. *Digest of UK Energy Statistics (DUKES)*. 2020. URL: https://www.gov.uk/government/collections/digest-of-uk-energy-statistics-dukes (cit. on p. 127).

[195] BEIS. *Greenhouse gas reporting: conversion factors 2019*. 2019. URL: https://www.gov.uk/government/publications/greenhouse-gas-reporting-conversion-factors-2019 (cit. on p. 127).

[196] Department for Transport. *Petroleum consumption by transport mode and fuel type: United Kingdom (ENV0101)*. 2020 (cit. on p. 132).

[197] Richmond, B., Misra, A., Brown, P., Karagianni, E., Murrells, T., Pang, Y., Passant, N., Pepler, A., Stewart, R., Thistlethwaite, G., Turtle, L., Wakeling, D., Walker, C. and Wiltshire, J. *UK Informative Inventory Report (1990 to 2018)*. Tech. rep. Ricardo Energy & Environment, 2020. URL: https://uk-air.defra.gov.uk/assets/documents/reports/cat07/2003131327_GB_IIR_2020_v1.0.pdf (cit. on p. 133).

[198] Carslaw, D. C., Farren, N. J., Vaughan, A. R., Drysdale, W. S., Young, S. and Lee, J. D. The diminishing importance of nitrogen dioxide emissions from road vehicle exhaust. *Atmospheric Environment: X* 1.2 (2019), p. 100002. DOI: 10.1016/J.AEAOA.2018.100002. URL: https://www.sciencedirect.com/science/article/pii/S2590162118300029 (cit. on p. 137).

[199] Dallmann, T., Bernard, Y., Tietge, U. and Muncrief, R. *Remote sensing of motor vehicle exhaust emissions in Paris*. Tech. rep. September. Washington DC: International Council on Clean Transportation, 2018. URL: https://theicct.org/publications/on-road-emissions-paris-201909 (cit. on pp. 138, 154).

[200] Wang, J., Chen, H., Hu, Z., Yao, M. and Li, Y. A Review on the Pd-Based Three-Way Catalyst. *http://dx.doi.org/10.1080/01614940.2014.977059* 57.1 (2014), pp. 79–144. DOI: 10.1080/01614940.2014.977059. URL: https://www.tandfonline.com/doi/abs/10.1080/01614940.2014.977059 (cit. on p. 141).

[201] Praveena, V. and Martin, M. L. J. A review on various after treatment techniques to reduce NOx emissions in a CI engine. *Journal of the Energy Institute* 91.5 (2018), pp. 704–720. DOI: 10.1016/J.JOEI.2017.05.010 (cit. on p. 141).

[202] Miller, J. and Jin, L. *Global progress toward soot-free diesel vehicles in 2019*. Tech. rep. Washington: International Council on Clean Transportation, 2019. URL: https://theicct.org/sites/default/files/publications/Global_progress_sootfree_diesel_2019_20190920.pdf (cit. on p. 141).

[203] Williams, M. and Minjares, R. *A technical summary of Euro 6/VI vehicle emission standards*. Tech. rep. Berlin: International Council on Clean Transportation, 2016. URL: www.theicct.org (cit. on p. 141).

[204] United States Environmental Protection Agency. *Final Rule for Control of Air Pollution from Motor Vehicles: Tier 3 Motor Vehicle Emission and Fuel Standards*. https://www.epa.gov/regulations-emissions-vehicles-and-engines/final-rule-control-air-pollution-motor-vehicles-tier-3. 2014 (cit. on p. 141).

[205] Matzer, C., Weller, K., Dippold, M., Lipp, S., Röck, M., Rexeis, M. and Hausberger, S. *Update of Emission Factors for HBEFA Version 4.1*. Tech. rep. Graz University of Technology, 2019. URL: http://ivt.tugraz.at (cit. on p. 142).

[206] Keller, M., Hausberger, S., Matzer, C. and Wüthrich, P. *Handbook emission factors for road transport—HBEFA Version 3.3*. Tech. rep. IVT Institute for internal combustion engines and thermodynamics, 2017. URL: http://www.hbefa.net/e/documents/HBEFA33_Documentation_20170425.pdf (cit. on p. 142).

[207] Bishop, G. A. and Stedman, D. H. A Decade of On-road Emissions Measurements. *Environmental Science and Technology* 42.5 (2008), pp. 1651–1656. DOI: 10.1021/ES702413B. URL: https://pubs.acs.org/doi/abs/10.1021/es702413b (cit. on p. 143).

[208] Huo, H., Yao, Z., Zhang, Y., Shen, X., Zhang, Q., Ding, Y. and He, K. On-board measurements of emissions from light-duty gasoline vehicles in three mega-cities of China. *Atmospheric Environment* 49 (2012), pp. 371–377. DOI: 10.1016/J.ATMOSENV.2011.11.005 (cit. on p. 143).

[209] Hao, L., Zhao, Z., Yin, H., Wang, J., Li, L., Lu, W., Ge, Y. and Sjödin, Å. Study of durability of diesel vehicle emissions performance based on real driving emission measurement. *Chemosphere* 297 (2022), p. 134171. DOI: 10.1016/J.CHEMOSPHERE.2022.134171. URL: https://linkinghub.elsevier.com/retrieve/pii/S0045653522006646 (cit. on p. 143).

[210] Chiang, H. L., Tsai, J. H., Yao, Y. C. and Ho, W. Y. Deterioration of gasoline vehicle emissions and effectiveness of tune-up for high-polluted vehicles. *Transportation Research Part D: Transport and Environment* 13.1 (2008), pp. 47–53. DOI: 10.1016/J.TRD.2007.07.004 (cit. on p. 143).

[211] Zhang, Q., Fan, J., Yang, W., Chen, B., Zhang, L., Liu, J., Wang, J., Zhou, C. and Chen, X. The effects of deterioration and technological levels on pollutant emission factors for gasoline light-duty trucks. *Journal of the Air & Waste Management Association* 67.7 (2017), pp. 814–823. DOI: 10.1080/10962247.2017.1301275. URL: https://www.tandfonline.com/doi/abs/10.1080/10962247.2017.1301275 (cit. on p. 143).

[212] Zhang, Q., Fan, J., Yang, W., Ying, F., Bao, Z., Sheng, Y., Lin, C. and Chen, X. Influences of accumulated mileage and technological changes on emissions of regulated pollutants from gasoline passenger vehicles. *Journal of Environmental Sciences* 71 (2018), pp. 197–206. DOI: 10.1016/J.JES.2018.03.021 (cit. on p. 143).

[213] Silge, J., Chow, F., Kuhn, M. and Wickham, H. *rsample: General Resampling Infrastructure*. R package version 0.0.9. 2021. URL: https://CRAN.R-project.org/package=rsample (cit. on p. 149).

[214] Chen, Y. and Borken-Kleefeld, J. Real-driving emissions from cars and light commercial vehicles – Results from 13 years remote sensing at Zurich/CH.

Atmospheric Environment 88 (2014), pp. 157–164. DOI: 10.1016/J.ATMOSENV.2014.01.040 (cit. on p. 155).

[215] Zhang, Q., Wei, N., Zou, C. and Mao, H. Evaluating the ammonia emission from in-use vehicles using on-road remote sensing test. *Environmental Pollution* 271 (2021), p. 116384. DOI: 10.1016/J.ENVPOL.2020.116384 (cit. on pp. 155, 156).

[216] Transport for London. *Ultra Low Emission Zone*. https://tfl.gov.uk/modes/driving/ultra-low-emission-zone. 2021 (cit. on p. 165).

[217] Office for Zero Emission Vehicles. *Outcome and response to ending the sale of new petrol, diesel and hybrid cars and vans*. 2021. URL: https://www.gov.uk/government/consultations/consulting-on-ending-the-sale-of-new-petrol-diesel-and-hybrid-cars-and-vans/outcome/ending-the-sale-of-new-petrol-diesel-and-hybrid-cars-and-vans-government-response (cit. on p. 175).

[218] Henry, L. and Wickham, H. *rlang: Functions for Base Types and Core R and 'Tidyverse' Features*. R package version 0.4.12. 2021. URL: https://CRAN.R-project.org/package=rlang (cit. on p. 178).

[219] Bache, S. M. and Wickham, H. *magrittr: A Forward-Pipe Operator for R*. R package version 2.0.1. 2020. URL: https://CRAN.R-project.org/package=magrittr (cit. on p. 178).

[220] Wickham, H. *rvest: Easily Harvest (Scrape) Web Pages*. R package version 1.0.2. 2021. URL: https://CRAN.R-project.org/package=rvest (cit. on p. 180).